

UNIVERSITY OF NOVI SAD
FACULTY OF TECHNOLOGY

УНИВЕРЗИТЕТ У НОВОМ САДУ
ТЕХНОЛОШКИ ФАКУЛТЕТ

**ACTA PERIODICA
TECHNOLOGICA**

ACTA PERIODICA TECHNOLOGICA (formerly Zbornik radova Tehnološkog fakulteta and Proceedings of Faculty of Technology) publishes articles from all branches of technology (food, chemical, biochemical, pharmaceutical), process engineering and related scientific fields.

Articles in Acta Periodica Technologica are abstracted by: Chemical Abstracts, Columbus, Ohio, Referativnyi zhurnal -Khimija, VINITI, Moscow, listed in Ulrich's International Periodical Directory, and indexed in the Elsevier Bibliographic databases – SCOPUS.

ISSN 1450-7188 (Print)
ISSN 2406-095X (Online)

CODEN: APTEFF
UDC 54:66:664:615

Publisher

University of Novi Sad, Faculty of Technology
Bulevar cara Lazara 1, 21000 Novi Sad, Serbia

For Publisher

Prof. Dr. Radomir Malbaša, Dean

Editor-in-Chief

Prof. Dr. Sonja Đilas

Editorial Board

From Abroad

Prof. Dr. Živko Nikolov

Texas A and M University, Biological and Agricultural Engineering
Department, College Station, TX, USA

Prof. Dr. Erika Békássy-Molnár

University of Horticulture and Food Industry, Budapest, Hungary

Prof. Dr. Željko Knez

University of Maribor,

Faculty of Chemistry and Chemical Technology, Maribor, Slovenia

Dr. T.S.R. Prasada Rao

Indian Institute of Petroleum, Dehra Dun, India

Prof. Dr. Đerd Karlović

Margarine Center of Expertise, Kruszwica, Poland

Dr. Szigmond András

Research Institute of Hungarian Sugar Industry, Budapest, Hungary

Dr. Andreas Reitzmann

Institute of Chemical Process Engineering, University Karlsruhe, Germany

From Serbia

Prof. Dr. Vlada Veljković

Prof. Dr. Spasenija Milanović

Prof. Dr. Vladimir Srdić

Prof. Dr. Slobodan D. Petrović

Prof. Dr. Jonjaua Ranogajec

Dr. Anamarija Mandić

CONTENT

FOOD TECHNOLOGY

<i>Miroljub B. Barać, Mirjana B. Pešić, Slađana P. Stanojević, Aleksandar Ž. Kostić, Slavica B. Čabrilo</i> TECHNO-FUNCTIONAL PROPERTIES OF PEA (<i>Pisum Sativum</i>) PROTEIN ISOLATES- A REVIEW	1
<i>Dušica S. Čolović, Jovanka D. Lević, Radmilo R. Čolović, Ljubinko B. Lević, Vojislav V. Banjac, Slađana M. Rakita, Olivera M. Đuragić</i> REDUCTION OF CYANOGENIC GLYCOSIDES BY EXTRUSION - INFLUENCE OF TEMPERATURE AND MOISTURE CONTENT OF THE PROCESSED MATERIAL.....	19
<i>Ljubica Dokić, Biljana Pajin, Aleksandar Fištes, Zita Šereš, Dragana Šoronja Simović, Veljko Krstonošić</i> RHEOLOGICAL AND TEXTURAL PROPERTIES OF CRACKER DOUGH WITH ADDITION OF PEA DIETARY FIBER	29
<i>Jelena S. Filipović¹*, Lato L. Pezo², Vladimir S. Filipović³, Gordana I. Ludajić</i> SPELT PASTA WITH INULIN AS A FUNCTIONAL FOOD	37
<i>Jovana R. Glušac, Milka J. Stijepić, Spasenija D. Milanović, Dragica M. Đurđević-Milošević</i> PHYSICOCHEMICAL PROPERTIES OF HONEYBEE POLLEN ENRICHED ACIDOPHILUS MILK AND PROBIOTIC YOGHURT.....	45
<i>Mirela D. Iličić, Spasenija D. Milanović, Dajana V. Hrnjez, Katarina G. Kanurić, Vladimir R. Vukić, Marjan I. Ranogajec</i> INFLUENCE OF FAT CONTENT AND STARTER CULTURES ON THE QUALITY OF FERMENTED DAIRY PRODUCTS.....	55
<i>Kristian A. Pastor, Marijana M. Ačanski, Djura N. Vujić, Ankica Đ. Kondić-Špika, Nikola S. Hristov</i> LIPID AND SUGAR PROFILES OF VARIOUS BARLEY CULTIVARS (<i>Hordeum vulgare</i>)	65

*Jelena M. Prodanović, Marina B. Šćiban, Mirjana G. Antov,
Dragana V. Kukić, Vesna M. Vasić*
TREATMENT OF SUGAR BEET EXTRACTION JUICE STILLAGE BY
NATURAL COAGULANTS EXTRACTED FROM COMMON BEAN 77

*Ahmed M. Saad, Ragab A. Elmassry, Khaled M.M. Wahdan,
Mohamed Fawzy Ramadan*
CHICKPEA (*Cicer arietinum*) STEEP LIQUOR AS
A LEAVENING AGENT: EFFECT ON DOUGH RHEOLOGY
AND SENSORY PROPERTIES OF BREAD 91

*Jelena J. Vulić, Jasna M. Čanadanović-Brunet, Gordana S. Četković,
Sonja M. Djilas, Vesna T. Tumbas Šaponjac, Sladjana M. Stajčić*
POLYFLORAL, LINDEN AND ACACIA HONEYS WITH DRIED CHERRIES
AFTER THREE MONTHS OF STORAGE – ANTIOXIDANT AND SENSORY
EVALUATION 103

*Danica B. Zarić, Biljana S. Pajin, Ivana S. Lončarević, Jovana S. Petrović
Marijana M. Stamenković Đoković*
EFFECTS OF THE AMOUNT OF SOY MILK ON
THERMORHEOLOGICAL, THERMAL AND TEXTURAL
PROPERTIES OF CHOCOLATE WITH SOY MILK 115

CHEMICAL TECHNOLOGY AND PROCESS ENGINEERING

Oluwaseyi A. Ajibade, Johnson O. Agunsoye, Sunday A. Oke
ANALYSIS OF THE FREE-SWELL BEHAVIOUR
OF ORANGE PEEL PARTICULATES..... 131

*Ana D. Đurović, Zorica S. Stojanović, Snežana Ž. Kravić, Zvonimir. J. Suturović,
Tanja Ž. Brezo, Nada L. Grahovac, Spasenija D. Milanović*
A COMPARISON OF DIFFERENT METHODS TO REMOVE
DISSOLVED OXYGEN: APPLICATION TO THE
ELECTROCHEMICAL DETERMINATION OF IMIDACLOPRID..... 149

Nataša Lj. Lukić, Predrag M. Tekić, Jelena B. Rađenović, Ivana M. Šijački
LATTICE BOLTZMANN SIMULATION OF TWO-SIDED
LID-DRIVEN FLOW IN DEEP CAVITIES..... 157

Sanja O. Podunavac-Kuzmanović, Jonjaua G. Ranogajec, Strahinja Z. Kovačević
CORRELATION AND PRINCIPAL COMPONENT ANALYSIS
IN CERAMIC TILES CHARACTERIZATION 169

<i>Vesna M. Vasić, Marina B. Šćiban, Dragana V. Kukić, Jelena M. Prodanović, Nikola R. Maravić</i>	
SEQUENTIAL MICRO AND ULTRAFILTRATION OF DISTILLERY WASTEWATER.....	177
<i>Vojkan M. Zorić, Željko Nikač, Radovan Radovanović</i>	
POLICE ASPECTS OF THE FORENSIC METHODS OF THE STUDY OF PERCENTAGE OF WATER CONTENT OF THE DETERMINE THE AGE OF THE FRESCOES	185

BIOCHEMICAL AND PHARMACEUTICAL ENGINEERING

<i>Bojana Ž. Bajić, Zorana Z. Rončević, Siniša N. Dodić, Jovana A. Grahovac, Jelena M. Dodić</i>	
GLYCEROL AS A CARBON SOURCE FOR XANTAN PRODUCTION BY <i>Xanthomonas campestris</i> ISOLATES.....	197
<i>Jovana J. Đuran, Zorana Z. Rončević, Bojana Ž. Bajić, Siniša N. Dodić, Jovana A. Grahovac, Aleksandar I. Jokić, Jelena M. Dodić</i>	
OPTIMIZATION OF ALCOHOLIC FERMENTATION USING IMMOBILIZED YEAST CELLS IN CALCIUM ALGINATE GEL.....	207
<i>Milica Ž. Karadžić, Davor M. Lončar, Lidija R. Jevrić, Sanja O. Podunavac-Kuzmanović, Strahinja Z. Kovačević, Stela D. Jokić</i>	
CHEMOMETRIC ESTIMATION OF THE RETENTION BEHAVIOR OF SELECTED ESTRADIOL DERIVATIVES.....	219
<i>Jaroslav M. Katona, Alena Tomšik, Sandra Dj. Bučko, Lidija B. Petrović</i>	
INFLUENCE OF IONIC STRENGTH ON THE RHEOLOGICAL PROPERTIES OF HYDROXYPROPYLMETHYL CELLULOSE-SODIUM DODECYLSULFATE MIXTURES.....	229
<i>Strahinja Z. Kovačević, Sanja O. Podunavac-Kuzmanović, Lidija R. Jevrić, Evgenija A. Djurendić, Jovana J. Ajduković, Pavle T. Jovanov</i>	
CHROMATOGRAPHIC LIPOPHILICITY AS A PREDICTOR OF ANTIPROLIFERATIVE ACTIVITY OF 17-PICOLYL AND 17-PICOLINYLDENE ANDROSTANE DERIVATIVES TOWARD PROSTATE CANCER.....	239
<i>Nada U. Perišić Janjić</i> <i>Katarina M. Penov Gaši, Evgenija A. Djurendić, Marina P. Savić, Strahinja Z. Kovačević, Stela D. Jokić, Sanja O. Podunavac-Kuzmanović</i>	
ESTIMATION OF CHROMATOGRAPHIC LIPOPHILICITY OF SOME D-HOMO ANDROSTENE DERIVATIVES	249

*Zoran P. Zeković, Snežana Dj. Filip, Senka S. Vidović,
Dušan S. Adamović, Ahmed M. Elgndi*

BASIL (*Ocimum basilicum* L.) ESSENTIAL OIL AND EXTRACTS
OBTAINED BY SUPERCRITICAL FLUID EXTRACTION..... 259

INSTRUCTION FOR MANUSCRIPT PREPARATION

САДРЖАЈ

ПРЕХРАМБЕНА ТЕХНОЛОГИЈА

<i>Мирољуб Б. Бараћ, Мирјана Б. Пешић, Слађана П. Станојевић, Александар Ж. Костић, Славица Б. Чабрило</i> ТЕХНО-ФУНКЦИОНАЛНЕ ОСОБИНЕ ИЗОЛАТА ПРОТЕИНА ГРАШКА	1
<i>Душица С. Чоловић, Јованка Д. Левић, Радмило Р. Чоловић, Љубинко Б. Левић, Војислав В. Бањац, Слађана М. Ракита, Оливера М. Ђурагић</i> РЕДУКЦИЈА ЦИЈАНОГЕНИХ ГЛИКОЗИДА ЕКСТРУДИРАЊЕМ – УТИЦАЈ ТЕМПЕРАТУРЕ И ВЛАГЕ ТРЕТИРАНОГ МАТЕРИЈАЛА	19
<i>Љубица Докић, Биљана Пајин, Александар Фиштеш, Зита Шереш, Драгана Шороња Симовић, Вељко Крстоношић</i> РЕОЛОШКЕ И ТЕКСТУРАЛНЕ ОСОБИНЕ ТЕСТА ЗА КРЕКЕРЕ СА ДОДАТКОМ ВЛАКАНА ГРАШКА	29
<i>Јелена С. Филиповић, Лато Л. Пезо, Владимир С. Филиповић, Гордана И. Људајић</i> ТЕСТЕНИНА ОД СПЕЛТЕ СА ИНУЛИНОМ КАО ФУНКЦИОНАЛНА ХРАНА	37
<i>Јована Р. Глушац, Милка Ј. Стијепић, Спасенија Д. Милановић, Драгица М. Ђурђевић-Милошевић</i> ФИЗИЧКОХЕМИЈСКЕ ОСОБИНЕ АЦИДОФИЛНОГ МЛЕКА И ПРОБИОТСКОГ ЈОГУРТА СА ДОДАТКОМ ПОЛЕНА	45
<i>Мирела Д. Иличић, Спасенија Д. Милановић, Дајана В. Хрњез, Катарина Г. Канурић, Владимир Р. Вукић, Марјан И. Раногајец</i> УТИЦАЈ САДРЖАЈА МЛЕЧНЕ МАСТИ И СТАРТЕР КУЛТУРЕ НА КВАЛИТЕТ ФЕРМЕНТИСАНИХ МЛЕЧНИХ ПРОИЗВОДА	55
<i>Кристиан А. Пастор, Маријана М. Ачански, Ђура Н. Вујић, Анкица Ђ. Кондић-Шпика, Никола С. Христов</i> ЛИПИДНИ И ШЕЋЕРНИ ПРОФИЛИ РАЗЛИЧИТИХ СОРТИ ЈЕЧМА (<i>Hordeum vulgare</i>)	65

*Јелена М. Продановић, Марина Б. Шћибан, Мирјана Г. Антов,
Драгана В. Кукић, Весна М. Васић*
ТРЕТМАН ЦИБРЕ ОД ЕКСТРАКЦИОНОГ СОКА ШЕЋЕРНЕ РЕПЕ
ПРИРОДНИМ КОАГУЛАНТИМА ЕКСТРАХОВАНИМ ИЗ ПАСУЉА 77

*Ахмед М. Саад, Рагаб А. Елмасру, Кхалед М.М. Вахдан,
Мохамед Фавзи Рамадан*
СУВИ ВОДЕНИ ЕКСТРАКТ ЛЕБЛЕБИЈЕ (*Cicer arietinum*)
КАО АГЕНС КВАСАЊА: УТИЦАЈ НА РЕОЛОГИЈУ ТЕСТА
И СЕНЗОРНЕ КАРАКТЕРИСТИКЕ ХЛЕБА..... 91

*Јелена Ј. Вулић, Јасна М. Чанадановић-Брунет, Гордана С. Тетковић,
Соња М. Ђилас, Весна Т. Тумбас Шапоњац, Слађана М. Стајчић*
ЛИВАДСКИ, ЛИПОВ И БАГРЕМОВ МЕД СА ДОДАТКОМ СУВЕ
ВИШЊЕ НАКОН 3 МЕСЕЦА СКЛАДИШТЕЊА – АНТИОКСИДАТИВНА
И СЕНЗОРСКА АНАЛИЗА 103

*Даница Б. Зарић, Биљана С. Пајин, Ивана С. Лончаревић, Јована С. Петровић
Маријана М. Стаменковић Ђоковић*
УТИЦАЈ КОЛИЧИНЕ СОЈИНОГ МЛЕКА НА ТЕРМОРЕОГРАФСКЕ,
ТОПЛОТНЕ И ТЕКСТУРАЛНЕ КАРАКТЕРИСТИКЕ ЧОКОЛАДЕ СА
СОЈИНИМ МЛЕКОМ 115

ХЕМИЈСКА ТЕХНОЛОГИЈА И ПРОЦЕСНО ИНЖЕЊЕРСТВО

Оливасеј А. Ајбаде, Џонсон О. Агумсој, Сандеј А. Оке
ИСПИТИВАЊЕ СЛОБОДНОГ БУБРЕЊА ПАРТИКУЛА
ПОМОРАНЦИНЕ КОРЕ..... 131

*Ана Д. Буровић, Зорица С. Стојановић, Снежана Ж. Кравић,
Звонимир. Ј. Сутуровић, Тања Ж. Брезе, Нада Л. Граховац,
Спасенија Д. Милановић*
ПОРЕЂЕЊЕ РАЗЛИЧИТИХ МЕТОДА ЗА УКЛАЊАЊЕ
РАСТВОРЕНОГ КИСЕОНИКА: ПРИМЕНА ПРИ
ЕЛЕКТРОХЕМИЈСКОМ ОДРЕЂИВАЊУ ИМИДАКЛОПРИДА 149

Наташа Љ. Лукић, Предраг М. Текић, Јелена Б. Рађеновић, Ивана М. Шијачки
СИМУЛАЦИЈА ТОКА ФЛУИДА У ДУБОКИМ ШУПЉИНАМА СА ДВА
ПОКРЕТНА ЗИДА ПРИМЕНОМ LATTICE VOLTZMANN МЕТОДЕ 157

Сања О. Подунавац-Кузмановић, Јоњауа Г. Ранозајец, Страхинја З. Ковачевић
КОРЕЛАЦИОНА АНАЛИЗА И АНАЛИЗА ГЛАВНИХ КОМПОНЕНАТА
У КАРАКТЕРИЗАЦИЈИ КЕРАМИЧКИХ ПЛОЧИЦА 169

*Весна М. Васић, Марина Б. Шћибан, Драгана В. Кукић,
Јелена М. Продановић, Никола Р. Маравић*
СЕКВЕНЦИЈАЛНА МИКРО И УЛТРАФИЛТРАЦИЈА
ОТПАДНЕ ВОДЕ ИЗ ДЕСТИЛЕРИЈЕ..... 177

Војкан М. Зорић, Жељко Никач, Радован Радовановић
ПОЛИЦИЈСКИ АСПЕКТИ ФОРЕНЗИЧКИХ МЕТОДА
СТУДИЈЕ ПРОЦЕНТА САДРЖАЈА ВОДЕ КОД
ОДРЕЂИВАЊА СТАРОСТИ ФРЕСАКА..... 185

БИОХЕМИЈСКО И ФАРМАЦЕУТСКО ИНЖЕЊЕРСТВО

*Бојана Ж. Бајић, Зорана З. Рончевић, Синиша Н. Додић,
Јована А. Граховац, Јелена М. Додић*
ГЛИЦЕРОЛ КАО ИЗВОР УГЉЕНИКА У ПРОИЗВОДЊИ
КСАНТАНА ПРИМЕНОМ ИЗОЛАТА *Xanthomonas campestris*..... 197

*Јована Ј. Ђуран, Зорана З. Рончевић, Бојана Ж. Бајић, Синиша Н. Додић,
Јована А. Граховац, Александар И. Јокић, Јелена М. Додић*
ОПТИМИЗАЦИЈА АЛКОХОЛНЕ ФЕРМЕНТАЦИЈЕ
ЋЕЛИЈАМА КВАСЦА ИМОБИЛИСАНИМ У КУГЛИЦАМА
КАЛЦИЈУМ-АЛГИНАТА. 207

*Милица Ж. Караџић, Давор М. Лончар, Лидија Р. Јеврић,
Сања О. Подунавац-Кузмановић, Страхиња З. Ковачевић, Стела Д. Јокић*
ХЕМОМЕТРИЈСКА ПРОЦЕНА РЕТЕНЦИОНОГ ПОНАШАЊА
ОДАБРАНИХ ДЕРИВАТА ЕСТРАДИОЛА 219

Јарослав М. Катона, Алена Томшиќ, Сандра Ђ. Бучко, Лидија Б. Петровић
УТИЦАЈ ЈОНСКЕ ЈАЧИНЕ НА РЕОЛОШКЕ ОСОБИНЕ
СМЕША ХИДРОКСИПРОПИЛМЕТИЛ ЦЕЛУЛОЗЕ
И НАТРИЈУМ ДОДЕЦИЛСУЛФАТА..... 229

*Страхиња З. Ковачевић, Сања О. Подунавац-Кузмановић, Лидија Р. Јеврић,
Евгенија А. Ђурендић, Јована Ј. Ајдуковић, Павле Т. Јованов*
ПРЕДВИЂАЊЕ АНТИКАНЦЕРОГЕНЕ АКТИВНОСТИ 17-ПИКОЛИЛ
И 17-ПИКОЛИНИЛИДЕН АНДРОСТАНСКИХ ДЕРИВАТА
НА ОСНОВУ ХРОМАТОГРАФСКЕ ЛИПОФИЛНОСТИ 239

*Нада У. Перичић Јањић, Катарина М. Пенев Гаши, Евгенија А. Ђурендић,
Марина П. Савић, Страхиња З. Ковачевић, Стела Д. Јокић,
Сања О. Подунавац-Кузмановић*
ПРОЦЕНА ХРОМАТОГРАФСКЕ ЛИПОФИЛНОСТИ
D-ХОМО АНДРОСТЕНСКИХ ДЕРИВАТА 249

Зоран П. Зековић, Снежана Ђ. Филип, Сенка С. Видовић,
Душан С. Адамовић, Ахмед М. Елгнди

ЕТАРСКО УЉЕ И ЕКСТРАКТИ БОСИЉКА (*Ocimum basilicum* L.)

ДОБИЈЕНИ СУПЕРКРИТИЧНОМ ЕКСТРАКЦИЈОМ 259

УПУТСТВО ЗА ПИСАЊЕ РАДА

FOOD TECHNOLOGY

TECHNO-FUNCTIONAL PROPERTIES OF PEA (*Pisum sativum*) PROTEIN ISOLATES- A REVIEW

Miroљub B. Barać^{1*}, Mirjana B. Pešić¹, Slađana P. Stanojević¹, Aleksandar Ž. Kostić¹
and Slavica B. Čabrilo²

¹ University of Belgrade, Faculty of Agriculture, Nemanjina 6, 11080 Beograd-Zemun, Serbia

² High Technical School of Vocational Studies, 12000 Požarevac, Nemanjina 2, Serbia

Due to high nutritive quality, good techno-functional properties and low cost, legume protein products are becoming the most appropriate alternative to protein products of animal origin. In food industries, these products are usually used as techno-functional additives which provide specific characteristics of final food products. Legume proteins are commonly used as flour, concentrates, and isolates. The greatest application on industrial scale has soy proteins, and to a lesser extent, in the past 20 years, pea protein isolates. The modest use of pea protein is partly a result of insufficient information relating to their techno-functional properties. This paper is an overview of techno-functional properties of pea proteins and their isolates. Also, the paper deals with the possible use of limited enzymatic hydrolysis as a method for the improvement of their techno-functional properties.

KEY WORDS: pea protein isolates, techno-functional properties, limited hydrolysis

INTRODUCTION

For a long time, legumes have been recognized as a valuable and low cost source of high quality protein products such as flour, concentrates and isolates. Nevertheless, the application on an industrial scale has only soybean proteins, whereas other vegetable proteins are less used. Over the last 20 years, especially in Canada and European countries, pea proteins are becoming a viable alternative to soy protein products because of techno-functional and nutritive characteristics (1), which can be as good as those of soybeans. Furthermore, pea seed have a lower content of anti-nutritive components, such as proteinase inhibitors and phytic acid (2) and caused less frequent allergic reactions in humans than soybean (3). In addition, they also contain good quality starch and fibers.

The most promising alternative to soy protein products are pea protein isolates. As in the case of soy protein isolates, techno-functional properties including solubility, emulsifying, foaming and gelling properties of pea isolates are well documented (4-10). In the current literature, opposite results were reported concerning techno-functional properties of pea and soy protein isolates. Some researches (11, 12) obtained better functionality of soy pro-

* Corresponding author: Miroљub B. Barać, University of Belgrade, Faculty of Agriculture, Nemanjina 6, 11080 Beograd-Zemun, Serbia, e-mail: baracm@agrif.bg.ac.rs

tein isolates, whereas some other (5, 13, 14) pointed out better properties of pea isolates. Variations in the results among different studies could be due to the differences in the protein purity of the studied samples, method of protein isolation, the specific conditions used for the tests, as well as the different processing conditions (7, 15). Furthermore, significantly different functionalities among pea isolates were observed. Maninder et al. (16) and Barac et al. (6, 17) attributed this to the different ratio of the major proteins, which is in turn influenced by genotype characteristics, environmental conditions, and processing conditions (10, 18-20). To avoid the difference caused by different processing conditions, Barac et al. (15) prepared and compared pea, soybean and adzuki isolates under the same conditions. The results of this investigation showed that techno-functional properties of the isolates prepared from different species depended on several factors such as: choice of species and varieties, preparation conditions, and the pH value at which specific properties were tested.

STORAGE PEA PROTEINS

Pea seeds contain about 22-23% proteins. The majority of pea proteins are globulins and albumins, which represent about 80% of total seed protein content. Albumins represent 18-25% and globulins 55-65% of total proteins (21). All globulins and some of albumins are storage proteins, which are used as nitrogen sources for the new embryos after seed germination (22).

Major pea storage proteins, legumin, vicilin and convicilin are globulins and represent 65-85% of total proteins (23). According to sedimentation properties these proteins are classified into two fractions, 7S (vicilin, convicilin) and 11S fraction (legumin). Molecular forms of the three major proteins are presented in Figure 1.

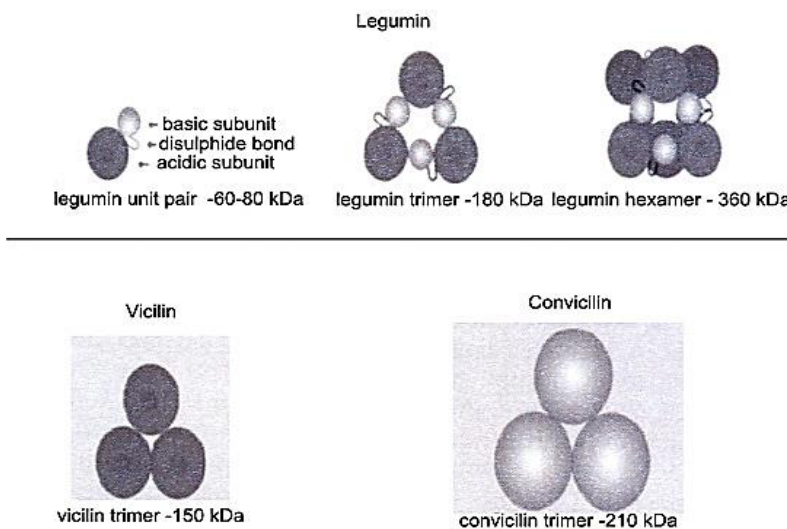


Figure 1. Molecular forms of legumin, vicilin and convicilin (22)

Legumin

Legumin is a protein with compact quaternary structure stabilized via disulphide, electrostatic and hydrophobic interactions. It is a hexamer with a molecular weight (Mw) ~320 to 380 kDa and with beta-sheet-rich structure (24). The mature proteins consist of six subunit pairs that interact non-covalently. Each of these subunit pairs consists of an acidic subunit of ~40 kDa and a basic subunit of ~20 kDa, linked by a single disulphide bond (25). As there are a number of legumin precursors originating from several gene families, different legumin polypeptides have been identified, e.g., 4-5 acidic (α) and 5-6 basic (β) polypeptides. The sizes of these polypeptides range from 38 to 40 kDa for the acidic polypeptides with the isoelectric point (pI) 4.5-5.8, and from 19 to 22 kDa for the basic polypeptides with the pIs of up to 8.8 (26). According to Gueguen et al. (25), more hydrophobic basic polypeptides are placed in the interior of the legumin molecule, whereas acidic polypeptides are oriented towards the outside of the molecule.

Due to its compact quaternary structure, legumin is a heat-stable protein. Thermal transition point of legumin is above 90°C. On the other hand, the quaternary structure of the legumin is more sensitive to pH and salt concentration. Pea legumin is present as a hexamer at the pH 7.0 and high ionic strength (0.1 M), but dissociates at, e.g., the pH 3.35 and 10.0, and, depending on the ionic strength, into a mixture of trimers, dimers, and monomers. Acidic conditions seem to be more drastic than alkaline ones, thus the native legumin is completely dissociated to monomers at the pH 2.4 (25).

As a food protein, legumin is recognized for its sulphur containing amino acid residues. It has been reported to contain approximately two cysteine and three methionine residues per 60-kDa subunit (27).

Vicilin

Vicilin is a trimeric protein of 150-170 kDa that lacks cysteine residues and hence cannot form disulphide bonds (27). The composition of vicilin subunits varies mostly because of post-translation processing. Mainly, vicilin consists of ~47 kDa, ~50 kDa, ~34 kDa and ~30 kDa subunits (28). Pea vicilin heterogeneity is more complex than the heterogeneity of legumin. Its heterogeneity derives from a combination of factors, including production of vicilin polypeptides from several small gene families encoding different primary sequences, differential proteolytic processing, and differential glycosylation (29). Thermal denaturation temperature of vicilin depends on ionic strength conditions. At low ionic strength conditions ($\mu = 0.08$) the thermal denaturation temperature is 71.7, whereas at higher ($\mu = 0.5$), it is 82.7°C (30).

Convicilin

A third major storage protein, distinct from legumin and vicilin, is convicilin. This protein has a distinctively different amino acid profile and unlike the 7S vicilin, contains very little carbohydrate and has a subunit molecular weight of 71,000 Da. The molecular weight of its native form is 290,000 Da including an N-terminal extension (8). Convicilin is not known to undergo any post-/co-translational modifications other than removal of the signal peptide, and it is not glycosylated. In opposite to vicilin, the residues of sulphur-amino

Commonly, protein concentrates are produced by air-classification of the pea flour (obtained from the milled seeds), which is a dry processing method that blows away the lighter starch granules, thus removing them from the protein. Concentrates have ~50% content of protein. Protein isolates instead undergo a wet processing in which low molecular weight water-soluble components and the salt soluble proteins are extracted from the flour and then the globular proteins are subsequently isolated by a selective precipitation step at the isoelectric point, neutralized and dried (Figure 3). Final protein content of isolates prepared by isoelectric precipitation is approximately about 85%. Protein extraction can be done under alkaline or acidic conditions. The schematic diagram of the most frequently used method based on aqueous alkaline extraction followed by isoelectric precipitation is presented in Figure 3.

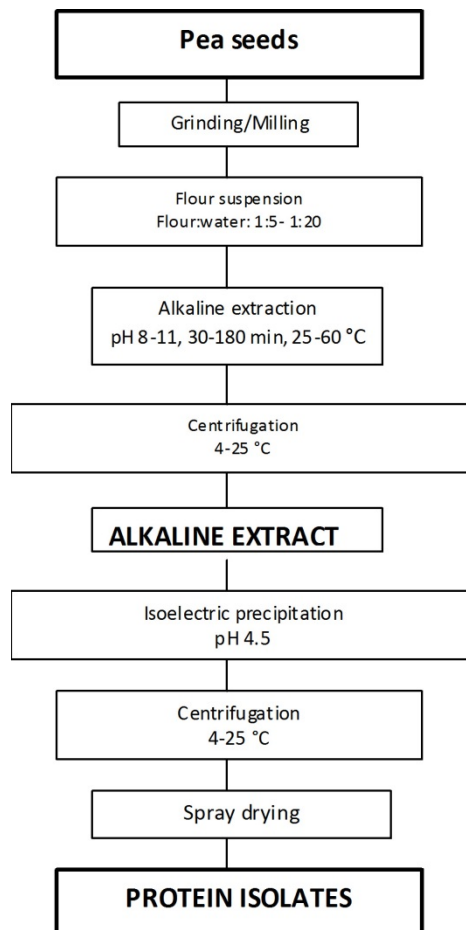


Figure 3. Schematic diagram of alkaline extraction and isoelectric precipitation process for production of pea protein isolates (8)

Alternatively, the isoelectric precipitation step can be substituted by ultrafiltration. The use of ultrafiltration increases the yield of isolates and change their composition. Isolates prepared by ultrafiltration contain 90-94% of protein (40). Besides globulins, these products contain other protein fractions and polysaccharides.

TECHNO-FUNCTIONAL PROPERTIES OF PEA PROTEINS AND THEIR PROTEIN PRODUCTS

In general, techno-functional properties of a protein are affected by numerous factors which can be classified into two groups, intrinsic and extrinsic factors. The intrinsic factors are: amino acid composition and sequence, shape, size, the ratio between hydrophobicity/hydrophilicity, conformation and reactivity. The extrinsic factors which can affect techno-functional properties of pure protein include pH, ionic strength, temperature, conformation, the ratio between hydrophobicity/hydrophilicity, method of extraction. Besides these factors, in the case of protein products, such as flour, concentrate and isolate, several additional factors, including the ratio of major proteins and processing conditions may have crucial effect on their techno-functional properties and consequently on their applicability in food systems.

Table 2. Techno-functional properties performed by functional proteins in food systems (41)

Techno-functional property	Mode of action	Food system
Solubility	Protein solvation	Beverages
Water absorption and binding	Hydrogen bonding of water; Entrapment of water (no drip)	Meat, sausages Breads, cakes
Viscosity	Thickening; water binding	Soups, gravies
Gelation	Protein matrix formation and setting	Meats, curds, cheese
Cohesion-adhesion	Protein act as adhesive material	Meats, sausages, baked goods, pasta
Elasticity	Hydrophobic binding in gluten; Disulfide links in gels	Meats, bakery
Emulsification	Formation and stabilization of fat emulsions	Sausages, bologna, soups, cakes
Fat absorption	Binding of free fat	Meats, sausages, doughnuts
Flavor-binding	Adsorption, entrapment, release	Simulated meats, bakery etc.
Foaming	Form stable film to entrap gas	Whipped toppings, chiffon desserts, angel cakes

Techno-functional properties required for a protein product vary due to its specific application in food and food systems (Table 2). In general, a good protein product has to possess multiple functionalities in order to perform well in food systems. The most important techno-functional properties of protein products are solubility, emulsification, foaming, and gelation.

Solubility of pea protein products

Good solubility of proteins is desired for optimal functionality in food processing applications (6). It is well known that other functional properties such as emulsification,

foaming, and gelation are dependent on the solubility of proteins. Solubility of proteins is variable and is influenced by the number of polar and apolar groups and their arrangement along the molecule (42). Solubility of protein depends on the pH and ionic strengths, whereas processing history of protein products has a great influence on this property (8, 15). Furthermore, the ratio of the major proteins in flour as starting material could affect the solubility of legumes protein product (6, 15, 44)

Major pea proteins are globulins with minimum solubility near the isoelectric point (pI 4.5), high solubility above and moderate below the isoelectric point (6, 11, 15, 46). The maximum value is observed in the pH range of 8-9 (11), whereas less than 20% of proteins are soluble at the pI value. Consequently, native pea proteins and their native products show U-shape of pH-solubility dependence, which is also typical for the other legume proteins (46, 15). However, the variations of solubility of pea protein isolates were observed. It is well known that native as well as thermally-treated proteins from legumes tend to form pH-induced aggregates (47, 48). So, Barac et al. (6, 44) attributed these variations to protein composition of pea isolate and different nature of complexes formed during the processing of the isolate (during isoelectric precipitation) and/or during the solubilization of the isolates at a specific pH.

Thermal treatments reduce the solubility of pea isolates (49). However, thermally treated pea protein products showed similar U-shape dependence (15). The effect of thermal treatment (90°C, 3 min) on pea protein isolate solubility is presented in Figure 4.

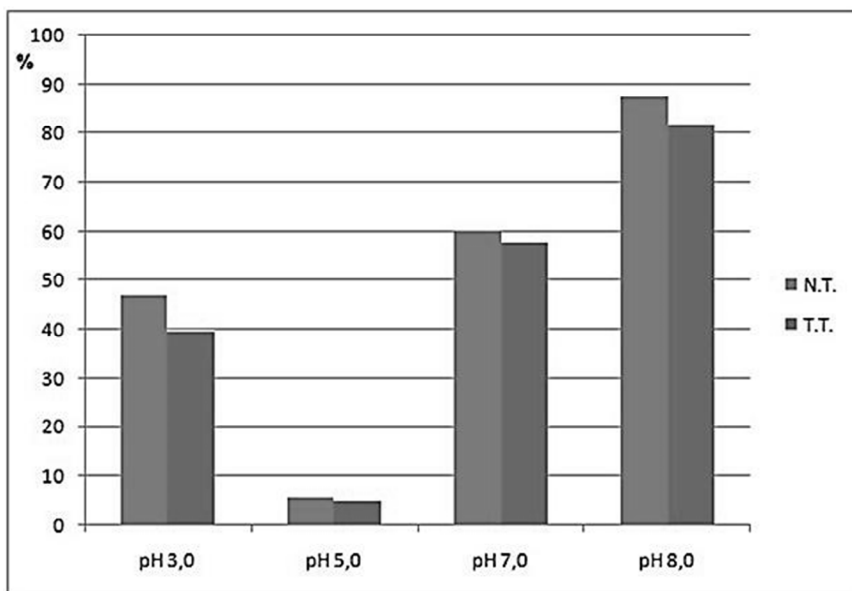


Figure 4. The influence of thermal treatment (90°C, 3 min) of neutralised suspensions of pea protein isolates on solubility at different pH values (15).

TT - thermally-treated, N.T. - non-treated

Emulsifying properties

Emulsions are disperse systems of immiscible liquids which are stabilized by emulsifiers – compounds which form interface films and thus prevent the disperse phases from flowing together. Proteins as surface-active and amphiphilic compounds can be used as emulsifying agents on a large scale during the production of food systems. Emulsifying properties of proteins are usually characterized as emulsifying ability or activity and emulsion stability. The emulsion stability is a measure of the stability of the emulsion over a certain time span and emulsion activity is a measurement of how much oil a protein can emulsify per unit protein (7).

Suitability of a pure protein and protein isolate as an emulsifier depends on the rate at which proteins diffuse into the interface and on the deformability of its conformation under the influence of interfacial tension (surface denaturation). A protein with ideal qualities as an emulsifier for an oil-in-water emulsion would have a relatively low molecular weight, a balanced amino acid composition in terms of charged, polar and non-polar residues, good water solubility, well-developed surface hydrophobicity, and a relatively stable conformation (42).

Different emulsifying properties of pure solutions of vicilin and legumin are documented. Results of several researchers (30, 36, 37, 50) showed that, in the native form, vicilin had better emulsifying properties than legumin. This could be attributed to the less compact and less rigid native structure of vicilin. Furthermore, due to conformational changes, emulsifying properties of vicilin and legumin are pH-dependent. Namely, the minimum emulsifying activity and stability the major pea proteins showed in the range of pI (4-5). Also, at the pI values their emulsions are extremely unstable. Above and below pI value, emulsifying properties increase due to intensive dissociation, which is more pronounced in the case of legumin (21). Due to this, besides the processing history of the isolate, the vicilin to legumin ratio has significant influence on the emulsifying properties.

Gharlsallaoui et al (51) investigated the emulsifying characteristics of acid-treated pea protein isolates. They showed that acid treated pea proteins adsorb faster on the water-oil interface at the pH 7.0 than at an acidic pH (pH 2.4). But, fast adsorption leads to the formation of more inhomogeneous film structures. In opposite to this, a slower adsorption is regular and slow but it leads to a higher surface viscoelasticity. Due to this, pea-protein-stabilized emulsions are more stable to creaming at acidic pHs, and their particle-size distributions are more homogeneous in these conditions.

Kimura et al. (30) investigated the emulsifying properties of pure 7S and 11S fractions of different legumes at the different pH and ionic strength. These authors showed that 7S fraction of pea had a slightly lower emulsifying ability and stability than 7S fraction of other legumes, whereas no significant differences were observed in the case of 11S globulins.

Several researchers compared the emulsifying properties of pea and soy protein isolates and opposite results were obtained. Earlier work of McWatters and Cherry (52) showed that the emulsifying properties of pea protein are minor compared to soy protein, but it is still able to produce both semi-thick and thick mayonnaise-like emulsions at different pH values. Vose (53) reported that pea isolate had similar or better emulsifying properties

than soy protein isolates. Also, Tömösközi et al. (46) found that pea isolates had quite good emulsifying capacity but low emulsion stability in comparison to soy protein isolate. Aluko et al. (45) and Adebisi and Aluko (54) showed that pea protein isolate had better emulsifying capacity than soy protein isolate when emulsions were prepared at different concentrations of isolate and at the pH 5.0 and 7.0. The better emulsifying capacity these authors attributed to the higher level of sugar in pea protein isolates than in soy protein isolates. Namely, a higher content of sugar may contribute to the increased protein solubility and emulsifying capacity. To avoid processing induced differences between soy and pea protein isolate, Barac et al. (15) compared these isolates prepared under the same conditions and showed that pea isolates in general had slightly lower emulsifying properties than those of soybean. However, they were quite usable in the food industry. Furthermore, this investigation clearly showed that the comparison of protein isolates from different species, even if they are prepared and used under the same conditions is difficult, as it is related to the selection of genotypes within species.

Foaming properties

In food systems (such as in baked goods, sweets and desserts), proteins function as foam-forming and foam-stabilizing components. Different proteins have different abilities to form and stabilize foams, and just as in the case of proteins and their different emulsifying properties, this is related to the different physico-chemical properties of the proteins. (6, 15, 55). The ideal foam-forming and foam-stabilizing protein is characterized by a low molecular weight, high surface hydrophobicity, good solubility, a small net charge in terms of the pH of the food, and easy denaturability (42). Foaming properties of proteins are usually characterized as foaming capacity (FC) and foaming stability (FS). FC is measured in volume (%) when whipped, while the volume of the foam over time (normally 0-30 min) gives the protein's FS (8).

Several authors investigated foam properties of pea protein isolates (6, 11, 55-57). According to these investigations, foaming properties of pea isolates are pH- and concentration-dependents. Furthermore, protein level and protein composition of starting seed, processing method used for their production affect foaming properties of pea protein products (7, 8, 20, 57, 47, 55).

Aluko et al. (45) compared foaming properties of soy and pea protein isolates. They showed that pea protein isolates were foaming agent with a more flexible polypeptide conformation at the pH 3.0 and 7.0 when compared to soy protein isolate. Similar observation was reported by Sosulski et al (14), whereas Tömösközi et al. (46) showed poorer foaming ability of pea protein isolate when compared to soy protein isolate. The opposite results of these authors could be attributed to numerous factors including processing conditions and different protein composition of the investigated isolates. To avoid the influence of processing conditions, Barac et al. (15) compared foaming properties of native and thermally treated soy and pea protein isolates prepared under the same conditions. They reported that pea protein isolates had slightly lower foam activity than soy protein isolates in a wide range of pH (3.0-8.0), but foams formed with pea protein isolates at the investigated pHs were more stable.

Gelling properties

Gel is a dispersed system of at least two components in which dispersant forms a cohesive network. It is characterized by the lack of fluidity and elastic deformability. Globular proteins, such as legume proteins, under specific conditions (after heating and denaturation), can form gel. Usually, this type of gel is characterized as aggregated dispersion (42). Namely, after the denaturation and further heating, the proteins will aggregate and interact with other proteins and form either a gel or a coagulum. Which type will be formed it depends on the conditions such as molecular weight, heating time and protein concentration (58). Gel formation is complicated and affected by the concentration of protein, amount of water, ionic strength, time and temperature, as well as by the pH and interaction with other components in the food system (58). These process conditions can be manipulated for gel formation.

Only a few authors investigated gelling properties of pure pea proteins and pea isolates. Shand et al (59) showed that both globulins and albumins of pea protein isolates contribute to gel formation. Studies on the gelation properties of mixed pea globulins, vicilin and legumin have been reported by Bora et al. (38) and O’Kane et al. (31, 1). It was found by Bora et al. (38) that pea globulin underwent heat-induced gelation, whereas pure legumin did not gel under the same conditions. According to these authors, the relationship between protein (globulin) concentration and log gel hardness was linear. Furthermore, at all protein concentrations studied, as proportion of legumin decreased, the gel hardness increased. In contrast to their findings, O’Kane et al. (1) and O’Kane (39) indicated that both pea vicilin and legumin could form gels. This was probably caused by a difference in pea cultivars since O’Kane et al. (1) indicated that the contribution of legumin to the pea protein gels was cultivar specific and related to its disulphide bonding ability rather than the absolute amount of legumin protein present. Furthermore, these authors showed that the third pea globulin can hinder the gel formation of pea protein isolates when present in sufficient quantity. In large amounts, this protein increases the minimum gelling concentration of purified pea proteins at a near-neutral pH, and causes formation of transparent heat-induced gels. This behaviour was attributed to the repulsive forces on the N-terminal extension region at a near-neutral pH, and was supported by the fact that no difference in the gelation behaviour of vicilin and convicilin fractions was observed at low pH values, where the repulsive charges would have been neutralised.

Most of the previously cited investigations were based on isolates prepared by isoelectric precipitation. Sun and Arntfield (12) showed that processing conditions significantly changed gelling properties of pea protein isolates. These authors investigated the heat-induced gelation properties of salt-extracted pea protein. They showed that the salt-extracted and freeze dried isolates formed gel at much lower concentrations than those prepared by isoelectric precipitation and spray drying. The minimum gelation concentration of salt-extracted pea protein isolate was 5.5%, while that of commercial pea protein isolate was 14.5%. Furthermore, Taherian et al. (10) showed that gelling temperatures of pea isolates prepared by water and KCl extraction and subsequent diafiltration at the pH 6.0 trimmed down to $75.7 \pm 0.63^\circ\text{C}$ and $81.6 \pm 0.55^\circ\text{C}$, in contrast to that of commercial isolate at above 90°C . Similarly, the formation of firm gels, after 1 h of heating at

90°C, was associated with membrane processed isolates, whereas commercial isolates did not develop any gel.

Pea protein form weak, heat-induced gels. The gelation of pea protein is temperature-dependent, and primarily influenced by the degree of protein denaturation. If the degree of denaturation is lower, a stronger gel is formed. Protein concentration also plays an important role in gelation properties. Higher concentrations generally produce stronger gels.

However, the gelling point was concentration independent. Heating and cooling rates are minor factors influencing the gelation properties of pea protein. The heating rate influenced the gelling point in the way that higher heating rates resulted in delayed gelling (higher gelling temperatures). Higher heating and cooling rates caused a weakening effect on gel elasticity.

O'Kane et al., (1) and Shand et al. (59) compared gelling properties of pea and soy protein isolates. Both groups of authors concluded that pea protein isolates formed more unstructured gel than soy protein isolates and thus their gelling properties are not that as good as those of soy. For example, Shand et al (59) showed that the optimal conditions for formation of strong heat-induced gels from the pea isolate were 19.6% (w/w) protein content, pH 7.1, 2.0% (w/w) NaCl, and heating at 93°C. The gels prepared with soy protein isolates under the same conditions were stronger and more elastic than those prepared with pea protein isolates. However, Nunes et al. (60), by studying pea protein as a replacer of dairy and egg proteins in a gelled vegetable dessert showed that pea proteins produced good gels that were highly applicable as a food product.

LIMITED PROTEOLYSIS AS A METHOD FOR IMPROVEMENT OF TECHNO-FUNCTIONAL PROPERTIES OF PEA PROTEIN ISOLATES

Techno-functional properties of pea protein isolates can be improved by chemical, physical and enzymatic treatments. From the standpoint of safety, the most appropriate method for modification of legume protein properties is limited proteolysis (61). Peptides produced by partial proteolysis have smaller molecular size and less compact structure than the original proteins. Such peptides contribute to the improvement of techno-functional properties compared to those of the native proteins (60). To obtain desirable techno-functional properties of pea protein hydrolysates, hydrolysis must be done under strictly controlled conditions to a specified degree of hydrolysis (DH). A limited DH usually improves solubility, as well as emulsifying and foaming capacities, whereas excessive hydrolysis often causes decline in some of these functionalities (62, 63, 44).

Partial enzymatic hydrolysis of plant proteins has been the subject of extensive research by various authors. Most of these studies have been conducted on soy protein products, including soy flour, concentrates and isolates (63-67). Less attention has been paid to pea proteins (44, 69-72). These studies have been conducted on pure proteins and pea isolates and showed that, as well as in the case of soybean proteins, 7S and 11S protein expressed different susceptibility to the enzyme-induced hydrolysis (70,73-75). Proteases preferentially hydrolyze vicilin over legumin (75). This is due to their different structures; the compact structure of legumin makes it difficult protease to act. Braudo et al. (77) compared susceptibility of pea legumin and soy glycinin and concluded that pea 11S

protein was more resistant to proteolysis than soy 11S protein. The differences between these two proteins were attributed to the differences in their primary structures.

In most of the studies reported in the literature, commercial proteases, such as trypsin, alcalase, papain and chymosin have been used for pea protein hydrolysis. In general, these investigations showed that the hydrolysis up to 10% significantly improved solubility, foaming, emulsifying and other properties. For example, the hydrolyzates (characterized with DH of 8%) prepared with trypsin had improved solubility, especially in the range of pH of 4-7 which was 90-98.6% (78). Furthermore, a linear dependence between the degree of hydrolysis and solubility of pea protein hydrolysates were registered. The later work of Huminski and Aluko (71) showed that trypsin isolates with higher DH values (18.28%) had better emulsifying properties than pea protein hydrolyzates obtained with papain, α -chymotrypsin, Alcalase and Flavourzyme. However, most of these studies were focused on the relationship between the action of one or several proteases and techno-functional properties of commercial or laboratory-prepared isolates of one variety. The influence of protein composition in the initial isolate on these properties was less investigated. Barac et al. (44) compared techno-functional properties of pea isolates from two different genotypes and those of modified with two different proteases (*Streptomyces griseus* protease and papain). They suggested that proper selection of pea variety (besides other factors) could result in the production of enzymatically-modified pea protein isolates with excellent functional properties.

CONCLUSION

This paper clearly showed that pea protein isolates can be a very useful substituent for soy protein products as techno-functional additives. Pea protein isolates could find application in a wide range of food products, but their proper selection and preparation conditions could be of great importance. Furthermore, the studies reported in the current literature suggest that physico-chemical properties of pea proteins could be extensively improved, and enzymatic hydrolysis is a good tool to achieve this.

Acknowledgement

The authors acknowledge financial support the Ministry of Education, Science and Technological Development of the Republic of Serbia, TR-31069, 2011-2015.

REFERENCES

1. O'Kane, F. E.; Vereijken, J. M.; Gruppen, H.: Van Boekel M. A. J. S. Gelation behavior of protein isolates extracted from 5 cultivars of *Pisum sativum* L. *J. Food Sci.* **2005**, *70*, 132-137.
2. Gwiazda, S.; Rutkowski, A.; Kocoń, J. Some functional properties of pea and soy bean protein preparations. *Nahrung* **1979**, *23*, 681-686.

3. San Ireneo, M.; Ibáñez Sandín, M.D; Fernández-Caldas, E.; Marañón Lizana, F.; Rosales Fletes, M.J., Laso Borrego, M.T. Specific IgE levels to *Cicer arietinum* (Chick pea) in tolerant and nontolerant children: evaluation of boiled and raw extracts. *Int. Arch. Allergy Imm.* **2000**, *121*, 137-143.
4. Karaca, A.C.; Low N.; Nickerson, M. Emulsifying properties of chickpea, faba bean, lentil and pea proteins produced by isoelectric precipitation and salt extraction. *Food Res Int.* **2011**, *44*, 2742-2750.
5. Aluko, R.E.; Mofolasayo, O.A.; Watts, B.M. Emulsifying and foaming properties of commercial yellow pea (*Pisum sativum* L.) seed flours. *J. Agric. Food Chem.* **2009**, *57*, 9793-9800.
6. Barac, M.; Cabrilo, S.; Pesic, M., Stanojevic, S.; Ristic, N. Profile and functional properties of seed proteins from six pea (*Pisum sativum*) genotypes. *Int. J. Mol. Sci.* **2010**, *11*, 4973-4990.
7. Boye, J.I.; Aksay, S.; Roufik, S.; Ribéreau, S.; Mondor, M.; Farnworth, E.; Rajamohamed, S.H. Comparison of the functional properties of pea, chickpea and lentil protein concentrates processed using ultrafiltration and isoelectric precipitation techniques. *Food Res. Int.* **2010a**, *43*, 537-546.
8. Boye, J.; Zare, F.; Pletch, A. Pulse proteins: processing, characterization, functional properties and applications in food and feed. *Food Res Int.* **2010b**, *43*, 414-431.
9. Adebisi, A.P.; Aluko, R.E. Functional properties of protein fractions obtained from commercial yellow field pea (*Pisum sativum* L.) seed protein isolate. *Food Chem.* **2011**, *128*, 902-908.
10. Taherian, A.R.; Mondor, M.; Labranche, J.; Drolet, H.; Ippersiel, D.; Lamarche, F. Comparative study of functional properties of commercial and membrane processed yellow pea protein isolates. *Food Res. Int.* **2011**, *44*, 2505-2514.
11. Fernandez-Quintela A.; Macarulla, M.T.; Del Barrio, A.S.; Martinez, J.A. Composition and functional properties of protein isolates obtained from commercial legumes grown in northern Spain. *Plant Foods Hum. Nutr.* **1997**, *51*, 331-342.
12. Sun, X.D.; Arntfield, S.D. Gelation properties of salt-extracted pea protein induced by heat treatment. *Food Res. Int.* **2010**, *43*, 509-515.
13. Sumner, A.K.; Nielsen M.A.; Youngs, C.G. Production and evaluation of pea protein isolate. *J Food Sci.* **1981**, *46*, 364-372.
14. Sosulski, F.W.; McCurdy, A.R. Functionality of flours, protein fractions and isolates from field peas and bean. *J. Food Sci.* **1987**, *52*, 1010-1014.
15. Barac, M.B.; Pesic, M.B.; Stanojevic, S.P.; Kostic, A.Z.; Bivolarevic, V. Comparative study of the functional properties of three legume seed isolates: adzuki, pea and soy bean. *J. Food Sci. Technol.* **2014**, in press, DOI 10.1007/s13197-014-1298-6.
16. Maninder, K.; Sandhu, K.S.; Singh N. Comparative study of the functional, thermal and pasting properties of flours from different field pea (*Pisum sativum* L.) and pigeon pea (*Cajanus cajan* L.) cultivars. *Food Chem.* **2007**, *104*, 259-267.
17. Barac, M.; Cabrilo, S.; Pesic, M.; Stanojevic, S.; Pavlicevic, M.; Macej, O.; Ristic, N. Functional properties of pea (*Pisum sativum*, L) protein isolates modified with chymosin. *Int. J. Mol. Sci.* **2011**, *12*, 8372-8387.

18. Periago, M.J.; Vidal, M.L.; Ros, G.; Rincón, F.; Martínez, C.; López, G., Rodrigo, J.; Martínez, I. Influence of enzymatic treatment on the nutritional and functional properties of pea flour. *Food Chem.* **1998**, *63*, 71-78.
19. Fuhrmeister, H.; Meuser, F. Impact of processing on functional properties of protein products from wrinkled peas. *J. Food Eng.* **2003**, *56*, 119-129.
20. Dua S.; Mahajan, A.; Sandal Gagan, M. Physico-chemical properties of defatted pea seed meal proteins with emphasis on salts and pH. *J. Food Sci. Tech.* **2009**, *46*, 251-254.
21. Tsoukala, A.; Papalamprou, E.; Makri, E.; Doxastakis, G.; Braudo, E.E. Adsorption at the air-water interface and emulsification properties of grain legume protein derivatives from pea and broad bean. *Colloids Surf. B* **2006**, *53*, 203-208.
22. Tzitzikas, E.N.; Vincken, J.P.; De Groot, J.; Gruppen, H.; Visser, R.G.F. Genetic variation in pea seed globulin composition. *J. Agric. Food Chem.* **2006**, *54*, 425-433.
23. Owusu- Anseh, Y. J.; McCurdy S.M. Pea Proteins: A review of chemistry, technology of production, and utilization. *Food Rev. Int.* **1991**, *7*, 103-134.
24. Schwenke, K. D.; Henning, T.; Dudek, S.; Dautzenberg, H.; Danilenko, A. N.; Kozhevnikov, G. O.; Braudo, E. E. Limited tryptic hydrolysis of pea legumin: molecular mass and conformational stability of legumin-T. *Int.l J. Biol. Macromol.* **2001**, *28*, 175-182.
25. Gueguen, J.C.M.; Barbot J.; Schaeffer F. Dissociation and aggregation of pea legumin induced by pH and ionic strength. *J. Sci. Food Agric.* **1988**, *53*, 167-182.
26. Heng, L.; Van Koningsveld, G.A.; Gruppen, H.; Van Boekel, M.A.J.S.; Vincken J.P.; Roozen, J.P.; Voragen, A.G.J. Protein-flavour interactions in relation to development of novel protein foods. *Trends Food Sci. Technol.* **2004**, *15*, 217-224.
27. Shewry, P. R.; Napier, J. A.; Tatham, A. S. Seed storage proteins: Structures and biosynthesis. *Plant Cell* **1995**, *7*, 945-956.
28. Griga, M.; Horáček, J.; Klenotičová, H. Protein patterns associated with *Pisum sativum* somatic embryogenesis. *Biol. Plantarum* **2007**, *51*, 201-211.
29. Casey, R.; Domoney, C. The biochemical genetics of pea seed storage proteins. *Kulturpflanze* **1984**, *32*, S99-S108.
30. Kimura, A.; Fukuda, T.; Zhang, M.; Motoyama, S.; Maruyama, N.; Utsumi S. Comparison of physicochemical properties of 7S and 11S globulins from pea, fava bean, cowpea, and French Bean with those of Soybean. French Bean 7S globulin exhibits excellent properties. *J. Agric. Food Chem.* **2008**, *56*, 10273-10279.
31. O'Kane, F.E.; Happe, R.P.; Vereijken, J.M.; Gruppen, H.; Van Boekel, M.A.J.S. Characterization of pea vicilin. 1. Denoting convicilin as the α -subunit of the pisum vicilin family. *J. Agric. Food Chem.* **2004**, *52*, 3141-3148.
32. Guleria, S.; Dua, S.; Chongtham, N. Analysis of variability in different genotypes of pea (*Pisum sativum* L.) on the basis of protein markers. *Legume Res.* **2009**, *32*, 265-269.
33. Wang, N.; Hatcher, D. W.; Warkentin, T. D.; Toews, R. Effect of cultivar and environment on physicochemical and cooking characteristics of field pea (*Pisum sativum*). *Food Chem.* **2010** *118*, 109-115.

34. Nikolopoulou, D.; Grigorakis, K.; Stasini, M.; Alexis, M. N.; Iliadis, K. Differences in chemical composition of field pea (*Pisum sativum*) cultivars: Effects of cultivation area and year. *Food Chem.* **2007**, *103*, 847-852.
35. Schroeder, H.E: Quantitative studies on the cotyledonary proteins in the genus *Pisum*. *J. Agric. Food Chem.* **1982**, *33*, 623-633.
36. Cserhalmi, Z.; Czukor, B.; Gajzágó-Schuster, I. Emulsifying properties, surface hydrophobicity and thermal denaturation of pea protein fractions. *Acta Aliment. Hung.* **1998**, *27*, 357-363.
37. Rangel, A.; Domont, G.B.; Pedrosa, C.; Ferreira, S.T. Functional properties of purified vicilins from cowpea (*Vigna unguiculata*) and pea (*Pisum sativum*) and cowpea protein isolate. *J. Agric. Food Chem.* **2003**, *51*, 5792-5797.
38. Bora, S.P.; Breeke, J.C.; Powers, R.J. Heat induced gelation of peas (*Pisum sativum*) mixed globulins, vicilin and legumin. *J. Food Sci.* **1994**, *59*(3), 594-596.
39. O'Kane, E.: O'Kane, E. Molecular Characterisation and Heat-Induced Gellation of Pea Vicilin and Legumin. Ph.D. Thesis, Wageningen University, November 2004.
40. Gueguen, J.; Cerletti, P. Protein of some legume seeds: soybean, pea, fababean and lupin. In *Developments in food proteins*; Hudson, B. J. Ed.; Elsevier Applied Science: London, 1994; pp 145-156.
41. Kinsella J.E.: Relationships between structure and functional properties of food proteins. In *Food proteins*; Fox, P.F., Condon, J.J. Eds.; Applied Science Publishers LT: England, 1982; pp 51-78.
42. Belitz, H.D.; Grosch, W.; Schieberle, P. *Food Chemistry*, Springer-Verlag, Berlin, 2009; pp 65- 95.
43. Pesic, M.B.; Vucelic-Radovic, B.V.; Barac, M.B.; Stanojevic, S.P. The influence of genotypic variation in protein composition on emulsifying properties of soy proteins. *J. Am. Oil Chem. Soc.* **2005**, *82*, 667-672.
44. Barac, M.; Cabrilo, S.; Stanojevic, S.; Pesic, M.; Pavlicevic, M.; Zlatkovic, B.; Jankovic M. Functional properties of protein hydrolysates from pea (*Pisum sativum*, L.) seeds. *Int. J. Food Sci. Technol.* **2012**, *47*, 1457-1467.
45. Aluko, R.E.; Mofolasayo, O.A.; Watts, B.M. Emulsifying and foaming properties of commercial yellow pea (*Pisum sativum* L.) seed flours. *J. Agric. Food Chem.* **2009**, *57*, 9793-9800.
46. Tömösközi, S.; Lásztity, R.; Haraszi, R.; Baticz O. Isolation and study of the functional properties of pea proteins. *Nahrung* **2001**, *45*, 399-401.
47. Ferreira, R.B.; Franco, E.; Teixeira, A.R. Calcium- and magnesium-dependent aggregation of legume seed storage proteins. *J. Agric. Food Chem.* **1999**, *47*, 3009-3015.
48. Yan, B.; Ren, J.; Zhao, M.; Luo, D.; Gu, L. Effects of limited enzymatic hydrolysis with pepsin and high-pressure homogenization on the functional properties of soybean protein isolate. *LWT- Food Sci. Technol.* **2012**, *46*, 453-459.
49. Habiba, R.A. Changes in anti-nutrients, protein solubility, digestibility, and HCl-extractability of ash and phosphorus in vegetable peas as affected by cooking methods. *Food Chem.* **2002**, *77*, 187-192.
50. Dagorn-Scaviner, C.; Gueguen, J.; Lefebvre J. Emulsifying properties of pea globulins as related to their adsorption behaviours. *J. Food Sci.* **1987**, *52*, 335-341.

51. Gharsallaoui, A.; Cases, E.; Chambin O.; Saurel R. Interfacial and emulsifying characteristics of acid-treated pea protein. *Food Biophys.* **2009**, *4*, 273-280.
52. McWaters, K.H.; Cherry, J.P. Emulsification, foaming and protein stability properties of defatted soybean, peanut, field pea and pecan flours. *J.Food Sci.* **1977**, *42*, 444-461.
53. Vose, J. R. Production and functionality of starches and protein isolates from legume seeds (field peas and horsebeans). *Cereal Chem.* **1980**, *57*, 406-410.
54. Adebisi, A.P.; Aluko, R.E. Functional properties of protein fractions obtained from commercial yellow field pea (*Pisum Sativum L.*) seed protein isolate. *Food Chem.* **2011**, *128*, 902-908.
55. Fuhrmeister, H.; Meuser, F. Impact of processing on functional properties of protein products from wrinkled peas. *J. Food Eng.* **2003**, *56*, 119-129.
56. Toews, R.; Wang N. Physicochemical and functional properties of protein concentrate from pulses. *Food Res. Int.* **2013**, *52*, 445-451.
57. Pedrosa, C.; Trisciuzzi, C.; Ferreira, S.T. Effects of glycosylation on functional properties of vicilin, the 7S storage globulin from pea (*Pisum sativum*). *J. Agric. Food Chem.* **1997**, *45*, 2025-2030.
58. Raikos, V.; Campbell, L.; Euston, S.R. Rheology and texture of hen's egg protein heat-set gels as affected by pH and the addition of sugar and/or salt. *Food Hydrocolloids* **2007**, *21*, 237-244.
59. Shand, P.J.; Ya, H.; Pietrasik, Z.; Wanasundara, P.K.J.P.D. Physicochemical and textural properties of heat-induced pea protein isolate gels. *Food Chem.* **2007**, *102*, 1119-1130.
60. Nunes, M. C.; Raymundo, A.; Sousa, I. Gelled vegetable desserts containing pea protein, K-carrageenan and starch. *Eur. Food Res. Technol.* **2006**, *222*, 622-628.
61. Barać, M.; Stanojević, S.; Jovanović, S.; Pešić M. Soy protein modification - A review. *APTEFF* **2004**, *35*, 3-17.
62. Adler-Nissen J. Some fundamental aspects of food protein hydrolysis. In *Enzymatic hydrolysis of food proteins*; Adler-Nissen, J. Ed; Elsevier Applied Science: London, 1986; pp 9-24.
63. Wu, W.; Hettiarachchy, N.; Qi, M. Hydrophobicity, solubility, and emulsifying properties of soy protein peptides prepared by papain modification and ultrafiltration. *J. Am. Oil Chem. Soc.* **1998**, *75*, 845-850.
64. Martinez, K. D.; Carrera Sanchez, C.; Rodriguez Patino, J. M.; Pilosof, A. M. R. Interfacial and foaming properties of soy protein and their hydrolysates. *Food Hydrocolloids* **2009**, *23*, 2149-2157.
65. Chen, L.; Chen, J.; Ren, J.; Zhao, M. Effects of ultrasound pretreatment on the enzymatic hydrolysis of soy protein isolates and on the emulsifying properties of hydrolysates. *J. Agric. Food Chem.* **2011**, *59*, 2600-2609.
66. Hou, Y.; Zhao, X. H. Limited hydrolysis of two soybean protein products with trypsin or neutrase and the impacts on their solubility, gelation and fat absorption capacity. *Biotechnology* **2011**, *10*, 190-196.
67. Jung, S.; Murphy, P. A.; Johnson, L. A. Physicochemical and functional properties of soy protein substrates modified by low levels of protease hydrolysis. *J. Food Sci.* **2005**, *70*, C180-C187.

68. Molina Ortiz, S.; Cristina A.N.M. Analysis of products, mechanisms of reaction, and some functional properties of soy protein hydrolysates. *J. Am. Oil Chem. Soc.* **2000**, *77*, 1293-1301.
69. Periago, M.J.; Vidal, M.L.; Ros, G.; Rincón, F.; Martínez, C.; López, G.; Rodrigo, J.; Martínez I. Influence of enzymatic treatment on the nutritional and functional properties of pea flour. *Food Chem.* **1998**, *63*, 71-78.
70. Le Gall, M., Gueguen, J.; Seve, B.; Quillien, L. Effects of Grinding and thermal treatments on hydrolysis susceptibility of pea proteins (*Pisum sativum L.*). *J. Agri. Food Chem.* **2005**, *53*, 3057-3064.
71. Humiski, L. M.; Aluko, R. E. Physicochemical and bitterness properties of enzymatic pea protein hydrolysates. *J. Food Sci.* **2007**, *72*, S605-S611.
72. Pownall, T. L.; Udenigwe, C. C.; Aluko, R. E. Amino acid composition and antioxidant properties of pea seed (*Pisum sativum L.*) enzymatic protein hydrolysate fractions. *J. Agri. Food Chem.* **2010**, *58*, 4712-4718.
73. Spencer, D.; Higgins, T.J.V.; Preer M.; Dove, H.; Coombe J.B. Monitoring the fate of dietary proteins in rumen fluid using gel electrophoresis. *Br. J. Nutr.* **1988**, *60*, 241-247.
74. Crévieu, I.; Carré, B.; Chagneau, A.M.; Quillien, L.; Guéguen, J.; Bérot, S. Identification of resistant pea (*Pisum stivum L.*) proteins in the digestive tract of chickens. *J. Agric. Food Chem.* **1997**, *45*, 1295-1300.
75. Gabriel, I.; Quillien, L.; Cassecuelle, F.; Marget, P.H.; Juin, H.; Lessire, M.; Sève, B.; Duc, G.; Burstin, J. Variation in seed protein digestion of different pea (*Pisum sativum L.*) genotypes by cecectomized broiler chickens: 2. Relation between in vivo protein digestibility and pea seed characteristics, and identification of resistant pea polypeptides. *Livest. Sci.* **2008**, *113*, 262-273.
76. Govindaraju, K.; Srinivas, H. Controlled enzymatic hydrolysis of glycinin: usceptibility of acidic and basic subunits to proteolytic enzymes. *LWT – Food Sci. Technol.* **2007**, *40*, 1056-1065.
77. Braudo, E.E.; Danilenko, A.N.; Guslyannikov, P.V.; Kozhevnikov, G.O.; Artykova, G.P.; Lapteva, N.A.; Vaintraub, I.A.; Sironi, E.; Duranti, M. Comparative effects of limited tryptic hydrolysis on physicochemical and structural features of seed 11S globulins, *Int. J. Biol. Macromol.* **2006**, *39*, 174-178.
78. Soral-Smietena, M.; Swigon, A.; Amarowicz, R.; Sijtsma, J. The solubility of trypsin pea hydrolysates. *Nahrung* **1998**, *42*, 217-218.

ТЕХНО-ФУНКЦИОНАЛНЕ ОСОБИНЕ ИЗОЛАТА ПРОТЕИНА ГРАШКА

Мирољуб Б. Бараћ¹, Мирјана Б. Пешић¹, Слађана П. Станојевић¹, Александар Ж. Костић¹, Славица Б. Чабрило²

¹ Универзитет у Београду, Пољопривредни факултет, Немањина 6, 11080 Београд-Земун, Србија

² Виша техничка школа струковних студија, Немањина 2, 12000 Пожаревац, Србија

Захваљујући високој нутритивној вредности, добрим техно-функционалним карактеристикама и ниској цени, протеини легуминоза постају најприхватљивија алтернатива за протеинске производе анималног порекла. У индустрији хране ови производи најчешће се користе као техно-функционални адитиви којима се обезбеђује нека од карактеристика финалног производа. Протеини легуминоза најчешће се користе као протеинска брашна, концентрати и изолати. У индустријским размерама највећу примену имају протеини соје и у знатно мањој мери, у последњих 20 година, протеински изолати грашка. Ређа употреба протеина грашка делом је последица још увек недовољно информација о њиховим техно-функционалним карактеристикама. Овај рад представља преглед техно-функционалних карактеристика протеина грашка и његових изолата. Такође, у овом раду разматра се и делимична протеолиза као метод за побољшање техно-функционалних карактеристика протеина грашка.

Кључне речи: протеински изолати грашка, техно-функционалне карактеристике, ограничена протеолиза

Received: 9 February 2015.

Accepted: 15 July 2015.

REDUCTION OF CYANOGENIC GLYCOSIDES BY EXTRUSION - INFLUENCE OF TEMPERATURE AND MOISTURE CONTENT OF THE PROCESSED MATERIAL

Dušica S. Čolović*, Jovanka D. Lević, Radmilo R. Čolović, Ljubinko B. Lević,
Vojislav V. Banjac, Slađana M. Rakita, Olivera M. Đuragić

University of Novi Sad, Institute of Food Technology, Bulevar cara Lazara 1, 21000 Novi Sad, Serbia

The paper presents results of the investigation of the influence of extrusion temperature and moisture content of treated material on the reduction of cyanogenic glycosides (CGs) in linseed-based co-extrudate. CGs are the major limitation of the effective usage of linseed in animal nutrition. Hence, some technological process must be applied for detoxification of linseed before its application as a nutrient. Extrusion process has demonstrated several advantages in reducing the present CGs, since it combines the influences of heating, shearing, high pressure, mixing, etc. According to obtained results, the increase in both temperature and moisture content of the starting mixture decreased the content of CGs in the processed material. HCN content, as a measurement of GCs presence, ranged from 25.42 mg/kg, recorded at the moisture content of 11.5%, to 126 mg/kg, detected at the lowest moisture content of 7%. It seems that moisture content and temperature had the impact on HCN content of equal importance. However, the influence of extrusion parameters other than temperature and moisture content could not be neglected. Therefore, the impact of individual factors has to be tested together.

KEY WORDS: Linseed, cyanogenic glycosides, extrusion, temperature, moisture, HCN

INTRODUCTION

Over fifty countries all over the world cultivate linseed (*Linum usitatissimum*) as a commercial plant (1-3). It has been considered the third most productive oil crop, after sunflower and winter oilseed rape (4, 5). It yields seeds whose maturity occurs 30-60 days after flowering, and which are a rich source of both edible and non-edible oils (6, 7). In addition to a large amount of oil, linseed contains approximately 20-30% of crude protein (1, 8). Although linseed oil is mostly used in chemical industry, there has been a growing interest in its usage as a food or feed, due to the high concentration of linoleic (LA, 18:2, n-6) and especially α -linolenic acid (ALA, 18:3, n-3), representatives of omega-6 (n-6) and omega-3 (n-3) polyunsaturated fatty acids (PUFAs) (9, 10). Moreover, linseed is the richest oilseed source of ALA (11). Cereals and oilseeds, or meals commonly used in animal diet

* Corresponding author: Dušica S. Čolović, University of Novi Sad, Institute of Food Technology, Bulevar cara Lazara 1, 21000 Novi Sad, Serbia, e-mail: dusica.ivanov@fins.uns.ac.rs

predominantly contain low level of n-3 FAs (12). Therefore, intensive inclusion of linseed in animal nutrition could have significant role in the improvement of FA composition of feed.

The main limitation in the exploitation of linseed as a nutrient lies in the presence of antinutritive components, which are cyanogenic glycosides (CGs) and antivitamin B6 (linatine). Negative effect of antivitamin B6 can be eliminated by adding vitamin B6 to the diet (13), which cannot be said for CGs. CGs may be defined chemically as glycosides of the α -hydroxynitriles, and are secondary metabolites produced by plants. They are amino acid-derived plant constituents (14). The reason for their toxicity is the release of hydrogen cyanide (HCN) due to the action of a β -glucosidase enzyme (oxynitrilase), thus their level in food or feed is expressed through the content of HCN (mg) per kg of examined material.

Different heat treatments, such as autoclaving, pelleting, extrusion or microwave roasting are commonly used to reduce the content of CGs (15-17). Dry heating is not recommended because the detoxification is based only on deactivation of glucosidase. Consequently, CGs can be synthesised again after entering into animal gut, and HCN can be released under the action of enzymes of intestinal microflora. High temperature in combination with moisture intensifies the hydrolysis of CGs, which results in intensive removal of HCN (15). Extrusion has been considered a suitable process for the removal of HCN from the material, because it combines a number of different processes: grinding, mixing, heating under high pressure in the presence of moisture, friction and shearing. However, the extrusion of oilseeds, such as linseed, is difficult to achieve due to the lubrication and limited expansion of the produced extrudates. Another disadvantage which is the separation of the oil from the solid phase, thereby changing the nutritional composition of produced extrudate, as is the case with the extrusion (17). In order to overcome the aforementioned problem, oil crops are often added to another raw material, usually a protein component, which shows good ability of oil adsorption, such as pea or sunflower meal (18-20).

Bearing in mind all the above, the aim of the present study was to find out how extrusion parameters affect temperature changes in the extruder barrel, and furthermore to examine the influence of the process temperature on reduction of CGs in linseed-sunflower meal co-extrudate. Since the presence of moisture highly influences CGs decomposition, three levels of moisture content of starting material were applied.

EXPERIMENTAL

Material

Linseed and sunflower meal used for production of co-extrudate originated from Serbia. Linseed indigenous sort "Ljupko" was cultivated in the valley of the river Beli Timok (South-Eastern Serbia). Before processing, linseed was cleaned and impurities were removed. Sunflower meal was produced in the local oil factory in Vojvodina (northern Serbian province), and it contained approximately 38% of protein expressed on dry matter (d.m.).

Extrusion process

All materials were milled on a laboratory hammer mill (ABC Engineering, Serbia) with sieve openings of 4 mm. The two components were mixed in 50:50 (w/w) ratio in double-

shaft paddle mixer - steam conditioner (Muyang SLHSJ0.2A, China). Water and steam were added into material during conditioning, in order to adjust the initial moisture content of the mixture at a desired level. Extrusion of the mixture was done on a single screw extruder (OEE 8, AMANDUS KAHL GmbH & Co., KG Germany), with the L/D ratio 8.5:1. The extrusion parameters were set according to the levels determined in the applied experimental design. The extruded product was dried in a fluid bed dryer/cooler (FB 500x200, AMANDUS KAHL GmbH & Co., KG Germany) for 10 minutes at the temperature of 25°C, and a material flow rate of 18 kg/h.

Determination of HCN in the co-extrudate

The determination of HCN was performed according to AOAC official method 915.03, part B, (alkaline titration method). Silver nitrate (AgNO₃) standard solution was used for titration. The volume of AgNO₃ standard solution consumed during the titration was recorded (21). Equation (1) was used to calculate the HCN content in the sample:

$$X = C \times V \times 54 \times \frac{\text{dilution}}{\text{aliquot}} \times \frac{1000}{m} \quad [1]$$

where *X* is the content of cyanide (including HCN) in the sample (mg/kg); *m* is the mass of the sample (g); *C* is the concentration of the AgNO₃ standard solution (mol/L); and *V* is the consumed volume of the AgNO₃ standard solution (mL).

All measurements were done in triplicate.

Experimental design, temperature measurement and statistical analysis

The effects of the following extrusion parameters on the temperature in the extruder barrel were examined: extrusion screw speed, moisture content of the starting mixture, feeding rate and total area of the die openings. The experiment was planned according to the Box-Behnken experimental design. The levels of independent parameters applied in the experiment are shown in Table 1.

Table 1. Independent process variables and their levels

Independent variable	Variable level		
	-1	0	1
Moisture content of the starting mixture (%)	7	11.5	16
Extrusion screw speed (rpm)	240	390	540
Feeding rate (kg/h)	16	24	32
Total area of the die openings (mm ²)	19.8	39.6	59.4

For monitoring the temperature in the extruder barrel, temperature contact sensors were used (produced by the Institute of Microelectronic Technologies and Single Crystals, Serbia). Temperature was monitored at the point just next to the die, at the end of the extruder barrel in seven replications.

STATISTICA software version 12 (Statsoft, Tulsa, OK, USA) was used to analyze variations (analysis of variance – ANOVA) and for Tukey’s HSD comparison of the means of measured temperatures and HCN content in the co-extrudates. Differences among means with the probability $p \leq 0.05$ were accepted as indicators of statistically significant differences, and the differences among means with $0.05 \leq p \leq 0.10$ were accepted as indicators of differentiating tendencies.

RESULTS AND DISCUSSION

The single screw extruder which was used in the experiment did not have the possibility of setting the temperature at a specific value. Thus, other extrusion parameters were varied, which indirectly affected the working temperature. Table 2 shows all temperatures measured in the experiment. As it can be seen, the process temperature ranged from 52.82 to 116.02°C.

Table 2. Influence of extrusion parameters on the temperature in the extruder barrel

Extrusion parameter				t (°C)
Moisture content of starting mixture (%)	Extrusion screw speed (rpm)	Feeding rate (kg/h)	Total area of the die openings (mm ²)	
11.5	240	32	39.6	57.52
11.5	540	32	39.6	73.33
11.5	240	16	39.6	71.38
11.5	540	16	39.6	73.94
11.5	390	24	39.6	75.18
11.5	390	24	39.6	74.03
11.5	390	24	39.6	74.60
16	390	24	19.8	53.16
16	240	24	39.6	63.80
16	540	24	39.6	68.54
16	390	32	39.6	58.99
16	390	16	39.6	52.82
16	390	24	59.4	70.23
11.5	390	16	19.8	82.50
11.5	390	32	19.8	79.18
11.5	540	24	19.8	79.16
11.5	240	24	19.8	78.00
11.5	390	16	59.4	84.93
11.5	390	32	59.4	70.38
11.5	240	24	59.4	67.75
11.5	540	24	59.4	76.53
7	390	24	19.8	113.14
7	240	24	39.6	104.51
7	540	24	39.6	114.39
7	390	32	39.6	111.18
7	390	16	39.6	116.02
7	390	24	59.4	109.81

As it is evident from the obtained results, the increase in the moisture content in the starting material resulted in a decrease of the temperature in the extruder barrel (Fig. 1 a), which was caused by lowering the viscosity of the material and its fast passage through the barrel of the extruder. The same trend was observed in the work of Abecassis et al.

(1994). According to their results, the increased moisture content of materials lowered the temperature, especially at the exit of the extruder barrel, while the effect was slightly lower in the extruder zone close to the entrance (22).

On the other hand, the increase of the extrusion screw speed increased the temperature, which was expected, since the increase in the extrusion screw speed influences intensification of the forces of shearing, torsion and friction, and consequently increase the working temperature (Fig. 1 b). The highest working temperatures at the constant intermediate levels of feeding rate and moisture content were achieved at the moisture content of 7% and extrusion screw speed of 540 rpm.

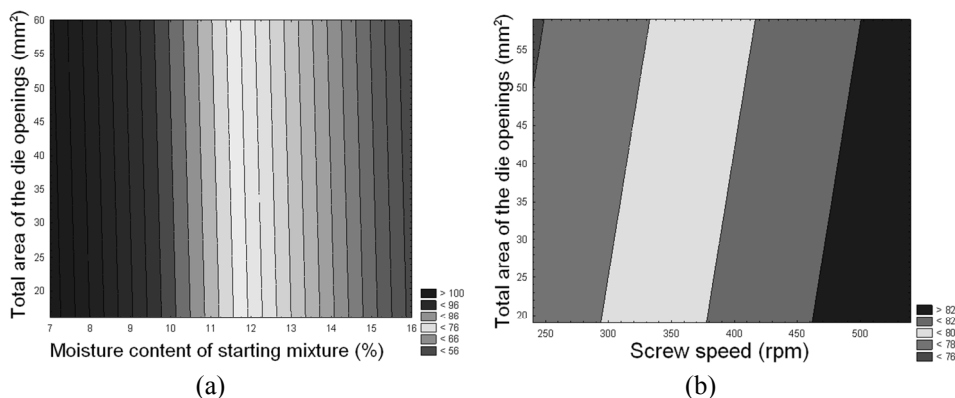


Figure 1. Influence of the process parameters on temperature in the extruder: moisture content of starting material and total area of the die openings (a); screw speed and total area of the die openings (b)

The lowest temperatures in the extruder barrel were achieved at the highest moisture content of 16% and the minimum feeding rate. In this case, the material remained shortly in the extruder and easily passed through the matrix, due to the compaction of the material and absence of the accumulation. Hence, the measured temperatures were low.

As already mentioned, high temperature in combination with the presence of moisture is the most important factor for the hydrolysis of CGs. Some authors have even reported that dry heat processing did not change the HCN content (23). This could be due to the fact that HCN formed after CGs hydrolysis remains in the linseed and its products, or deactivated glucosidase in the plant tissue could be replaced by the glucosidase formed by gut microflora (24). Effective linseed processing requires more than CGs hydrolysis and deactivation of glucosidase alone. Beneficial effects of the increased temperature combined with moisture remove permanently HCN from the material by evaporation (15, 18). The highest HCN content in the experiment (126 mg/kg) was recorded under conditions of the lowest moisture content of the starting material (7%) and temperature of 116.02°C, while the lowest content of HCN (25.42 mg/kg) was measured at the moisture content of 11% and temperature of 70.2°C. This temperature was recorded when an intermediate screw speed (390 rpm) and feeding rate (24 kg/h) were applied. Under such conditions,

the material remained in the extruder barrel long enough so that the temperature of approx. 70°C was sufficiently high to accelerate the hydrolysis of CGs.

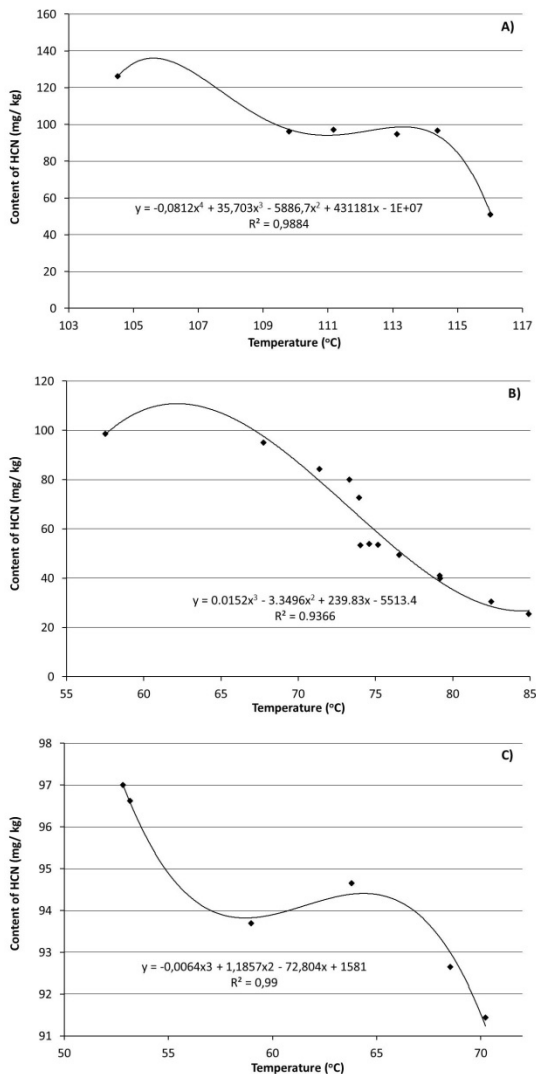


Figure 2. Influence of temperature on the HCN content in the co-extrudate at a constant moisture content of the starting material: 7% (A), 11.5% (B) and 16% (C)

Figure 2 shows the changes in the HCN content with increase in the temperature at the same level of moisture content of the starting material. The HCN content ranged from 50.99 to 126 mg/kg at the moisture content of 7%, from 25.42 to 98.46 mg/kg at the moisture content of 11.5%, and from 83.69 to 97 mg/kg at the moisture content of 16%.

Based on the obtained results it can be concluded that the HCN content decreased with the increase in temperature at constant moisture content. However, if we compare the results for the different moisture contents, no regularity can be seen. The reason for that could be that the other process parameters (pressure, friction, milling, etc.) influenced the CGs reduction. It also seems that the influences of temperature and moisture content of the material are equally important for the hydrolysis of CGs. Extrusion is considered to be very suitable for detoxification of linseed because of the simultaneous effect of several factors on the CGs. Milling and heating of the material in the presence of moisture accelerates the process of hydrolysis and the formation of HCN. After the decrease in the operating pressure at the exit of the material from the barrel of the extruder, the acid formed evaporates rapidly together with water. At the same time, the high pressure in the extruder barrel destroys molecules CGs, thereby preventing the release of HCN (15, 18).

CONCLUSION

The present study demonstrated how the temperature and content of moisture reduce the content of CGs in linseed-based product during the extrusion process. The highest HCN content in the experiment (126 mg/kg) was recorded at the lowest moisture content of the starting material (7%) and temperature of 116.02°C, while the lowest content of HCN (25.42 mg/kg) was measured at the moisture content of 11% and temperature of 70.2°C. It was found that the increase in the temperature decreased the HCN content, and that increased moisture content positively affected the HCN reduction. However, the effectiveness of the HCN reduction varied depending on several process factors. Since extrusion is a complex process, the impacts of individual factors cannot be considered independently from the influence of other process parameters.

Acknowledgement

The presented results are part of the Integrated and Interdisciplinary Research Project No. III 46012, funded by the Ministry of Education, Science. and Technological Development of the Republic of Serbia.

REFERENCES

1. Karlović, Đ.; Andrić, N. *Kontrola kvaliteta semena uljarica*. Tehnološki fakultet Novi Sad, Savezni zavod za standardizaciju, Beograd, Serbia, 1996.
2. Gabiana, C.P.: Gabiana, C.P. *Response of linseed (*Linum usitatissimum* L.) to irrigation, nitrogen and plant population*. MSc Thesis, Lincoln University, Canterbury, New Zealand, 2005.
3. Copur, O; Gur, M.; Karakus, M.; Demirel, U. Determination of correlation and path analysis among yield components and seed yield in oil flax varieties (*Linum usitatissimum* L.). *J. Biol. Sci.* **2006**, *6*, 738-743.
4. Aufhammer, W.; Wägner, W.; Kaul, H.-P.; Kübler, E. Radiation used by oilseed crops – a comparison of winter rape, linseed and sunflower. *J. Agron. Crop Sci.* **2000**, *184*, 277-286.

5. Zajač, T.; Olesky, A.; Stokłosa, A.; Klimek-Kopyra, A.; Kulig, B. The development competition and productivity of linseed and pea-cultivars grown in a pure sowing or in a mixture. *Eur. J. Agron.* **2013**, *44*, 21-33.
6. Rubilar, M.; Gutiérrez, C.; Verdugo, M.; Shene, C.; Sineiro, J. Flaxseed as a Source of Functional Ingredients. *J. Soil Sci. Plant Nutr.* **2010**, *10* (3), 373-377.
7. Matheson, E.M. *Vegetable Oil Seed Crops in Australia*; Holt, Rinehart & Winston, Sydney, Australia, 1976, pp. 111-121.
8. Ivanov, D.; Kokić, B.; Brlek, T.; Čolović, R.; Vukmirović, Đ.; Lević, J.; Sredanović, S. Effect of microwave heating on content of cyanogenic glycosides in linseed. *Ratarstvo i povrtarstvo* **2012**, *49*, 63-68.
9. Beare – Rogers, J.; Dieffenbacher, A.; Holm, J.V. Lexicon of lipid nutrition (IUPAC Technical report). *Pure Appl. Chem.* **2001**, *73* (4), 685-744.
10. Lukaszewicz, M.; Szopa, J.; Krasowska, A. Susceptibility of lipids from different flax cultivars to peroxidation and its lowering by added antioxidants. *Food Chem.* **2004**, *88*, 225-231.
11. Juárez, M.; Dugan, M. E. R.; Aldai, N.; Aalhus, J. L.; Patience, J.F.; Zijlstra R.; Beau-lieu A. D. Feeding co-extruded flaxseed to pigs: Effects of duration and feeding level on growth performance and backfat fatty acid composition of grower-finisher pigs. *Meat Sci.* **2010**, *84*, 578-584.
12. Csengeri, I. Dietary effects on fatty acid metabolism of common carp. *Arch. Anim. Nutr.* **1996**, *49* (1), 73-92.
13. Klosterman, H.J. Vitamin B6 antagonist of natural origin. *J. Agr. Food Chem.* **1974**, *22* (1), 13-16.
14. Vetter, J. Plant cyanogenic glycosides. *Toxicon* **2010**, *38*, 11-36.
15. Feng, D.; Shen, Y.; Chavez, E. Effectiveness of different processing methods in reducing hydrogen cyanide content of linseed. *J. Sci. Food Agr.* **2003**, *83*, 836-841.
16. Wu, M.; Li, D.; Zhou, Y.-G.; Brooks, M.S.-L.; Chen, X.D.; Mao, Z.H. Extrusion detoxification technique on linseed by uniform design optimization. *Sep. Purif. Tech.* **2008**, *61*, 51-59.
17. Ivanov, D.; Čolović, R.; Vukmirović, Đ.; Lević, J.; Kokić, B.; Lević, Lj.; Đuragić, O. Influence of process parameters on temperature profile and nitrogen solubility index of linseed co-extrudate, 1st International Symposium on Animal Science, Belgrade, 8-10. October, 2012, Book of papers, 511-515.
18. Čolović, D. Ispitivanje uticaja procesa ekstrudiranja na dobijanje i stabilnost funkcionalnog hraniva za životinje na bazi lanenog semena. Ph.D. Thesis, Univeristy of Novi Sad, June 2014.
19. Htoo, J.K.; Meng, X.; Patience, J.F.; Dugan, M.E; Zijlstra, R.T. Effects of coextrusion of linseed and field pea on the digestibility of energy, ether extract, fatty acids, protein, and amino acids in grower-finisher pigs. *J. Anim. Sci.*, **2008**, *86* (11), 2942-2951.
20. Thacker, P.A.; Racz, V.J.; Soita, H.W. Performance and carcass characteristics of growing-finishing pigs fed barley-based diets supplemented with Linpro (extruded whole linseed and peas) or soybean meal. *Can. J. Anim. Sci.* **2004**, *84* (4), 681-688.
21. AOAC (2000) In *Official Methods of Analysis, 17th edn.* Ed. W. Horwitz, AOAC Int, Arlington, VA, USA.

22. Abecassis, J.; Abbou, R.; Chaurand, M.; Morel, M.-H.; Vernoux, P. Influence of extrusion conditions on extrusion speed, temperature and pressure in the extruder and on pasta quality. *Cereal Chem.* **1994**, *71* (3), 247-253.
23. Mayak, W.; McDiarmid, R.E.; Hall, J.W.; Cheng, K.J. Factors that determine rate of cyanogenesis in bovine ruminal fluid in vitro. *J. Anim. Sci.* **1990**, *68*, 1648-1655.
24. Mazza, G.B.; Oomah, D. Flaxseed, dietary fiber, and cyanogens, In *Flaxseed in Human Nutrition*; Cunnane S.C. and Thompson L.U. Eds.; AOCS Press, University of Illinois, Champaign, Ill, 1995, pp. 56-81.

РЕДУКЦИЈА ЦИЈАНОГЕНИХ ГЛИКОЗИДА ЕКСТРУДИРАЊЕМ - УТИЦАЈ ТЕМПЕРАТУРЕ И ВЛАГЕ ТРЕТИРАНОГ МАТЕРИЈАЛА

Душица С. Чоловић, Јованка Д. Левић, Радмило Р. Чоловић, Љубинко Б. Левић,
Војислав В. Бањац, Слађана М. Ракита, Оливера М. Ђурагић

Универзитет у Новом Саду, Институт за прехранбене технологије, Булевар цара Лазара 1,
21000 Нови Сад, Србија

У овом раду представљени су резултати експеримента који се бавио испитивањем утицаја температуре екструдирања и почетног садржаја влаге материјала који је третиран на редукцију цијаногених гликозида (ЦГ) присутних у ко-екструдату на бази ланеног семена. ЦГ представљају главну препреку у масовнијој употреби ланеног семена у исхрани животиња. Стога је, пре употребе, обавезно третирати ланено семе неким технолошким процесом, како би се ЦГ уклонили, а оно детоксификовало. Екструдирање је показало читав низ предности у односу на друге процесе детоксификације, нарочито у поређењу са сувим загревањем, јер комбинује утицаје неколико фактора: загревања, смицања, мешања, високог притиска, итд. На основу добијених резултата, потврђено је да пораст температуре и присутне влаге у третираном материјалу поспешује и убрзава реакцију хидролизе ЦГ, што је евидентирано смањењем садржаја HCN у добијеном ко-екструдату, као мерила присутних ЦГ. Садржај HCN се у огледу кретао од 25.42 mg/kg, што је забележено при вредностима влаге материјала од 11.5%, до 126 mg/kg, што је измерено при влази материјала од 7% (минимална влага у експерименту). Може се рећи да су утицаји процесне температуре и влаге присутне у материјалу од једнаког значаја за детоксификацију ланеног семена. Ипак, када се посматрају добијени резултати садржаја HCN између третмана који подразумевају различит садржај влаге уз различиту процесну температуру, не може се утврдити нека правилност. Разлог за то огледа се у утицају осталих процесних параметара при екструдирању. Због сложености самог процеса, најпожељније је анализирати заједничко дејство и интеракције свих параметара процеса.

Кључне речи: Ланено семе, цијаногени гликозиди, екструдирање, температура, влага, HCN

Received: 8 April 2015.
Accepted: 10 June 2015.

RHEOLOGICAL AND TEXTURAL PROPERTIES OF CRACKER DOUGH WITH ADDITION OF PEA DIETARY FIBER

Ljubica Dokić¹, Biljana Pajin¹, Aleksandar Fištes¹, Zita Šereš¹,
Dragana Šoronja Simović¹ and Veljko Krstonošić²*

¹University of Novi Sad, Faculty of Technology, Bulevar cara Lazara 1, Novi Sad, Serbia

²University of Novi Sad, Faculty of Medicine, Hajduk Veljkova 11, Novi Sad, Serbia

Consumers are becoming aware of health benefits of dietary fiber intake. In past years, the development of products containing different fiber is increasing. The aim of this research was to look into the effect of addition pea fiber to dough for crackers. Rheological and textural properties were evaluated. In order to develop dough in which wheat flour was partly substituted with pea fiber, it was necessary to increase water content. The addition of 5% and 10% of pea fiber affected intramolecular linkages of gluten and lowered elastic properties of the dough. Dough with addition of 30% of fiber was brittle, grainy and impossible to process.

KEY WORDS: dietary fiber, rheology, texture, dough

INTRODUCTION

Dietary fibers relate to a heterogeneous group of components with different functional properties. The fibers swell in aqueous media of intestinal juices, absorb water and small molecules. Between the fibers and the molecules that surround them, different types of bonds are formed, such as ionic, hydrogen, weak hydrophobic bonds and dispersion forces, which may influence the absorption of minerals and steroids (1,2).

Numerous studies show that the consumption of fibers protect against heart disease and cancer, normalize the lipid content in the blood, affect the glucose level and insulin secretion, prevent the constipation and digestive tract diseases (3,4). The enrichment of food with dietary fibers aims to increase the dietary fibers intake. It is mainly done in case if bakery products, cookies, crackers, and other products that may contain cereals have been done. However, as a source of fibers, different by-products of milling of wheat, maize, sorghum and other cereals can be used, as well as the products obtained by wet milling of corn and wheat. There are many other potential sources of fibers, such as fruits, vegetables, and infrequently used grains (5,6). Soluble dietary fibers, including pectin and hydrocolloids are found in fruits, nuts, vegetables, legumes (7). Insoluble fibers, including cellulose and hemicelluloses, may be found in whole grain cereals. Dietary fibers from cereals include 50% of all sources, 30-40 % is obtained from vegetables,

* Corresponding author: Ljubica P. Dokić, University of Novi Sad, Faculty of Technology, Bulevar cara Lazara 1, 21000 Novi Sad, Serbia, e-mail: ldbaucal@tf.uns.ac.rs

about 16% are of the fruit, and the remaining 3% is from other sources of dietary fibers (8).

The important technological characteristics of dietary fiber that determine the possibilities for their application are water holding capacity, capacity of fat binding, viscosity, gel forming ability, chelating capacity, and the influence on food texture. The water holding capacity is associated with the length and density of the fibers. Also, the pH of the environment affects the water retention capacity. Capacity of fat binding is more dependent on the porosity of the fibers, than the molecular affinity. Fibers such as pectin, gums and β -glucan form solutions with large viscosity, and they are commonly used as thickeners (9). Viscosity of insoluble and some soluble fibers, such as inulin, is minimal. The ability to form a gel is the most important feature in using fibers as a fat replacer. This ability is provided by cross-linking of polymeric units and by retention of water or other solvents in the gel structure. This characteristic depends on a number of factors, such as concentration, temperature, the presence of certain ions, and the pH of the environment.

The objective of this study was to determine the rheological and textural properties of dough for crackers with addition of pea dietary fibers.

EXPERIMENTAL

Materials

Materials used in cracker formulation were wheat flour (type T-500, Danubius, Novi Sad, Serbia) pea dietary fiber (EF150, J. Rettenmaier & Son, Rosenberg, Germany), vegetable fat (Dijamant, Zrenjanin, Serbia), yeast, leavening agent NaHCO_3 , NaCl and water.

Methods

Alkaline water retention capacity (AWRC) of wheat flour and wheat flour-pea fiber mixtures was determined according to AACC 56-10 method (10).

Dough preparation: The control sample contained only wheat flour. The wheat flour was substituted at the levels of 5, 10 and 30% by pea dietary fibers, to produce dietary fibers containing samples.

The dough for crackers was prepared according to the long fermentation process. The process includes two phases: mixing of the sour dough and mixing of dough in the vertical spindle mixer. The dough for cracker is of soft consistency, with 30% of moisture. The sour dough contained wheat flour (70% of total amount of flour), yeast (0.4%) and water (30%). The mixing time was 10 min at 27°C, and the fermentation process was 18 h at relative humidity of 80-90%. The dough contained wheat flour (30% of total amount of flour), vegetable fat (11%), NaCl (1.5%) and NaHCO_3 (1.0%). The ingredients for the dough were added to sour dough and mixed for 5 min. The second fermentation process was 5 h at 27-29°C and relative humidity of 80-90%.

After the second fermentation, rheological and textural measurements were performed.

Rheological properties: Rheological properties of cracker dough were determined using a rotational viscometer HAAKE RheoStress RS600 (Thermo Electron Corporation, Karlsruhe, Germany) with plate–plate sensor PP60 Ti (plate diameter was 60 mm and gap 1 mm). The measurements were done at $27 \pm 0.1^\circ\text{C}$.

Viscoelastic properties of the dough, defined by storage modulus (G') and loss modulus (G''), were determined by dynamic oscillatory measurements in the range of linear viscoelastic regime (LVE). The moduli were observed during increased frequency from 1 to 10 Hz, and at constant shear stress of 10 Pa. The results were expressed as value $\tan \delta = G''/G'$.

Viscoelastic response of the samples at a constant stress, as well as the sample behavior after removing the stress, were determined by creep and recovery test. The test was performed in the LVE regime in which the deformation amplitude was proportional to the applied stress amplitude. The creep time with constant stress ($\sigma=10$ Pa) was 150 s, and the recovery period after removing the stress was 300 s.

The creep data were analyzed by the Burger's model [1].

$$J(t) = J_0 + J_1 \times (1 - \exp(-t/\lambda)) + t/\eta_0 \quad [1]$$

For the recovery phase, the equation of the Burger's model is [2].

$$J(t) = J_{max} - J_0 - J_1 \times (1 - \exp(-t/\lambda)) \quad [2]$$

The value J_0 is the instantaneous compliance, J_1 is the retarded (viscoelastic) compliance, J_{max} is the maximum compliance, λ is the mean retardation time, and η_0 is the Newtonian viscosity. Also, the relative elastic part J_e/J_{max} and relative viscous part J_v/J_{max} of the maximum creep compliance were determined from creep and recovery curves.

Textural properties: Textural properties of the dough for crackers were determined on a Texture Analyzer TA.HD Plus (Stable Micro Systems, Godalming, U.K.).

Hardness of the dough was determined by penetration test using the cylindrical element (P/6) 6 mm in diameter.

Extensibility was determined by the method specified by the device producer, *Extensibility of dough and measure of gluten quality*. The load cell of 5 kg was used.

RESULTS AND DISCUSSION

Alkaline water retention capacity is a parameter by which quantity of water needed to obtain optimal consistency of dough is calculated. For the control dough, 30.59g of water was added. The AWRC values for the examined samples are given in Table 1. Since pea flour is a typical hydrocolloid macromolecule its water retention capacity is high, and increases the AWRC values of flour mixtures compared to wheat flour. Due to this effect, the increase in water content in order to develop dough was necessary. Water quantities added to flour mixtures were 45.51g, 50.44g and 73.47g for the mixtures containing 5%, 10% and 30% of pea dietary fiber, respectively. Even though water quantity was increased when wheat flour was replaced with 30% of pea fiber, the presence of fiber resulted in so high colloidal bonding of water that the obtained dough was brittle, grainy and un-

able to stretch, so that measurements were not possible to perform. Hence, the measurements were done and rheological and textural properties determined only for the samples containing 5% and 10% of pea fiber.

Table 1. AWRC of wheat flour, pea dietary fiber and flour-pea dietary fiber mixtures

Sample	Wheat flour	PF	Mixture 5%PF	Mixture 10%PF	Mixture 30%PF
AWRC (%)	70.59	600.01	88.29	101.04	160.59

PF-pea dietary fiber

The viscoelastic properties are presented in Figure 1. As expected, the elastic modulus is higher than the viscous one, since the dough is a highly viscoelastic system. Due to the hydrocolloid nature of the pea fiber and water bonding, the elastic modulus of the dough with 5% of pea fiber was higher than of the control. On the contrary, the dough with 10% of pea fiber had lower value compared to the control sample. Replacement of wheat flour with pea fiber in the dough formulation resulted in a lower gluten content, which was replaced with non-stretchable cellulose as the main component of the pea fiber.

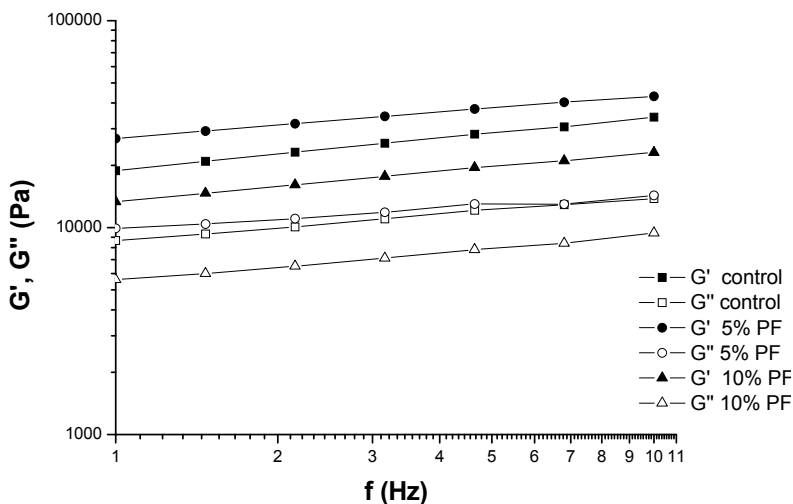


Figure 1. Elastic (G') and viscous (G'') moduli of dough

The calculated values of the $\tan\delta$ were 0.432, 0.345 and 0.407 for the control, 5% PF and 10% PF, respectively. Such values of $\tan\delta$ are characteristic for amorphous polymer systems.

The creep and recovery tests were performed, and the parameters are given in Tables 2 and 3. Under the constant stress, applied in the linear viscoelastic region, which does not disrupt sample structure intermolecular bonds, are stretched and deformed. The resulting

value of J_0 (instantaneous compliance) is the result of elastic deformations, while retarded compliance J_1 is a result of viscoelastic deformations. The control sample in which gluten content was the highest had the highest elastic instantaneous compliance, i.e. elastic deformation. The intramolecular disulfide bonds between the gluten molecules are highly stretchable. Replacement of protein molecules with rigid cellulose ones resulted in a significant decrease in J_0 . When flour is replaced with pea fiber, the decrease in J_{max} implies that the obtained material possesses greater resistance to deformation than the control. The flour upon the addition of fiber becomes stronger. But, increased addition of water to the dough with dietary fiber increased the viscous component η_0 .

Table 2. Creep phase parameters

Sample	Creep phase					r
	J_0 ($\times 10^5$) [Pa ⁻¹]	J_1 ($\times 10^4$) [Pa ⁻¹]	η_0 ($\times 10^{-5}$) [Pas]	λ_1 [s]	J_{max} ($\times 10^5$) [Pa ⁻¹]	
Control	132.7	8.820	1.692	196.7	267.3	0.9995
5% PF	4.981	2.488	6.003	196.8	75.39	0.9992
10%PF	10.80	4.599	3.248	196.8	135.8	0.9981

After the removal of the stress, in the recovery phase, one part of deformation remains to represent the viscous part (J_v) of the maximum compliance, whereas the recovery represents the total elastic component (J_e) of the maximum compliance. The values of the relative elastic part J_e/J_{max} and relative viscous part J_v/J_{max} of the sample maximum compliance were calculated from the recovery curve. The elastic recovery reflects the extent of bonding between the structural elements of dough. The increase in the elasticity means less deformation of the components network in the presence of the fiber, as noticed by other authors with different fiber (11).

Table 3. Recovery phase parameters

Sample	Recovery phase					
	J_0 ($\times 10^5$) [Pa ⁻¹]	J_1 ($\times 10^5$) [Pa ⁻¹]	η_0 ($\times 10^{-6}$) [Pas]	λ_1 [s]	r	J_e/J_{max}
Control	260.1	75.55	0.3292	327.7	0.9865	14.36
5% PF	70.19	18.78	1.325	327.8	0.9611	24.51
10%PF	125.6	2.446	75.88	457.5	0.9899	49.39

Texture analysis was performed in order to determine the behavior of the dough in case of large deformations. These tests are useful in getting information on the behavior in processing under the real production conditions. The results are given in Table 4. The values of the hardness, resistance to extension and extensibility, decreased with the addition of pea fiber. Such behavior was also reported by other authors (12). Increased addition of water did not improve the dough ability to stretch, since the excessive water was tightly bonded to cellulose fibers. Such dough should be harder to laminate into thin dough sheets in cracker production. This is the reason why the dough with 30% of pea fiber was unable to produce.

Table 4. Penetration and extensibility parameters

Sample	Hardness (g)	Resistance to extension (g)	Extensibility (mm)
	F _{max sr} ± SD	F _{sr} ± SD	X _{sr} ± SD
Control	48.417±3.118	21.22±2.37	16.99±0.74
5% PF	46.048± 0.697	21.51±1.06	12.81±0.91
10%PF	23.609± 0.530	13.30±0.59	12.07±1.17

CONCLUSION

Substitution of wheat flour with pea dietary fiber is possible, but dynamic oscillatory parameters, creep recovery test and textural properties showed that the addition of pea fiber increased the stiffness, resistance to deformation, flowability and elasticity of the dough.

Acknowledgement

This research is conducted within the project “Cookies and crackers with functional characteristics aimed for consumers with special dietary needs“, supported by the Provincial Secretariat for Science and Technological Development of Vojvodina.

REFERENCES

1. Kay R. M. Dietary fiber, *J. Lipid Res.* **1982**, 23, 221-234
2. Borderias, A.J; Sanchez-Alonso, I; Perez-Mateos, M. New Applications of Fibres in Foods: Addition to Fishery products, *T. Food Sci. Tehn.* **2005**, 16 (10), 458-465.
3. Marlet, J.A; McBurney, M.I; Slavin, J.L. Health implications of dietary fiber, *J. Am. Diet. Assoc.* **2002**, 102 (7), 993-1000.
4. Slavin, J.L. Dietary fiber and body weight, *Nutrit.* **2005**, 21, 411-418.
5. McKee, L.H; Latner, T.A. Underutilized sources of dietary fiber: A review, *Plant Foods Hum. Nutr.* **2000**, 55, 285-304.
6. Masoodi, F.A; Sharma, M; Chauhan, G.S. Use of apple pomace as a source of dietary in cakes, *Plant Foods Hum. Nutr.* **2002**, 55, 121-128.
7. Grigelmo-Miguel, N; Gorinstein, S; Marton-Belloso, O. Characterisation of peach dietary fibre concentrate as a food ingredient, *Food Chem.* **1999**, 65, 175-181.
8. Mezger, T. *The Rheology Handbook: For users of rotational and oscillation rheometers*", VincentzVerlag., Hannover, 2002, pp. 86-99.
9. Lazaridou, A; Duta, D; Papageorgiou, M; Belc, N; Biliaderis, C.G. Effects of hydrocolloids on dough rheology and bread quality parameters in gluten-free formulations. *J. Food Eng.* **2007**, 79 1033-1047.
10. AACC, *Approved methods of the AACC (10th ed)*, American Association of Cereal Chemists, st. Paul, MN, 2000.

11. Skendi, A; Papageorgiou, M; Biliaderis, C.G. Effects of barley β -glucan molecular size and level on wheat dough rheological properties. *J. Food Eng.* **2009**, *91* 594-601.
12. Rouille, J; Della Valle, G; Lefebvre, J; Sliwinski, E; van Vliet, T. Shear and extensional properties of bread dough affected by their minor components. *J. Cereal Sci.* **2005**, *42* 45-57.

РЕОЛОШКЕ И ТЕКСТУРАЛНЕ ОСОБИНЕ ТЕСТА ЗА КРЕКЕРЕ СА ДОДАТКОМ ВЛАКАНА ГРАШКА

Љубица Докић¹, Биљана Пајин¹, Александар Фиштеш¹, Зита Шереш¹, Драгана Шороња Симовић¹, Вељко Крстоношић²

¹ Универзитет у Новом Саду, Технолошки факултет, Булевар цара Лазара 1, Нови Сад, Србија

² Универзитет у Новом Саду, Медицински факултет, Хајдук Вељкова 11, Нови Сад, Србија

У скорије време, свест потрошача о корисном здравственом дејству прехранбених влака расте. Из тог разлога све већи број производа на тржишту који у свом саставу имају повећан садржај влакана. Последњих година, почела је производња прехранбених влакана из мање познатих сировима, као што су махунарке. У овом раду испитиван је утицај додатка прехранбених влакана грашка на реолошке и текстуралне карактеристике теста за производњу крекера. Пшенично брашно у формулацији за крекере је замењено са 5%, 10% и 30% влакана грашка. Да би се могло формирати тесто, на основу одређене моћи задржавања воде дефинисана је количина воде коју је потребно додати у замес. Додатком влакана потребно је повећати количину воде у односу на контролни узорак. На основу реолошких и текстуралних мерења утврђено је да се еластичност теста са додатком влакана смањила. Тесто са 30% влакана се лако кидало и било ситнозрнасто, тако да се није могло развући те ова количина влакана није погодна за производњу крекера.

Кључне речи: прехранбена влакна, реологија, текстура, тесто

Received: 15 June 2015.

Accepted: 23 September 2015.

SPELT PASTA WITH INULIN AS A FUNCTIONAL FOOD

Jelena S. Filipović^{1*}, Lato L. Pezo², Vladimir S. Filipović³ and
Gordana I. Ludajić⁴

¹ University of Novi Sad, Institute for Food Technology, Bulevar cara Lazara 1, 21000 Novi Sad, Serbia

² University of Belgrade, Institute of General and Physical Chemistry, Studentski Trg 12-16,
11000 Beograd, Serbia

³ University of Novi Sad, Faculty of Technology, Bulevar cara Lazara 1, 21000 Novi Sad, Serbia

⁴ Higher Technical School of Professional Studies, Đorđa Stratimirovića 23, 23000 Zrenjanin, Serbia

Spelt wheat growing without use of pesticides is a suitable raw material for whole meal products. The aim of this study was to enhance the fiber content in spelt pasta by adding inulin HPX. Inulin HPX replaced the spelt farina in the quantity of 0%, 5%, 10% and 20%, thus contributing to a decrease in the toughness, and improving color of the pasta. The presence of inulin can be clearly distinguished from other polysaccharides components by ¹³C MAS NMR spectroscopy. A simultaneous increase in the area of the peaks at 81, 74, 64 and 58 ppm, obtained during the deconvolution analysis of the NMR spectra, is directly associated with the increase in the inulin content. Inulin contributes positively to the nutritive and technological characteristics of the pasta. Spelt pasta with 20 % of inulin is a new functional product with modified nutritional properties and with decreased digestible carbohydrates in the amount of 43.2% and reduced energy of 27.2%.

KEY WORDS: pasta, inulin, nutritive value, texture color, ¹³C MAS NMR

INTRODUCTION

The relationship between food and health has an increasing impact on food innovation due to the popularity of the concept of functional food. Dietary fibers in pasta are versatile functional food ingredients, which are beneficial to human health (1-4). One of dietary fibers used by food industry is inulin, a non-digestible fructo-oligosaccharide. It acts as a prebiotic by stimulating the growth of healthy bacteria in the colon. Inulin is a linear polydisperse carbohydrate material consisting mainly of D – fructose joined by β-(2/1) linkages (1, 3, 5). Pasta containing inulin alters nutritive and sensory properties, has a positive effect on certain functions in the organism, and improves psychical condition. The functionality of the food with increased content of inulin can be seen in the positive effect of reducing the risk from numerous non-infectious diseases (1, 2, 6). The aim of this study was to investigate the quality of pasta with inulin, in an effort of obtaining new products with alte-

* Corresponding author: Jelena S. Filipović, University of Novi Sad, Institute for Food Technology, Bulevar cara Lazara 1, 21000 Novi Sad, Serbia, e-mail: jelena.filipovic@fins.uns.ac.rs

red nutritional properties, to classify and discriminate the analyzed samples by principal component analysis (PCA) using ^{13}C MAS NMR spectroscopy data and presented technological data. Pattern recognition technique was applied within assay descriptors, to characterize and differentiate various samples.

EXPERIMENTAL

Material and methods

Wholemeal flour of spelt grown in the year 2012 in Serbia was used for pasta production. Chemical analyses (protein, starch, lipid, sugar, cellulose, and total dietary fiber) of pasta were determined according to the official methods of AOAC (7) and AOAC (8). Inulin HPX is a commercial product obtained from the root of Jerusalem artichoke, produced by "ORAFIT Active Food Ingredients", Tienen, Belgium, with average $\text{DP} \geq 23$. Pasta with inulin HPX (0, 5, 10 and 20%) was made using the La Parmigiana D45 MAC 60 procedure described by Filipović et al, (9). Textural properties of cooked pasta and pasta color were measured using Texture analyzer TA.HD plus (Stable Micro System, U.K.) and colorimeter Chroma meter (CR-400, Konica, Minolta, Japan), respectively, as described by Filipović et al, (9, 10). The ^{13}C MAS NMR spectra were recorded at 100.627 MHz using a Bruker MSL 400 NMR spectrometer with a TecMag console upgraded (Texas, USA), according to the procedure described by Filipović et al, (11). Descriptive statistical analyses for all the obtained results were expressed as the mean \pm standard deviation (SD), one-way ANOVA and principal component analysis (PCA) analyses were described by Filipović et al, (10). Furthermore, PVA was applied successfully to classify and discriminate the different samples based on the NMR spectra (peak width) and technological parameters.

RESULTS AND DISCUSSION

Quality of spelt pasta with different quantities of inulin. Based on chemical properties of the pasta with different quantities of inulin, ANOVA, coupled with Tukey's HSD test, were evaluated for a comparison of the parameters. These tests showed statistically significant differences in protein content among the values of pastas with 0 and 5% inulin and pasta with 10% and 20% inulin (Table 1).

The addition of inulin (5%, 10% and 20%) to pasta also results in a statistically significant difference in the starch content, because one part of flour is replaced by inulin and the quantity of available starch is reduced. Tukey's HSD test showed statistically significant differences in the values of cellulose in pasta with inulin (5%, 10% and 20%) and pasta without inulin, since inulin is a macromolecule with chemical structure containing the same molecules as cellulose.

Table 1 shows that the increase in the inulin content indicates a statistically significant increase in the sugar content and a statistically significant decrease of the lipid content. Tukey's HSD test indicates statistically significant differences in dietary fiber content in pasta with 0%, 5%, 10% and 20% inulin, which confirms that inulin is one type of non-digestible carbohydrates.

Table 1. Chemical properties of pasta with different contents of inulin

Chemical property	Content of inulin (%)			
	0	5	10	20
Protein content (% d. m)	15.87±0.21 ^c	15.53±0.13 ^c	14.56±0.10 ^b	12.85±0.11 ^a
Starch content (% d. m)	56.49±0.39 ^d	53.67±0.57 ^c	51.53±0.89 ^b	38.07±0.28 ^a
Cellulose content (% d. m)	2.0±0.04 ^a	2.28±0.05 ^b	2.68±0.04 ^c	2.94±0.06 ^d
Sugars content (% d. m)	2.42±0.02 ^b	2.53±0.02 ^c	2.55±0.02 ^c	2.35±0.01 ^a
Lipids content (% d. m)	2.70±0.02 ^d	2.54±0.07 ^c	2.42±0.07 ^b	2.35±0.05 ^a
Dietary fibers content (% d. m)	5.62±0.13 ^a	8.21±0.17 ^b	10.81±0.08 ^c	16.0±0.11 ^d

^{a, b, c, d} Values with the same letter are not statistically different at the p<0.05 level (according to post-hocTukey's HSD test)

By increasing the quantity of inulin from 0 to 20, sugar, contents of lipid and dietary fibers can be calculated as follows:

$$\text{Sugars content} = (2.42 \pm 0.00) + (0.03 \pm 0.00) \times \text{Inulin} \quad (r^2=0.999, p<0.05)$$

$$\text{Lipids content} = (2.70 \pm 0.00) - (0.04 \pm 0.00) \times \text{Inulin} \quad (r^2=0.999, p<0.05)$$

$$\text{Dietary fibers content} = (5.62 \pm 0.22) + (0.52 \pm 0.0) \times \text{Inulin} \quad (r^2=0.999, p<0.05).$$

Table 2 shows a significant reduction of digestible carbohydrates, which contributes to the reduction of the energy value and increase in the functionality of food. By daily average consumption of 100 g pasta with inulin 0% and 20% inulin, the intake of fiber is 7.7 and 18.9 g per day, respectively. Therefore, this kind of pasta can have positive long-term effects in the prevention of non-infectious diseases caused by irregular diet (12). It is worth to point out that pasta with 20% inulin is a product with a significant decrease of digestible carbohydrates (by 43.2%) and significant reduction of energy (by 27.2%).

Table 2. Nutritive properties of pastas with different contents of inulin

Nutritive properties	Content of inulin (%)			
	0	5	10	20
Decrease of digestible carbohydrates (%)	-	10.0±0.16 ^a	18.8±0.12 ^b	43.2±0.11 ^c
Content of non-digestible carbohydrates (g) in 100 g of pasta	7.7±0.21 ^a	10.9±0.21 ^b	13.5±0.21 ^c	18.9±0.21 ^d
Energy (kJ)	1373.9	1315.9	1258.8	1000.7
Decrease in the energy of pasta (%)	-	4.2	8.4	27.2

^{a, b, c, d} Values with the same letter are not statistically different at the p<0.05 level (according to post-hocTukey's HSD test)

For the increase of the inulin content from 0 to 20, the content of non-digestible carbohydrates can be calculated as follows:

$$\text{Non-digestible carbohydrates content} = (7.75 \pm 0.18) + (0.61 \pm 0.05) \times \text{Inulin} \quad (r^2=0.999, p<0.05)$$

The textural characteristics and color of pasta play an essential role in determining the final acceptance by consumers (6). The ANOVA and the following post-hoc Tukey's HSD tests (Table 3) showed that the addition (5%, 10 % and 20%) of inulin statistically significantly decreased the hardness and toughness of the pasta in comparison to pasta without inulin, which indicates that inulin weakens the structure of pasta dough, which is due to the gluten dilution. Tukey's HSD test showed that inulin statistically significantly increased the adhesiveness of pasta, because inulin hydrates faster than the starch and protein components of flour, in turn leading to starch and fiber fractions of the pasta being less incorporated in the matrix. If the starch is not encapsulated within a protein matrix, cooking contributes to a sticky layer at the surface of the product, resulting in higher levels of adhesiveness (6, 13, 14).

Table 3. Textural and color properties of pasta with different contents of inulin

Textural property	Content of inulin (%)			
	0	5	10	20
Hardness (g)	3117.5±13.1 ^c	2498.7±27.9 ^b	2439.1±43.8 ^b	1860.7±20.0 ^a
Adhesiveness (gsec)	2.02±0.05 ^a	2.59±0.04 ^b	6.37±0.12 ^c	9.15±0.09 ^d
Work of Shear - toughness	13.44±0.14 ^d	8.9±0.12 ^c	6.19±0.15 ^b	4.35±0.10 ^a
Pasta color				
L Brightness	76.00±0.32 ^a	76.41±0.12 ^a	76.90±0.24 ^a	79.36±43.8 ^a
a*Share of red color	2.27±0.08 ^a	2.12±0.02 ^a	2.03±0.05 ^a	1.54±0.02 ^a
b* Share of yellow color	13.35±0.00 ^a	13.23±0.09 ^a	13.16±0.12 ^a	12.74±0.13 ^a
C* Differences in coloration	13.35±0.14 ^a	13.41±0.10 ^a	13.50±0.19 ^a	12.83±0.18 ^a

^{a, b, c, d} Values with the same letter are not statistically different at the p<0.05 level (according to post-hoc Tukey's HSD test)

For the increase in the inulin content from 0 to 20, the toughness can be calculated as follows:

$$\text{Toughness} = (13.39 \pm 0.17) - (1.01 \pm 0.44) \times \text{Inulin} + (0.03 \pm 0.00) \times \text{Inulin}^2 \quad (r^2 = 0.999, p < 0.05)$$

The use of a tristimulus colorimeter permits the simultaneous measurements of brightness and yellowness, the most appreciated pasta attributes. Table 3 shows that there is a statistically insignificant difference in the brightness, share of red color and yellow color, and differences in the coloration in pasta with the addition of 20% of inulin and pastas with 0%, 5% and 10% of inulin. The content of inulin increased the brightness, reduced the proportion of red color and increased the differences in coloration of the product. The share of yellow color decreased with the increased content of inulin in pasta, since one part of wholemeal flour was replaced by inulin, so that the quantity of available flour was reduced.

The ¹³C MAS NMR characterization of spelt pasta with different quantities of inulin. As stated in our previous study (11), due to a similar chemical environment of detectable groups, the NMR analysis of the most polysaccharides, shows that the shifts overlap to a large extent. The positions of the peaks of inulin and spelt pasta samples, reveal the possibility of obtaining discrimination of the inulin component from other pre-

sent components in the spectrum. The distinction of the peak position of inulin compared to other polysaccharides (such as starch) enables also the evaluation of their content in the sample. This difference in the peak position of inulin in comparison to the position of the dominant peaks originated from the starch is especially pronounced for peaks positioned at 81, 64 and 58 ppm. Furthermore, based on the results of deconvolution analysis of polysaccharides region in the ^{13}C MAS NMR spectra, the peak at 75 ppm (basically originated from the C(4) carbon in the starch structure) also provides the continual gain in the values of the area ascribed to this peak, which is consistent with the added amount of inulin. Generally, a continuous increase of the area for any of particular peak mentioned above can be observed, which can be clearly correlated with the amount of added inulin for each of the samples shown. During the deconvolution analysis, the peaks at 64 and 58 ppm are incorporated only in the case of the samples with inulin (samples 2 and 3), whereas the peaks positioned at 81 and 74 ppm are overlapped to some extent with neighboring peaks belonging to the starch component. However, the results of deconvolution analysis were not affected substantially for that reason, indicating the same correlation dependence as was observed for other mentioned peaks.

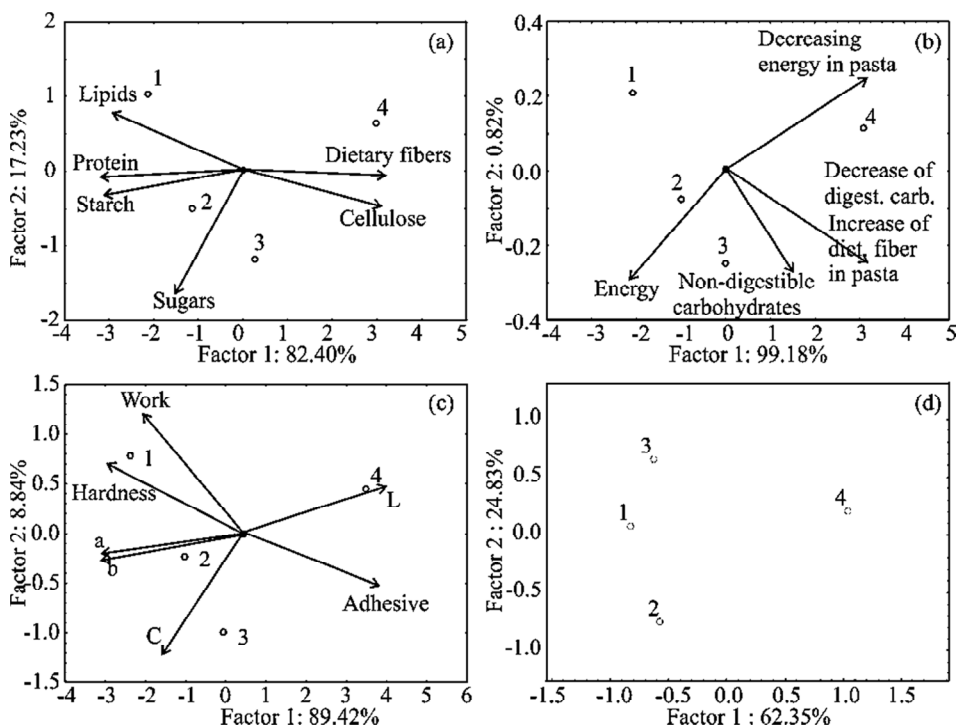


Figure 1. PCA biplots for: chemical properties of pasta (a), nutritive properties of pasta (b) textural properties and color of pasta (c), biplot for ^{13}C MAS NMR spectra of different samples of pasta (d)

The PCA allows a considerable reduction in the number of variables and the detection of the structure in the relationship between the measured parameters and different samples that give complementary information. In this study, four different data sets were submitted to PCA: chemical properties of pasta (Table 1), nutritive properties of pasta (Table 2), textural properties and color of pasta (Table 3) and ^{13}C MAS NMR spectrum (peak width). For visualizing the data trends and the discriminating the efficiency of the used descriptors, a scatter plot of samples using the first two PCs resulting from the PCA of the data matrix is obtained (Fig. 1).

As can be seen, there is a neat separation of samples according to chemical properties of pasta, nutritive properties of pasta, textural properties and color of pasta and NMR spectra. Chemical data showed that the first two PCs explained 99.63% of the total variability. Protein, starch and cellulose content, as well as lipids and dietary fibers content contributed almost equally to the calculation of the first PC, while sugars content contributed the most to the second PC (75%). The first two PCs of the nutritive properties data (Table 2) accounted for 100% of the total variability. All variables contributed almost equally to the calculation of the first PCs, while the content of non-digestible carbohydrates contributed the most to the second PC. The textural properties (hardness, adhesiveness and toughness) and color of pasta (brightness, shares of red and yellow color and differences in coloration) explained 98.26% of the total variability. The first PC is explained almost equally by all variables (both textural and color properties), while the second PC is mostly calculated by C and toughness). The ^{13}C MAS NMR results showed that the first two PCs accounted for 87.18% of the total variability.

CONCLUSION

Based on the investigation of the influence of inulin content on the nutritive and textural properties of pasta and the possibility of inulin identification by ^{13}C MAS NMR spectrum it can be concluded: that the pasta obtained by adding 5, 10 or 20% of inulin is characterized by a significant decrease of digestible carbohydrates (10.0, 18.8 and 43.2%) and increased content of non-digestible carbohydrates (10.9, 13.5 and 18.9%). An average daily consumption of 100 g of pasta with 20% of inulin contributes to the fiber intake of 18.94 g per day. The pasta with 20% of inulin is a new functional product with modified nutritional properties, with reduced energy in the amount of 27.2%. The addition of inulin influenced adversely the pasta texture (decreased toughness) and positively the pasta color (increased brightness, reduced share of red color and differences in coloration). The presence of inulin can be clearly identified by ^{13}C MAS NMR spectroscopy. The increase in the area of the peak positioned at 81, 74, 64 and 58 ppm, obtained during the deconvolution analysis of the NMR spectra, was directly associated with the increase in the inulin content. PCA appeared to be a useful tool for providing a neat separation of the samples according to chemical, nutritive textural pasta properties, pasta color and ^{13}C MAS NMR spectra.

Acknowledgement

These results are part of the projects III 46005 and TR 31029, supported by the Ministry of Education, Science and Technological Development of the Republic of Serbia.

REFERENCES

1. Mastromatteo, M., Iannetti, M., Civica, M., Sepielli, G., Del Nobile, M. A. Effect of the Inulin Addition on the Properties of Gluten Free Pasta. *Food Nutr. Sci.*, **2012**, *3*, 22-27.
2. Brennan, C., Cleary, L. The potential use of cereal (1 \rightarrow 3, 1 \rightarrow 4)- β -D-glucans as functional food ingredients. *J. Cereal Sci.*, **2005**, *42*, 11-13.
3. Filipović, J., Filipović, N., Filipović, V. The effects of commercial fibres on frozen bread dough. *J. Serb. Chem. Soc.* **2010**, *75*, 195-207.
4. Brennan, C., Tudorica, C. Evaluation of potential mechanisms by which dietary fiber additions reduce the predicted glycemic index of fresh pasta. *Int. J. Food Sci. Tech.* **2008**, *43*, 2151-2162.
5. Filipović, J., Filipović, N. Fibres in the dough influencing freezing and thawing kinetics. *Int. J. Food Sci. Tech.* **2010**, *45* (1) 1-6.
6. Tudorică, C., Kuri, V., Brennan, C. Nutritional and physicochemical characteristics of dietary fibre enriched pasta. *J. Agr. Food Chem.* **2002**, *50* 347-356.
7. AOAC, Official methods of analysis. 17ed. Washington Association of Official Analytical Chemists, 2000.
8. AOAC, Official Methods of Analysis of the Association of Official Analytical Chemists, Vol. II, 15th ed. Sec. 985.29. The Association Arlington, VA, 1990.
9. Filipović, J., Pezo, L., Filipović, N., Filipović, V., Brkljača, J., Jevtić-Vukmirović, J. Optimization of Spelt Pasta Composition, Regarding Inulin HPX Content and Eggs Quantity. *J. Food Nutr. Res.* **2014**, *2*, 167-173.
10. Filipović, J., Pezo, L., Filipović, N., Filipović, V., Bodroža-Solarov, M., Plančak, M. Mathematical approach to assessing spelt cultivars (*Triticum aestivum subsp. spelt*) for pasta making. *Int. J. Food Sci. Tech.* **2013**, *48*, 195-203.
11. Filipović, J., Miladinović, Z., Pezo, L., Filipović, N., Košutić, M., Brkljača, J. Identification of Inulin HPX in pasta by ^{13}C MAS NMR Spectroscopy, *PTEP*, **2012**, *12*, 169-172.
12. Novaković, B; Mirosavljev, M. Higijena ishrane, Univerzitet u Novom Sadu, Medicinski fakultet, Novi Sad, 2002.
13. Aravind, N., Sissons, M., Egan, N., Fellows, C. Effect of insoluble dietary fibre addition on technological, sensory and structural properties of durum wheat spaghetti. *Food Chem.* **2012a**, *130*, 299-309.
14. Aravind, N., Sissons, M., Fellows, C., Blazek, J., Gilbert, E. Effect of inulin soluble dietary fibre addition on technological, sensory and structural properties of durum wheat spaghetti *Food Chem.* **2012b**, *132*, 993 -1002.

ТЕСТЕНИНА ОД СПЕЛТЕ СА ИНУЛИНОМ КАО ФУНКЦИОНАЛНА ХРАНА

*Јелена С. Филиповић¹, Лато Л. Пезо², Владимир С. Филиповић³,
Гордана И. Лудајић⁴*

¹ Универзитет у Новом Саду, Институт за прехранбене технологије, Булевар цара Лазара 1,
21000 Нови Сад, Србија

² Универзитет у Београду, Институт за општу и физичку хемију, Студентски трг 12 - 16,
11000 Београд, Србија

³ Универзитет у Новом Саду, Технолошки факултет, Булевар цара Лазара 1, 21000 Нови Сад

⁴ Висока техничка школа струковних студија, Борђа Стратимировића 23, 23000 Зрењанин

Спелта је погодна сировина за производе од целог зрна јер се узгаја без примене пестицида. Са циљем да се повећа садржај влакана у овом раду је испитан квалитет тестенине од спелте са додатком инулина НРХ. Количина инулина је додавана у интервалу од 0%, 5%, 10% и 20%, као замена за брашно, при чему долази до смањења жилавости и побољшања боје тестенине. Резултати испитивања су показали да се присуство инулина НРХ у тестенини од спелте може јасно доказати коришћењем ¹³C MAS NMR спектроскопије. Пораст површине пикова позиционираних на 81, 74, 64 и 58 ppm, добијене деконволуцијом NMR спектара, директно је повезан са повећањем садржаја инулина у одговарајућим узорцима. Инулин позитивно утиче на сензорне и нутритивне особине тестенине. Тестенина од спелте са 20% инулина представља нов функционални производ са смањеним садржајем сварљивих угљених хидрата од 43,2% и смањеном енергијом од 27,2%.

Кључне речи: тестенина, инулин, нутритивна вредност, текстура, боја, ¹³C MAS NMR

Received: 10 December 2014.
Accepted: 25 May 2015.

PHYSICOCHEMICAL PROPERTIES OF HONEYBEE POLLEN ENRICHED ACIDOPHILUS MILK AND PROBIOTIC YOGHURT

Jovana R. Glušac^{1*}, Milka J. Stijepić¹, Spasenija D. Milanović²
and Dragica M. Đurđević-Milošević³

¹School of Applied Medical Sciences, Nikole Pašića 4a, 79101 Prijedor, Bosnia and Herzegovina

²University of Novi Sad, Faculty of Technology, Bulevar cara Lazara 1, 21000 Novi Sad, Serbia

³MP Lab, MP Bio d.o.o., Prokupačka 41, 11000 Belgrade, Serbia

*The aim of this work was to examine the possibility of preparation of acidophilus milk and probiotic yoghurt by processing of milk (1%, 2.8% and 3.2% w/w fat) enriched with honeybee pollen (0.6% w/w). The quality of produced fermented milks was followed by comparing pH value during fermentation and storage time, as well as of lactic acid content and sensory properties during 14 days of storage. Fermentation time was influenced more the type of the starter culture than by honeybee pollen addition or fat level. The addition of honeybee pollen increased the production of lactic acid, regardless of the fat level. The effects of different starters (*L. acidophilus* LA-5, *S. thermophilus* and *L. Delbrueckii* ssp. *bulgaricus*) on the production of lactic acid were also different, but not as obvious as that due to pollen addition. The obtained results revealed that honeybee addition had positive effects on the physicochemical and sensory properties of produced acidophilus milk and probiotic yoghurt.*

KEY WORDS: acidophilus milk, probiotic yoghurt, honeybee pollen, physicochemical characteristics

INTRODUCTION

Among many fermented dairy products, the most notable fermented milks are yoghurt, kefir, kumiss, acidophilus milk, buttermilk, and Bulgarian buttermilk. Recently, acidophilus milk is becoming one of the most desirable natural products for human nutrition due to its beneficial health effects (1). Furthermore, *Lactobacillus acidophilus* is the most commonly suggested organism for dietary use. All these positive findings have emerged for the consumption of acidophilus milk. Traditional acidophilus milk is made from low-fat milk, sterilized at 120°C for 15 minutes to stimulate growth of *L. acidophilus*. The high-heat treatment of milk is used to denature and release peptides from milk proteins, which helps the growth of *L. acidophilus*, due to its lack of a good proteolytic system for hydrolyzing milk proteins (2). Original acidophilus milk is a highly acidic product with no balancing

* Corresponding author: Jovana R. Glušac, School of Applied Medical Sciences, Nikole Pašića 4a, 79101 Prijedor, Bosnia and Herzegovina, e-mail: jovanaglusac@yahoo.com

flavours. However, because of its acidic flavour, most consumers do not generally relish it (3). Recently, honeybee pollen, as well as other apicultural products, has gained increased attention for its high nutritive value. Honeybee pollen is a rich source of protein (25%); essential amino acids; oil (6%), containing more than 51% polyunsaturated fatty acids (PUFA), of which 39% of linolenic, 20% palmitic and 13% of linoleic acids; more than 12 vitamins; 28 minerals; 11 enzymes or co-enzymes; 11 carbohydrates (35-61%); flavonoids and carotenoids; phytosterols (4). Honeybee pollen was found to have therapeutic properties (5,6). It is considered a nutrient-rich perfect food, and is promoted as a commercially available supplement (7).

In recent years, the physiological functionality of natural and functional foods has received much attention due to the increasing interest in human health. As far as we know, the use of honeybee pollen as a food supplement in dairy products is rare. Therefore, the objective of the present work was to investigate the influence of the honeybee addition and different starter culture (LA-5 and probiotic) on the physicochemical and sensory properties of fermented milk products manufactured from milk with different fat content (1%, 2.8% and 3.2% w/w fat) after the production and during 14 days of storage.

EXPERIMENTAL

Materials

The following milk samples: 1) 3.2 % fat content (3.2% proteins, 4.6% lactose, polyunsaturated fatty acids), obtained from „VITALIA, IMLEK“, d.d. Mlijekoprodukt (Kozarska Dubica, Bosnia and Herzegovina); 2) 2.8% fat content (3.4% proteins, 4.6% lactose pH 6.82 ±0.02), obtained from MEGGLE Mljekara d.o.o. (Bihać, Bosnia and Herzegovina); 3) 1% fat content obtained from the "d.d. Varaždin" (Croatia) were used for the production of fermented milk. Physical, chemical and microbiological characteristics of milk samples were entirely in accordance with the pertinent standards. Probiotic monoculture *Lactobacillus acidophilus* LA-5 (Chr. Hansen, Denmark) was applied to achieve a concentration of 0.05g/l (w/v) in manufacturing fermented milks. Probiotic yoghurt containing: *L.acidophilus* LA-5 was made in combination with yoghurt starter culture YC-X16 (*Streptococcus thermophilus* and *L. delbrueckii* ssp. *bulgaricus*, Chr. Hansen, Denmark) in the ratio of 4:1. Commercial polyfloral honeybee pollen (Prijedor, Bosnia and Herzegovina) was powdered and used in the concentration of 0.6% w/w in manufacturing both types of fermented milk products.

Fermented milks manufacturing

Milks with different fat content were heated at 95°C for 10 min. The milk and bacteria mixture was incubated at 38°C for 4 hours and the fermented milk formed was stored at 4°C and used as a starter culture next day. Two series of yoghurt were made: 1) acidophilus milk (LA-5) without and with addition of honeybee pollen, and 2) probiotic yoghurts made with: LA-5 + yoghurt starter (YS) (LA-5 + YS-X16= 4:1), without and with pollen

addition. For each treatment, the pollen powder was dispersed in an aliquot of heat-treated milk, and then mixed thoroughly with the remaining milk to achieve the desired concentration. The milk was cooled to the optimal temperature (38°C), inoculated with the yoghurt starter-mother culture (50 ml) and incubated at the same temperature until pH 4.7 to 4.6 was reached. Fermentations were stopped by rapid cooling to 20°C and the fermented milks were placed in a cold storage at 5°C ±1. Each trial was repeated three times.

Methods

After manufacturing, fermented milks were analyzed by measuring the pH value, lactic acid content and sensory properties. pH was measured using pH 510/mV Meter (Eutech Instruments, England) during fermentation and during 14 days of storage. Lactic acid content was calculated on the basic titratable acidity (8) during 14 days of storage. Sensory evaluation of yoghurt was profiled after the 1st and 14th day in the cold store. The sensory properties of yoghurt were evaluated by 5 trained panellists using the International Dairy Federation (IDF) method (9). The sensory attributes consisted of flavour, odour, general appearance, colour and consistency, and the coefficients of significance (Fv) were: 2.4 for taste; 0.4 for odour; 0.2 for appearance and for colour and 0.8 for consistency. Maximum score was 20, and the sensory scores were awarded for each attribute using a rating scale ranging between 1 and 5. The average value of 3 measurements was taken for further analysis. Values of different tests were expressed as the mean ± standard deviation ($\bar{x} \pm SD$). All data were subjected to one-way ANOVA and means were compared by the Holm-Sidak test (SigmaPlot 11.0, Systat Software, Inc. USA). The level of significance was set at $p < 0.05$.

RESULTS AND DISCUSSION

Fermentation of all produced samples lasted between 3 and 10 hours (Fig. 1). The shorter fermentation time (about 4 hours) resulted in probiotic yoghurt samples comparable to acidophilus milks, regardless of the milk fat content. The addition of honeybee pollen caused a slight decrease in the fermentation time of probiotic yoghurt samples made from milk with the highest fat content (Fig. 2A), probably due to the presence of various carbohydrates, mainly glucose, fructose and sucrose (4).

However, the fermentation time was influenced more by different types of starter culture than by honeybee pollen addition or fat levels. As is evident from Fig. 1A, acidophilus milks had the longest fermentation time (9-10 hours), regardless of different fat level. According to the results of Iancu et al. (10), the strain of *L. delbrueckii* ssp. *bulgaricus* is faster than the other lactobacilli in producing lactic acid, so this could explain the observed shorter fermentation time of probiotic yoghurt samples.

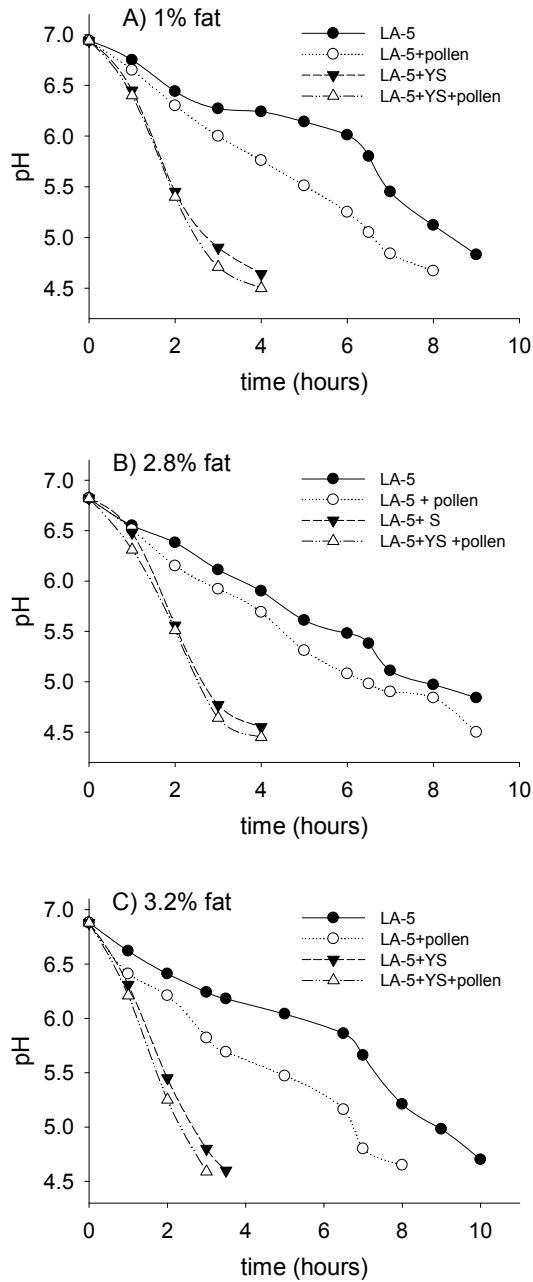


Figure 1. Fermentation time of acidophilus milk and probiotic yoghurt made of milk with 1% (A), 2.8% (B) and 3.2% fat (C) enriched with honeybee pollen (0.6%)

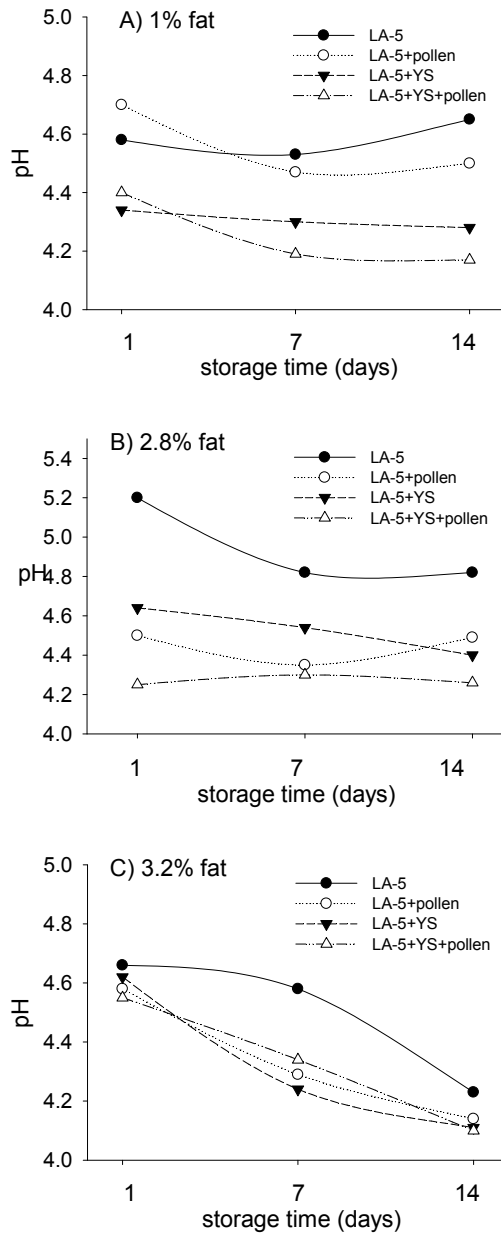


Figure 2. Changes in pH over the storage time of acidophilus milk and probiotic yoghurt made of milk with 1% (B, E), 2.8% (C, F) and 3.2% fat (D, G) enriched with honeybee pollen (0.6%)

The pH value and lactic acid content (%) of all fermented milks changed slightly during the storage period (Fig. 2). The highest pH value during 14 days of storage (ranging from 4.81 to 4.15) had acidophilus milks, regardless of the different fat level. The pH values were lower in the fermented milks enriched with honeybee pollen than in samples without it, which was previously reported (11). The decrease in the pH value was between 0.2 and 0.4 pH units in all fermented milks during 14 day of storage. The highest decrease in the pH was observed in the fermented milks produced from milk with the highest fat content (Fig. 2C).

The highest content of lactic acid on the 1st day of storage had the fermented milks produced from 2.8% fat milk (Fig. 3). Lactic acid content ranged from 0.742 to 1.035% for the samples made with 1% fat milk, from 0.675 to 1.008% for the samples made with 2.8% fat milk, from 0.765 to 1.026% for the samples made with 3.2% fat milk.

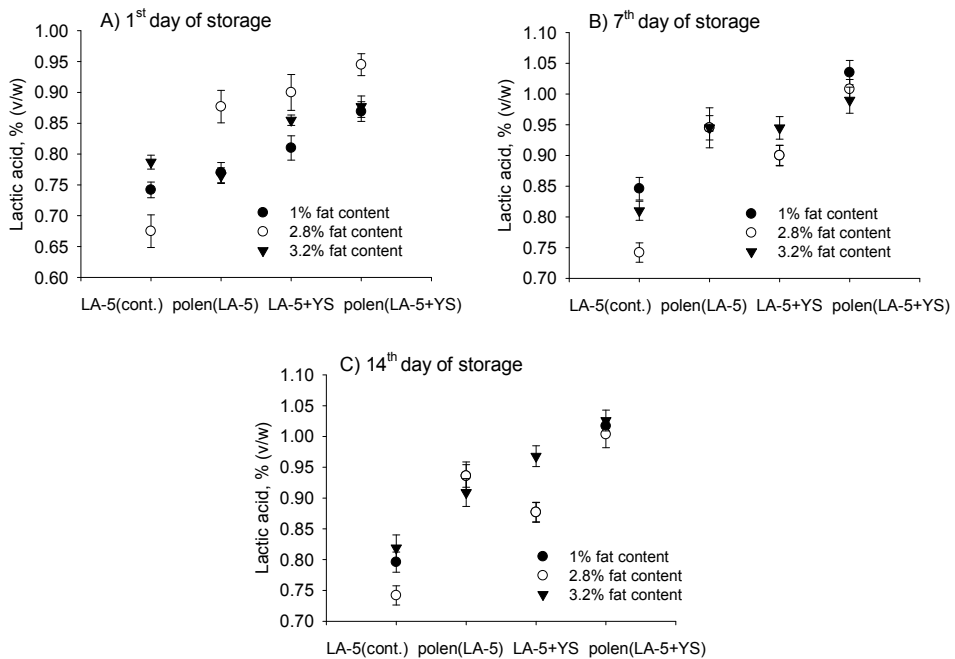


Figure 3. Lactic acid content (%) of acidophilus milk and probiotic yoghurt depending of milk fat content after 1st (A), 7th (B) and 14th storage days (C)

On the other days of storage, the production of lactic acid was not influenced by the fat level. The previously reported results by Shakerian et al. (12) showed that different levels of fat had significant effects on the acetic and lactic acid production in *B. animalis* and *L. acidophilus* yoghurt, but the trend was not linear. Furthermore, it was observed that the addition of honeybee pollen increased the production of lactic acid, regardless of the fat level (Fig. 3), which is in agreement with the results obtained by Khider et al. (11)

who found that different types of honeybee pollen induced an increase in the lactic acid production in yoghurts.

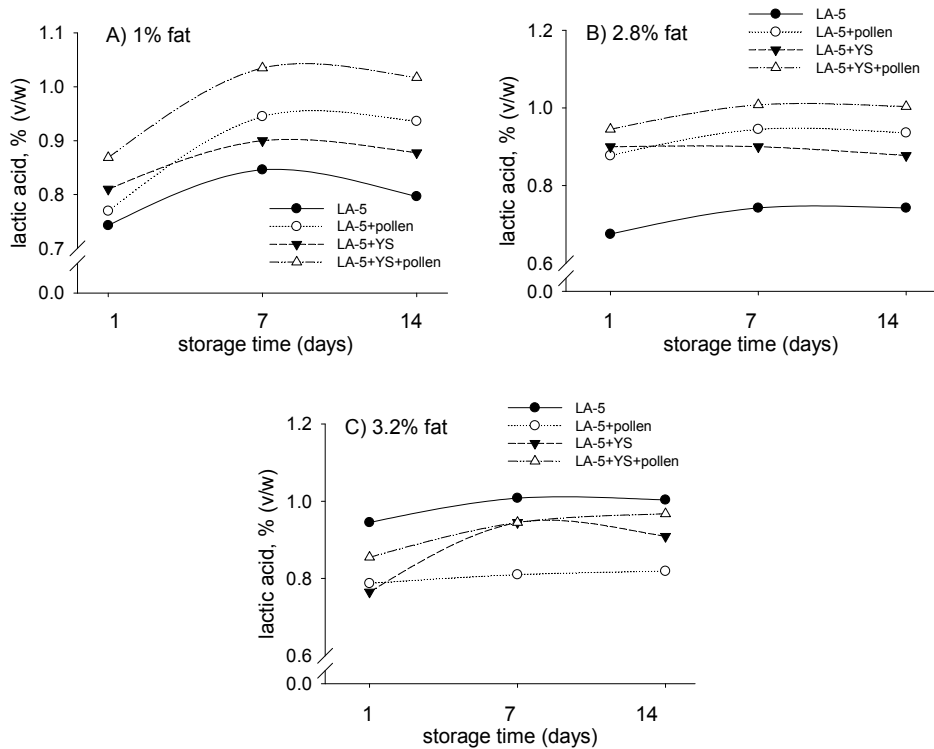


Figure 4. Lactic acid content (%) of acidophilus milk and probiotic yoghurt depending of storage time and honeybee pollen addition (0.6%) in acidophilus milk and probiotic yoghurt made from milk with different fat content: 1% fat (A), 2.8% fat (B) and 3.2% fat (C)

The effects of the addition of honeybee pollen on the production of lactic acid were significantly higher ($p < 0.05$) after the 7th and 14th day of storage for all fermented milks produced from 1% and 2.8% fat milk (Fig. 4.A,B). Furthermore, the effects of different starters on the production of lactic acid were also different, but not as obvious as that due to pollen addition. The production of lactic acid was in favour of probiotic yoghurt, respectively addition of yoghurt starter (*S. thermophilus* and *L. delbrueckii* ssp. *bulgaricus*) induced an increase in the production of lactic acid than *L. acidophilus* LA-5 alone. However, it is well known that *L. acidophilus* LA-5 with lactic acid content in range 1-2% w/w is acid-tolerant in acidophilus milk (13). This is not observed in our studies, probably due to a low inoculation rate compared with the rate recommended in the literature (2-5% inoculum) (13).

The data presented in Table 1 show the values of total solids in the fermented milks. There were significant differences ($p \leq 0.05$) in the total solids between probiotic yoghurt and acidophilus milk made with 2.8% fat milk, but no significant differences ($p \geq 0.05$) were observed due to the honeybee pollen addition. Generally, it was noticed that the lower values of total solids were recorded for probiotic yoghurt, which could be related to better consumption of lactose by *Sc. thermophilus* and *L. delbrueckii* ssp. *bulgaricus*, than by *L. acidophilus* LA-5, which was previously reported (14).

Table 1. Total solids of acidophilus milk, probiotic yoghurt, raw milks and honeybee pollen (mean±SD)

Sample	Milk fat content (% w/w)		
	1%	2.8%	3.2%
	LA-5	9.049±0.032 ^a	10.600±0.127 ^{ab}
LA-5+pollen	9.414±0.260 ^a	10.895±0.078 ^b	11.275±0.304 ^a
LA-5+YS	8.884±0.005 ^a	10.150±0.028 ^c	10.870±0.042 ^a
LA-5+YS+pollen	9.011±0.028 ^a	10.450±0.085 ^{ac}	11.035±0.106 ^a
Milk	9.000±0.033	10.790±0.027	11.005±0.054
Pollen	76.952±0.999		

^{abc} Means in a column with different letters differ significantly ($p \leq 0.05$, Holm-Sidak test)

Sensory evaluation scores of fermented milks after 14th day of storage are presented in Fig. 5. The appearance, colour, odour, and consistency had the highest scores for all samples at the beginning (data not shown) and at the end of the storage.

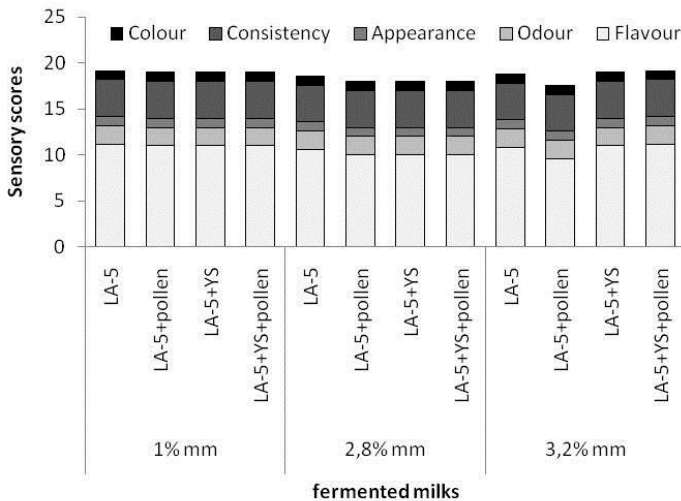


Figure 5. Sensory evaluation scores of fermented milks products after 14th day of storage

The best average flavour scores at the end of storage had acidophilus milk made from 1% fat milk. The addition of honeybee pollen caused slightly bean-like flavour but acceptable, which was previously reported also for date palm pollen (11). The effects of different starters (*L. acidophilus* LA-5, *Sc. thermophilus* and *L. delbrueckii* ssp. *bulgaricus*) or different fat levels did not influence the taste of the fermented milks or flavour scores.

CONCLUSION

The obtained results showed that the addition of honeybee pollen had a positive effects on the physicochemical and sensory properties of produced acidophilus milk and probiotic yoghurt. The results indicate that honeybee pollen may encourage the growth of lactic acid bacterial starters used and subsequently increase the lactic acid production, which also led to a slight decrease in the pH values during the storage. The knowledge obtained from this study could be applied for the development of a novel formulation for functional food enriched with honeybee pollen.

Acknowledgement

The authors would like to thank MTC-SO, Sombor, Serbia, for supplying free samples of starter culture.

REFERENCES

1. de Vrese, M.; Kristen, H.; Rautenberg, P.; Laue, C.; Schrezenmeir, J. Probiotic lactobacilli and bifidobacteria in a fermented milk product with added fruit preparation reduce antibiotic associated diarrhea and Helicobacter pylori activity. *J.Dairy Res.* **2011**, *78* (4), 1-8.
2. Kosikowski, F.V. and Mistry, V.V. Fermented milks. In *Cheese and Fermented Milk Foods*. Vol. 2. 3rd, Eds., F. V. Kosikowski, F.V., Westport, CT; 1997; pp 57-75.
3. Vedamuthu, E.R. Other fermented and culture-containing milks. In *Manufacturing Yogurt and Fermented Milks*, Eds. Chandan, R.C., and Kilara, A.; Wiley-Blackwell, New Jersey, 2013; pp 404-406.
4. Xu, X.; Sun, L.; Dong, J., Zhang, H. Breaking the cells of rape bee pollen and consecutive extraction of functional oil with supercritical carbon oxide. *Innovat. Food Sci. Emerg. Tech.* **2009**, *10*, 42-46.
5. Carpes, S.T.; Mourao, G.B.; Alencar, S.M.; Masson, M.L. Chemical composition and free radical scavenging activity of *Apis mellifera* bee pollen from Southern Brazil. *Brazilian J. Food Technol.* **2009**, *12*, 220-229.
6. Graikou, K.; Kapeta, S.; Aligiannis, N.; Sotiroidis, G.; Chondrogianni, N.; Gonos, E.; Chinou, I. Chemical analysis of Greek pollen - Antioxidant, antimicrobial and protease activation properties. *Chem Cent. J.* **2011**, *5* (33). doi: 10.1186/1752-153X-5-33.
7. Nakajima, Y.; Tsuruma, K.; Shimazawa, M.; Mishima S.; Hara, H. Comparison of bee products based on assays of antioxidant Capacities. *BMC Complement Altern Med.* **2009**, *9* (4) doi: 10.1186/1472-6882-9-4.

8. Sabadoš, D. Kontrola i ocjenjivanje kakvoće mlijeka i mliječnih proizvoda, 2. Dopunjeno izdanje, Hrvatsko mljekarsko društvo RH, Zagreb, 1996.
9. International Dairy Federation method, IDF 1984. Fermented milks, Bulletin of the IDF 179.
10. Iancu, B.; Nicolau, I. Attempts to obtain a new symbiotic product based on soy milk. *Innovative Romanian Food Biotechnology*. **2010**, 7, 21-29.
11. Khider, M.; Elbanna, K.; Mahmoud, A.; Owayss, A.A. Egyptian honeybee pollen as antimicrobial, antioxidant agents, and dietary food supplements. *Food Sci. Biotechnol.* **2013**, 22(5), 1-9.
12. Shakerian, M.; Hadi Razavi, S.; Khodaiyan, F.; Ziai, S. A.; Saeid Yarmand, M.; Moayedi, A. Effect of different levels of fat and inulin on the microbial growth and metabolites in probiotic yogurt containing nonviable bacteria. *Int. J Food Sci. Tech.* **2014**, 49, 261-268.
13. Niamsiri, N. Dairy Products. In *Encyclopedia of Microbiology*, Third Edition, Schaechter, M., Elsevier Inc., 2009, pp.42
14. Sodini, I.; Lucas, A.; Oliveira, M.N.; Remeuf, F.; Corrieu, G. Effect of Milk Base and Starter Culture on Acidification, Texture, and Probiotic Cell Counts in Fermented Milk Processing. *J Dairy Sci.* **2002**, 85(10), 2479-88.

ФИЗИЧКОХЕМИЈСКЕ ОСОБИНЕ АЦИДОФИЛНОГ МЛЕКА И ПРОБИОТСКОГ ЈОГУРТА СА ДОДАТКОМ ПОЛЕНА

Јована Р. Глушац¹, Милка Ј. Ступевић¹, Спасенија М. Милановић²,
Драгица М. Ђурђевић-Милошевић³

¹ Висока медицинска школа Приједор, Николе Пашића 4а, 79101 Приједор, Босна и Херцеговина,

² Универзитет у Новом Саду, Технолошки факултет, Булевар Цара Лазара 1, Нови Сад, Србија

³ МП Лаб, МП Био д.о.о., Прокупачка 41, Београд, Србија

У раду је испитана могућност производње ацидофилног млека и пробиотског јогурта од млека са различитим садржајем млечне масти (1%, 2.8% и 3.2%) и уз додатак полена (0.6%). Квалитет произведених узорака праћен је мерењем рН вредности током ферментације и складиштења, те мерењем садржаја млечне киселине и сензорских особина током 14 дана складиштења. На брзину ферментација је знатно више утицала starter култура, него додатак полена или садржај млечне масти. Доплатак полена је значајно утицао на продукцију млечне киселине током складиштења, без обзира на ниво млечне масти. Утицај starter култура (*L. acidophilus* LA-5, *S. thermophilus* and *L. delbrueckii ssp. bulgaricus*) на продукцију млечне киселине није био тако значајан као утицај додатка полена. Генерално, додатак полена је утицао на побољшање физичкохемијских и сензорских карактеристика произведеног ацидофилног млека и пробиотског јогурта.

Кључне речи: ацидофилно млеко, пробиотски јогурт, полен, физичкохемијске карактеристике

Received: 9 February 2015.

Accepted: 15 July 2015.

INFLUENCE OF FAT CONTENT AND STARTER CULTURES ON THE QUALITY OF FERMENTED DAIRY PRODUCTS

Mirela D. Iličić*, Spasenija D. Milanović, Dajana V. Hrnjez, Katarina G. Kanurić,
Vladimir R. Vukić and Marjan I. Ranogajec

University of Novi Sad, Faculty of Technology, Bulevar cara Lazara 1, 21000 Novi Sad, Serbia

The objective of this study was to investigate the effect of fat content and type of the starter culture (traditional or probiotic) on physico-chemical quality, rheological and textural characteristics of the fermented dairy products during 14 days of storage. Seven different fermented dairy products of two different groups: stirred and set yoghurts were used in this study. The rheological and textural characteristics of the analyzed type of fermented dairy products after the production and during storage are dependent on the chemical composition, particularly fat content.

KEY WORDS: fermented milk products, starter cultures, rheology, texture

INTRODUCTION

Fermented dairy products play an important role in the human diet, as a very important part of the modern life style. These products are very diverse groups of high valuable nutritional products. They are produced in strictly controlled and technologically defined conditions by fermentation with selected microorganisms – starter cultures (1, 2). Great progress in modern technology of fermented dairy products has been made by the development of new types of starter culture – probiotic bacteria, like *Lactobacillus* and *Bifidobacterium* strains (3). These strains can be used instead of the traditional thermophilic starter cultures (*Streptococcus thermophilus* and *Lactobacillus delbrueckii* spp. *bulgaricus*) (4). Nowadays, the fermented dairy beverages are produced with different fat content and enriched with a variety of ingredients (milk proteins concentrate, whey proteins concentrate, skim milk powder, casein, vitamins, inulin, etc.), different aromatic and functional ingredients (5-8).

In order to enhance the quality of fermented dairy products, beside the optimization of a technological process and choice of starter culture, a variety of ingredients with known chemical composition is used (9-13). Structure of the gel and its textural characteristics are influenced by several factors, including proteins concentration, incubation temperature, heat treatment of the milk, and type of starter culture (14).

* Corresponding author: Mirela D. Iličić, University of Novi Sad, Faculty of technology, Bulevar cara Lazara 1, 21000 Novi Sad, Serbia, e-mail: panim@uns.ac.rs

The aim of this study was to investigate the influence of fat content and type of the starter culture (traditional or probiotic) on physico-chemical quality, rheological and textural characteristics of the fermented dairy products during 14 days of storage.

EXPERIMENTAL

Materials

In this study, the quality of seven different commercial fermented dairy products were analyzed:

- Sample 1 – yoghurt produced from pasteurized milk with 3.2% milk fat;
- Sample 2 – yoghurt produced from pasteurized skim milk with 0% fat;
- Sample 3 – fermented dairy product from pasteurized milk with 1% fat and probiotic starter cultures and 1.5% oligofructose;
- Sample 4 – yoghurt produced from pasteurized milk with 2% fat;
- Sample 5 – sour milk produced from organic milk with 2.8% fat;
- Sample 6 – Greek style yoghurt from pasteurized and homogenized extra fat milk with 9.7% fat;
- Sample 7 – sour milk produced from milk with 6% fat.

Methods

Physico-chemical analyses of different types of fermented dairy products were performed by the following methods (15): pH value – with a pH meter (EcoScan pH6, Eutech Instruments, Nijkerk, Netherlands); total solids (TS)-(IDF/ISO21:2010); total proteins - by Kjeldahl method (SRPS EN ISO 8968-1:2008); ash content - by the incineration at the temperature of 550°C (IDF 90:1979); while total sugar content was calculated as follows:

$$\text{total sugar} = \text{total solids} - (\text{total proteins} + \text{milk fat} + \text{ash}) \quad [1]$$

and the energy value from the following formula:

$$\text{Energy value} = (\text{protein \%} \times 4.4 + \text{milk fat \%} \times 9.3 + \text{total sugar \%} \times 4.1) \times 4.186 \text{ (kJ/100g)} \quad [2]$$

Textural characteristics (firmness, consistency, cohesiveness and index of viscosity) were measured on a Texture Analyser TA XD plus (Stable Micro System, Godalming, England) at +4°C. The force of compression was measured using back extrusion cell (A/BE) with a diameter of 35 mm, and using 5 kg load cell. The option „Return to Start“ was used and a speed disk displacement before and during the test was 1.0 mm/s. The disk had exceeded the distance of 30 mm. Replicate measurements of firmness for each sample were done independently after 1st, 7th and 14th day of storage.

Viscosity of samples was measured at +4°C using a viscometer HAAKE RheoStress 600HP (Karlsruhe, Germany) with cone and plate sensor PP60Ti (gap 1 mm). Hysteresis loop area was recorded at increasing shear rate from 0 to 200 s, followed by its decrease in

the same span within 180 s of downward flow curve. The thixotropic test was initially applied to characterize the flow behavior of the samples and was calculated by RheoWin Data Manager 4 program package (Thermo Haake, Karlsruhe, Germany).

Statistical analysis of the results was carried out using the computer software program "Statistica 9" and were expressed as average, standard deviation of values obtained in three independent experiments.

RESULTS AND DISCUSSION

Physico-chemical characteristics of fermented dairy products

According to the results presented in Table 1, the pH values of stirred yoghurt (samples 1, 2, 3 and 4) were between 4.22 (sample 1) and 4.40 (sample 3). The values for set yoghurt varied between 4.17 (sample 7) and 4.54 (sample 6). The content of total solids and milk components depended on product type. The lowest total solids had stirred yoghurt – sample 2 (9.05%). Energy values of fermented products varied in dependence of milk fat content.

Table 1. Chemical composition and energy value of fermented dairy products

Sample	pH	Total solids (%)	Total solids without fat (%)	Ash (%)	Total protein (%)	Total sugar (%)	Energy value (kJ/100g)
1	4.22	11.59	8.29	0.77	2.99	4.53	261
2	4.23	9.05	8.95	0.70	3.12	5.03	148
3	4.40	11.14	10.04	0.76	3.08	6.20	206
4	4.30	10.63	7.54	0.74	2.93	3.86	241
5	4.28	11.85	7.67	0.71	3.06	3.88	286
6	4.54	17.35	8.11	0.89	3.29	3.97	487
7	4.17	16.16	8.68	0.86	3.48	4.32	430

Rheological characteristics of fermented dairy products

The rheological characteristics were analyzed after production and after 14th day of storage of the samples at +4°C. The obtained results indicate that all samples are thixotropic system (Figure 1). All fermented dairy products exhibited a typical shear thinning, thixotropic and time-dependent flow behavior as described by Rohm (1993) (8) and Patocka et al. (2007) (10). A higher yield stress was noticed in the type of set yoghurts than in stirred yoghurts, which is a result of better networking of its matrix and absence of final stirring. It was noticed that the samples produced from milk with 3.2% fat had significantly higher yield shear stress than samples produced from milk with 0 and 1.0% fat in the group of stirred yoghurts. These values were in accordance with the literature data (16-18).

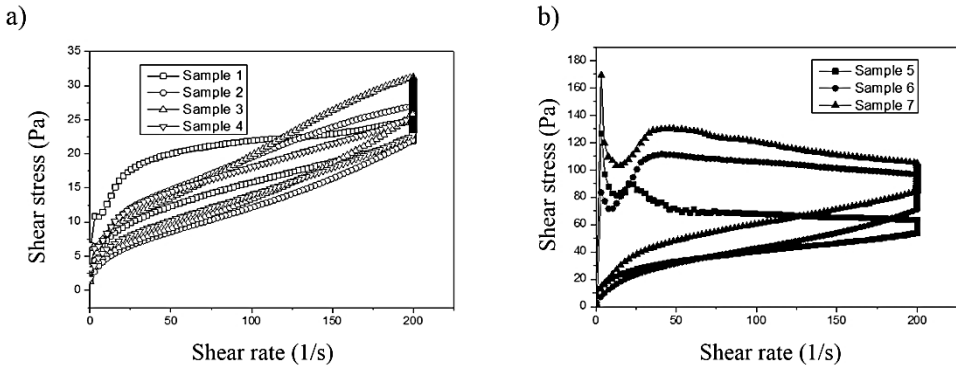


Figure 1. The flow curves after production at +4°C: a) stirred yoghurt, b) set yoghurt.

During the storage (14 days), all samples of stirred yoghurt showed similar rheological characteristics compared to this properties after the production. Two set yoghurt (samples 5 and 7) had better rheological properties and higher value of yield stress compared to the values after production (Figure 2).

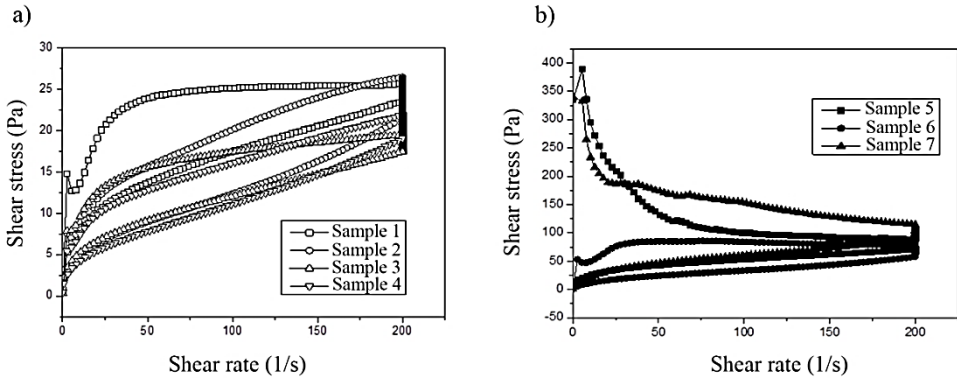


Figure 2. The flow curves after 14 day of storage at +4°C: a) stirred yoghurt and b) the set yoghurt.

Values of the hysteresis loop area were calculated based on the flow curves of fermented dairy products (Figure 3). The hysteresis loop area (HLA) is the indicator of yoghurt structural breakdown and rebuilding (degree of thixotropy) during shearing (19, 20). Samples of the set yoghurts showed the highest hysteresis loop area values at +4°C, followed by the samples of stirred yoghurt. The highest values of HLA in set yoghurt indicate better structural reversibility of these samples during the shearing. The differences in the value of HLA among different types of fermented milk products could be explained by a structuring effect of using starter culture, different chemical composition of samples, and process parameters during the manufacture (18, 21). The average HLA va-

lue of stirred fermented dairy products is 1180 Pa/s. The set yoghurt samples had much higher values of HLA, then stirred yoghurt, and also higher values in comparison to the literature data.

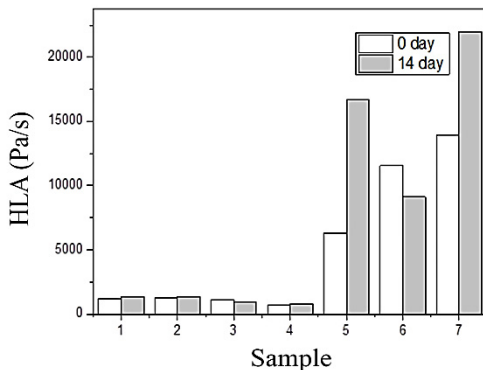


Figure 3. Hysteresis loop area of fermented milk products

These results are in correlation with the results of textural characteristics which were also higher after 14 days of storage.

Textural characteristics of fermented dairy products

Textural characteristics of fermented dairy products after the production are presented in Table 2. The type of fermented milk products and its chemical composition had significant impact on the overall textural characteristics of the samples, which is also presented in the literature (22, 23).

Table 2. Textural characteristics of fermented dairy products after production

Sample	Firmness (g)	Consistency (gs)	Cohesiveness (g)	Index of viscosity (gs)
1	17.207±1.27	435.508±30.84	-11.352±1.40	-7.556±1.89
2	13.979±0.22	354.037±4.88	-8.632±0.29	-3.109±0.10
3	13.468±0.13	346.188±5.77	-8.384±0.10	-3.048±0.07
4	13.949±0.36	352.534±5.57	-8.241±0.11	-2.975±0.16
5	192.268	3667.425	-101.455	-206.740
6	38.157±0.68	914.412±46.12	-25.824±0.66	-75.135±1.61
7	356.994	7119.068	-177.505	-338.767

The lowest firmness was obtained for the samples of stirred yoghurts. The firmness of stirred yoghurt (samples 1, 2, 3 and 4) was between 13.468 g (sample 3) and 17.207g (sample 1). The lowest firmness for the set yoghurt had sample 6 (38.157g) and the highest sample 7 (356.994g). Like firmness, the lowest cohesiveness was obtained for stirred yog-

hurt, between -8.241g (sample 4) and -11.352g (sample 1). The set yoghurts had higher cohesiveness. Among them, sample 6 again had the lowest (-25.824 g) and sample 7 the highest value (-177.505g).

Moreover, sample 7 of set yoghurt had the highest value of textural characteristics, which is in correlation with the chemical composition. As it was expected, the stirred yoghurt had significantly lower values of all textural characteristics due to the different technological process of production and final stirring of the products. Even, addition of 1.5 % oligofructose to samples 3 did not improve its textural characteristics, which indicated a more significant impact of the milk fat content (sample 1-3.2% milk fat, sample 3-1.0% milk fat) on textural characteristics of this type of fermented milk products. These results are in correlation with the rheological characteristics and chemical compositions of the samples.

During the storage, the textural characteristics of all types of fermented dairy products changed. The changes of firmness of the samples are shown in Figure 4. The obtained values of firmness were higher on the 14th day than on the 7th day of storage. The activity of the applied starter culture (postacidification) and fat content during the storage had a great influence on the measured values of firmness. These results are in concordance with the previous data (17,18).

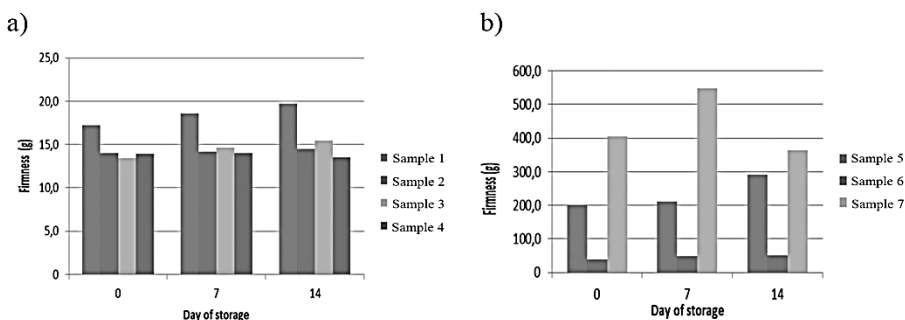


Figure 4. Firmness of fermented milk products during storage: a) stirred yoghurt, b) set yoghurt

CONCLUSION

The differences in the physico-chemical, rheological and textural characteristics between two groups (seven samples) of fermented dairy products after the production and during 14 days of storage were observed.

The obtained results showed that the total solids, milk fat content and starter cultures had great influence on the quality of the analyzed samples. The highest yield stress and hysteresis loop area were noticed in the type of set yoghurts. The results of the rheological parameters of fermented dairy products are in correlation with their textural characteristics.

Set yoghurts had better textural characteristic (firmness, consistency, cohesiveness and index of viscosity) in comparisons to stirred yoghurt samples. Generally, during the

storage samples of stirred and set yoghurt showed better rheological properties and higher firmness compared to the values after the production.

Acknowledgement

Authors want to thank the Ministry of Education, Science and Technological Development of the Republic of Serbia for the financial support of investigations presented in this article, Project No. III 46009.

REFERENCES

1. Surono, I.S.; Hosono, A. Fermented milks, Types and standards of identity. In: *Encyclopedia of Dairy Sciences*, Fuquay, P.F, Fox, P.L.H, McSweeney, J.W. (Eds) Press: Elsevier, Academic Press: London, UK, 2011; pp 470-476.
2. Morgensen, G.; Salminen, S.; O'Brien, J.; Ouwehand, A.C.; Holzapfel, W.H.; Shortt, C. Food microorganisms: Health benefits, safety evaluation and strains with documented history of use in foods. *Bulletin - International Dairy Federation*. **2002**, 377, 4-9.
3. Matilla-Sandholm, T.; Myllarinen, P.; Crittenden, R.; Mogensen, G.; Fonden, R., Saarela, M. Technological challenges for future probiotic food. *Int Dairy J*. **2002**, 12, 173-182.
4. Marafon, A.P.; Sumi, A.; Alcântara, M.R.; Tamime, A.Y.; Oliveira, M.N. Optimization of rheological properties of probiotic yoghurts supplemented with milk proteins. *LWT-Food Sci Technol*. **2011**, 44, 511-519.
5. Stijepić, M.; Milanović, S.; Glušac, J.; Đurđević-Milošević, D. Primjena različitih do-dataka u proizvodnji fermentisanih mliječnih napitaka. *Prehrambena industrija-Mleko i mlečni proizvodi*. **2013**, 24, 29-37.
6. Milanović, S.; Iličić, M.; Đurić, M.; Carić, M. Effect of transglutaminase and whey protein concentrate on textural characteristics of low fat fermented milk produced with probiotic starter. *Milchwissenschaft*. **2009**, 4, 388-392.
7. Madjoska, V.; Srbínovska, S.; Sterjovski, S. The influence of whey proteins on the sensory properties of yoghurt. *Prehrambena industrija-Mleko i mlečni proizvodi*. **2013**, 24, 1, 37-42.
8. Rohm, H.: Influence of dry matter fortification on flow properties of yoghurt 2. Time dependant behavior. *Milchwisenschaft*. **1993**, 48, 614-617.
9. Oliveira, R.P.S.; Florence, A.C.R.; Silva, R.C.; Prego, P.; Converti, A.; Gioielli, L.A.; Oliveira, M.N. Effect of different prebiotics on the fermentation kinetics, probiotic survival and fatty acids profiles in nonfat symbiotic fermented milk. *Int J Food Microbiol*. **2009**, 128, 467-472.
10. Patocka, G.; Cervenkova, R.; Narine, S.; Jelen, P. Rheological behaviour of dairy products as affected by soluble whey protein isolate. *Int Dairy J*. **2005**, 16, 399-405.
11. Hoppert, K.; Zahn, S.; Jänecke, L.; Mai, R.; Hoffmann, S.; Rhom, H.: Consumer acceptance of regular and reduced-sugar yoghurt enriched with different types of dietary fiber. *Int Dairy J*. **2013**, 28, 1, 1-7.
12. Loveday, S.; Sarkar, A.; Singh, H. Innovative yoghurts: Novel processing technologies for improving acid milk gel texture. *Trends Food Sci Tech*. **2013**, 33, 5-20.

13. Harte, F.; Luedecke, L.; Swanson, B.; Barbosa-Cánovas, G.V. Low-fat set yogurt made from milk subjected to combinations of high hydrostatic pressure and thermal processing. *J Dairy Sci.* **2003**, *86*, 1074-1082.
14. Sandoval-Castilla, O.; Lobato-Calleros, C.; Aguirre-Mandujano E.; Vernon-Carter, E. J.: Microstructure and texture of yogurt as influenced by fat replacers. *Int Dairy J.* **2004**, *14* (2), 151-159.
15. Carić, M.; Milanović, S.; Vucelja, D. *Standardne metode analize mleka i mlečnih proizvoda*, Prometej, Novi Sad, 2000, pp 25-91.
16. Iličić, M.; Milanović, S.; Carić, M.; Vukić, V.; Kanurić, K.; Ranogajec, M.; Hrnjez, D. The effect of transglutaminase on rheology and texture of fermented milk products. *J Texture Stud.* **2013**, *44*, 160-168.
17. Vélez-Ruiz, J. F. Rheological Properties of Yoghurt. In: Progress in Food Engineering Research and Development, Cantor, J. M., Ed.; Nova Science Publishers, Inc.: New York, 2008; pp. 223-242.
18. Tamime, A.Y., Robinson, R.K. *Yoghurt, Science and Technology*; Woodhead Publishing Limited: Cambridge England, 2004; pp.619.
19. Paseophol, T.; Small, D.; M., Sherkat, F. Rheology and texture of set yoghurt as affected by inulin addition. *J Texture Stud.* **2008**, *39*, 617-634.
20. Hassen, A.N.; Ipsen R.; Janzen, T.; Qvist, K. B. Microstructure and rheology of yoghurt made with culture differing only in their ability to produce exopolysaccharides. *J Dairy Sci.* **2003**, *86*, 1632-1638.
21. Iličić, M.; Milanović, S.; Kanurić, K.; Vukić, V.; Hrnjez, D. The effect of processing parameters on the structure of fermented milk products with transglutaminase addition during storage. *APTEFF.* **2013**, *44*, 67-73.
22. Kip, P.; Meyer, D.; Jellema, R. H. Inulins improve sensoric and textural properties of low-fat yoghurts. *Int Dairy J.* **2006**, *16*, 1098-1103.
23. Guggisberg, D.; Cuthbert-Steven, J.; Piccinah, P.; Butikofer, U.; Eberhard, P. Rheological, microstructural and sensory characterization of low-fat and whole milk set yogurt as influenced by inulin addition. *Int Dairy J.* **2009**, *19*, 107-115.

УТИЦАЈ САДРЖАЈА МЛЕЧНЕ МАСТИ И СТАРТЕР КУЛТУРЕ НА КВАЛИТЕТ ФЕРМЕНТИСАНИХ МЛЕЧНИХ ПРОИЗВОДА

*Мирела Д. Иличих**, *Спасенија Д. Милановић*, *Дајана В. Хрњез*,
Катарина Г. Канурић, *Владимир Р. Вукић*, *Марјан И. Раногајец*

Универзитет у Новом Саду, Технолошки факултет, Булевар цара Лазара 1, 21000 Нови Сад, Србија

Испитан је утицај масти и врсте стартер културе на физичко-хемијски квалитет, реолошке и текстуалне карактеристике ферментисаних млечних производа током 14 дана складиштења. Анализиране су две различите групе ферментисаних млечних производа: течни и чврсти јогурт.

Узорци чврстог јогурта имају боља реолошка својства и веће вредности текстуалних карактеристика (чврстоћа, конзистенција, кохезивност и индекс вискозитете-

та) у поређењу са узорцима течног јогурта. Током периода складиштења узорци течног јогурта показују сличне карактеристике, као и након производње. Вредности приносног напона, површине хистерезисне петље и чврстоће су веће код два узорка чврстог јогурта током складиштења у поређењу са анализираним параметрима након производње.

Кључне речи: ферментисани млечни производи, стартер културе, реологија, текстура

Received: 14 July 2015.
Accepted: 11 October 2015.

LIPID AND SUGAR PROFILES OF VARIOUS BARLEY CULTIVARS (*Hordeum vulgare*)

Kristian A. Pastor^{1*}, Marijana M. Ačanski¹, Djura N. Vujić¹, Ankica Đ. Kondić-Špika²
and Nikola S. Hristov²

¹ University of Novi Sad, Faculty of Technology, Bulevar cara Lazara 1, 21000 Novi Sad, Serbia

² Institute of Field and Vegetable Crops, Maksima Gorkog 30, 21000 Novi Sad, Serbia

*The lipid components and soluble sugars in flour samples of different cultivars of barley (*Hordeum vulgare*), involving winter malting barley, winter forage barley, spring barley, and hullless barley, were identified). Fatty acids were extracted from flour samples with n-hexane, and derivatized into volatile methyl esters, using TMSH (trimethylsulfonium hydroxide) in methanol. Soluble sugars were extracted from defatted and dried samples of barley flour with 96% ethanol, and further derivatized into the corresponding trimethylsilyl (TMS) oximes, using hydroxylamine hydrochloride solution and BSTFA (N,O-bis-(trimethylsilyl)-trifluoroacetamide). The hexane and alcoholic extracts of barley cultivars were analyzed by GC-MS system. Lipid and sugar compositions were very similar in all barley cultivars. Therefore, multivariate analysis was applied to numerical values of automatically integrated areas of the identified fatty acid methyl esters and TMS oximes of soluble sugars. The application of hierarchical cluster analysis showed a great similarity between the investigated flour samples of barley cultivars, according to their fatty acid content (0.96). Also, significant, but somewhat less similarity was observed regarding the content of soluble sugars (0.70). These preliminary results indicate the possibility of distinguishing flour made of barley, regardless of the variety, from flours made of other cereal species, just by the analysis of the contents of fatty acids and soluble sugars.*

KEY WORDS: barley cultivars, lipid composition, soluble sugar composition, GC-MS, cluster analysis

INTRODUCTION

Research involving non-wheat flours has been stimulated tremendously by world food problems resulting primarily from expanding populations. Developing countries are much too dependent on costly imported grain; insufficient food and inadequate nutrition are widespread problems. Non-wheat flours have the potential of being economically benefi-

* Corresponding author: Pastor Kristian, University of Novi Sad, Faculty of Technology, Bulevar Cara Lazara 1, 21000 Novi Sad, Serbia, e-mail: pastor@tf.uns.ac.rs

cial to both developing and industrial countries and of making large nutritional contributions, particularly in developing countries (1). Small grains of high quality have been dominant on the world market in the last decade. Special importance is given to the improvement of yield and quality potential of alternative small grains due to their constant demand and shortage on the world market. Improvement of small grains processing has great potential primarily in increasing quality of raw materials, improvement of processing equipment and quality of final products, which would significantly affect the commercial sector (new products, new processing methods, expanding the range of small grain products etc.) (2). Barley (*Hordeum vulgare*) is used almost entirely as feed and as a grain for brewing and for ethanol production (1). Fortification of bread with barley significantly improves the nutritional quality of bread due to increased levels of dietary fiber and β -glucans, and qualifies the product (in some countries) to carry a health claim, relating the presence of β -glucans with reducing the risk of cardiovascular diseases, heart diseases, constipation (3) and type II diabetes (4).

Barley is a rich source of tocopherols, including tocopherols and tocotrienols, which are known to reduce serum LDL cholesterol through their antioxidant action (5). Soong et al. (2014) investigated total phenolic content, which is found to be positively correlated with total antioxidative capacity in muffins made of different cereal species. They proved that muffins made with barley flour had the highest phenolic content compared to corn, oat, wheat and rice (6). Wholegrain barley foods also appear to be associated with increased satiety and weight loss.

There is great potential to utilize barley in a large number of cereal-based food products as a substitute partially or wholly for currently used cereal grains such as wheat (*Triticum aestivum*), oat (*Avena sativa*), rice (*Oryza sativa*), and maize (*Zea mays*).

Barley is arguably the most widely adapted cereal grain species with production at higher latitudes and altitudes and farther into deserts than any other cereal crop. It is in extreme climates that barley remains a principal food source today, e.g., Himalayan nations, Ethiopia, and Morocco.

The aim of this study consists of two different parts: (i) the application of gas chromatography-mass spectrometry system (GC-MS) to determine lipid and soluble sugar composition in hexane and ethanol extracts of various barley cultivars; and (ii) the application of multivariate data analysis to investigate the similarity of analyzed cultivars and the possibility to determine the authenticity of barley flour based upon mutual similarities among the samples, considering the importance of barley flour addition in non-wheat and mixed flour bakery products. These results could be integrated in the procedures for flour quality assurance.

EXPERIMENTAL

Sample preparation

All analyzed barley samples were obtained from the Small Grains Department at the Institute of Field and Vegetable Crops "NS Seme", Novi Sad, Serbia: three cultivars of winter malting barley (Novosadski 525 - B1, NS Pinon - B2, NS Zitos - B3), three culti-

vars of winter forage barley (Atlas - B4, Somborac - B5, Rudnik - B6), one spring barley cultivar (NS Marko - B7), and one hullless barley cultivar (Golijat - B8). All barley samples were grown in the same year and at the same location, thus enabling a comparison independent from the differences in the environmental conditions.

About 10 g of each barley cultivar were ground using a laboratory mill (Falling number 3100, Sweden). An amount of 0.5 g of barley flour sample was poured in a 12 mL cuvette for centrifugation. The cuvette was afterwards filled with 5 mL of n-hexane and stirred on Vortex for 2 min, after which the mixture was centrifuged at 2000 rpm for 5 min. A volume of 3.00 mL of clear supernatant of each sample was separated into a 10 mL glass beaker and dried under nitrogen flow. The residue was first dissolved in 400 μ L of methylene chloride, and then 100 μ L of 0.2 M *trimethylsulfonium hydroxide* in methanol (TMSH, Macherey–Nagel) was added, to achieve the derivatization into volatile methyl-esters (7).

After removing the hexane fractions, the barley flour samples remained defatted. Samples of defatted flour were dried in the air. 5 mL of 96% ethanol (Merck) was added to each dried sample. The mixture was vortexed for 2 min and centrifuged at 2000 rpm for 5 min. A volume of 2.00 mL of clear supernatant was separated and 50 μ L of 10% sodium hydroxide in ethanol and 50 μ L of 10% hydroxylamine hydrochloride solution were then added, through which oximes of sugars were obtained in ethanol solution. The mixture was dried under nitrogen flow. The residue was first dissolved in 400 μ L of methylene chloride and 50 μ L of BSTFA (N,O-bis-(trimethylsilyl)-trifluoroacetamide, Macherey-Nagel) was added, by oximes were derivatized into trimethylsilyl-oximes (TMSO) (8). By creating TMSO, two peaks corresponding to the syn (E) and anti (Z) forms per reducing sugar are obtained and a single peak for any non-reducing carbohydrate which does not form oximes. These derivatives are applicable to both aldoses and ketoses, and have been widely used for the determination of carbohydrate complex mixtures, such as flour of cereals, as they present good GC properties and provide simple chromatograms (9).

All samples were prepared and analyzed in triplicates.

GC-MS analysis

The GC-MS analyses were performed on an Agilent Technologies 7890 gas chromatograph coupled to 5975 mass spectrometer (Agilent Technologies, Palo Alto, CA, USA), operating in EI mode at 70 eV. A DB-5 MS column (30m \times 0.25mm \times 25 μ m) was used. The same experimental conditions were used to determine both lipid and simple sugar profiles. The temperature program was: 50-130°C at 30°C/min and 130-300°C at 10°C/min. The injector temperature was 250°C. The flow rate of the carrier gas (helium) was 0.8 mL/min. A split ratio of 1:50 was used for the injection of 1 μ L of sample solutions.

Data processing

The analysis of the obtained chromatograms was performed using the MSD Productivity ChemStation program. WILEY 275 library was used for the mass spectra analysis.

PAST program was used for statistical data processing (10). Hierarchical cluster analysis of integrated surface areas of derivatized lipid and simple sugar compounds were performed. Data points were clustered using paired group algorithm and correlation similarity measure.

RESULTS AND DISCUSSION

Figure 1 shows the overlaid chromatograms of 8 samples of barley flour extracts: (A) overlaid chromatograms of lipid components; (B) overlaid chromatograms of soluble sugar components.

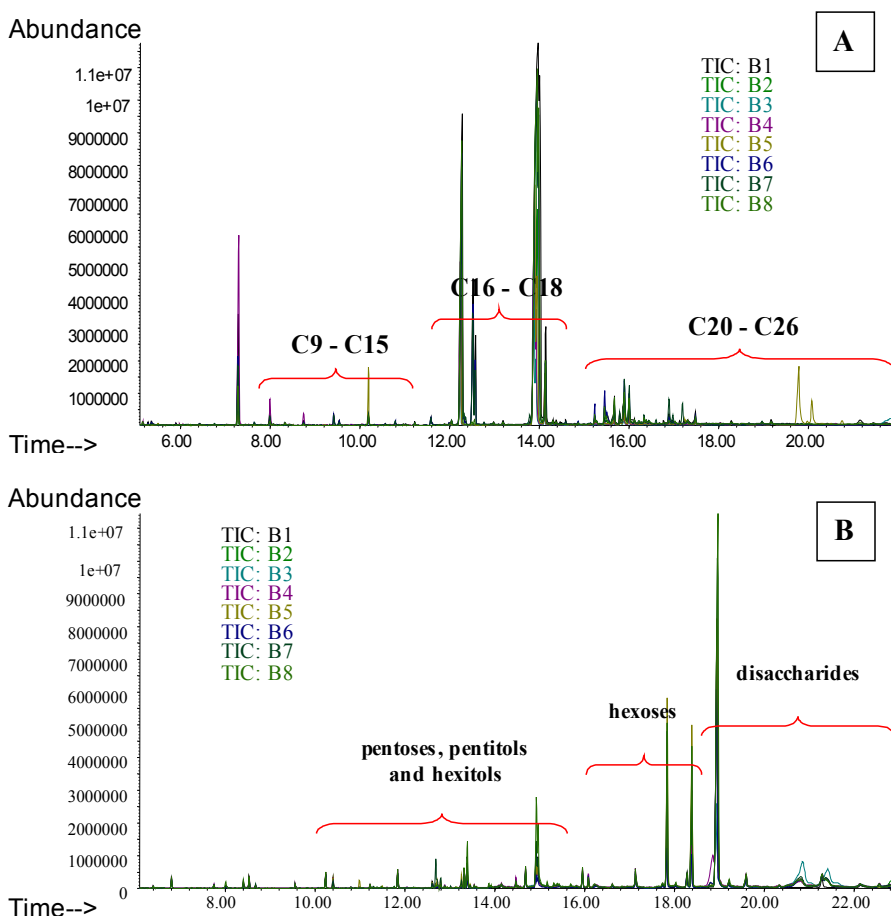


Figure 1. Overlaid chromatograms of 8 samples of barley flour: (A) lipid components; (B) soluble sugar components

The Wiley 275 mass spectra library was used for the identification of detected components in both hexane and ethanol extracts. The components of each barley flour extract were identified according to the characteristic fragmentations for each group of compounds – lipid and soluble sugar compounds.

Using the MSD Productivity ChemStation program the peaks of compounds of interest were integrated automatically from the chromatograms of both hexane and ethanol extracts of barley flour samples. The numerical values of integrated surface areas were subjected to the multivariate analysis using PAST program. A fundamental idea in multivariate data analysis is to regard the distance between objects in the variable space as a measure of the similarity of the objects. Hierarchical cluster analysis is a complementary, nonlinear, and widely used method for cluster analysis, with the result represented by a dendrogram (11). Paired group algorithm and correlation similarity measure were applied in all cases, because it provided the highest values of cophenetic correlation coefficient.

Hexane extracts analysis

Table 1 lists the identified lipid components in hexane extracts.

Table 1. Compounds detected in hexane extracts of analyzed barley samples

Lipid compound	Rt
Dodecanoic acid, methyl ester	8.08
<i>Nonanedioic acid, dimethyl ester</i>	8.34
<i>Tetradecanoic acid, methyl ester</i>	10.20
9-Dodecenoic acid, methyl ester, (E)-	10.98
<i>Pentadecanoic acid, methyl ester</i>	11.23
<i>9-Hexadecenoic acid, methyl ester</i>	12.04
<i>Hexadecanoic acid, methyl ester</i>	12.25
<i>Heptadecanoic acid, methyl ester</i>	13.19
<i>9,12-Octadecadienoic acid (Z, Z), methyl ester</i>	13.92
<i>9-Octadecenoic acid (Z)-, methyl ester</i>	13.96
<i>Octadecanoic acid, methyl ester</i>	14.12
<i>11-Eicosenoic acid, methyl ester</i>	15.67
<i>Eicosanoic acid, methyl ester</i>	15.90
Heneicosanoic acid, methyl ester	16.69
Ricinoleic acid methyl ester	16.90
Octadecanoic acid, 9,10-dihydroxy-methyl ester	17.23
<i>13-Docosenoic acid, methyl ester</i>	17.31
<i>Docosanoic acid, methyl ester</i>	17.48
15-Tetracosenoic acid, methyl ester	18.98
<i>Tetracosanoic acid, methyl ester</i>	19.17
Hexacosanoic acid, methyl ester	21.45

*The components written in italic are present in all barley flour samples

By looking at the overlaid chromatograms in Figure 1 (A) and Table 1 it can be said that the chromatograms can be divided into three different parts. First part includes methyl esters of minor fatty acids with less than 16 carbon atoms in the molecule ($R_t \leq 11.23$ min). The second part includes methyl esters of the most abundant fatty acids, i.e. saturated and unsaturated fatty acid methyl esters with 16 and 18 carbon atoms in the molecule ($R_t=12.04\div 14.12$ min): hexadecanoic (palmitic), 9,12-octadecadienoic (linoleic), 9-octadecenoic (oleic), and octadecanoic (stearic) acid. 9-hexadecenoic (palmitoleic) and heptadecanoic (margaric) acid methyl esters were also detected in the second part, but in much smaller quantities. The third part of the chromatograms is composed of methyl esters of saturated and unsaturated fatty acids with more than 18 carbon atoms in the molecule, which also appear in smaller amounts in all barley samples ($R_t \geq 15.25$ min).

The dendrogram of 8 barley flour samples constructed based on the lipid components detected in the hexane extracts is presented in Figure 2.

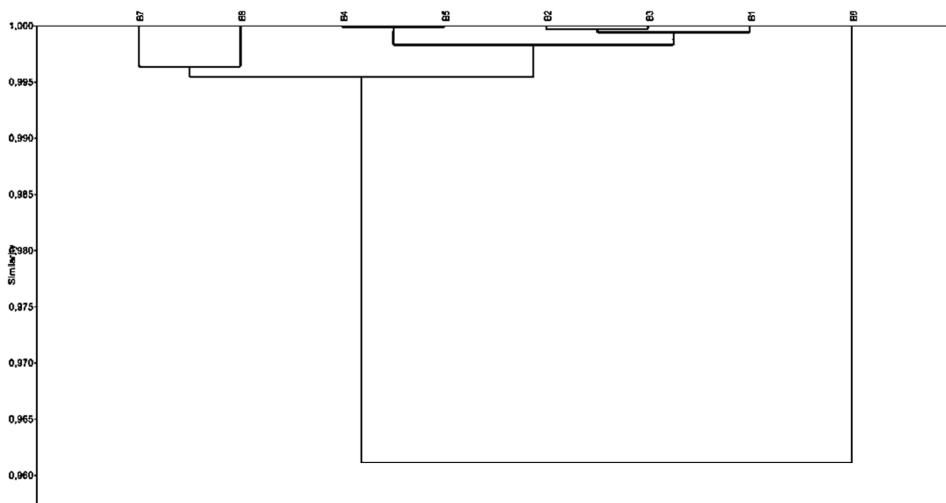


Figure 2. Dendrogram of lipid component correlations from Table 1, present in 8 samples of barley flour

The correlation similarity measure among barley samples is very high ($r \geq 0.96$). The flour samples of barley hybrids are divided in three groups (B1, B2, B3), (B4, B5), (B7, B8), but they still represent great similarities between the groups. The properties of barley flour sample B6 slightly differ compared to the other barley samples, regarding its lipid composition, but its similarity with the other samples is still very high ($r \sim 0.96$).

The obtained value of cophenetic correlation coefficient was very high (0.9951), which means that the dendrogram preserves very faithfully the pairwise distances between the original unmodeled data points.

Analysis of ethanol extracts

Table 2 lists the identified soluble sugars in ethanol extracts of 8 barley flour samples.

Table 2. Compounds detected in ethanol extracts of the analyzed barley samples

Simple sugar compound	Rt
<i>Xylitol, 1,2,3,4,5-pentakis-O-(trimethylsilyl)-</i>	10.40
<i>Arabinopyranose, tetrakis-O-(trimethylsilyl)-α-D-</i>	11.30
<i>D-Mannitol, 1,2,3,4,5,6-hexakis-O-(trimethylsilyl)-</i>	12.61
<i>D-Glucitol, 1,2,3,4,5,6-hexakis-O-(trimethylsilyl)-</i>	12.69
<i>Xylitol, 1,2,3,4,5-pentakis-O-(trimethylsilyl)-</i>	12.80
<i>D-Glucitol, 1,2,3,4,5,6-hexakis-O-(trimethylsilyl)-</i>	13.25
<i>D-Glucopyranose, 1,2,3,4,6-pentakis-O-(trimethylsilyl)-</i>	16.09
<i>α-D-Glucopyranoside, 1,3,4,6-tetrakis-O-(trimethylsilyl)-β-D-fructofuranosyl 2,3,4,6-tetrakis-O-(trimethylsilyl)-</i>	17.84
<i>α-D-Glucopyranoside, 1,3,4,6-tetrakis-O-(trimethylsilyl)-β-D-fructofuranosyl 2,3,4,6-tetrakis-O-(trimethylsilyl)-</i>	18.38
<i>D-Turanose, heptakis(trimethylsilyl)-</i>	18.57
<i>Melibiose, octakis(trimethylsilyl)-</i>	18.80
<i>α-D-Glucopyranoside, 1,3,4,6-tetrakis-O-(trimethylsilyl)-β-D-fructofuranosyl 2,3,4,6-tetrakis-O-(trimethylsilyl)-</i>	18.92
<i>α-D-Glucopyranoside, 1,3,4,6-tetrakis-O-(trimethylsilyl)-β-D-fructofuranosyl 2,3,4,6-tetrakis-O-(trimethylsilyl)-</i>	20.85
<i>α-D-Glucopyranoside, 1,3,4,6-tetrakis-O-(trimethylsilyl)-β-D-fructofuranosyl 2,3,4,6-tetrakis-O-(trimethylsilyl)-</i>	21.39

* The components written in italic are present in all barley flour samples

By observing the overlaid chromatograms in Figure 1 (B) and the detected components in Table 2 it can be concluded that soluble sugar components, present in all the barley flour samples include monosaccharides and sugar alcohols: pentose and pentitol (arabinose and xylitol), hexose and hexitols (glucose, glucitol and mannitol), but also some reducing disaccharides (turanose and melibiose). The most abundant component detected in the chromatograms of ethanol extracts is definitely a disaccharide, identified as the non-reducing sugar - sucrose, which represents the highest peaks on the chromatograms, eluting at 17.84 min, 18.38 min and 21.39 min.

The similarity of the barley flour samples obtained by applying hierarchical cluster analysis of compounds selected in the chromatograms of the ethanol extracts, by using all sugar components that are present in the obtained chromatograms (monosaccharides, disaccharides and sugar alcohols), is shown in Figure 3. The figure depicts the dendrogram of the analyzed barley samples obtained according to soluble sugars.

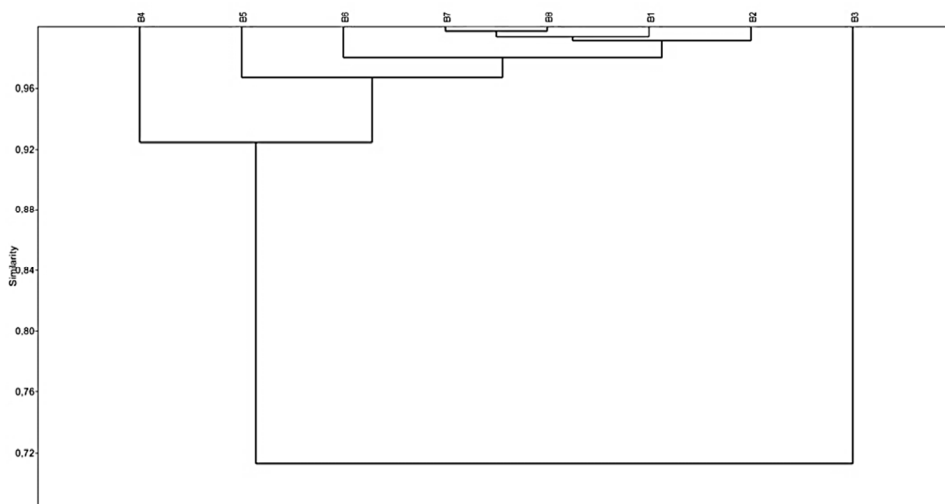


Figure 3. Dendrogram of simple sugar component correlations from Table 2, present in 8 samples of barley flour

In this case, based on the soluble sugar content, the branch with the sample B3 is separated from the other samples, which are much more similar among each other. The correlation similarity measure for all the samples was, however, very high, above $r \geq 0.995$. According to the soluble sugar content, samples B7 and B8 are grouped together in one branch because of the highest similarity, while samples B1, B2, B6, B5 and B4 manifest slight differences and their branches join individually in the order mentioned.

It can be said that the similarity among the barley samples, when comparing their ethanol extracts, was above 0.70, which is significantly lower compared to the similarity between the hexane extracts of the same samples, but still represents a relatively high similarity.

The obtained value of cophenetic correlation coefficient was again very high (0.9837).

CONCLUSIONS

All samples of flour produced of different barley cultivars give similar chromatograms of hexane and ethanol extracts, lipid and soluble sugar compositions and, therefore, high values of similarity measures. With the application of multivariate analyses to integrated surface areas of identified lipid and soluble sugar compounds, the samples of barley flour of different cultivars can be grouped together into clusters on the dendrograms based on the mutual similarities of their hexane and ethanol extracts. Studies regarding various cultivars of other cereal (corn, wheat) and pseudocereal species (amaranth, buckwheat), as well, has already proven high similarities of the lipid and simple sugar profiles of samples with the same botanical origin. In this way, our future research will be direc-

ted towards the identification of barley flour during procedures concerning the flour quality control on the world market, apart from the analyzed samples of barley cultivars.

Acknowledgement

The authors gratefully acknowledge the financial support of the Ministry of Education, Science and Technological Development of the Republic of Serbia (Project TR 31066) and of the Provincial Secretariat for Science and Technological Development of Vojvodina (Project No. 114-451-1361/2014-03).

REFERENCES

1. Penfield, M.P.; Campbell, A.M. Flour. In *Experimental Food Science*; Penfield, M.P., Campbell, A.M., Eds.; Academic press: London, UK, 1990; pp 384-405.
2. Vujić, Dj.N.; Ačanski, M.M.; Bodroža-Solarov, M.I.; Hristov, N.S.; Krunić, M.N. Performance of GC-MS analysis for differentiation of various types of flour by creating dendrogram of liposoluble extract. *Chem. Ind. Chem. Eng. Q. (CI&CEQ)* **2012**, *18* (4), 555-561.
3. Izydorczyk, M.S.; McMillan, T. Chapter 31: Barley β -Glucans and Fiber-Rich Fractions as Functional Ingredients in Flat and Pan Bread. In *Flour and Breads and their Fortification in Health and Disease Prevention*; Preedy, V.R., Watson, R.R., Patel, V.B. Eds.; Elsevier: USA, 2011; pp 337-353.
4. King, R.A.; Noakes, M.; Bird, A.R.; Morell, M.K.; Topping, D.L. An extruded breakfast cereal made from a high amylose barley cultivar has a low glycemic index and lower plasma insulin response than one made from a standard barley. *J. Cereal Sci.* **2008**, *48*, 526-530.
5. Baik, B.-K.; Ullrich, S.E. Barley for food: Characteristics, improvement, and renewed interest. *J. Cereal Sci.* **2008**, *48*, 233-242.
6. Soong, Y.Y.; Tan, S.P.; Leong, L.P.; Henry, J.K. Total antioxidant capacity and starch digestibility of muffins baked with rice, wheat, oat, corn and barley flour. *Food Chem.* **2014**, *164*, 462-469.
7. Ačanski, M.M.; Vujić, Dj.N.; Psodorov Dj.B. Practical method for the confirmation of authentic flours of different types of cereals and pseudocereals. *Food Chem.* **2015**, *172*, 314-317.
8. Ačanski, M.M.; Vujić, Dj.N. Comparing sugar components of cereal and pseudo-cereal flour by GC-MS analysis. *Food Chem.* **2014**, *145C*, 743-748.
9. Ruiz-Matute, A.I.; Hernández-Hernández, O.; Rodríguez-Sánchez, S.; Sanz, M.L.; Martínez-Castro, I. Derivatization of carbohydrates for GC and GC-MS analyses. *J. Chromatogr. B*, **2011**, *879*, 1226-1240.
10. Hammer, O.; Harper, D.A.T.; Ryan, P.D. *PAST-Paleontological statistics software package for education and data analysis*; Palaeontologia Electronica 4(1): Oslo, Norway, 2001; pp 4-11.
11. Varmuza, K.; Filzmoser, P. *Introduction to Multivariate Statistical Analysis in Chemometrics*; CRC Press Taylor & Francis Group: Boca Raton, FL, 2008; 265-270.

12. Pastor, K.A.; Ačanski, M.M.; Hristov, N.S.; Vujić, Dj.N.; Kondić-Špika, A.Dj. Application of multivariate analysis in wheat and corn flour differentiation, 4th International Congress Engineering, Environment and Materials in Processing Industry, Jahorina, Pale, Bosnia and Herzegovina, 4-6 March 2015, Book of Abstracts, pp 69-70.
13. Pastor, K.A.; Ačanski, M.M.; Bekavac, G.F.; Vujić, Dj.N. Qualitative analysis of liposoluble flour extracts of different corn hybrids using GC-MS system, 4th International Congress Engineering, Environment and Materials in Processing Industry, Jahorina, Pale, Bosnia and Herzegovina, 4-6 March 2015, Book of Abstracts, pp 349-350.
14. Psodorov, Dj.B.; Ačanski, M.M.; Vujić, Dj.N.; Brkljača, J.; Psodorov, D.Dj. Homogeneity of oil and sugar components of amaranth flour investigated by GC-MS. *Chem. Ind. Chem. Eng. Q. (CI&CEQ)* **2015**, 21 (1), 71-76.
15. Ačanski, M.M.; Pastor, K.A.; Razmovski, R.N.; Kravić, S.Ž.; Psodorov, Đ.B.; Vujić, Đ.N. Homogeneity of oil and sugar components of buckwheat flour investigated by GC-MS system and multivariate analysis, International Congress on Natural Science and Engineering, Kyoto, Japan, 7-9 May 2015, Conference Proceedings, Part 2, pp 403-410.

ЛИПИДНИ И ШЕЋЕРНИ ПРОФИЛИ РАЗЛИЧИТИХ СОРТИ ЈЕЧМА (*Hordeum vulgare*)

Кристиан А. Пастор¹, Маријана М. Ачански¹, Бура Н. Вујић¹,
Анкица Ђ. Кондић-Шника², Никола С. Христов²

¹ Универзитет у Новом Саду, Технолошки факултет, Булевар цара Лазара 1, 21000 Нови Сад, Србија

² Институт за ратарство и повртарство, Максима Горког 30, 21000 Нови Сад, Србија

У овом раду идентификоване су липидне компоненте и растворљиви шећери у узорцима брашна различитих сорти јечма (*Hordeum vulgare*). Испитане су следеће сорте јечма: 3 узорка сорте озимог пивског јечма, 3 узорка сорте озимог сточног јечма, и по један узорак сорти јарог и голозимог јечма. Из узорка брашна јечма прво су хексаном екстраховане масне киселине, које су затим дериватизоване у одговарајуће, испарљиве метил-естре, применом реагенса за дериватизацију TMSH (триметилсулфонијум-хидроксид у метанолу). Након тога, обезмашћени и осушени узорци јечменог брашна подвргнути су екстракцији 96%-тним етанолом, чиме су издвојени растворљиви шећери, који су даље дериватизовани у одговарајуће TMS-оксиде, применом раствора хидроксиламин-хидрохлорида и BSTFA (Н, О-бис-(триметилсиллил)-трифлуороацетамид). Хексански и алкохолни екстракти сорти јечма анализирани су применом гасне хроматографије - масене спектрометрије (GC-MS). Састав липидних, као и шећерних компонената је био врло сличан код свих сорти. Стога је за даљу обраду података примењена мултиваријантна анализа нумеричких вредности интегрисаних површина идентификованих метил-естара масних киселина и триметилсиллил-оксима растворљивих шећера. Примена хијерархијске кластер анализе показује веома велике сличности између испитаних узорка брашна сорти јечма, по садржају масних киселина (0.96). Такође значајна, али нешто ма-

ња сличност установљена је код садржаја растворљивих шећера (0,70). Ови прелиминарни резултати указују на могућност разликовања јечменог брашна, без обзира на сорту, од брашна других житарица анализом садржаја масних киселина и растворљивих шећера.

Кључне речи: сорте јечма, липидни састав, састав простих шећера, GC-MS, кластер анализа

Received: 9 April 2015.
Accepted: 18 June 2015.

TREATMENT OF SUGAR BEET EXTRACTION JUICE STILLAGE BY NATURAL COAGULANTS EXTRACTED FROM COMMON BEAN

Jelena M. Prodanović*, Marina B. Šćiban, Mirjana G. Antov, Dragana V. Kukić
and Vesna M. Vasić

University of Novi Sad, Faculty of Technology, Bulevar cara Lazara 1, 21000 Novi Sad, Serbia

Distillery wastewaters have a great pollution potential, and pollution caused by them is one of the most critical environmental issues. This study is concerned with the coagulation efficiency of a new, environmental friendly, natural coagulant extracted from common bean seeds in the primary treatment of distillery wastewater in the bioethanol production from sugar beet juice. Active coagulation components were extracted from ground seeds of common bean with 0.5 mol/L NaCl. The obtained raw extract was used as a coagulant. The coagulation efficiency was measured by jar test at different pH values of wastewater, and a decrease in organic matter content was determined. The experiments confirmed that natural coagulant from common bean could be successfully used for the treatment of extraction juice distillery wastewater. The highest coagulation efficiencies were achieved at the pH 5.2 with a coagulant dose of 30 mL/L, and at the pH 8.5 with a coagulant dose of 5 mL/L, and they were 64.71% and 68.75% respectively. These encouraging results indicate that natural coagulant from common bean seeds is a potential alternative to conventional chemical coagulant/flocculant agents for treatment of wastewaters.

KEY WORDS: Natural coagulants, common bean, distillery wastewater, organic matter removal

INTRODUCTION

Bioethanol, both clean and renewable fuel, is believed to be a good alternative to oil and expected to play a more significant role in the future (1-3). The worldwide prognoses are the further increase in the production and consumption of biofuels, among other bioethanol (4).

Molasses, a by-product of sugar production from sugar beet, is commonly used feedstock for bioethanol production. Besides, some intermediate products from sugar production can be used for fermentative bioethanol production, and these are: extraction juice, thin juice and thick juice. Among these juices, extraction juice is the most suitable for

* Corresponding author: Jelena M. Prodanović, University of Novi Sad, Faculty of Technology, Bulevar Cara Lazara 1, 21000 Novi Sad, Serbia, e-mail: jejap@uns.ac.rs

ethanol production from the economic point of view, since the cost of its production is considerably lower than the cost of production from the other two juices.

During bioethanol production, the distillery wastewater (spent wash or stillage) is generated in large quantities. The production and properties of stillage are highly variable and depend on the feedstocks and various aspects of the bioethanol production process. In general, distillery wastewaters have an extremely high pollution potential: high biological oxygen demand (BOD), chemical oxygen demand (COD) and high BOD/COD ratio. They also contain substances such as potassium, phosphates, nitrogen, calcium and sulphates (5,6). Inappropriate disposal of the stillage leads to pollution of soil, surface- and ground-waters. As awareness regarding the environmental impacts caused by the uncontrolled disposal of stillage grows, the bioethanol production sector faces noticeable challenges.

Stillage volume is approximately 10 times that of ethanol produced, so that properly use of this by-product is an important issue to address. Since stillage contains many valuable ingredients, it is used as fodder, as a base for further microbiological production (for example biogas, SCP etc.), as a fertilizer, etc. (7). The stillage can be processed as a whole or it is screened or centrifuged to produce thin stillage and wet distillers' grain. Separation of wastewaters to tin and concentrated fractions gives new possibilities of their uses (8).

Thin stillage could be obtained from whole stillage, also by settling enhanced by coagulation and flocculation. Coagulation and flocculation are the essential processes used for the removal of particulates and organic matter from wastewaters, and are usually conducted by adding chemicals such as salts of aluminium and iron and polyelectrolytes. The sludge remaining after coagulation and flocculation cannot be used as fertilizer or feed, since it contains residues of coagulants and flocculants that are potentially hazardous to health (9-12). Besides, the alum sludges are gelatinous, acidic and difficult to de-water and to dispose of in the environment (13). Also, a biological post-treatment of this sludge may be problematic, since the residues of coagulants and flocculants can cause obstructions during this process. The lowering of the pH of treated water, and the increase in the conductivity are additional disadvantages of alum usage (13).

Recently, intensive investigations of natural coagulants have been conducted in order to replace above chemical coagulants and flocculants for water and wastewater treatment. Natural coagulants are mainly extracted from plant tissues. It is believed that they are not harmful, and besides, the resulting biodegradable sludge can be simply anaerobically treated and disposed in the nature without any harmful influence. Compared to chemical coagulants, natural coagulants are relatively cost-effective and can be easily processed in a usable form (14). Also, compared to alum, they generate up to six times less sludge volume (15-17).

The most investigated plant in terms of natural coagulants derivation is *Moringa oleifera*. *M. oleifera* seed extract is very efficient for water (18-22) and wastewater treatment (15,17,23-25). There are only some data on the performance of other plant extracts as natural coagulants. Although natural coagulants from *M. oleifera* are undoubtedly good, it is a plant widespread in tropical areas. Because of that it is also necessary to investigate the possibility of extraction of natural coagulants from sources that are

cheap and easily available in tempered climate zone. Our previous investigations confirmed the fact that seed extracts of various strains of Leguminose (*Fabaceae*) family could be used as natural coagulants (26-28). This research was aimed to investigate the efficiency of the use of natural coagulants extracted from common bean seeds (*Phaseolus vulgaris*) for treatment of wastewater remaining after bioethanol production on sugar beet extraction juice as a substrate. Beside its availability, common bean seeds do not contain oil unlike *M. oleifera* seeds (29) – there is no need for oil extraction by organic solvents, thus a delipidation step can be avoided, which is beneficial for both economic and environmental reasons.

EXPERIMENTAL

Fermentation and wastewater

The fermentation process of bioethanol production based on sugar beet extraction juice was carried out in laboratory, as described previously (30). Bioethanol and other evaporative components were isolated from the fermented mash by distillation. The distillation was ended when 10% of the volume of the fermented mash vaporized and condensed. The residue of the fermented mash which comes out as a liquid waste is termed as distillery wastewater, spent wash or stillage. Distillery wastewater was stored in a refrigerator at +4°C.

Natural coagulant

Natural coagulant was obtained in accordance with our previous investigations (26, 31), in the following way: common bean (*P. vulgaris*) seeds were ground and sieved through a sieve with 0.4 mm pore size. An amount of 10 g/L of the smaller fraction was suspended in 0.5 mol/L solution of NaCl. This suspension was stirred 10 minutes on a magnetic stirrer in order to extract active coagulant. After that, the suspension was filtered through filter paper Macherey-Nagel MN 651/120. The obtained filtrate was stored in a refrigerator at +4°C, and used as natural coagulant.

Coagulation test

Coagulation activity was assessed by the jar test using wastewater obtained after bioethanol production. The traditional experimental method, one variable (dose of coagulant) at a time was applied at different pH values of the wastewater. The wastewater pH value was adjusted by adding 33% NaOH just before performing the coagulation test. The jar test was carried out by adding different amounts of extract to 150 mL of wastewater. After fast stirring at 150 rpm for 1 minute in order to disperse the coagulant, it was continued with slower stirring at 60 rpm for 30 minutes in order to promote the flocculation of the suspended and colloidal particles present in the wastewater, and after that the system was left for 1 h for sedimentation. The same coagulation test was conducted with no coagulant as a blank. After 1 hour of sedimentation, the residual COD was determined in the upper clarified liquid fraction and coagulation activity was calculated as:

$$\text{Coagulation activity (\%)} = (\text{COD}_b - \text{COD}_s) \cdot 100 / \text{COD}_b \quad [1]$$

where COD_b and COD_s are the COD of the blank and the sample, respectively.

All experiments were performed in duplicate, and the mean value is given as the final result.

Analytical methods

In distillery wastewater the following parameters were determined: pH, Dry matter, Fixed residue, Suspended solids, Fixed residue of suspended solids, Settleable matter, Total nitrogen, Phosphates, and COD. All of the parameters were determined according to Standard Methods for the Examination of Water and Wastewater (32).

RESULTS AND DISCUSSION

Analysis of wastewater

Wastewater remaining after laboratory bioethanol production from extraction juice, were analyzed. Since the quantity of wastewater obtained from one fermentation experiment was not large, it was prepared over and again, and the average values with standard deviations of the determined parameters are presented in Table 1.

Table 1 Results of the analysis of the wastewater obtained after bioethanol production from extraction juice

Parameter	Mean value	Standard deviation	Coefficient of variation ^a (%)
pH	4.32	0.13	3.0
Dry matter (g/L)	41.04	0.55	1.3
Ash (g/L)	4.88	0.51	10.5
Organic dry matter (g/L)	35.66	0.36	1.0
% of organic dry matter	86.88	0.29	
Suspended solids (g/L)	14.66	0.26	1.8
Fixed residue of suspended solids (g/L)	1.21	0.3	24.8
Organic dry matter of suspended solids (g/L)	13.64	0.21	1.5
Settleable matter (mL/L)	9.25	3.88	41.9
Total nitrogen (mg/L)	1 323	224	18.4
Phosphates (mg/L)	17	4	23.5
COD (mg O ₂ /L)	83 178	4 356	5.2

^a Coefficient of variation = (Standard deviation/Mean)·100

Considering data given in the works of Mutton et al. (5) and Wilkie et al. (6), it can be concluded that the values of COD of investigated extraction juice stillage are similar to

those of sugarcane molasses stillage and higher than those of sugarcane juice stillage. At the same time, sugar beet molasses stillage has higher COD values than the extraction juice stillage (5,30), which can be explained by the presence of melanoidins formed in the Maillard reaction of sugars with proteins and other coloured compounds, such as phenolics (tannic and humic acids), caramels from overheated sugars and furfurals from acid hydrolysis (33). Although data for a large number of different stillages are presented in the paper of Wilkie et al. (6), this cannot be a general conclusion since the coefficients of variation (when calculated for the data given in that study) are considerably high – in the range of 25% - 75%. Compared to data on cane molasses stillage presented in the paper of Mohana et al. (34), most of the parameters of extraction juice wastewater shown in Table 1 are much lower.

The quantity of settleable matter in the investigated stillage is very low compared to the quantity of suspended solids, which make up about 35% of dry matter. This means that suspended solids are stable in the stillage, and it is necessary to apply coagulation to ensure their destabilization.

Wastewater treatment by natural coagulant

The efficiency of common bean extract as a natural coagulant for organic matter removal from wastewater was investigated. The extracts of bean seeds contain different substances with coagulation ability: proteins, carbohydrates, phytic acid etc. (35). Because of that, the very complex reactions can occur during the coagulation, which is considerably influenced by the pH value of the wastewater. The coagulation activity was assessed by the jar test at the different pH values of wastewater and different applied doses of the coagulant. It is well known the pH value influences the charge of colloid particles (generally of organic matter) and, as a result, affect the coagulation. Because of that, the investigations of the coagulation were done in a wider pH range around the neutral point, from the original pH 4.23 to the pH 8.50, with the steps of around 0.8 pH unit.

The first coagulation test was conducted at the original pH of the stillage, 4.23 and the results are shown in Figure 1.

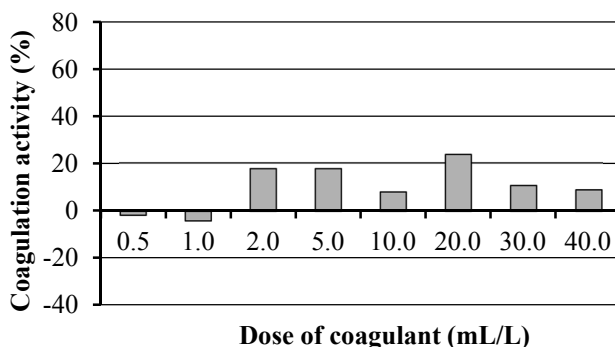


Figure 1. The influence of the coagulant dose on the coagulation activity at the pH 4.23

As it can be seen from Figure 1, better results were achieved with higher coagulant doses. The best coagulation activity, 23.53%, was attained with the applied coagulant dose of 20 mL/L. The doses of coagulant lower than 2 mL/L did not prove to be good for coagulation at this pH, since COD in the wastewater even increased after their application. This result can be explained by the fact that the natural coagulant is of organic nature, and since there was no coagulation, it contributed to the increase in the organic matter content.

In the next experiment, the wastewater pH was adjusted to 5.2 by adding 33% NaOH just before performing the coagulation test. The dependence of the coagulation activity on the applied dose of the coagulant is shown in Figure 2.

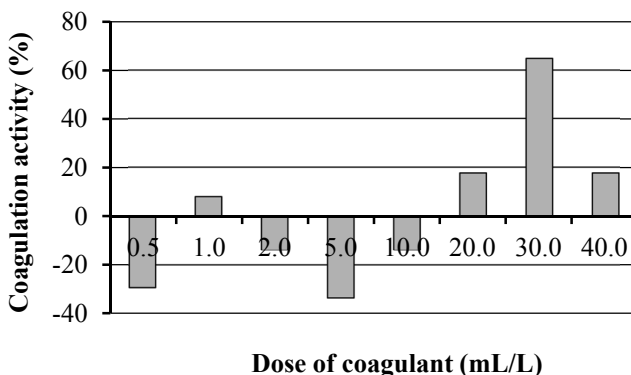


Figure 2. The influence of the coagulant dose on the coagulation activity at the pH 5.20

In comparison to the previous experiment, the pH increase to 5.2 led to a more efficient organic matter removal from the wastewater when higher coagulant doses were applied. It was demonstrated that the highest coagulation efficiency was achieved with a dosage of 30 mL/L, resulting in the organic matter decrease of 64.71%. At this pH, lower coagulant doses appeared to be even less efficient than at the pH 4.23, as the organic matter increase was considerable after the coagulation tests performed with the coagulant doses of 0.5 mL/L and 5 mL/L.

The next coagulation test was carried out at the pH 6, and the results are shown in Figure 3. The best coagulation activity was at the same coagulant dose applied (30 mL/L) as it was in the coagulation test performed at the pH 5.2, but it was almost twice lower – 37.5%. With a coagulant dose of 20 mL/L a little bit lower coagulation efficiency was achieved (35.42%), so it can be a recommended dose for this pH, because almost the same effect was achieved with the dose lower by one third.

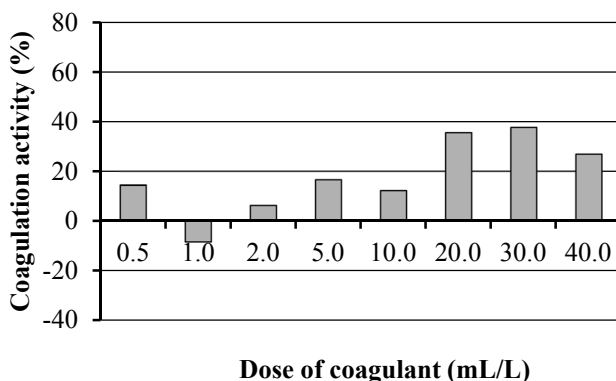


Figure 3. The influence of the coagulant dose on the coagulation activity at the pH 6

For the next coagulation test the pH 6.7 was adjusted in the spent wash. The influence of the coagulant dose on the coagulation activity at this pH is presented in Figure 4. The highest coagulation activity was obtained with a coagulant dose of 2 mL/L, and it was 24.32%.

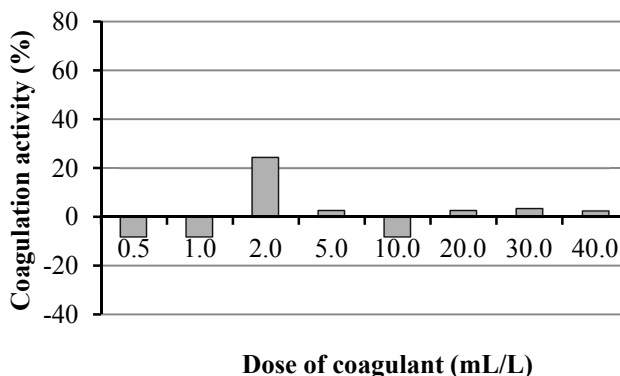


Figure 4. The influence of the coagulant dose on the coagulation activity at the pH 6.7

The influence of the coagulant dose on the coagulation activity at the pH 7.5 is shown in Figure 5.

As it can be seen in Figure 5, the pH 7.5 proved to be inappropriate for organic matter removal from the extraction juice wastewater. At this pH, the coagulation activity was inappreciable at almost all of the coagulant doses applied. A possible explanation could be the chemical complexity of sugar beet extraction juice. Namely, sugar beet juice contains carbohydrates, proteins, amino acids, organic acids, pectic substances, fat, saponins, mineral matter (36). Also, the chemical composition of common bean extract is very com-

plex. Regarding this, some reactions can take place at the pH values approximating 7.5. These reactions can block either the compounds which show coagulation activity or compounds of pollution – in any case, the coagulation process is disabled. Considering the achieved results of the previous and this experiment, it can be said that the pH 6.7 and pH 7.5, i.e. at neutral pH range, are not suitable for this kind of treatment of extraction juice stillage.

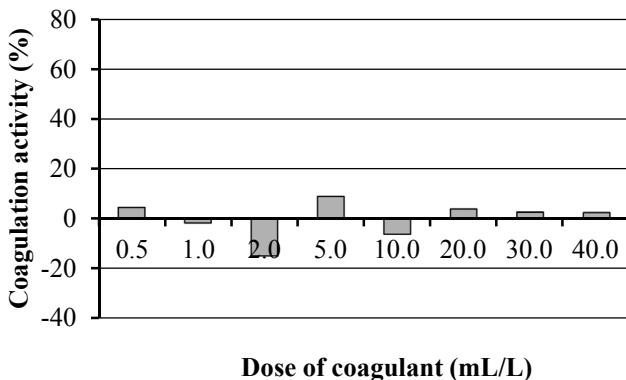


Figure 5. The influence of the coagulant dose on the coagulation activity at the pH 7.5

The coagulation efficiency of common bean coagulant in a low alkaline medium was investigated at the pH 8.5, and the results are shown in Figure 6. In this experiment, a 5 mL/L coagulant dose was determined as the most appropriate, giving the highest organic matter decrease of 68.75%, which was the highest coagulation activity among all the experiments performed. A similar coagulation activity was achieved at the pH 5.2, but with a six times higher dose of the coagulant. Contrary to all the other investigated pH values, the increase of the organic matter content in the treated wastewater was not noticed at this pH.

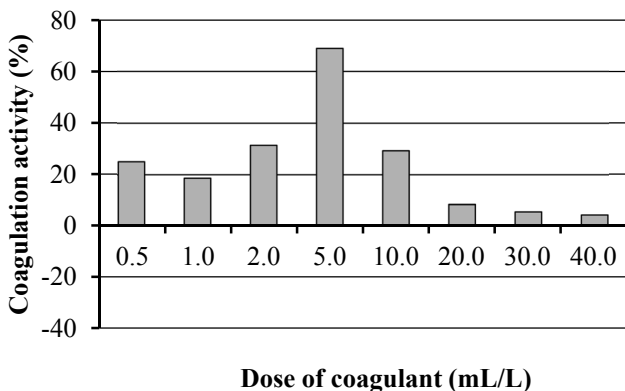


Figure 6. The influence of the coagulant dose on the coagulation activity at the pH 8.5

Considering the results of the above experiments, the pH 5.2 with a coagulant dose of 30 mL/L and pH 8.5 with a coagulant dose of 5 mL/L appeared to be the most appropriate for the treatment of the extraction juice wastewater.

The consumption of alkali, salt and ground bean

With regard to the fact that the best coagulation efficiencies were achieved at the pH 5.2 and the pH 8.5 with the coagulant doses of 30 mL/L and 5 mL/L, respectively, in this part of investigation, the consumption of NaOH required for the pH adjustment and quantities of ground bean, and 0.5 mol/L NaCl required for the preparation of the natural coagulant extract were determined in order to estimate which combination of treatment parameters would be more suitable from the economic point of view.

First, the change of the pH of the wastewater with the addition of 2 mol/L solution of NaOH was investigated. The amounts of 2 mol/L NaOH required for the pH adjustment in 100 mL of wastewater to the pH 5.2 and the pH 8.5 were determined, and they were 1.53 mL and 2.65 mL, respectively. Considering this, the amounts of pure NaOH required for the pH adjustment to 5.2 and 8.5 in 1 m³ of wastewater were calculated.

As the highest coagulation activities at the pH 5.2 and 8.5 were achieved with the coagulant doses of 30 mL/L and 5 mL/L, respectively, and considering the extraction ratio, the amounts of common bean and 0.5 mol/L NaCl required for treatment of 1 m³ of wastewater were calculated. The calculated consumptions are presented in Table 2.

Table 2 The estimated consumption of alkali, common bean and salt for treatment of 1 m³ of wastewater at the pH 5.2 and the pH 8.5

pH	Coagulant dose (mL/L)	Consumption of:		
		NaOH (g)	Ground bean (g)	NaCl (g)
5.2	30	1 203	300	877.5
8.5	5	2 120	50	146.3

The results shown in Table 2 indicate that the pH 8.5 is more suitable for the wastewater treatment with natural coagulant extracted from common bean than the pH 5.2, since although more NaOH (approximately 2 times) is required for the pH correction than in the case of treatment at the pH 5.2, much less (approximately 6 times) common bean and NaCl are estimated to be consumed. In any case, in order to make clear decision which pH is more suitable, a detailed economic analysis should be conducted.

CONCLUSION

Considering the performed experiments and obtained results, it is possible to derive the following conclusions:

- Natural coagulant extracted from common bean showed potential to be used for the extraction juice distillery wastewater treatment. It presents a viable alternative coagulant to alum, which is in line with the sustainable development initiatives.

- The pH value of the stillage influenced the coagulation activity of the natural coagulant.
- The highest coagulation activities were achieved at the pH 5.2 with the applied coagulant dose of 30 mL/L and at the pH 8.5 with the applied coagulant dose of 5 mL/L, and they were 64.71% and 68.75%, respectively.
- Comparing the estimated consumptions of NaOH, NaCl and ground bean required for the treatment of 1 m³ of wastewater at the pH 5.2 and 8.5, it can be concluded that the pH 8.5 is more suitable for wastewater treatment with natural coagulant extracted from common bean.

Acknowledgement

This research was supported by the grant No. III 43005, given by the Ministry of Education, Science and Technological Development of the Republic of Serbia.

REFERENCES

1. Agarwal, A.K. Biofuels Alcohols and Biodiesel Applications as Fuels for Internal Combustion Engines. *Prog. Energy Combust. Sci.* **2007**, *33*, 233-271.
2. Nigam, P.S.; Singh, A. Production of Liquid Biofuels from Renewable Resources. *Prog. Energy Combust. Sci.* **2011**, *37*, 52-68.
3. Prasad, S.; Singh, A.; Joshi, H.C. Ethanol as an Alternative Fuel from Agricultural, Industrial and Urban Residues. *Resour. Conserv. Recycl.* **2007**, *50*, 1-39.
4. Demirbas, A. Biofuels Sources, Biofuel Policy, Biofuel Economy and Global Biofuel Projections. *Energy Convers. Manag.* **2008**, *49*, 2106-2116.
5. Mutton, M.A.; Rossetto, R.; Mutton, M.J.R. Agricultural Use of Stillage. In *Sugarcanne Bioethanol - R&D for Productivity and Sustainability*; Cortez, L.A.B., Ed.; Edgard Blücher: São Paulo, 2014; pp 423-440.
6. Wilkie, A.C.; Riedesel, K.J.; Owens, J.M. Stillage Characterization and Anaerobic Treatment of Ethanol Stillage from Conventional and Cellulosic Feedstocks. *Biomass Bioenerg.* **2000**, *19*, 63-102.
7. Qian, P.; Schoenau, J.; Urton, R. Effect of Soil Amendment with Thin Stillage and Glycerol on Plant Growth and Soil Properties. *J. Plant Nutrition.* **2011**, *34*, 2206-21.
8. de Sena, R.F.; Claudino, A.; Moretti, K.; Bonfanti, I.C.P.; Moreira, R.F.P.M.; José, H.J. Biofuel Application of Biomass Obtained from a Meat Industry Wastewater Plant through the Flotation Process - A Case Study. *Resour., Conserv. Recycl.* **2008**, *52*, 557-569.
9. Becaria, A.; Lahiri, D.K.; Bondy, S.C.; Chen, D.-M.; Hamadeh, A.; Li, H.; Taylor, R.; Campbell, A. Aluminium and Copper in Drinking Water Enhance Inflammatory or Oxidative Events Specifically in the Brain. *J. Neuroimmunol.* **2006**, *176*, 16-23.
10. Bondy, S.C. The Neurotoxicity of Environmental Aluminium is Still an Issue. *Neuro-Toxicology* **2010**, *31*, 575-581.
11. Chico Galdo, V.; Massart, C.; Jin, L.; Vanvooren, V.; Caillet-Fauquet, P.; Andry, G.; Lothaire, P.; Dequanter, D.; Friedman, M.; Van Sande, J. Acrylamide, an in Vivo

- Thyroid Carcinogenic Agent, Induces DNA Damage in Rat Thyroid Cell Lines and Primary Cultures. *Mol. Cell. Endocrinol.* **2006**, 257-258, 6-14.
12. Walton, J.R.; Wang, M.-X. APP Expression, Distribution and Accumulation are Altered by Aluminium in a Rodent Model for Alzheimer's Disease. *J. Inorg. Biochem.* **2009**, 103, 1548-1554.
 13. Ndabigengesere, A.; Narasiah, K.S. Quality of Water Treated by Coagulation Using *Moringa oleifera* Seeds. *Water Res.* **1998**, 32, 781-791.
 14. Yin, C.-Y. Emerging Usage of Plant-Based Coagulants for Water and Wastewater Treatment. *Process Biochem.* **2010**, 45, 1437-1444.
 15. Bhuptawat, H.; Folkard, G.K.; Chaudhari, S. Innovative Physico-Chemical Treatment of Wastewater Incorporating *Moringa oleifera* Seed Coagulant. *J. Hazard. Mater.* **2007**, 142, 477-482.
 16. Narasiah, K.S.; Vogel, A.; Kramadhathi, N.N. Coagulation of Turbid Waters Using *Moringa oleifera* Seeds from Two Distinct Sources. *Water Sci. Technol.* **2002**, 2, 83-88.
 17. Ndabigengesere, A.; Narasiah, K.S. Use of *Moringa oleifera* Seeds as a Primary Coagulant in Wastewater Treatment. *Environ. Technol.* **1998**, 19, 789-800.
 18. Beltrán-Heredia, J.; Sánchez-Martín, J.; Delgado-Regalado, A. Removal of Dyes by *Moringa oleifera* Seed Extract. Study through Response Surface Methodology. *J. Chem. Technol. Biotechnol.* **2009**, 84, 1653-1659.
 19. Beltrán-Heredia, J.; Sánchez-Martín, J.; Delgado-Regalado, A.; Jurado-Bustos, C. Removal of Alizarin Violet 3R (Anthraquinonic Dye) from Aqueous Solutions by Natural Coagulants. *J. Hazard. Mater.* **2009**, 170, 43-50.
 20. Beltrán-Heredia, J.; Sánchez-Martín, J. Removal of Sodium Lauryl Sulphate by Coagulation/Flocculation with *Moringa oleifera* Seed Extract. *J. Hazard. Mater.* **2009**, 164, 713-719.
 21. Ghebremichael, K.; Abaliwano, J.; Amy, G. Combined Natural Organic and Synthetic Inorganic Coagulants for Surface Water Treatment. *J. Water Supply: Res. Technol.-AQUA* **2009**, 58, 267-276.
 22. Okuda, T.; Baes, A.U.; Nishijima, W.; Okada, M. Isolation and Characterization of Coagulant Extracted from *Moringa oleifera* Seed by Salt Solution. *Water Res.* **2001**, 35, 405-410.
 23. Bhatia, S.; Othman, Z.; Ahmad, A.L. Pretreatment of Palm Oil Mill Effluent (POME) Using *Moringa oleifera* Seeds as Natural Coagulant. *J. Hazard. Mater.* **2007**, 145, 120-126.
 24. Bhatia, S.; Othman, Z.; Ahmad, A.L. Coagulation-Flocculation Process for POME Treatment Using *Moringa oleifera* Seeds Extract: Optimization Studies. *Chem. Eng. J.* **2007**, 133, 205-212.
 25. Krishna Prasad, R. Color Removal from Distillery Spent Wash through Coagulation Using *Moringa oleifera* Seeds: Use of Optimum Response Surface Methodology. *J. Hazard. Mater.* **2009**, 165, 804-811.
 26. Antov, M.; Šćiban, M.; Petrović, N. Proteins from Common Bean (*Phaseolus vulgaris*) Seed as a Natural Coagulant for Potential Application in Water Turbidity Removal. *Bioresour. Technol.* **2010**, 101, 2167-2172.

27. Šćiban, M.; Vasić, M.; Prodanović, J.; Antov, M.; Klačnja, M. The Investigation of Coagulation Activity of Natural Coagulants Extracted from Different Strains of Common Bean. *APTEFF* **2010**, *41*, 141-147.
28. Šćiban, M.; Klačnja, M.; Stojimirović, J. Investigation of Coagulation Activity of Natural Coagulants from Seeds of Different Leguminose Species. *APTEFF* **2005**, *36*, 81-87.
29. Muyibi, S.A.; Noor, M.J.M.M.; Tan, K.L.; Lam, H.L. Effect of Oil Extraction from *Moringa oleifera* Seeds on Coagulation of Turbid Water. *Int. J. Environ. Stud.* **2002**, *59*, 243-254.
30. Prodanović, J.; Šćiban, M.; Antov, M.; Dodić, J. Comparing the Use of Common Bean Extracted Natural Coagulants with Centrifugation in the Treatment of Distillery Wastewaters. *Rom. Biotechnol. Lett.* **2011**, *16*, 6638-6647.
31. Antov, M.; Šćiban, M.; Adamović, S.; Klačnja, M. Investigation of Isolation Conditions and Ion-Exchange Purification of Protein Coagulation Components from Common Bean Seeds. *APTEFF* **2007**, *38*, 81-87.
32. *Standard Methods for the Examination of Water and Wastewater*; 20th ed.; American Public Health Association, American Water Works Association, Water Pollution Control Federation: Washington, DC, 1998.
33. Kort, M.J. *Colour in the Sugar Industry*; Science and Technology, Applied Science: London, 1979.
34. Kukić, D.; Šćiban, M.; Tepić, A.; Prodanović, J. Influence of the Composition of Common Bean Extracts on their Coagulation Ability. *APTEFF* **2011**, *42*, 71-79.
35. Mohana, S.; Acharya, B.K.; Madamwar, D. Distillery Spent Wash: Treatment Technologies and Potential Applications. *J. Hazard. Mater.* **2009**, *163*, 12-25.
36. Petrov, S. Chemical Composition of Sugar Beet (in Serbian). In *Fundamentals of Sugar Technology* (in Serbian); Šušić, S., Koronovac, B., Svorcan, R., Eds.; Sugar Industry of Yugoslavia „Jugošećer“: Beograd, 1994; pp 49-93.

ТРЕТМАН ЦИБРЕ ОД ЕКСТРАКЦИОНОГ СОКА ШЕЋЕРНЕ РЕПЕ ПРИРОДНИМ КОАГУЛАНТИМА ЕКСТРАХОВАНИМ ИЗ ПАСУЉА

*Јелена М. Продановић**, *Марина Б. Шћибан*, *Мирјана Г. Антов*,
Драгана В. Кукић, *Весна М. Васић*

Универзитет у Новом Саду, Технолошки факултет, Булевар цара Лазара 1, 21000 Нови Сад, Србија

Отпадне воде дестилерија имају велики потенцијал загађивања животне средине. У овом раду је испитана ефикасност примене новог, еколошки прихватљивог, природног коагуланта екстрахованог из зрна пасуља, за примарни третман отпадне воде од производње биоетанола на екстракционом соку шећерне репе. Отпадна вода је добијана из лабораторијских огледа производње биоетанола на овом супстрату. Отпадна вода има низак рН и висок садржај суспендованих честица, органске материје и азота, услед чега потенцијално има врло велики негативан утицај уколико би се непречишћена испуштала у животну средину. Активне коагулантне суп-

станце су екстраховане из самлевоног зрна пасуља са 0,5 mol/L раствором NaCl. Добијени сирови екстракт је коришћен као коагулантно средство. Ефикасност коагулације је испитивана цар тестом, при различитим рН вредностима отпадне воде и различитим количинама коагуланта. Праћено је смањење садржаја органске материје у обрађеној води након коагулације и таложења флокула. Органска материја је одређивана преко хемијске потрошње кисеоника. Експерименти су потврдили да се природни коагуланти из зрна пасуља могу успешно применити за примарну обраду отпадне воде од производње биоетанола на екстракционом соку, али под одговарајућим условима. Највеће ефикасности коагулације су постигнуте на рН 5,2 са дозом коагуланта од 30 , и на рН 8,5 са дозом коагуланта од 5, и износиле су 64,71% и 68,75%, следствено. Израчунавањем потребне количине средства за подешавање рН вредности и потребне количине зрна пасуља за добијање коагуланта за ове две рН вредности, установљено је да је економичнији рад на рН 8,5. Ови обећавајући резултати указују да се природни коагуланти из зрна пасуља могу сматрати потенцијалном алтернативом хемијским коагулантима/флокулантима за третман отпадних вода.

Кључне речи: природни коагуланти, пасуљ, отпадна вода дестилерије, уклањање органске материје

Received: 6 July 2015.
Accepted: 16 October 2015.

CHICKPEA (*Cicer arietinum*) STEEP LIQUOR AS A LEAVENING AGENT: EFFECT ON DOUGH RHEOLOGY AND SENSORY PROPERTIES OF BREAD

Ahmed M. Saad¹, Ragab A. Elmassry¹, Khaled M.M. Wahdan¹
and Mohamed Fawzy Ramadan^{1,2*}

¹ Department of Agricultural Biochemistry, Faculty of Agriculture, Zagazig University, Egypt.

² Deanship of Scientific Research, Umm Al-Qura University, Makkah, Kingdom of Saudi Arabia

Dough fermentation is one of the oldest process in food technologies. It has been recently intensively studied for its impact on the sensory, structural, nutritional and shelf life properties of leavened baked products. The goals of this work were to investigate chickpea steep liquor (CSL) as a dough-leavening agent and to study the effect of CSL on the dough rheology and sensory properties of leavened bread. CSL was prepared by submerging chickpea seeds in boiled distilled water (1:2, w/v) for 24 h at 37°C, and then obtained liquor was filtered and freeze-dried to obtain CSL. The addition of CSL to wheat flour (WF) brought changes in the dough mixing behavior as measured by the farinograph. An increase in the farinograph water absorption of WF dough was observed when 4.5% CSL and 1.5% yeast was added, while arrival time was not affected. Addition of CSL to the dough at a content of 4.5, 9.0 and 13.5 g CSL/300 g WF caused an increase in dough stability. The CSL addition also increased mechanical tolerance index, dough weakening and mixing time. Dough development time for all blends was higher than the control (1.2-1.5 min), while between the CSL samples no significant difference was observed. The loaf weight slightly increased from 146.2 g for control to 152.2 g for CSL-fermented bread, whereas the loaf volume and specific volume of CSL-fermented bread were lower than the control. The combination of yeast and CSL increased the acceptability of bread with the increasing level of both leavening agents'. The results show that CSL could be used as an alternative to yeast for syngas fermentation. On the other hand, CLS is rich in nutrients and lower in cost compared to yeast.

KEY WORDS: Dough, baking, functional features, bakery products, farinograph, fermentation, gassing power.

INTRODUCTION

Cereals are important diet constituents, which provide carbohydrates, proteins, dietary fibers and vitamins. Bread is one of the major product items in the human diet, as the an-

* Corresponding author: Prof. Dr. Mohamed Fawzy Ramadan, Agricultural Biochemistry Department, Faculty of Agriculture, Zagazig University, Zagazig 44519, Egypt, e-mail: hassanienmohamed@yahoo.com

nual intake of bread in European countries was reported to be in the range from 46 to 100 kg per capita (1). Dough fermentation represents an old food biotechnology process, which has been studied for its effect on the sensory, structural and shelf-life characteristics of leavened baked products. The literature is rich in reports that show how the dough fermentation may affect the functional features of leavened baked products (2). The dough suitable for production of biologically leavened baked products needs to have characteristics that enable dough to stretch in response to the expansion of leavening gas. In addition, dough films surrounding gas bubbles must have sufficient strength to prevent collapse, but at the same time, be capable of stretching (extensibility) without rupturing (3, 4).

Chickpea (*Cicer arietinum* L.) is a valuable leguminous plant and the third most important legume after bean (*Phaseolus vulgaris*) and pea (*Pisum sativum*), based on world production estimates (5, 6). Seeds of chickpea are a good source of protein, carbohydrates, and minerals in the diet (7). In some Mediterranean countries, fermented chickpea was used as a leavening agent to make baked products. Addition of fermented chickpea to the wheat flour (WF) enhanced the nutritional quality and expanded the shelf life of WF (8). In Greece, a traditional type of bread is made with chickpea fermented in water as a leavening agent (9).

Steep fermented liquor of some plants, such as corn steep liquor is a cheap and environmental-friendly leavening agent in many functional food products. The development of an alternative low-cost fermentation medium containing main nutrients required for cell growth would reduce the cost of the fermentation process. Standard medium for *Clostridium* strain contain yeast extract, vitamins, minerals, trace metals and reducing agent (10, 11). Apart from the reducing agent, yeast extract is the most expensive component. Some cheap nutrients that could replace yeast extract are corn steep liquor, hydrolyzed cottonseed flour, hydrolyzed soy flour and ethanol stillage (12).

During chickpea steep liquor (CSL) fermentation, the levels of free fatty acids, reducing sugars and free amino acids were increased while the pH was decreased (9). After 10 h of fermentation, the degradation of chickpea proteins became obvious due to the proteolytic activities of *Bacillus* spp. The microflora that developed during a submerged fermentation of ground chickpea in water was studied in (9). Indigenous *bacilli* and *clostridia* in the fermented CSL may cause changes in the enzyme activities and its chemical composition. Changes in the chemical composition of CSL can be attributed to *bacilli*, until 10 h of fermentation, and then to *clostridia* until 18 h. Fermenting broth was not toxic to mice and the product was reported to be safe for consumption (9).

Baker's yeast is of the species *Saccharomyces cerevisiae* that is used as a leavening agent in bakery products, where it converts the fermentable sugars found in dough into CO₂ and ethanol. Using of water from potato boiling in bread dough provides food for the growth of yeasts (13). Al Khafaji *et al.* (14) used fermented CSL instead of baker's yeast in preparation of some leavened baked products, such as white breads, loaf bread, and flat tannour bread. The results revealed the superiority of leavened baked products prepared with CSL for most of the evaluated characteristics, especially leavening of loaf.

The continuous search for novel processes and products, which provides ingredients with new functionalities and cost-effective manufacturing, emphasizes the potential of food-grade fermentation and microbial bioconversion, that is crucial for the production of

functional leavened baked products (2, 15). The present work focuses on that, how a CSL fermentation process improves the quality of bread with particular attention to its effect on the rheological properties of WF dough and quality of the leavened bread.

MATERIALS AND METHODS

Materials

Chickpea (*Cicer arietinum*) seeds were obtained from local market in Zagazig city (Egypt). Seeds were hand-sorted to remove wrinkled and moldy seeds as well as foreign material, then stored in polyethylene bags in the refrigerator (4°C). Chickpea seeds were used to make a starter in fermentation experiments.

Methods

Preparation of chickpea steep liquor (CSL). Chickpea seeds (250 g) were submerged and soaked in 500 mL boiled distilled water (1:2, w/v) for 24 h at 37°C. After incubation of 24 h, foam was formed and the beaker was taken from the incubator. In another 500 mL beaker, filtration was performed on Whatman paper No.1 and about 300 mL of CSL was recovered. The obtained CSL was then freeze-dried using lyophilizer (Thermo Fisher).

Preparation of dough blends:

1. 98.5% wheat flour (WF) 72% extraction rate + 1.5% yeast (control).
2. 98.5% WF + 1.5% CSL.
3. 97% WF + 3% CSL.
4. 95.5% WF + 4.5% CSL.
5. 97% WF + 1.5% yeast + 1.5% CSL.
6. 95.5% WF + 1.5% yeast + 3% CSL.
7. 94% WF + 1.5% yeast + 4.5% CSL.

Baking process. Bread formula consisted of 500 g flour, 25 g sugar, 5 g salt and 25 g corn oil. The dough was divided into 150 g pieces. Each piece was molded on matrix of bread. The dough samples were left for fermentation at 37°C and 85% relative humidity for 60 min. The bread samples were proofed at 32-3°C and 85% relative humidity for 60 min, and then baked at 270-280°C for 20 min. Bread loaves were cooled at room temperature for about 60 min before evaluation and then were packed in polyethylene bags.

Rheological properties of dough formula. Rheological properties of dough samples were evaluated using Brabender farinograph according to the AACC method 56-50 (16).

Farinograph test. Brabender farinograph (Duisburg, Germany) test was carried out to determine the water absorption, arrival time, stability time, dough development time (DDT) and dough weakening of WF. Flour (300 g on modified moisture 14%) was placed in the farinograph bowl and the burette was filled with water at room temperature,

and then adjusted at zero. The machine was set at high speed and run for 1 min until zero-minute line was reached. Water was added immediately to the side of the bowl from the burette, nearly to the volume expected to be the right absorption of flour. When the dough begins to form, the dough was scraped down from the sides of the bowl. When the mixing curve levelled at a value larger than 500 BU, more water was added and the bowl was covered with a glass plate to prevent evaporation. Subsequent titration was needed to adjust the absorption curve at 500 BU. For final titration, the total volume of water was added within 25 seconds after opening burette's stopcock. Absorption values were corrected to the nearest 0.1% and values were calculated on 14% moisture basis using the following equation:

$$\text{Absorption (\%)} = (X+Y-300)/3$$

where X is the volume (mL) of water required to produce curve with maximum consistency entered on 500 BU line and Y is the weight (g) of flour equivalent to 300 g (14% moisture basis).

Fermentograph (gassing power) of CSL and yeast. The leavening ability of yeast and freeze-dried CSL blends (1.5% yeast + 1.5% CSL, 1.5% yeast + 3% CSL, and 1.5% yeast + 4.5% CSL) as well as CSL without yeast (1.5%, 3% and 4.5%) in dough preparations was determined by measuring gas volume developed in standard dough at 30°C for 2 h. The composition of standard dough was 10 g flour, 5.5 mL distilled water (containing 0.5 g glucose and 0.1 g NaCl), wherein the weight of tested dough was 0.5 g. The aforementioned ingredients (standard dough) were quickly mixed for 1 min, then placed in a test tube (24 X 200 mm) and kept at 30°C. The gas evolved from the dough that passed into graduated measuring cylinder (filled with saturated NaCl solution) was measured.

Evaluation of bread quality and sensory characteristics. Evaluation of the baked loaves quality characteristics was carried out following cooling to room temperature according to Paraskevopoulou *et al.* (17). A panel of ten judges assessed the sensory characteristics evaluation of panelists. They were asked to use the control sample as the basis for determining acceptance by first assigning score, and then to evaluate each test sample in comparison to the control.

Statistical analysis. Data obtained during dough and bread quality measurements were subjected to the analysis of variance (ANOVA) and Duncan's test using the software program of Statistical Package for the Social Sciences (SPSS, edition 16.0), in order to assess significant differences among samples. Differences were considered significant when $p < 0.05$.

RESULTS AND DISCUSSION

The results indicated that 8.2 g of freeze-dried CSL were obtained from 250 g of chickpea seeds (3.28%, w/w) after 24 h of fermentation at 37°C. The chemical composition of WF (72% extraction) used in this study consisted of 13.8% moisture, 10.15% protein, 0.74% lipids, 0.76% fiber, 0.61 ash and 87.74 carbohydrates.

During baking, bread ingredients undergo some changes such as evaporation of water, volume expansion, protein denaturation, starch gelatinization and crust formation (6, 18). Activation of some enzymes, acidification, proteolysis and the synthesis of microbial metabolites cause several physicochemical changes during dough fermentation, which affect the dough nutritional and functional properties. The WF digested *via* proteases and selected *lactobacilli* can be considered as safe for celiac patients (2). When CSL is fermented, bacilli initially and subsequently clostridia grow to high levels and degrade the constituents liberated from the chickpea into the water producing gas as the main end product. Enzymes such as cellulase, α -galactosidase, invertase, amylase and proteinase were detected in CSL and their maximal activities were recorded (9).

Rheological properties of WF dough affected by fermentation with CSL. Rheological properties of dough are useful for predicting the potential application of WF and the quality of the product (6). Dough properties can be measured using numerous rheological techniques wherein the common used instruments are farinograph, mixograph and extensograph (19). The Brabender farinograph was designed to record changes of dough consistency during kneading. Farinographs are commonly used for determination of the water absorption of flour (20). The flour is placed into a bowl, and while being kneaded, water is added to reach 500 FU (farinographic units) dough consistency. This value was obtained empirically and is considered the optimal consistency of WF dough used in the production of biologically leavened bread (4, 21).

In this study, CSL was fermented and used for leavening WF dough. The addition of CSL to WF brought some changes in its dough mixing behavior as measured by the farinograph. Farinogram values of flour doughs were affected by fortification with CSL compared with yeast (control), as shown in Table 1. The addition of CSL to the flour dough at 4.5, 9 and 13.5 g CSL/300 g WF caused a slightly decreased of water absorption, while arrival time was not affected. An increase in the farinograph water absorption of the dough was observed only in the case of 4.5% CSL and 1.5% yeast addition. The quantity of added water is considered very important for the distribution of the dough materials, their hydration and the gluten protein network development (6, 17).

Table 1. Effect of yeast and CSL on the farinograph characteristics of WF

Treatment	Dough formulation	Farinograph values				
		Water absorption %	Arrival time (min)	Dough development time (min)	Dough stability (min)	Degree of weakening (BU)
1	98.5% WF + 1.5% yeast	58.9	0.5	1.0	4.5	60
2	98.5% WF + 1.5% CSL	51.2	0.5	1.5	4.5	120
3	97% WF + 3% CSL	53.5	0.5	1.2	5.5	100
4	95.5% WF + 4.5% CSL	56.4	0.5	1.2	5.5	90
5	94% WF + 4.5% CSL + 1.5% yeast	60	0.5	1.2	7.5	80

Regarding dough stability, it appears that the dough samples containing CSL exhibited higher stability and resistance to mechanical mixing than the control. The addition of CSL to the flour dough at 4.5, 9 and 13.5 g CSL/300 g WF caused an increase in dough stability. Stability values increased from 4.5 min for the control sample to 4.5, 5.5 and 5.5 min for samples containing 4.5, 9 and 13.5 g CSL/300 g flour, respectively. In

general, the stability value is an index of the dough strength, with higher values indicating stronger dough.

The CSL addition also increased mechanical tolerance index and dough weakening. The addition of 13.5 g CSL, 4.5 g yeast/300 g WF caused a slight increase in the mechanical tolerance index, dough weakening and mixing time as shown in Figure 1. Maforimbo *et al.* (22) suggested that the weakening of WF dough by soy protein was the result of increased sulphhydryl concentration.

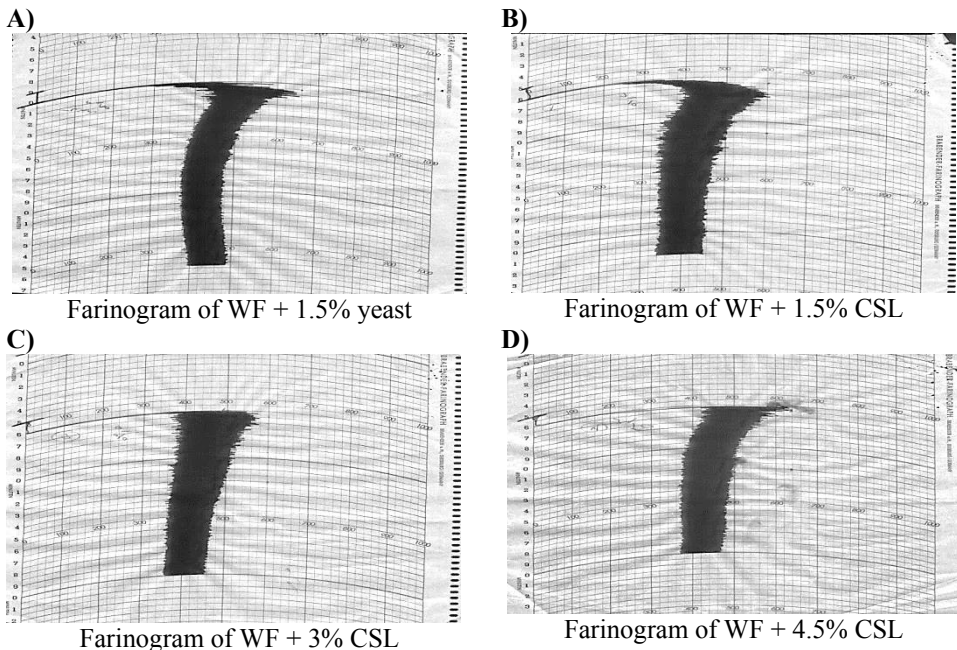


Figure 1. Farinograms of dough formulated from WF, yeast and CSL

The time required for the control dough to reach 500 BU consistency was also slightly modified by the CSL addition. During this phase of mixing, the water hydrates WF components and the dough is developed. The dough development time (DDT) was higher for all blends than for the control (1.2-1.5 min), while no significant difference was observed between the CSL samples (Table 1). The increase in DDT resulting from CSL addition could be due to the differences in the physicochemical properties between the constituents of the CSL on the one hand and those of the WF on the other.

Fermentograph (gassing power) of CSL and yeast. Leavening ability of yeast as well as blends of yeast and CSL in WF dough were determined after 16 h of fermentation. The results expressed as mL of CO₂ per gram of dough are presented in Table 2 and illustrated in Figures 2 and 3.

Table 2. Leavening ability of yeast and blends of yeast and CSL in WF dough

Dough sample	Fermentation time (min)								
	0	15	30	45	60	75	90	105	120
Control	13	20	28	45	57	67	68	68	69
CSL (1.5%)	13	13	14	14	14	14	14	14	14
CSL (3%)	13	13	14	14	14	14	14	14	14
CSL (4.5%)	13	13	13	13	13	13	13	13	13
Control + CSL (1.5%)	13	20	29	43	58	69	71	73	75
Control + CSL (3%)	13	20	29	37	52	65	71	73	75
Control + CSL (4.5%)	13	20	24	33	43	58	64	68	70

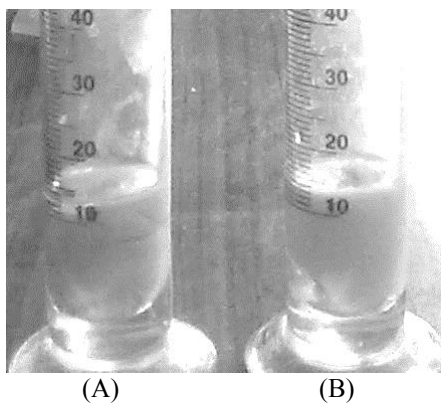


Figure 2. Leavening ability after 90 min of dough made with 3% CSL (A) and 4.5% CSL (B) without yeast

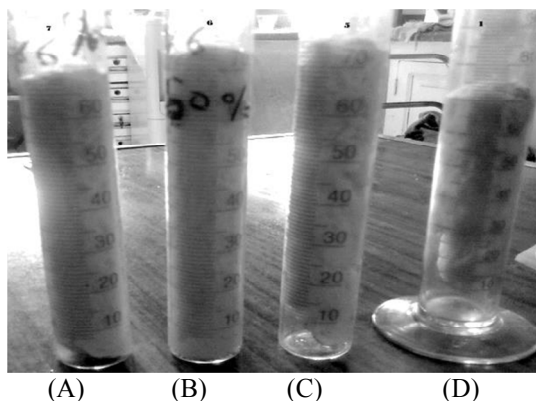


Figure 3. Leavening ability after 90 min fermentation of dough made with 1.5% yeast + 1.5% CSL (A), 1.5% yeast + 3% CSL (B), 1.5% yeast + 4.5% CSL (C) and control (D)

It can be noticed that the production of CO₂ was gradually increased with increasing the fermentation period for the formulation treatments 1, 2, 3 and 4. On the other hand, the production of CO₂ was constant in the formulation treatments 5, 6 and 7. The amount of gas production increased with the increase of fermentation time and CSL level. These results verified that CSL played an important role for improving the leavening ability of yeast in the production of dough. The increasing in the production of CO₂ may be due to the ability of microorganisms in CSL to produce CO₂. The ability of *S. cerevisiae* to produce CO₂ was enhanced in the presence of *Bacillus megitherum* and *Bacillus subtilus* in CSL (9).

The leavening of dough can be attributed to residual enzyme activity and enzymes liberated after cell lysis by the declining microbial population of *bacilli* and *clostridia* during dough rising. *B. cereus* and *C. perfringens*, predominantly growing during fermentation, do not seem to form toxins, and any health hazard after consumption of the bread, properly baked, seems improbable (9). In addition, the properties of WF dough and the quality of leavened bread mainly affect by the amount and quality of gluten. During dough development, proteins form a gluten network with unique viscoelastic characteristics. Due to its strength and extensibility, leavening gas is retained in the dough and the typical foam structure is created (4).

Physical properties of bread. Weight (g), volume (cm³), and specific volume (cm³/g) as a function of CSL content are presented in Table 3 and Figure 4. It was observed that the loaf weight slightly increased from 146.2 g for control to 152.2 g for bread fermented with 1.5 g CSL. While the loaf volume and specific volume of bread fermented with 1.5 g and 4.5 g CSL had a lower volume than the control bread. In addition, the specific volume of the loaf fermented with 1.5 g yeast and 3 g CSL had higher values than the bread fermented with CSL and the control bread.

Table 3. Physical properties of bread produced with or without CSL

Sample	Weight (g)	Volume (cm ³)	Specific volume (cm ³ /g)
Control (1.5% yeast)	146.2	515	3.52
1.5% CSL	152.2	85	0.55
3% CSL	152.2	95	0.65
4.5% CSL	152.7	100	0.65
1.5% yeast + 1.5% CSL	146.5	505	3.44
1.5% yeast + 3% CSL	147.0	520	3.53
1.5% yeast + 4.5% CSL	150.4	460	3.05

Crumb structure of baked products is a very important factor for the determination of the sensorial quality (6, 18). Examination of the loaf internal structure revealed that the crumb of the CSL-fermented bread contained a greater number of small gas cells compared to the control (Figure 4). Formation of large cells in bread is due to gluten elasticity that allows cell expansion by gas pressure during fermentation and oven spring. CSL are not as elastic as gluten, so they did not form a network and did not allow cell expansion, so the crumb appears more compact. This probably adversely affected bread volume, sug-

gesting that incorporation of CSL into WF resulted in a dough with more stable gas cells which did not coalesced readily during baking. Bread made with CSL-fermented WF exhibited an increased number of large cells probably due to an enhancement of the gas retention capacity of the gluten network.

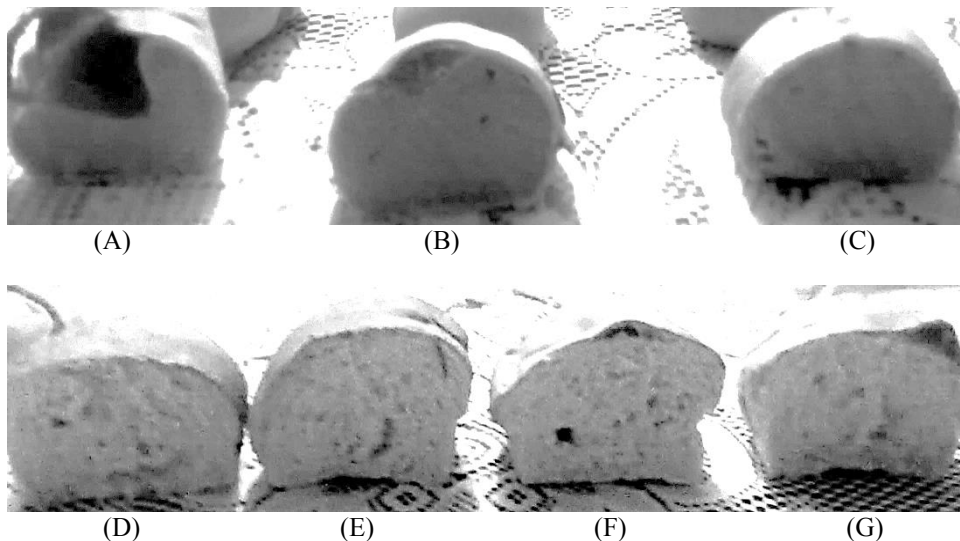


Figure 4. Sections of bread crumbs formulated with (A) 1.5% CSL without yeast, (B) 3% CSL without yeast, (C) 4.5% CSL without yeast, (D) control, (E) 1.5% yeast + 1.5% CSL, (F) 1.5% yeast + 3% CSL and (G) 1.5% yeast + 4.5% CSL

Sensory characteristics. The measured sensory characteristics included external characteristics (appearance and crust color), internal characteristics (texture, crumb quality, taste, odor, crumb color and volume) and the overall acceptability (Table 4).

Table 4. Sensory characteristics of bread formulated with or without CSL

Sample	External characteristic		Internal characteristic					Overall acceptability 100	
	Appearance 10	Crust color 10	Texture 15	Grain 15	Taste 15	Odor 15	Crumb color 10		Volume 10
Control (1.5% yeast)	9.4±0.16 ^a	9.4±0.16 ^a	14.3±0.26 ^a	14.2±0.20 ^a	14.2±0.25 ^a	14.1±0.23 ^a	9.6±0.16 ^a	9.4±0.22 ^a	94.5±0.89 ^a
1.5% CSL	4.1±0.23 ^d	6.8±0.20 ^d	7±0.26 ^c	7±0.21 ^d	7±0.33 ^c	8.4±0.31 ^d	6.2±0.2 ^d	4±0.15 ^f	49.2±0.74 ^d
3% CSL	3.6±0.22 ^{de}	4±0.26 ^c	8±0.21 ^d	6.2±0.20 ^e	4.8±0.29 ^d	5.1±0.23 ^c	3.8±0.13 ^c	5.4±0.22 ^d	41.4±0.81 ^c
4.5% CSL	3.5±0.22 ^c	3.8±0.29 ^c	7.3±0.33 ^{de}	6±0.37 ^c	4.7±0.26 ^d	5±0.33 ^c	3.6±0.27 ^c	4.7±0.15 ^e	38.4±1.11 ^f
1.5% yeast + 1.5% CSL	8.3±0.15 ^b	8.8±0.20 ^b	13±0.26 ^b	13.4±0.22 ^{ab}	12.7±0.26 ^b	13.1±0.23 ^b	8.8±0.20 ^b	8.3±0.21 ^b	86.4±0.87 ^b
1.5% yeast + 3% CSL	8±0.21 ^b	7.8±0.13 ^c	12.2±0.36 ^{bc}	13±0.26 ^{bc}	12.6±0.27 ^b	12.3±0.21 ^c	7.8±0.20 ^c	8±0.15 ^b	81.7±1.05 ^c
1.5% yeast + 4.5% CSL	7.3±0.21 ^c	8.4±0.16 ^b	12.1±0.28 ^c	12.5±0.27 ^c	12.3±0.30 ^b	12±0.21 ^c	7.9±0.18 ^c	7.4±0.22 ^c	80.4±1.05 ^c
Least significant difference (L.S.D.)	0.53	0.58	0.80	0.68	0.78	0.67	0.53	0.54	2.59

*Properties with the same letter differed no significantly at the 0.05 probability level.

The results indicated that the addition of 1.5, 3.0 and 4.5% CSL + 1.5% yeast caused significant differences in the external, internal characteristics and overall score of the CSL-fermented bread in comparison with the control. A decrease in the acceptability of the CSL-fermented bread was noticed in comparison with the control. The decrease in the sensory characteristics was high in bread samples made without yeast. The data in Table 4 show that the combination of yeast and CSL increased the acceptability of bread with the increasing level of the both materials. CSL might be like egg yolk with emulsifying action that could improve structural characteristics and may influence the flavor and color of the bakery products.

CONCLUSION

Although a very few studies in the literature showed the functional potential of the CSL fermentation, the interim prospect would probably be to consider the CSL fermentation like a cell factory to modify cereals for functionally and nutritionally tailored food. The formation or modification of bioactive compounds during CSL fermentation should expand the toolset to develop CSL-fermented baked goods. It appears that the addition of CSL to WF modified the rheological properties of the dough as well as the characteristics of the baked bread. An increase in the farinograph water absorption of the dough was recorded in the case of CSL and yeast addition, presumably due to greater water requirement of its proteins in order to become hydrated. The CSL addition increased the dough development time and stability. This was attributed mainly to possible association between the gluten and some of the CSL constituents. The development of such functional foods would be beneficial to improve the nutritional status of consumers.

REFERENCES

1. Scazzina, F.; Del Rio, D.; Pellegrini, N.; Brighenti, F. Sourdough bread: starch digestibility and postprandial glycemic response. *J. Cereal Sci.* **2009**, *49*, 419-421.
2. Gobetti, M.; Rizzello, C.G.; Di Cagno, R.; De Angelis, M. How the sourdough may affect the functional features of leavened baked goods. *Food Microbiol.* **2014**, *37* 30-40.
3. Singh, H.; MacRitchie, F. Application of polymer science to properties of gluten. *J. Cereal Sci.* **2001**, *33*, 231-243.
4. Buresova, I.; Kracmar, S.; Dvorakov, P.; Streda, T. The relationship between rheological characteristics of gluten-free dough and the quality of biologically leavened bread. *J. Cereal Sci.* **2014**, *60*, 271-275.
5. FAO. Bulletin of Statistics. Food and Agriculture Organization, 2001.
6. Mohammed, I.; Ahmed, A.R.; Senge, B. Dough rheology and bread quality of wheat-chickpea flour blends. *Ind. Crops Prod.* **2012**, *36*, 196-202.
7. Kaur, M.; Singh, N. Studies on functional, thermal and pasting properties of flours from different Chickpea (*Cicer arietinum* L.) cultivars. *Food Chem.* **2005**, *91*, 403-411.

8. Tulbek, M.C.; Hall, C.; Schwarz, J.G. Abstract in IFT Annual Meeting, Chicago, **2003**, 13-16.
9. Hatzikamari, M.; Kyriakidis, D.A.; Tzanetakis, N.; Biliaderis, C.G.; Litopoulou-Tzanetaki, E. Biochemical changes during a submerged chickpea fermentation used as a leavening agent for bread production. *Euro. Food Res. Technol.* **2007**, *224*, 715-723.
10. Saxena J. Development of an Optimized and cost-effective medium for ethanol production by clostridium strain P11. PhD, University of Oklahoma, Norman, OK, **2008**, p. 110.
11. Saxena, J.; Tanner, R.S. Effect of trace metals on ethanol production from synthesis gas by the ethanologenic acetogen, *Clostridium ragsdalei*. *J. Ind. l Microbiol. Biotechnol.* **2011**, *38*, 513-521.
12. Witjitra, K.; Shah, M.M.; Cheryan, M. Effect of nutrient sources on growth and acetate production by *Clostridium thermoaceticum*. *Enz. Microb. Technol.* **1996**, *19*, 322-327.
13. Aslankoochi, E.; Rezaei, M.N.; Vervoort, Y.; Courtin, C.M.; Verstrepen, K.J. Glycerol Production by Fermenting Yeast Cells Is Essential for Optimal Bread Dough Fermentation. *PLoS ONE*, **2015**, *10*(3), 1-13. doi:10.1371/journal.pone.0119364.
14. Al-Khafaji, Z.M.; Abdul-Hussien, S.S.; Awadala, R.A. Using of fermented chickpea infusion in some bakeries. *Iraqi J. Agric. Sci.* **1999**, *30*, 523-530.
15. De Vos, W.M.; Frontiers in food biotechnology- Fermentations and functionality. *Current Opinion in Biotechnology*, **2005**, *16*, 187-189.
16. AACC-American Association of Cereal Chemists. Approved methods of the AACC (Method 54-21, appr. Apr 1961, rev. Oct 1982, 8th ed.) St Paul: AACC, 1983.
17. Paraskevopoulou, A.; Provatidou, E.; Tsotsiou, D.; Kiosseoglou, V. Dough rheology and baking performance of wheat flour–lupin protein isolate blends. *Food Res. Inter.* **2010**, *43*, 1009-1016.
18. Regier, M.; Hardy, E.H.; Knoerzer, K.; Leeb, C.V.; Schuchmann, H.P. Determination of structural and transport properties of cereal products by optical scanning, magnetic resonance imaging and Monte Carlo simulations. *J. Food Eng.* **2007**, *81*, 485-491.
19. Dobraszczyk, B.J.; Morgenstern, M.P. Rheology and the breadmaking process. *J. Cereal Sci.* **2003**, *38*, 229-245.
20. Mondal, A.; Datta, A. Bread baking: A review. *J. Food Eng.* **2008**, *86*, (2008) 465-474.
21. Kuktaite, R.; Larsson, H.; Johansson, E. The influence of dough mixing time on wheat protein composition and gluten quality for four commercial flour mixtures. In *Wheat Production in Stressed Environments*; Buck, H.T., Nisi, J.E., Salomon, N., Eds.; Springer, New York, 2007; pp. 543-548.
22. Maforimbo, E.; Skurray, G.; Uthayakumaran, S.; Wringley, C. Incorporation of soy proteins into the wheat–gluten matrix during dough mixing. *J. Cereal Sci.* **2007**, *47*, 380-385.

СУВИ ВОДЕНИ ЕКСТРАКТ ЛЕБЛЕБИЈЕ (*Cicer arietinum*) КАО АГЕНС КВАСАЊА: УТИЦАЈ НА РЕОЛОГИЈУ ТЕСТА И СЕНЗОРНЕ КАРАКТЕРИСТИКЕ ХЛЕБА

*Ахмед М. Саад¹, Рагаб А. Елмасри¹, Калед М.М. Вахдан¹,
Мохамед Фавзи Рамадан^{1,2*}*

¹ Универзитет у Загазигу, Пољопривредни факултет, Департман пољопривредне биохемије, Египат

² Универзитет Ум Ал-кура, Деканат за научна истраживања, Мака, Краљевина Саудијска Арабија

Ферментација теста је један од најстаријих процеса у технологијама хране. Овај процес се у новије време интензивно проучава због свог утицаја на сензорне, структурне и нутриционе карактеристике, као и на одрживост пецива од киселог теста. Циљ овог рада је био да се испита утицај сушеног екстракта леблебије (СЕЛ) као агенса квасања теста на реологију теста и сензорне карактеристике хлеба. СЕЛ је био припремљен мочеем семена леблебије у прокуваној дестилованој води (1:2) у току 24 сата на 37°C, после чега је филтрирани екстракт лиофилизиран, да би се добио СЕЛ. Додавање СЕЛ у пшенично брашно (ПБ) довело је до промена у понашању теста при мешању, што је праћено помоћу фаринографа. Примећено је да тесто има повећану моћ апсорпције воде када му се дода 4,5% СЕЛ и 1,5% квасца, што није утицало на време надолажења. Додавање СЕЛ тесту у количини од 4,5, 9,0 и 13,5 г СЕЛ/300 г ПБ довело је до повећане стабилности теста. Такође, то је довело и до повећања индекса механичке толеранције воде, слабљења теста и времена мешања. Време нарастања теста за све смеше било је дуже у поређењу са контролом (1,2-1,5 мин), док се узорци са СЕЛ нису значајно разликовали. Тежина векне се мало повећала, са 146,2 г (контрола) на 152,2 г за хлеб ферментисан помоћу СЕЛ, док су запремина векне и специфична запремина узорака са СЕЛ биле мање него код контроле. Комбинација пекарског квасца и СЕЛ довела је до повећања прихватљивости производа са повећањем нивоа оба агенса квасања. Резултати су показали да се СЕЛ може користити као алтернатива квасцу у ферментацији. С друге стране, СЕЛ је богат нутријентима и има нижу цену од квасца.

Кључне речи: Тесто, печење, функционалне карактеристике, пециво, фаринограф, ферментограф

Received: 14 July 2015.
Accepted: 11 October 2015.

POLYFLORAL, LINDEN AND ACACIA HONEYS WITH DRIED CHERRIES AFTER THREE MONTHS OF STORAGE – ANTIOXIDANT AND SENSORY EVALUATION

Jelena J. Vulić*, Jasna M. Čanadanović-Brunet, Gordana S. Četković, Sonja M. Djilas, Vesna T. Tumbas Šaponjac and Sladjana M. Stajčić

University of Novi Sad, Faculty of Technology, Bulevar cara Lazara 1, 21000 Novi Sad, Serbia

Samples of three types of honey: polyfloral (PH), linden (LH) and acacia (AH), without and with addition of dried cherries (40%) were analyzed before and after three months of storage. The total phenol (TPh), flavonoid (TFd) and anthocyanin (TAn) contents, antioxidant activities and sensory properties of honeys with and without the addition of dry cherries were evaluated. TPh and TFd increased with addition of dried cherries to the honey, while enriched honeys showed high TAn. The LH sample with dried cherries showed the highest anthocyanins content (41.41mgCGE/100g). The antioxidant activity increased with addition of dried cherries in honey in the DPPH test and reducing power. The PH and enriched PH exhibited the best antiradical activity compared to LH and AH. The EC_{50}^{DPPH} values were: 23.81 for PH and 24.19 mg/mL for PH, while the EC_{50}^{DPPH} were: 1.16 mg/mL for PH40 and 1.18 mg/mL for PH40s. $RP_{0.5}$ values were: 57.00 mg/mL for PH40 and 56.00 mg/mL for PH40s, while $RP_{0.5}$ were: 15.05 mg/mL for PH40 and 15.18 mg/mL for PH40s. The statistical analysis showed that TPh, TFd and TAn, and antioxidant activity of honeys and enriched honeys showed significant correlation. Sensory analysis of honey with dried cherries, before and after storage, indicated very good sensory characteristics.

KEY WORDS: Honey, dried cherry, antioxidant activity, sensory analysis, storage

INTRODUCTION

Honey is a natural food product well known for its high nutritional and prophylactic-medicinal value (1). It is often used as a sugar substitute, an ingredient or a natural preservative in many of manufactured foods, because of its sweetness, color and flavor. Also, it can prevent oxidation reactions in foods (e.g., lipid oxidation in meat (2) and enzymatic browning of fruits and vegetables (3)). Numerous flavonoids (such as apigenin, pinocembrin, pinobanksin, kaempferol, quercetin, galangin, chrysin, and luteolin) and phenolic acids (caffeic, gallic, cinnamic, protocatechuic, *p*-coumaric, and chlorogenic acids) were identified in honey samples (4,5). Several studies have shown that the varia-

* Corresponding author: Jelena J. Vulić, University of Novi Sad, Faculty of Technology, Bulevar cara Lazara 1, 21000 Novi Sad, Serbia, e-mail: jvulic@uns.ac.rs

bility in sugars and secondary metabolites are related to the source and botanical origin of the nectar (6). Apitherapy (the medical use of honeybee products) has recently become the focus of attention as a folk and preventive medicine for treating certain conditions and diseases, as well as promoting overall health and well-being (7). Serbia has a very long tradition of beekeeping. Its favorable climate, good geographical conditions and a variety of botanical species provide great potential for the development of apiculture (8).

Honeys are divided as monofloral or polyfloral. Monofloral honeys are produced from one plant species containing predominantly its nectar with minor nectar contributions from other botanical origins. Polyfloral honey has several plant sources, none of which is predominant. In practical terms it can be considered as a blend of several monofloral honeys with significant nectar or honeydew contributions from different plants [9]. In Serbia, honey is consumed in original form and as a comb honey or with the addition of propolis, pollen or other bee products. Also, some nuts or dried fruits can be added to honeys and used as a very delicious dessert.

Fruits are considered as a natural source of antioxidants, including anthocyanins and phenolics (10). These compounds can reduce the risk of degenerative diseases caused by oxidative stress, such as cancer and cardiovascular diseases (11). The production of cherry fruit is on the third place in Serbia. It is a highly profitable fruit variety, because it is relatively easy growing and has a good demand on market (12). Phenolic contents in cherries are influenced by the cultivar, the growing season and the growing location (13,14). Drying is one of the oldest methods for food preservation (15).

To our knowledge, this is the first study of the antioxidant and sensory characteristics of honeys with dried cherries. The aim was to evaluate total phenolic, flavonoid and anthocyanin contents, antioxidant activity and sensory properties of polyfloral, linden and acacia honeys with dried cherries before and after three months of storage. Antioxidant characteristics were determined by 2,2-diphenyl-1-picrylhydrazyl (DPPH) test and reducing power (RP).

EXPERIMENTAL

Chemicals and reagents

The chemicals used for these investigations were Folin-Ciocalteu reagent (Fluka Chemical Co., Buchs, Switzerland), trichloroacetic acid, 2,2-diphenyl-1-picrylhydrazyl (Sigma Chemical Co., St. Louis, Mo, USA). All other chemicals and reagents were of the highest analytical grade, obtained from J.T. Baker (Deventer, Holland). The total phenolic, flavonoid, anthocyanin, DPPH free radical scavenging assays and reducing power were determined using an UV-1800 spectrophotometer (Schimadzu, Kyoto, Japan).

Honey and dried cherries samples

The honeys with dried cherries were prepared from polyfloral (P), linden (L) and acacia (A) honey (obtained from the honeybee farm „Simonović“, Belgrade, Serbia). Dried cherries (produced by Agranela, Valjevo, Serbia) were added to the honey in 40%

mass concentrations (PH40, LH40, and AH40). The enriched honeys before and after three months storage were grounded in domestic food processor (Bosh, Compact Kitchen Mashine 4420, Gerlingen-Stuttgart, Germany).

Total phenolic content (TPh)

Total phenolics were determined spectrophotometrically by the Folin-Ciocalteu method [16]. The content of total phenolics was expressed as mg of gallic acid equivalents per 100 g of honey sample (mg GAE/100 g).

Total flavonoid content (TFd)

Total flavonoids were measured by the aluminium chloride spectrophotometric assay [17]. Total flavonoid content was expressed as mg of rutin equivalents per 100 g of honey sample (mg RE/100 g).

Total anthocyanin content (TAn)

Total anthocyanins were determined spectrophotometrically by the Markham et al. method [18]. The content of total anthocyanins was expressed as mg of cyanidin-3-O-glucoside equivalents per 100 g of honey sample (mg CGE/100 g).

DPPH free radical scavenging assay

Homogenized honeys were dissolved in methanol, and each sample (1.5 mL) or methanol (1.5 mL, blank) was mixed with DPPH solution in methanol (3 mL, 0.02 mg/mL) in appropriate range of investigated concentrations (for honeys: 0.56-500 mg/mL; for enriched honeys: 0.11-55.56 mg/mL). The mixtures were left for 15 min at room temperature and then the absorbances was measured at 517 nm against reference mixtures that were prepared in the similar manner, by replacing the DPPH solution with methanol. The ability of honey samples to scavenge DPPH radicals, SA_{DPPH} value, was calculated using the following equation: $SA_{DPPH} (\%) = 100 \times (A_0 - A_x) / A_0$, where A_0 and A_x are the absorbances of the blank and the sample, respectively.

Reducing power

The solution of honeys and enriched honeys (1.5 – 300 mg/mL) in distilled water (1 mL) or distilled water (1 mL, blank) was mixed with phosphate buffer (1 mL, pH 6.6) and potassium ferricyanide, $K_3[Fe(CN)_6]$, (1 mL, 1 w/w). The mixture was incubated at 50°C for 20 min and then rapidly cooled. Following this, trichloroacetic acid (1 mL, 10%) was added and the mixture was then centrifuged at 1811.16 g for 10 min. An aliquot (2 mL) of the upper layer, mixed with distilled water (2 mL) and $FeCl_3$ (0.4 mL, 0.1%), was left to stand for 10 min. The absorbance of the mixture was measured at 700 nm against the blank.

Sensory analysis

Sensory analysis was conducted according to the general guidelines regarding the design of test rooms (19), general sensory analysis guidance (20) and training of assessors (21). Sensory evaluation was carried out by seven experienced panelists (ages 35 to 60) selected from previously trained academic staff of the Faculty of Technology, Novi Sad. Drinking water was provided for palate cleansing between each sample. Sensory profiling was performed using a generic descriptive analysis technique, according to Piana et al. (22). Sensory evaluation included the selected representative properties of honey samples: density, intensity of color, aroma and odor. These properties were evaluated using a 3-point method. Marks were given based on the scale from 0 “unacceptable product” to 3 “optimal quality level”.

Statistical analysis

All analyses were run in triplicate and the results were expressed as means \pm standard deviation (SD) except for sensory analysis ($n=7 \times 7$). Statistical analyses were done by using Microsoft Office Excel 2007 software. Significant differences were calculated by ANOVA test and least significant difference (LSD) test ($P < 0.05$).

RESULTS AND DISCUSSION

Polyfloral (P), linden (L) and acacia (A) honeys were used to prepare honey samples with 40% of dried cherries (PH40, LH40 and AH40). Also, the changes in the antiradical activity of honeys after three months of storage (PH40s, LH40s and AH40s) were investigated. The comparative evaluation of the phenolic composition of honey samples was based on: total phenolics (TPh), total flavonoids (TFd), total anthocyanins (TAn) content, the ratio of TFd in relation to TPh (TFd/TPh) and the ratio of TAn in relation to TPh (TAn/TPh) (Table 1).

The TPh and TFd increased with the addition of dried cherries to honey, while enriched honeys showed high TAn. TAn were not detected in raw honeys. LH40 showed the highest anthocyanins content (41.41mgCGE/100g). In comparison to honey, the TPh increase was by 1.45 times for PH40, 1.21 times for LH40 and 2.17 times for AH40, while in the honeys after three months of storage the TPh increased by 1.40 times for PH40s, 2.31 times for LH40s, and 2.15 times for AHs. The increase in TFd was approximately 2.81 times for PH40, 1.21 times for LH40 and 1.44 times for AH40, while after three months of storage TFd increased 2.84 times for PH40s, 1.16 times for LH40s and 1.45 times for AH40s. The TAn contents were determined only in enriched honeys, before and after storage. The determined TAn contents in enriched honeys were slightly lower after three months of storage.

It can be concluded that enriched honeys possess higher content of phenolics in comparison to raw honeys. Honeys and enriched honeys after storage had almost the same phenolics content like before the storage time. The amount of phenolics in honeys is closely related not only to the floral variety but also to the specific parameters such as soil

composition and meteorological conditions [23]. The botanical origin of honey is one of its main quality parameters, and its price is very often related to the floral origin (1).

Table 1. Phenolics composition of honeys with and without addition of dried cherries

Sample	TPh (mg GAE/100 g) ¹	TFd (mg RE/100 g) ²	TAn (mgCGE/100g) ³	TFd/TPh ⁴	TAn/TPh ⁵
PH	38.50±1.7 ^a	8.32±0.34 ^a	-	0.22	-
PHs	38.40±1.14 ^a	8.06±0.25 ^a	-	0.21	-
PH40	55.77±2.13 ^b	23.41±0.69 ^b	37.91±1.43 ^a	0.42	0.68
PH40s	53.88±2.14 ^b	22.86±1.09 ^{b,c}	37.57±1.66 ^a	0.42	0.70
LH	23.96±1.62 ^{*c}	18.11±0.81 ^{*d}	-	0.76	-
LHs	23.01±0.99 ^c	17.56±0.64 ^d	-	0.76	-
LH40	53.96±2.45 ^b	21.84±0.78 ^{b,c,d}	41.41±1.86 ^a	0.40	0.77
LH40s	53.13±2.02 ^b	20.42±1.01 ^d	40.41±1.97 ^a	0.38	0.76
AH	20.04±0.88 ^c	14.03±0.56 ^e	-	0.70	-
AHs	19.66±0.72 ^c	13.88±0.49 ^e	-	0.71	-
AH40	43.40±1.77 ^a	20.26±0.89 ^d	31.23±1.46 ^b	0.47	0.72
AH40s	42.20±1.56 ^a	20.18±0.77 ^{c,d}	30.06±1.43 ^b	0.48	0.71

*Taken from Cetkovic et al. (2014)

¹Total phenol content expressed as mg gallic acid equivalents per 100 g of honey sample; ²Total flavonoid content expressed as mg rutin equivalents per 100 g of honey sample; ³Total anthocyanin content expressed as mg cyanidin-3-O-glucoside equivalents per 100 g of honey sample; ⁴TFd/TPh: the ratio of TFd in relation to TPh; ⁵TAn/TPh: the ratio of TAn in relation to TPh. TPh, TFd and TAn values are mean ± SD of three replicates. Values sharing the same letters in the same column are not significantly different from each other at the level of 5%.

Tumbas et al. (24) reported that the addition of 40% of prunes to raw acacia honey, increased the content of total phenolics content by 2.5 times (from 16.18 to 41.64 mgGAE/100g), while the flavonoid level was increased approximately by 11.15 times (from 2.65 to 30.86 mgRE/100g). The results in this study are in accordance for phenolics, while the flavonoids content increased less from raw to honey with dried cherries, than in the study by Tumbas et al. (24). Beretta et al. (25) and Bertoncelej et al. (26) reported the phenolics contents of acacia honeys: 5.52 mgGAE/100g of commercial acacia honey and 4.48 mgGAE/100g of Slovenian acacia honey, respectively. The results shown in Table 1. have higher values.

In our research we evaluated the antioxidant activity of honeys and honeys with dried cherries using two spectrophotometric methods: DPPH test and reducing power. The antioxidant molecules can quench DPPH free radicals (i.e. by providing hydrogen atoms or by electron donation, conceivably via a free-radical attack on the DPPH molecule) and convert them to a colorless/bleached product (i.e. 2,2-Diphenyl-1-hydrazine, or a substituted analogous hydrazine), resulting in a decrease in the absorbance at 517 nm (27). The presence of reductants (i.e. antioxidants) causes the reduction of the ferric–ferricyanide complex to the ferrous–ferricyanide complex of Perl’s Prussian blue. Therefore, Fe²⁺ can be monitored by measuring the absorbance at 700 nm in reducing power method (28).

The honeys with dried cherries exhibited higher antioxidant activity than honeys without dried cherries, while the honeys after three months of storage did not exhibit big changes in the antioxidant activity. Cetkovic et al. (5) showed that the antioxidant activity

increased with increasing the concentration of dried apricots in linden honey and that it could be explained by the fact that bioactive components of dried apricot were transferred to linden honey, while the same trend of honey samples antiradical activity remained after the storage period. Vulic et al. (29) reported an increase in the phenolics content and antioxidant activity of polyfloral honey with dried apricots. Also, after one-year storage there was no significant changes in antioxidant activity. Canadanovic-Brunet et al. (30) reported that dried apricot has good antioxidant activity and that phenolic compounds in dried apricot appear to be the main contributors to their antioxidant capacity. Besides phenolics present in honeys, the compounds present in dried cherries were most probably the key constituents contributing to the antioxidant capacity of the enriched honey samples.

The EC₅₀, defined as the concentration of extract required for 50% scavenging of DPPH radicals under experimental condition employed, was used to measure the free radical SA [31], while for RP it is the concentration of the antioxidant assigned at 0.5 value of absorption. The rResults are presented in Table 2.

Table 2. Antioxidant activities of honeys with and without addition of dried cherries

Sample	EC ₅₀ ^{DPPH} (mg/mL) ¹	RP _{0.5} (mg/mL) ²
PH	23.81±1.02 ^a	57.00±2.67 ^a
PHs	24.19±1.09 ^{a,b}	56.00±2.65 ^a
PH40	1.16±0.02 ^c	15.05±0.71 ^b
PH40s	1.18±0.03 ^c	15.18±0.69 ^b
LH	189.83±6.24 ^{*d}	169.00±6.06 ^{*c}
LHs	190.01±8.99 ^d	170.11±8.00 ^c
LH40	1.42±0.07 ^c	16.09±0.73 ^b
LH40s	1.41±0.06 ^c	15.21±0.64 ^b
AH	314.80±14.77 ^c	256.64±11.65 ^d
AHs	315.03±14.98 ^c	257.99±11.99 ^d
AH40	1.69±0.07 ^c	17.60±0.54 ^b
AH40s	1.71±0.08 ^c	15.96±0.70 ^b

*Taken from Cetkovic et al. [5]

¹the concentration of antioxidant necessary to decrease the initial concentration of DPPH radicals by 50%; ²the concentration of antioxidant assigned at 0.5 value of absorption; EC₅₀^{DPPH} and RP_{0.5} values are mean ± SD of three replicates. Values sharing the same letters in the same column are not significantly different from each other at the level of 5%.

The PH and enriched PH exhibited the best antioxidant activity comparing to LH, AH, LH40 and LH40, before and after storage. The EC₅₀^{DPPH} values were: 23.81 for PH and 24.19 mg/mL for PHs, while the EC₅₀^{DPPH} were: 1.16 mg/mL for PH40 and 1.18 mg/mL for PH40s. RP_{0.5} values were: 57.00 mg/mL for PH40 and 56.00 mg/mL for PH40s, while RP_{0.5} were: 15.05 mg/mL for PH40 and 15.18 mg/mL for PH40s. It can be concluded that during the three months honeys and enriched honeys retained good antioxidant activities.

Because of the great variation in honey composition, the biological activities exhibited by the honey samples varied according to the geographical and botanical origin of honey, while processing and storage condition might affect the biological activities only to a minor degree (32).

For the correlation analysis, the EC₅₀ values were transformed into their reciprocal values, 1/EC₅₀. The 1/EC₅₀ values are more representative of the presented activity because they follow the increasing trend of honey samples in tested assays (Figure 1).

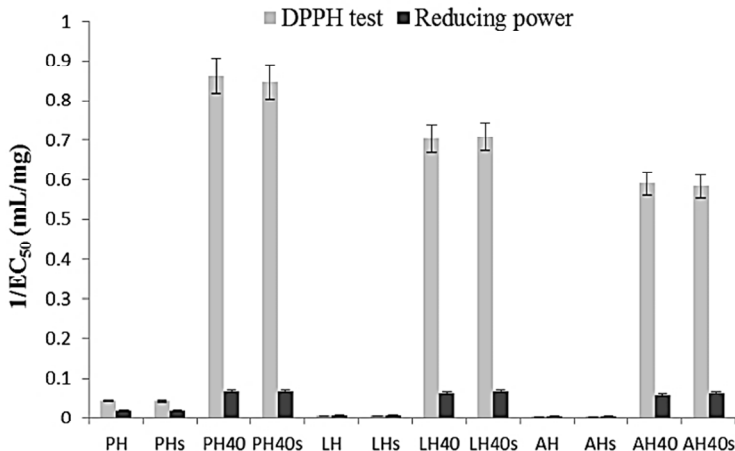


Figure 1. 1/EC₅₀ values of honeys with and without addition of dried cherries

Statistical tool can be considered as a useful complimentary approach to investigate the relationship between the antioxidant activities of honey and its biochemical composition. Pearson’s correlation coefficients (R) between the composition and the antioxidant activities of honey samples are shown in Table 3.

Table 3. Pearson’s coefficients of correlation between the composition and the antioxidant activities of honey samples

		TPh (mg GAE/100 g)	TFd (mg RE/100 g)	TAn (mgCGE/100g)	1/EC ₅₀ (mL/mg)	
					DPPH	RP
1/EC ₅₀ (mL/mg)	RP	0.93	0.73	0.57	0.99	-
	DPPH	0.91	0.81	0.62	-	
TPh (mg GAE/100 g)		-	0.74	0.96		
TFd (mg RE/100 g)			-	0.70		
TAn (mgCyG/100g)				-		

There was a very good correlation between the total phenolic contents and the analyzed antioxidant activities of honey samples (0.91 for DPPH radical scavenging activity and 0.93 for reducing power). The correlation coefficients for the relation between the analyzed antioxidant activities and flavonoids (0.81 for DPPH radical scavenging activity and 0.73 for reducing power) and anthocyanins (0.62 for DPPH radical scavenging activity and 0.57 for reducing power) were slightly lower. Cetkovic et al. (5) and Vulic et

al. (29) also reported high correlation factors between the phenolics and flavonoid contents, and antioxidant activity of honeys.

Based the high correlation coefficients, it can be noticed that phenolics, flavonoids and anthocyanins play very important role in the antioxidant activity of honeys and honeys with dried cherries. Dai et al. (33) reported that, although the mechanisms behind the bioactivities of phenolics and anthocyanins involve many pathways, the most remarkable aspect of their activities may be their ability to act as either antioxidants or prooxidants in some biological environments. Significant correlations between the color parameters, phenolics, and antioxidant capacity have been demonstrated by Beretta et al. (34), Ferreira et al. (35) and Bertoneclj et al. (36).

An important parameter of honey is its color, which reflects the floral source (36). PH, LH and AH with and without dried cherries, before and after storage, were evaluated by a 7-member trained expert descriptive attribute sensory panel. The sensory quality of honey samples was defined based on density, intensity of color, aroma and odor. Samples were scored using the 0 to 3 intensity scale and the results are presented in Figure 2.

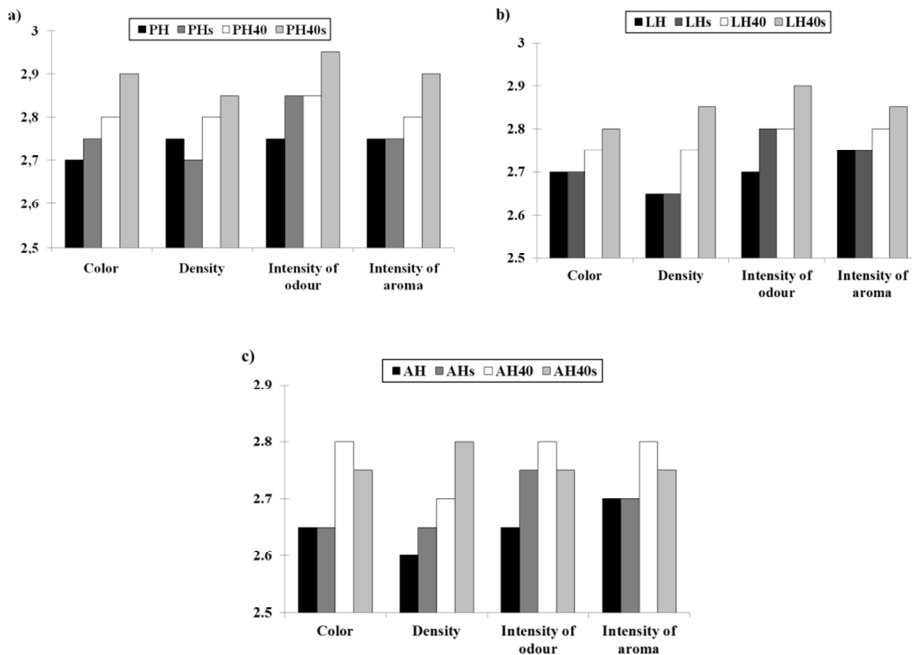


Figure 2. Sensorial characteristics of honey samples. a) PH and PH with addition of dried cherries, before and after storage; b) LH and LH with addition of dried cherries before and after storage; c) AH and AH with addition of dried cherries before and after storage.

Scores are means of seven evaluations by seven panelists. Scores: 0 - unacceptable, 1 - acceptable, 2 - good, 3 - optimal quality level.

Darker honeys tend to have higher antioxidant activity and an increased concentration of phenolic compounds (37). Ferreira et al. (35) showed that dark honeys were richer in phenolics and had a higher antioxidant activity. Sensorial descriptive profiling of all honeys indicated very good quality. Panelists' evaluations of honeys indicated that polyfloral honeys with the addition of dried cherries showed the best sensory properties. Dried cherries in PH improved density, color, odor and aroma. The total sensory scores, increased from 2.73 for PH to 2.88 for PH40 and 2.78 for PHs to 2.86 for PH40s, which shows that the quality of honey samples was improved with addition of dried cherries. Good sensory characteristics of honey enriched with dried cherry remained practically unchanged after three months of storage.

CONCLUSION

This study showed that polyfloral, linden and accacia honeys and honeys with dried cherries, before and after three months storage, contained high amounts of bioactive compounds and possessed good antioxidant activity. Also, high level of correlation between the phenolics, flavonoids and anthocyanins content and antioxidant activities of all studied honeys confirmed that they may be products of wide use due to good consumers acceptance. The addition of dried cherries improved the sensory properties of investigated honeys. The three-month storage of the raw and enriched honeys did not affect the good quality of the samples.

Acknowledgement

This research is part of the Project No. 114-451-964/2015-02, which is financially supported by the Provincial Secretariat for Science and Technological Development of the Autonomous Province of Vojvodina, Republic of Serbia.

REFERENCES

1. Pyrzynska, K.; Biesaga, M. Analysis of phenolic acids and flavonoids in honey. *Trends Anal. Chem.* **2009** 28(79), 893-902.
2. Nagai, T.; Inoue, R.; Kanamori, N.; Suzuki, N.; Nagashima, T. Characterization of honey from different floral sources. Its functional properties and effects of honey species on storage of meat. *Food Chem.* **2006**, 97, 256-262.
3. Ibanez, E.; Cifuentes, A. New analytical techniques in food sciences. *Crit. Rev. Food. Sci.* **2000**, 41, 413-450.
4. Gašić, U.; Keckes, S.; Dabic, D.; Trifkovic, J.; Milojkovic-Opsenica, D.; Natic, M.; Tešić, Z. Phenolic profile and antioxidant activity of Serbian polyfloral honeys. *Food Chem.* **2014**, 145, 599-607.
5. Cetkovic, G.; Canadanovic-Brunet, J.; Vulic, J.; Djilas, S.; Tumbas Saponjac, V. Antioxidant and sensorial properties of linden honey with dried apricots. *Chem. & Biod.* **2014**, 11(11) 1861-1870.

6. Pontis, J.A.; Costa, L.A.M.A.; Silva, S.J.R.; Flach, A. Color, phenolic and flavonoid content, and antioxidant activity of honey from Roraima, Brazil. *Food Sci. Technol.* **2014**, 34(1) 69-73.
7. Inoue, K.; Murayama, S.; Seshimi, F.; Takeba, K.; Yoshimura, Y.; Nakazawa, H. *J. Sci. Food Agric.* **2005**, 85, 872-878.
8. Maćukanović-Jocić, M. *The biology of melliferous plants with an atlas of Serbian apiflora*. Belgrade, Serbia, Faculty of Agriculture (on Serbian), 2008.
9. Gašić, U.; Šikoparija, B.; Tosti, T.; Trifković, J.; Milojković-Opsenica, D.; Natić, M.; Tešić, Ž. Phytochemical fingerprints of lime honey collected in Serbia. *J. AOAC Intern.* **2014**, 97(5) 1259-1267.
10. Kaur, C.; Kapoor, H.C. Antioxidants in fruits and vegetables – the millennium's health. *Int. J. Sci. Technol.* **2001**, 36, 703-725.
11. Ma, Q.; Kinner, Q. Chemoprotection by phenolic antioxidants. Inhibition of tumor necrosis factor alpha induction in macrophages. *J. Biol. Chem.* **2002**, 227, 2477-2484.
12. Fotiric, M.; Nikolic, D.; Rakonjac, V. Variability components and heritability of pomological and chemical characteristics in sour cherry clones of cultivar Montmorency. *Genetica* **2007**, 39, 297-304.
13. Kim, D.O.; Heo, H.J.; Kim, Y.J.; Yang, H.S.; Lee, C.Y. Sweet and sour cherry phenolics and their protective effects on neuronal cells. *J. Agric. Food Chem.* **2005**, 53, 9921-9927.
14. Kirakosyan, A.; Seymour, E.M.; Urcuyo Leanes, D.E.; Kaufman, P.B.; Bolling, S.F. Chemical profile and antioxidant capacities of tart cherry products. *Food. Chem.* **2009**, 115, 20-25.
15. Izli, N.; Yildiz, G.; Unal, H.; Isik, E.; Uylaser, V. Effect of different drying methods on drying characteristics, color, total phenolic content and antioxidant activity of Goldenberry (*Physalis peruviana* L.). *Intern. J. Food Sci. Techn.* **2014**, 49, 9-17.
16. Singleton, V.L.; Orthofer, R.; Lamuela-Raventos, R.M. *Methods in Enzymology, oxidant and antioxidant, Part A*, Packer, L. Ed.: Academic Press, San Diego, CA, pp. 152, 299, 1999.
17. Jia, Z.; Tang, M.; J. Wu, J. The determination of flavonoids content in mulberry and their scavenging effect on superoxide radicals, *Food Chem.* **1999**, 64, 555-599.
18. ISO 8589 (1988). Sensory analysis – General guidance for the design of test rooms, International Organization for Standardization, Geneva [Online] Available at: <http://www.iso.org>. Accessed on 12 December 2013.
19. ISO 6658, *Sensory analysis – Methodology – General guidance*, International Organization for Standardization, Geneva (1985) (Online, available at: <http://www.iso.org>. Accessed on 12 December 2013).
20. ISO 8586-1, *Sensory analysis – General guidance for the selection, training and monitoring of assessors - Part 1: Selected assessors*, International Organization for Standardization, Geneva (1993). (Online, available at: <http://www.iso.org>. Accessed on 12 December 2013).
21. ISO 8586-2, *Sensory analysis – General guidance for the selection, training and monitoring of assessors – Part 2: Experts*, International Organization for Standardization, Geneva (1994) (Online, available at: <http://www.iso.org>. Accessed on 12 December 2013).

22. Piana, M.L.; Persano Oddo, L.; Bentabol, A.; Bruneau, E.; Bogdanov, S.; Guyot Declerck, C. Sensory analysis applied to honey: state of the art. *Apidologie*, **2004**, 35, S26-S37.
23. Bilandzic, N.; Dokic, M.; Sedak, M.; Solomun Kolanovic, B.; Varenina, I.; Koncurat, A.; Gajger, I.T. Determination of trace elements in croatian floral honey originating from different regions. *Food Chem.* **2011**, 128, 4, 1160–1164.
24. Tumbas, V.; Vulić, J.; Čanadanović-Brunet, J.; Djilas, S., Četković, G., Stajčić, S.; Štajner, D.; Popović, B. Antioxidant and sensorial properties of acacia honey supplemented with prunes. *Acta Period. Technol.* **2012**, 293-304.
25. Beretta, G.; Granata, P.; Ferrero, M.; Orioli, M.; Facino, R.M. Standardization of antioxidant properties of honey by a combination of spectrophotometric/fluorimetric assays and chemometrics. *Anal. Chim. Acta* **2005**, 533, 185-191.
26. Bertoneclj, J.; Doberšek, U.; Jamnik, M.; Golob, T. Evaluation of the phenolic content, antioxidant activity and colour of Slovenian honey. *Food Chem.* **2007**, 105, 822.
27. Işik, E.; Şahin, S.; Demir, C.; Türkben, C. Determination of total phenolic content of raspberry and blackberry cultivars by immobilized horseradish peroxidase bioreactor. *J. Food Comp. Anal.* **2011**, 24, 944-949.
28. Chung, Y.C.; Chang, C.T.; Chao, W.W.; Lin, C.F.; Chou, S.T. Antioxidative activity and safety of the 50% ethanolic extract from red bean fermented by *Bacillus subtilis* IMR-NK1. *J. Agric. Food Chem.* **2002**, 50, 2454–2458.
29. Vulic, J.; Canadanovic-Brunet, J., Cetkovic, G., Djilas, S., Tumbas Saponjac, V. Antioxidant and Sensorial Properties of polyfloral Honey with Dried Apricots after One Year of Storage. *J. Chem.* 2015.
30. Čanadanović-Brunet, J.; Vulić, J.; Četković, G.; Djilas, S.; Tumbas Šaponjac, V. Bioactive compounds and antioxidant properties of dried apricot. *Acta Periodica Technologica*, **2013**, 44, 193-205.
31. Cuvelier, M.-E.; Richard, H.; Berset, C. Comparison of the Antioxidative Activity of Some Acid-phenols: Structure-Activity Relationship. *Biosci., Biotechn. Biochem.* **1992**, 56, 324-325.
32. Gheldof, N.; Wang, X.; Engeseth, N.J. Identification and quantification of antioxidant components of honeys from various floral sources. *J. Agric. Food Chem.* **2002**, 50, 21 5870-5877.
33. Dai J, Gupte A, Gates L and Mumper RJA, Comprehensive study of anthocyanin-containing extracts from selected blackberry cultivars: extraction methods, stability, anticancer properties and mechanisms. *Food Chem. Toxicol.* **47**, 837-847 (2009).
34. Beretta, G.; Granata, P.; Ferrero, M.; Orioli, M.; Facino, R.M. Standardization of antioxidant properties of honey by a combination of spectrophotometric/fluorimetric assays and chemometrics. *Anal. Chim. Acta*, **2005**, 533, 185-191.
35. Bertoneclj, J.; Doberšek, U.; Jamnik, M.; Golob, T. Evaluation of the phenolic content, antioxidant activity and colour of Slovenian honey. *Food Chem.* **2007**, 105, 822-828.
36. Ferreira, I.C.F.R.; Aires, E.; Barreira, J.C.M.; Estevinho, L.M. Antioxidant activity of Portuguese honey samples: Different contributions of the entire honey and phenolic extract. *Food Chem.* **2009**, 114, 1438-1443.
37. Kaškonienė, V.; Maruška, A.; Kornyšova, O. Quantitative and qualitative determination of phenolic compounds in honey. *Cheminé Technol.* **2009**, 52(3), 74-80.

ЛИВАДСКИ, ЛИПОВ И БАГРЕМОВ МЕД СА ДОДАТКОМ СУВЕ ВИШЊЕ НАКОН 3 МЕСЕЦА СКЛАДИШТЕЊА – АНТИОКСИДАТИВНА И СЕНЗОРСКА АНАЛИЗА

*Јелена Ј. Вулић, Јасна М. Чанадановић-Брунет, Гордана С. Ђетковић,
Соња М. Ђилас, Весна Т. Тумбас, Слађана М. Стајчић*

Универзитет у Новом Саду, Технолошки факултет, Булевар цара Лазара 1, 21000 Нови Сад, Србија

Ливадски (ПХ), липов (ЛХ) и багремов (АХ) мед, без и са сувом вишњом (40%), пре и након 3 месеца складиштења, су анализирани у овом раду. Одређени су укупни феноли, флавоноиди, антоцијани, антиоксидативна активност и сензорске карактеристике. Садржаји укупних фенола и флавоноида су порасли са додатком суве вишње у мед, а обogaћени медови су показали висок садржај укупних антоцијана. ЛХ40 имао је највећи садржај укупних антоцијана (41,41 мгЦГЕ/100г). Антиоксидативна активност је порасла са додатком сувих вишања у мед код ДППХ' теста и редукционе способности. ПХ и обogaћени ПХ показао је најбољу антиоксидативну активност у поређењу са ЛХ и АХ. $EC_{50}^{ДППХ}$ вредности су: 23,81 за ПХ и 24,19 мг/мл за ПХс, док су $EC_{50}^{ДППХ}$: 1,16 мг/мл за ПХ40 и 1,18 мг/мл за ПХ40с. $RP_{0,5}$ вредности су: 57,00 мг/мл за ПХ40 и 56,00 мг/мл ПХ40с, док су $RP_{0,5}$: 15,05 мг/мл за ПХ40 и 15,18 мг/мл за ПХ40с. Статистичке анализе су показале да су укупни феноли, флавоноиди и антоцијани и антиоксидативна активност снажно повезани. Сензорска анализа медова са додатком суве вишње, пре и након складиштења, је указала на веома добре сензорске карактеристике.

Кључне речи: мед, сува вишња, антиоксидативна активност, сензорска анализа, складиштење

Received: 14 July 2015.
Accepted: 11 October 2015.

EFFECTS OF THE AMOUNT OF SOY MILK ON THERMORHEOLOGICAL, THERMAL AND TEXTURAL PROPERTIES OF CHOCOLATE WITH SOY MILK

Danica B. Zarić¹, Biljana S. Pajin², Ivana S. Lončarević^{2}, Jovana S. Petrović²
and Marijana M. Stamenković Đoković³*

¹IHIS Tehno Experts d.o.o. Research & Development Center, 11080 Belgrade, Serbia

²University of Novi Sad, Faculty of Technology, Bulevar cara Lazara 1, 21000 Novi Sad, Serbia

³IHIS Science & Technology Park Zemun, 11080 Belgrade, Serbia

Chocolate is a two-phase rheological system. The solid phase, consisting of non-fat cocoa particles, sugar and soy milk is wrapped in a fat phase - cocoa butter. Physical, thermal, textural and organoleptic properties of chocolate depend on the composition of the ingredients, manufacturing process and a properly conducted pre-crystallization phase.

For this study, two chocolate masses were produced in a ball mill: one with 15% of soy milk powder (R1) and the other with 20% of soy milk powder (R2). The chocolate mass was produced at different milling times (30, 60 and 90 min), and pre-crystallization temperature (26, 28 and 30°C). The aim of the study was to evaluate the changes caused by different amounts of soy milk powder on the quality of the chocolate. The quality of chocolate was evaluated by comparing the nutritional composition, hardness, thermorheological and thermal properties of the chocolate mass. The results show that chocolate mass R2, due to the presence of higher amounts of soy milk proteins, should be milled longer, and also needs lower temperatures for pre-crystallization.

KEY WORDS: chocolate, ball mill, soy milk, thermal properties, hardness

INTRODUCTION

The chocolate with soy milk which was tested in this work was produced in a ball mill, used to manufacture chocolate and chocolate-like products. The ball mill replaces the two phases in a standard production process, as milling and conching are performed simultaneously. It is a vertical cylinder with a double wall for hot water circulation (1). In the central part of the cylinder there is a mixer with paddles. The mixer paddles rotate at a speed of 50-70 rpm, causing the collision of chocolate mass particles with the mill balls and due to the effects of force of impact, friction and shear stress, the size of the solid particles of the chocolate mass decreases (2). The mill is equipped with a mass recircula-

* Corresponding author: Ivana S. Lončarević, University of Novi Sad, Faculty of Technology, Bulevar cara Lazara 1, 21000 Novi Sad, Serbia, e-mail: ivana.radujko@tf.uns.ac.rs

tion system, so that the mass passes several times through the thick layer of moving balls and is fragmented many times and is submitted to the effects of shear stress and friction. The speed of recirculation of the mass is 3-6 kg/min. Depending on the length of grinding, an optimum distribution of particles by size is achieved (3).

The optimal parameters for production of chocolate with soy milk, used in this study, were determined in the work by Pajin et al. (4).

Melted chocolate is a complex rheological system, where solid particles are dispersed in the fat phase. The fat phase consists of cocoa butter and soybean oil from soy milk. The solid phase is not a uniformly dispersed phase, as the particles have a different distribution by size, shape, and surface properties. The influence of milling on the chocolate mass is reflected in the gradual reduction of shear stress due to which it achieves the appearance of a homogeneous suspension that starts to flow. Before forming the stable chocolate mass, it is tempered to form centers of crystallization of cocoa butter in a stable V crystalline form (5). The formed crystals allow the proper formation and solidification of chocolate, thus providing optimal physical and sensory properties of chocolate (6).

The greatest impact on the thermorheological, thermal and textural properties of chocolate has the composition of the ingredients, fat content, selection of emulsifiers, size distribution of solid particles, and particles packing method. The significance of densely packed particles and their mutual interactions in chocolate can be seen when cow's milk powder is substitute with soy milk powder. The replacement leads to high elastic properties of chocolate with soy milk. These properties are due to the presence of soy proteins: β -conglycinin and glycinin. β -conglycinin is prone to the processes of association and dissociation, and it appears in seven polymorphic forms. Each polymorphic form is a trimer and is composed of the same subunit or a combination of different subunits (7). Both soy milk proteins create intermolecular bonds, which influence the high elastic properties of the chocolate. At higher temperatures and at neutral pH, β -conglycinin and glycinin form a gel. The minimum concentration of protein at which the gel can be formed is 8%. The gel can be formed at lower concentrations, but at higher temperatures or longer heating times. Formation of disulfide bonds and electrostatic interactions are responsible for the gelation of glycinin. Glycinin forms a stable gel with a cylindrical structure. β -Conglycinin forms an irregular gel, the process being governed by the formation of hydrogen bonds. The resulting gel has a double helix structure, with a multitude of cross-links (8). Actually, gel formation and emulsifying properties of soy proteins are the primary requirements for making a good quality chocolate with soy milk in a ball mill (working conditions: temperature of $50 \pm 2^\circ\text{C}$, neutral pH, and the pressure caused by the movement of the balls).

The quality of chocolate with soy milk varies depending on the amount of soy milk, which contains significant antioxidant activity. Isoflavones, flavonoids and other soy polyphenols act as antioxidants and protect the low-density lipoprotein from oxidation, and also have a positive effect on blood plasma lipids as they inhibit platelet aggregation (9). Also, soy milk contains more protein and less fat than cow's milk (10), and no cholesterol or lactose. It has a low content of saturated fatty acids and a high content of polyunsaturated fatty acids. The contents of iron, niacin, and thiamin are also higher than in cow's milk. The advantage of using soy milk is reflected in its high digestibility.

The objective of this study is to find optimal conditions for the preparation of chocolate with soy milk with different amounts of soy milk, while endeavoring not to infringe the thermorheological, thermal and textural (hardness) properties of the chocolate.

EXPERIMENTAL

Materials

The raw materials used for chocolate production included cocoa butter (Theobroma, Amsterdam), cocoa liquor (Cargill, Italia), medium-grain sugar (Crvenka AD, Serbia), soy milk powder with 26% of total fat, 44% of proteins and 18.5% of carbohydrates (Provesol PSA, Brazil), hazelnut paste with 25% of a total, 28% of proteins 28% and 37% of carbohydrates 37% (Arslanturk, Turkey), ethylvanilin (FCC, Norway), soy lecithin with a minimum content of 65% insoluble in acetone (Soyaprotein AD, Serbia), polyglycerol polyricinoleate (PGPR) (Danisco, Malaysia).

Methods

Production of chocolate mass in a ball mill. The chocolate was manufactured in a laboratory ball mill with a homogenizer (capacity 5 kg), of a domestic manufacturer – Mašinoprodukt, Crvenka. The raw materials (cocoa butter, cocoa liquor, sugar, soy milk, hazelnut paste, ethylvanilin, soy lecithin and PGPR) needed for the production of chocolate mass were measured and simultaneously dosed into the homogenizer (except for 10% of cocoa butter which was dosed 10 minutes before taking out the mass from the ball mill), in which mixing was done for 20 minutes, at the temperature of 50°C and mixer rotation speed of 50 r/min. The homogenous mass was then transferred into the ball mill (ball diameter 9.1 mm; ball mass 30 kg; mixer rotation speed 50 rpm; mill inner diameter 0.250 m; height 0.31 m.; volume of space provided for balls and 5 kg of chocolate mass 0.0152 m³).

Chemical analyses. The basic chemical composition was determined using standard AOAC methods (11), as shown in Table 1.

Table 1. Chemical methods for determining basic chemical composition of the chocolate mass with soy milk

Quality parameter	Method/Principle
Moisture [%]	Thermogravimetric
Total fat [% d.m.]	Determination of the petrol ether extract
Proteins [% d.m.]	Kjeldahl method
Carbohydrates [% d.m.]	Polarimetric
Cocoa solids [% d.m.]	Spectrophotometric
Non-fat cocoa components [% d.m.]	Spectrophotometric
Sucrose [% d.m.]	Polarimetric
Lactose [% d.m.]	Iodine metric titration
Amino acid content [%]	Ion chromatography
Fatty acid content [%]	Gas chromatography

Pre-crystallization of the chocolate mass. The pre-crystallization of the chocolate mass was performed in a modified Brabender Farinograph laboratory pre-crystallizer (12). The process of pre-crystallization was controlled indirectly by the changes of the mass resistance during mixing, which was registered on a force/time diagram – the thermorheogram. The following pre-crystallization temperatures were applied: 26, 28 and 30°C for both chocolate masses.

Sample names. Sample names of the chocolate masses used in the work are listed in Table 2.

Table 2. Sample names of the chocolate masses mentioned in the paper

Symbol of the chocolate mass	Refining time (min)	Pre-crystallization temperature (°C)
R1-90-26	90	26
R1-90-28	90	28
R1-90-30	90	30
R1-60-26	60	26
R1-60-28	60	28
R1-60-30	60	30
R1-30-26	30	26
R1-30-28	30	28
R1-30-30	30	30
R2-90-26	90	26
R2-90-28	90	28
R2-90-30	90	30
R2-60-26	60	26
R2-60-28	60	28
R2-60-30	60	30
R2-30-26	30	26
R2-30-28	30	28
R2-30-30	30	30

Determination of phase transitions by differential scanning calorimetry method.

Differential scanning calorimetry (DSC) is a method that is based on the measurement of calorific value (heat flow in mW) which occurs while heating (or cooling) the test and reference samples at a specified speed, i.e. when they are exposed to the same temperature regime. The DSC instrument used was a TA Instruments Q20.

Determination of chocolate hardness. The determination of the chocolate textural properties was performed using a texture analyzer, following the original method 3-Point Bending Rig HDP/3PB. The working conditions were: measuring cell 5 kg; temperature 20°C; speed of the cylindrical probe before the analysis 1.0 mm/s; speed of the cylindrical probe during the analysis: 3.0 mm/s; speed of the cylindrical probe after the analysis: 10.0 mm/s; distance 40 mm; texture measurement was repeated on three times after seven days of stabilization of the manufactured chocolate. The measured parameter was the intensity of the force used to crush the chocolate.

Statistical analyses. The results of measuring hardness and the total number of pondered points were processed by statistical testing for significant difference between two means using t-test at the significance threshold of 95%, $\alpha = 0.05$ (program packages Statistica 8.0 and Origin 6.1). The influence of independent variables (x and y) on the above dependent variables (z) was mathematically defined by means of regression analysis of experimental values. The response function z was defined by the regression equation (mathematical model) of the following form:

$$z = b_0 + b_1x + b_2y + b_{11}x^2 + b_{12}xy + b_{22}y^2, \quad [1]$$

where: b_0 , b_1 , b_2 , b_{11} , b_{12} and b_{22} are regression coefficients; x is the pre-crystallization temperature (t_p); y is the refining time (τ); z is the response function of a characteristic parameter value: the chocolate hardness and the total number of points for sensory quality. The regression coefficients b_1 and b_2 indicate a linear effect of the independent variables x and y on the dependent variable z, b_{11} , and b_{22} indicate the square effect, while b_{12} indicates linear interaction of the independent variables.

On the basis of obtained experimental - real (z_e) and theoretical - expected values (z_t), the following statistical parameters were calculated: the standard error of the regression σ , p and t-values, the coefficient of determination and analysis of variance for the selected regression expression.

The standard error of the regression is defined by the following relation:

$$\sigma = \sqrt{\frac{\sum(z_e - z_t)^2}{n - 2}} \quad [2]$$

The calculation of the coefficient of determination (r^2) was solved to determine the discrepancy between the experimental and the theoretical values.

RESULTS AND DISCUSSION

Chemical composition of the chocolate mass

The chocolate mass with 15% of soy milk (R1) contains 2.2% less protein than the chocolate mass made with 20% of soy milk (R2). Therefore, chocolate mass R1 does not achieve the critical percentage of 9% of soy protein required for the formation of gel under the conditions of the ball mill operation. Chemical composition of chocolate mass R1 and R2 is shown in Table 3.

The changes in the composition of the ingredients have also led to a slight difference in amino acid composition. Chocolate mass R2 was characterized by better nutritional properties because of the higher percentage of essential amino acids (lysine, cysteine, tryptophan, threonine, isoleucine, leucine, phenylalanine and valine). The changes in the composition of acids fatty yielded an increase in the nutritional value of chocolate mass R2.

Table 3. Chemical composition of chocolate mass R1 and R2

Quality parameters	R1	R2
Moisture (%)	1.1	1.1
Total fat (% d.m.)	32.44	32.44
Protein (% d.m.)	7.71	9.91
Carbohydrates (% d.m.)	54.25	52.07
Cocoa solids (% d.m.)	30.14	30.14
Non-fat cocoa components (% d.m.)	4.74	4.74
Cocoa butter (% d.m.)	25.5	25.5
Milk fat (% d.m.)	-	-
Soybean oil (% d.m.)	4.2	5.2
Hazelnut oil (% d.m.)	2.7	1.7
Sucrose (% d.m.)	54.25	52.07
Emulsifiers (% d.m.)	0.5	0.5
Lactose [% d.m.]	-	-
Energy value, kcal	539.53	539.61
Energy value, kJ	2255.24	2255.55
Amino acids	%	
Lysine	0.5	0.8
Alanine	0.51	0.69
Threonine	0.27	0.34
Glycine	0.27	0.34
Valine	0.31	0.4
Serine	0.41	0.51
Proline	0.36	0.47
Isoleucine	0.45	0.52
Leucine	0.32	0.42
Methionine	0.05	0.07
Histidine	0.25	0.33
Phenylalanine	0.4	0.51
Glutamate	1.5	1.8
Aspartate	0.98	1.21
Cysteine	0.07	0.09
Tyrosine	0.25	0.43
Fatty acids	%	
Palmitic	7.45	7.45
Stearic	9.59	9.61
Oleic	10.71	10.51
Linoleic	4.02	4.2
Linolenic	0.32	0.4
Arachidonic	0.04	0.04
Gadoleic	0.05	0.04
Behenic	0.1	0.07

Both chocolate masses had the same percentage of palmitic acid, while chocolate mass R2 had a slightly higher content of stearic acid (by 0.02%), linoleic acid (by 0.18%)

and linolenic acid (by 0.08%) compared to chocolate mass R1. Chocolate mass R2 contained less oleic acid (by 0.2%), gadoleic acid (by 0.01%) and behenic acid (by 0.03%) compared to chocolate mass R1. Neither of chocolate masses contained cholesterol or lactose.

Thermorheological properties of the chocolate masses

The torque value of chocolate mass R2 was higher compared to chocolate mass R1 because of the higher content and complexity of the structure of soy proteins. The concentration of soy protein in this chocolate mass was critical (9%) and sufficient for gel formation and interconnection, which was particularly reflected in the increase of the torque value during longer milling times of 60 and 90 minutes. The optimal torque value (13), which gives the chocolate mass of the appropriate rheological properties, is about $250-350 \times 10^2$ Nm, which corresponds to chocolate mass R1-30-30 and R2-90-30. The higher content of unsaturated fatty acids in chocolate mass R2 did not affect the rate of crystallization, i.e. the extension of time needed to achieve maximum torque. The results are shown in Figure 1.

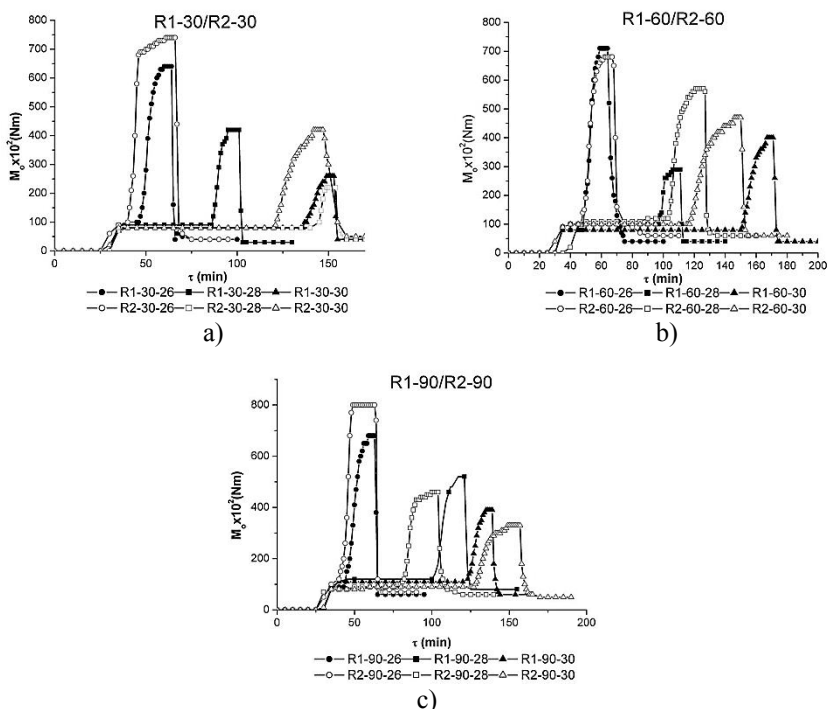
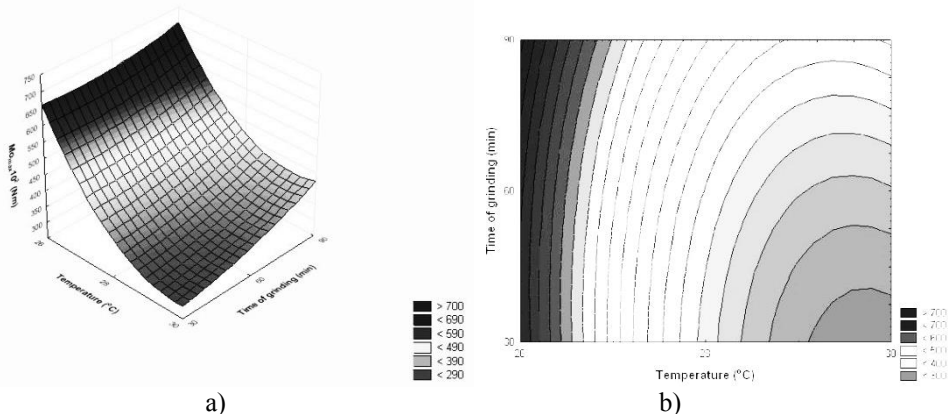


Figure 1. Comparison of the thermorheograms of chocolate masses R1 and R2 regarding: a) milling time (90 min) and pre-crystallization temperature (26°C, 28°C, 30°C); b) milling time (60 min) and pre-crystallization temperature (26°C, 28°C, 30°C); c) milling time (30 min) and pre-crystallization temperature (26°C, 28°C, 30°C)

By testing the statistical significance of the individual parameters of the regression equation it was noticed that none of the parameters had a statistically significant effect on the change of torque value in chocolate mass R1 (calculated t-values < tabular 3.128).

The regression coefficients b_0 , b_1 and b_{11} also indicate specific changes of the dependent variable - z (torque value) with the change of the independent variable - x (temperature of pre-crystallization).

The calculated value of the standard error of regression ($\sigma = 194.35$) confirms that the used of the chosen mathematical model gave a large dispersion of the experimental values. The value of the coefficient of determination ($r^2 = 0.938$) indicates that the torque value of chocolate R2 is determined by variations of independent variables with 93.8%. Analysis of the variance of the regression equation confirms it at a significance level of 95% ($\alpha = 0.05$). Using a selected regression equation, the behavior of the torque value can be predicted for chocolate R2 when changing the milling time and pre-crystallization temperature (calculated $F = 42.777 > \text{tabular } F_{0.05; 6; 3} = 8.94$). The results of statistical data are shown in the 3D and contour diagram in Figure 2.

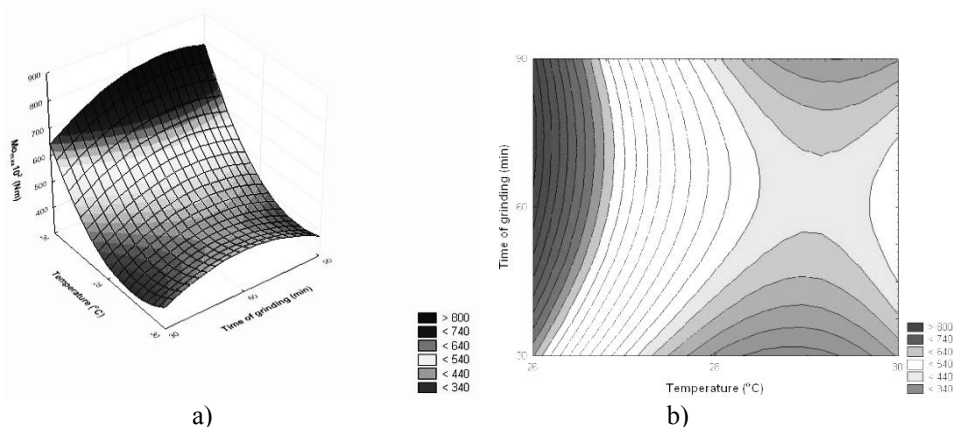


$$Z_1 = 23511.11 - 1550.83 t_p - 11.44 \tau + 25.83 t_p^2 + 0.37 t_p \tau + 0.02 \tau^2$$

Figure 2. The influence of milling time and pre-crystallization temperature on maximum torque value of chocolate mass R1, a) 3D diagram b) contour diagram

Using statistical data the functional dependence of the maximum torque value of chocolate mass R2 on pre-crystallization temperature and milling time was calculated. The results indicate that the pre-crystallization temperature had a higher impact on the maximum torque value than the milling time. By comparing the obtained t-values with the tabular value $t_{0.05;3} = 3.182$ it can be noticed that the most important parameters in the regression equation were b_0 , b_1 and b_{11} , i.e. the elements which indicate the significance of the pre-crystallization temperature. The values of the standard error of regression indicate a significant dissipation of the experimental values from the theoretical ones ($\sigma = 89.35$). The results of the analysis of variance ($F = 24.12$ is greater than the tabular value $F_{0.05;6;3} = 8.94$) with the

risk of error $\alpha = 0.05$ ($p < 0.05$), confirm that the applied regression equation as a whole significantly defines the dependence of the torque value on the independent parameters. The torque value for chocolate R2 is determined by variations in the pre-crystallization temperature and milling time by 90.01% ($R^2 = 0.901$). The results are shown in Figure 3.



$$Z_1 = 32075.5556 - 2239.1667 t_p + 29.1111 \tau + 39.1667 t_p^2 - 0.625 t_p \tau - 0.087 \tau^2$$

Figure 3. The influence of milling time and pre-crystallization temperature on the maximum torque value of chocolate mass R2, a) 3D diagram b) contour diagram

Comparison of thermal properties of chocolate masses R1 and R2

The thermal properties of chocolate with soy milk are most influenced by soy proteins (14), as well as by particle size. Disulfide bonds and electrostatic interactions are responsible for gelling of soy protein - glycinin. Glycinin forms a stable gel with a cylindrical structure, while an irregular gel is formed by β -conglycinin, for which most responsible are hydrogen bonds. Gel is formed by aggregation of molecules and has a double helix structure with a variety of cross-links (15).

It was observed that the pre-crystallization temperature of chocolate mass R1 tended to increase the value of T_{index} regardless of the milling time. Afoakwa et al. (16) also reported that the melting interval increased with a decrease in the particle size, due to stronger interactions between the components. The results of thermal properties of chocolate masses R1 and R2 are shown in Table 4.

The values shown in Table 4 are the average values of the largest cocoa particles. Regarding chocolate mass R2, the increase in the amount of soy milk from 15 to 20% resulted in an increase of the T_{index} value on average by about 2°C. Samples of R2-90 had a lower T_{index} value because the R2-90 samples had fewer crystallizing forms, which resulted in a shorter melting interval.

Table 4. Thermal properties of chocolate masses R1 and R2

Sample	T _{onset} (°C)	T _{end} (°C)	T _{peak} (°C)	T _{index} (°C)	ΔH _{melt} (J/g)	Particle size (μm)
R1-30-26	26.88	36.66	33.66	9.78	29.40	106.15
R1-30-28	29.49	37.35	34.19	7.86	21.11	
R1-30-30	27.81	39.66	34.41	11.85	24.97	
R1-60-26	27.71	40.19	34.72	12.48	24.73	86.33
R1-60-28	27.69	40.16	34.60	12.47	21.30	
R1-60-30	27.92	40.87	35.05	12.95	25.17	
R1-90-26	31.24	35.49	33.52	4.25	28.19	78.48
R1-90-28	27.31	35.80	33.28	8.49	30.37	
R1-90-30	27.74	35.95	33.29	8.21	27.27	
R2-30-26	27.07	35.87	33.24	9.59	27.09	104.61
R2-30-28	25.13	33.68	32.11	12.22	25.54	
R2-30-30	31.44	34.49	32.68	8.22	30.58	
R2-60-26	25.58	35.41	32.03	14.61	28.55	85.25
R2-60-28	26.79	35.75	32.73	13.37	29.14	
R2-60-30	27.31	35.32	33.14	13.56	32.88	
R2-90-26	29.60	34.20	32.27	5.89	29.78	72.92
R2-90-28	26.55	35.92	33.01	9.25	29.36	
R2-90-30	26.76	35.72	32.76	9.19	27.07	

All samples showed a tendency to increase enthalpy with the increase in the retention time in the mill because the decrease in the particle size is accompanied by an enhanced interaction between the components, and the system requires more energy for melting. The lowest values of enthalpy showed samples with a retention period of 30 min in the ball mill, which can be attributed to an insufficient time of milling, resulting in a system with non-uniform particle size. Samples of chocolate mass with optimum enthalpy are R2-90, and especially sample R2-90-30.

Comparison of the textural properties

Experimental results of measuring hardness of chocolate R1 and R2 as a function of milling time and pre-crystallization temperature are shown in Figure 4.

As can be seen, milling time and pre-crystallization temperature had an equal influence on the hardness of chocolate R1. The best hardness has the chocolate that was pre-crystallized at 26°C and milled for 90 min. Finer milling results in a decrease of the chocolate hardness, and an extended milling time requires a lower pre-crystallization temperature. To achieve an optimum hardness, the chocolate mass with higher content of soy milk (R2) needed a lower pre-crystallization temperature and shorter milling time. Chocolate mass R2 was harder than chocolate mass R1 by an average of 42%.

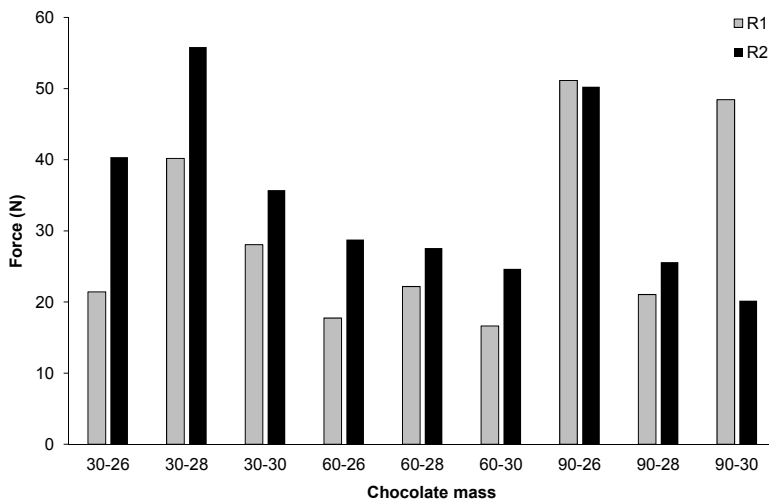


Figure 4. Effect of pre-crystallization temperature and milling time on hardness of chocolate R1 and R2

CONCLUSIONS

The increase in the amount of soy milk from 15% to 20% did not cause a change in the rate of crystallization of chocolate mass, regardless of the applied temperature, but resulted in an increase in torque values. The optimum torque value ($250-350 \times 10^2 \text{ Nm}$) that provided adequate rheological properties of chocolate mass was achieved at the pre-crystallization temperature of 30°C , regardless of the amount of soy milk. Regardless of the milling time and the pre-crystallization temperature, chocolate mass R2 had higher T_{index} values, as well as the enthalpy values comparing to chocolate mass R1. Chocolate R2 is harder than chocolate R1 on an average by 42% for all tested milling time and pre-crystallization temperatures.

Acknowledgement

This study was funded by the Ministry of Education, Science and Technological Development of the Republic of Serbia (Project TR 31014).

REFERENCES

1. Lucisano, M.; Casiraghi, E.; Mariotti, M. Influence of formulation and processing variables on ball mill refining of milk chocolate. *Eur. Food Res. Technol.* **2006**, *223*, 797-802.

2. Beckett, S.T. *Science of Chocolate*; RSC Publishing: Cambridge, England, 2008; pp 61-152.
3. Afoakwa, E.O.; Paterson, A.; Fowler, M.; Vieira, J. Relationship between rheological, textural and melting properties of dark chocolate as influenced by particle size distribution and composition. *Eur. Food Res. Technol.* **2008**, *227*, 1215-1223.
4. Pajin B.; Zarić D.; Dokić Lj.; Šereš Z.; Šoronja Simović D.; Omorjan R.; Lončarević I. Influence of emulsifier on the optimization of precessing parameters of refining milk chocolate in the ball mill. *Acta Periodica Technologica*, **2011**, *42*, 101-110.
5. Zarić, D. Optimising the production of chocolate soy milk in a ball mill. Ph.D. Thesis, University of Novi Sad, 2011.
6. Popov-Raljić, J.V.; Laličić-Petronijević, J.G. Sensory properties and Color Measurements of Dietary Chocolate with Different Compositions During Storage for Up to 360 Days. *Sensors*. **2009**, *9*, 1996-2016.
7. Morr, C.W. Current status of soy protein functionality in food systems. *J. Am. Oil Chem. Soc.* **1990**, *67*, 267-271.
8. Wolf, W.J. Soybeans proteins. Their functional, chemical, and physical properties. *J. Agric. Food Chem.* **1970**, *18*, 369-373.
9. Wei, H.; Bowen, R.; Cai, Q.; Wang, Y. Antioxidant and antipromotional effects of the soybean isoflavone genistein. *Proc. Soc. Expe. Biol. Med.* **1995**, *208*, 124-130.
10. Akinwale, T.O. Development and organoleptic assesment of soya-fortified chocolate products. *Eur. Food. Res. Technol.* **2000**, *211*, 269-271.
11. AOAC, *Official Methods of Analysis*; Association of Official Analytical Chemist: Maryland USA, 2000.
12. Pajin, B. *Praktikum iz tehnologije konditorskih proizvoda*; Faculty of Technology, University of Novi Sad: Novi Sad, Srbija, 2009, 36-39.
13. Pajin, B., Influence of milk fat fractions on rheological properties and quality of chocolate, Ph.D. Thesis, University of Novi Sad, Faculty of technology 2001, 39-42.
14. Pajin, B.; Dokić, Lj.; Zarić, D.; Šoronja-Simović, D.; Lončarević, I.; Nikolić, I. Crystallization and rheological properties of soya milk chocolate produced in a ball mill. *J. Food Eng.* **2013**, *114*, 70-74.
15. Renkema, J.M.S. Formation, structure and rheological properties of soy protein gels. Ph.D. Thesis, University of Netherlands, 2001.
16. Afoakwa, E.O.; Paterson, A.; Fower, M. Effects of particle size distribution and composition on rheological properties of dark chocolate. *Eur. Food. Res. Technol.* **2008**, *6*, 1259-1268.

УТИЦАЈ КОЛИЧИНЕ СОЈИНОГ МЛЕКА НА ТЕРМОРЕОГРАФСКЕ, ТОПЛОТНЕ И ТЕКСТУРАЛНЕ КАРАКТЕРИСТИКЕ ЧОКОЛАДЕ СА СОЈИНИМ МЛЕКОМ

Даница Б. Зарић¹, Биљана С. Пајин², Ивана С. Лончаревић^{2}, Јована С. Петровић²,
Маријана М. Стаменковић³*

¹ IHIS Tehno Eksperts d.o.o. Истраживачко развојни центар, 11080 Београд, Србија

² Универзитет у Новом Саду, Технолошки факултет, Булевар цара Лазара 1, 21000 Нови Сад, Србија

³ IHIS Научно-технолошки парк, 11080 Београд, Србија

Чоколада представља двофазни реолошка систем. Чврста фаза коју чине немасне какао честице, шећер и сојино млеко обавијена је масном фазом - какао маслацем. Физичке, топлотне, текстуралне и органолептичке особине чоколаде зависе од сировинског састава, поступка производње и правилно вођене фазе преткристализације.

У овом раду су произведене у кугличном млину две чоколадне масе: са 15% сојиног млека у праху (R1) и 20% сојиног млека (R2). При производњи чоколадних маса, време уситњавања чоколадне масе се варирало (30, 60 и 90 мин), као и температура преткристализације (26, 28 и 30°C). Циљ рада је да се утврде промене које изазива различита количина сојиног млека у праху на квалитет чоколаде. Квалитет чоколаде је праћен упоређивањем нутритивног састава, чврстоће, термореографских и топлотних карактеристика чоколадних маса. Резултати показују да је чоколадној маси R2, због присуства веће количине протеина сојиног млека потребно дуже време млевења, али и нижа температуре преткристализације.

Кључне речи: чоколада, куглични млин, сојино млеко, топлотне карактеристике, чврстоћа

Received: 22 October 2014.

Accepted: 21 October 2015.

CHEMICAL TECHNOLOGY AND PROCESS ENGINEERING

ANALYSIS OF THE FREE-SWELL BEHAVIOUR OF ORANGE PEEL PARTICULATES

Oluwaseyi A. Ajibade¹, Johnson O. Agunsoye¹ and Sunday A. Oke^{2*}

¹ University of Lagos, Faculty of Engineering, Department of Metallurgical and Materials Engineering, Lagos, Nigeria

² University of Lagos, Faculty of Engineering, Department of Mechanical Engineering, Lagos, Nigeria

Orange peel particulates (OPPs) are interesting materials for the sport equipment production and other industrial applications from the economic and ecological perspectives. Free swell experiments were used to observe the possible behaviour of orange peel filler materials as inputs to orange peel reinforced composites when used in outdoor water-based applications. Experimental data were collected for 10 days on 24-hourly measurements. Holtz and Gibb's free swell model was applied in terms of five parameters: Free swell (S_f); final volume (V_f); mass of water (M_w); mass of solution (M_s); and volume of solution (V_s). The particle diameter sizes considered in the experiments are 0.075, 0.150, 0.212, 0.300, 0.425 and 0.600 mm. The analysis showed the level of water swelling abilities of the various particulate sizes, which could give an informed decision on possible behaviour of orange peel particulates in outdoor applications.

KEY WORDS: swelling parameters, experiments, free swell, green composites

INTRODUCTION

In the citrus family, sweet orange is a very important agricultural product from an economic perspective. Sweet orange (*Citrus sinensis*), is a small edible fruit with a spherical shape and having an orange colour. It remains one of the most economically important fruits in Brazil, USA, Japan, China, Mexico, Pakistan and other countries of the Mediterranean region (1) as well as Nigeria (2), Bangladesh (3) and India (4). It has a sweet taste and is relatively cheap. It is available during the harvest seasons when large quantities of it are lost due to post-harvest preservation problems. OPPs have important applications in green composite fabrication for use in a variety of sporting equipment systems. Green composites have started playing a key role in the economic development of countries. Conventional materials used for structural, non-structural, constructional and sporting equipment manufacturing purposes are no longer adequate to meet the challenge of reducing the environmental impacts of replaced deteriorated infrastructures and new structural members.

* Corresponding author: Sunday A. Oke, Department of Mechanical Engineering, Room 10, Mezzanine Complex, Faculty of Engineering, University of Lagos, Akoka-Yaba, Lagos, Nigeria, e-mail: sa_oke@yahoo.com

Since orange peel particulates are newly recognised as useful composite fillers, sufficient literature information is not available concerning the free swell behaviour of this material and such information is needed to understand the possible responses of orange peel particulate-filled composites in natural conditions of rain, water immersion and humidity in outdoor applications.

In experimental studies concerning sweet orange, chemical analytical investigations have been the focus of a wide range of research and different hotspots have been studied with relevance to a number of areas. A considerable body of knowledge exists on the chemical properties of orange peels (5-8) while the understanding of the physical properties (9, 10) of the same material is evolving as an interest among composite fabricators. There is a large pool of information in literature concerning the chemical properties of pectin content (7), essential oil composition (5), identifying phenols and anti-oxidant levels of orange (11).

Investigations by Yeoh *et al.* (7), as well as Pandharipande and Makode (8) are based on the extraction of pectin content of the orange peels. Similarly, Vora *et al.* (9), Pino *et al.* (10), investigated the chemical composition of orange oil concentrates to determine its uses. These authors contributed towards the definition of the appropriate levels of pectin contents, and on the chemical composition of orange oil. Furthermore, Kamal *et al.* (1) investigated the chemical composition of orange oils from fresh, ambient and oven-dried orange peels. Also, Banidadr and Asempour (11) investigated the ability of ferric salt of orange peels to accelerate photo-oxidation and bio-degradation in low density polyethylene soil environments.

The relevance of the chemical property experimental debates on orange peels to the current work lies in the fact that the central debate so far has been on pectin and ferric salts' chemical analysis, among others, whereas physical analysis has been recognised only more recently. However, very scanty information exists on the physical properties of orange peels till date. The growing environmental concern of the potential risks associated with indiscriminate dumping of orange peel wastes in communities ignites an increasing interest towards making an economic utilisation of these wastes. Although chemical analyses are important, they are not sufficient for a thorough understanding of the properties of the orange peel grain structure. This is because the physical properties helps to explain different ways in which the particulate sweet orange peels could be applied in green composite fabrication. However, the existing studies on orange and orange peels lacks the potentials of suggesting what the free swell properties of the orange peels are when used as an input for green composite fabrication. This will help to determine the mix ratio of orange peels filler to matrix in order to have high strength characteristics of the composite that finally emerges from the fabrication process.

A scanty number of publications exist with particular reference to the analysis and study of swell behaviour of composites but the independent investigations of the swell behaviour of the comprising materials of the composites seem unattended to in literature. van den Brom *et al.* (12) investigated the swelling behaviour of thermo responsive hydrogen/silica nano-particle composites using water-swollen films by means of surface plasmon resonance and optical waveguide spectroscopy. In another investigation, Abd-El-Salam *et al.* (13) found a correlation between the position annihilation parameters of silicone rubber polydimethyl siloxane composite that was loaded and the different con-

ductive fillers against their swelling prospectus. The parameters used to evaluate swell were the maximum degree of swell, Q_m %, and the penetration rate, P , diffusion coefficient, D , was reported to decrease with increasing filler content as a result of the reduced size of free-volume. It was noted that carbon black-filled composites showed low values of P , D and Q_m % as compared with graphite-filled composites. The differences were attributed to physical properties of the filler, particle size, surface area and the tendency of the filler particles to make aggregates. Yet in another study, Masoodi and Pillai (14) investigated the swelling and weight gain behaviour of bio-based composite made from jute fibers and bio-based or ordinary epoxy.

In the above-mentioned investigations, all the articles focused exclusively on the composite swell behaviour and the characteristics and data related to how the reinforcement behave when subjected to moist environments, as indicative of the results obtained from water-dipped particle analysis of orange peel particulates, as revealed in the laboratory is conspicuously missing in the literature. It is necessary to understand how reinforcements would behave in moist conditions in order to use the knowledge to understand in what quantities the reinforcement are to be combined with the matrix in moist environment. An urgent attention must be paid to this literature deficiency.

Undoubtedly, there exists several problems with the traditional engineering materials used presently for fabrication purposes; huge costs of product and seemingly interrupted imports due to government changing regulations. However, it is necessary to overcome these difficulties and challenges since wastes in forms of orange peels are abundantly available in many societies, particularly the Nigerian environment that this study originated from. These problems could be overcome by developing an adequate understanding of the system of processing the raw orange peels. Exhaustive literature search and scrutiny reveals that polymer-based raw materials such as polyethylene (low and high densities) are gaining an increased attention. Still, their usage and processing documentation is at the infant level. More investigations are needed to breakthrough this area and pass the bundle of benefits to users and researchers interested in this area. So, new knowledge on the free swell of particulate orange peels was developed while the effect of variation of sizes of particulates was studied.

Motivated by the aforementioned investigations and the possible applications in which orange peel particulates could be made use of, it is of particular interest to the current investigators to study the problem of free swell orange peel particulates through laboratory experiments. There are unfortunately no recommendations about the free swell behaviour that is presented for the various grades of particulate orange peels by the different aperture sizes: 0.075, 0.150, 0.212, 0.300, 0.425, and 0.600 mm. In addition, no detailed data and direction is given in the current literature on composite materials as to how the free swell of orange peels particulates could be determined. This aspect urgently needs research attention. The approach uses collection of waste samples from the field, grinding them into particulates, sieving them into various sizes, and carrying out volumetric and weight measurements on each of the particulate sizes to establish the behaviour of this material in water solution and therefore have an understanding of the possible behaviour of the material in outdoor applications where the material (in its composite form) would likely be run over by liquids such as water throughout its lifespan.

It is generally accepted that being a waste material, orange peels have great potentials in bringing down the cost of fabrication of composites. Others consider it as a potential raw material for the industry and one that will bring down manufacturing cost (2). Yet, very little has been documented relative to orange peels being investigated for its free swell properties. The current work applies parameters including measures of volume of orange peel particulates in dried and swollen forms and measures of water to create a broader investigation of the free swell behaviour of orange peel particulates for understanding the possible behaviour of outdoor applications of orange peel particulate-based composites during its actual field applications. Free swell experimentation has been conventionally used for soil particle analysis. Here, it is used for orange peel particulates following the knowledge of shared properties of soil particles with orange peels particulates by adapting the Holtz and Gibbs' (1956) free swell model.

The paper is organised as follows. Section 1 presents the motivation for the work and the purpose of the study. Section 2 proposes the structure of the research methodological framework for the current study, which presents the flow of work from the motivation through the study objective to the parametric determination of quantities through experimental investigations. This is followed by experimental method specification and observations with results specification. Section 3 shows the experimental results concerning the relationship among the important parameters in the study. In section 4, concluding remarks are made.

RESEARCH METHODOLOGY

Orange peel particulates obtained from grinding of dried orange peels were sieved using a British Standard test sieve Wykeham Farrance to obtain 0.075, 0.150, 0.200, 0.300, 0.425, 0.600 and 1.18 mm aperture sizes. However, the 1.18 mm size was not used in the experiment due to its minute quantity obtained during sieving. It is desired to know what each sample size would exhibit in terms of distinct or otherwise of swell properties, which are hitherto unknown. For this purpose, free swell experiments were set up for each of the samples in accordance with universally acceptable standards. The experiments were carried out in line with literature documentation by Holtz and Gibbs. 6 measuring cylinders of known capacity were filled with 100 cm³ of water, orange peels particulates of each sample size were dissolved into water in the calibrated measuring cylinders of capacity. The setting up of the experiments and the taking of readings after 24 hours of dissolution is referred to as a run. For simplicity and consistency, ten experimental runs were performed for each of the sample sizes. This is for statistical acceptability of experiments. Also, a number of intricate parametric quantities helpful in understanding the free swell behaviour were also determined. This yielded a broader insight into the dynamics of free swell for the orange peel samples. These quantities are initial volume, mass of solute, final volume, volume of water, mass of water, volume of solution before free swell, volume of solution after free swell, increase in volume of specimen and increase in volume of solution.

The measurement of dry orange peel particulates before dissolution is the initial volume V_i while the 100 cm³ of water in the cylinders is taken as the volume of water, V_w . The

mass of water in the measuring cylinders is designated as M_w , while the mass of the dry solute poured into the water is taken as M_s . The volume of solution before 24 hours of dissolution is taken as V_b , while the volume after the completion of the process is given as V_a . The difference between the volume of solution after free swell V_a , and the volume of the solution before free swell V_b , is the increase in volume of the solution, V_{inc} .

The volume of solution before 24 hours of dissolution is taken as V_b , after free swell has taken place; the volume of the solute in water was given as the final volume, V_f . The new level of the solution is the volume of the solution after free swell. Other quantities obtained are the increase in the volume of the specimen is the difference between V_f and V_i is denoted by H , while the increase in volume of solution is given as V_{inc} . The V_i , M_s , V_w and M_w are the measurements that takes place before the free swell of the orange peel particulates. On the other hand, V_f , V_a , V_b , V_{inc} , and H are obtainable after the free swell process has been completed. Free swell is obtained by calculation, using the Holtz and Gibbs model. Readings were taken repeatedly for all the sample sizes with a 24-hour interval between the runs from the time the last dissolution was made. Graphs were used to study the interactions of the different parametric quantities and for their individual influence on free swell values. From these calculations and analyses, the free swell behaviour of each sample size was established. Results are explained and the conclusions reached in terms of practical applications and implications for the material science society are documented. The chemical composition of orange is shown in Table 1.

Table 1. Chemical composition of orange per 100g

S/No.	Chemical composition	Value	S/No.	Chemical composition	Value
1	Carbohydrates	11.54g	10	Vitamin B ₆	0.051mg (4%)
2	Sugars	9.14g	11	Folate (Vit. B ₉)	17mg (4%)
3	Dietary Fiber	2.4g	12	Vitamin C	45mg (54%)
4	Fat	0.21	13	Calcium	43mg (4%)
5	Protein	0.70g	14	Iron	0.09mg (1%)
6	Thiamine (Vit. B ₁)	0.100mg (9%)	15	Magnesium	10mg (3%)
7	Riboflavin (Vit. B ₂)	0.040mg (3%)	16	Phosphorus	12mg (2%)
8	Niacin (Vit. B ₃)	0.400mg (3%)	17	Potassium	169mg (4%)
9	Panto thenic Acid (B ₅)	0.250mg (5%)	18	Zinc	0.08mg (1%)

Source: Onward Paper Mill

The procedural calculation of free swell is shown in Figure 1. An explanation of the structure and these steps will be done in this section.

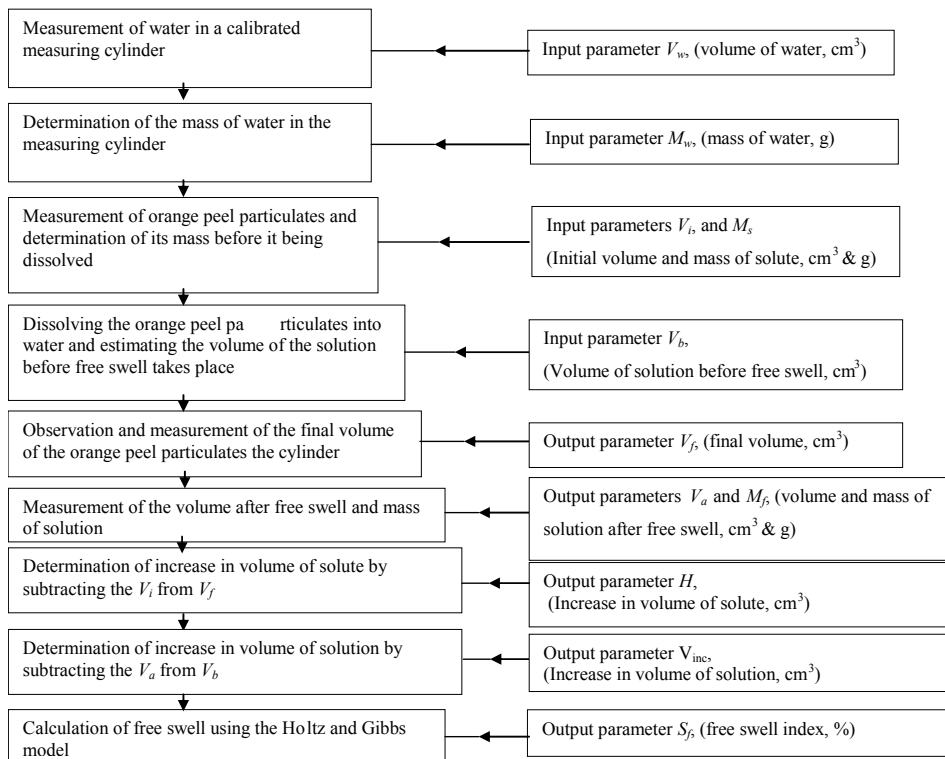


Figure 1. Flow chart for the calculation of free swell of orange peel particulates in water

THE SWELLING BEHAVIOUR DETERMINATION

A careful investigation has been carried out to describe the free swell characteristics of particulate orange peels. Free swell experiments were conducted on six different sample sizes of orange peel particulates. Various parametric measurements were made throughout the conduct of the experiments in order to understand the dynamics of free swell and the contribution of each parameter to the free swell process. The interaction of the various parametric quantities, namely, V_f , V_{soltm} , V_{inc} , M_w , M_{soltm} , M_{inc} , d_{soltm} and d_{inc} with free swell (S_f) were made graphically from which useful observations and conclusions were reached. The analysis presented below is based on each sample size as follows.

The relationship between final volume and the free swell indices of the 0.075 sample involves three volumetric measurements, plotted against the free swell simultaneously as seen in Figure 2. The final volume V_f is observed to have a linear relationship. This clearly indicates that the free swell of orange peels particulate has a direct dependence on its final volume after 24 hours of dissolution. The curve rises through 20 to 34 cm³ on the

vertical volume axis which translates to 100 to 240 % on the free swell axis. During this ascent, the free swell is seen to increase for every rise in the final volume which means that free swell is dependent on the final volume. In practical terms, the volumetric changes in a 0.075 orange peels reinforced composite can be used to estimate the amount of free swell which has taken place. The interaction of volume of solution and free swell indices of the sample produces a curve with steep movements. The curve is seen to have a peak at 104 cm³ which corresponds to 240 and 200 % on the free swell indices. The curve rises to its first peak with a corresponding increase in the free swell.

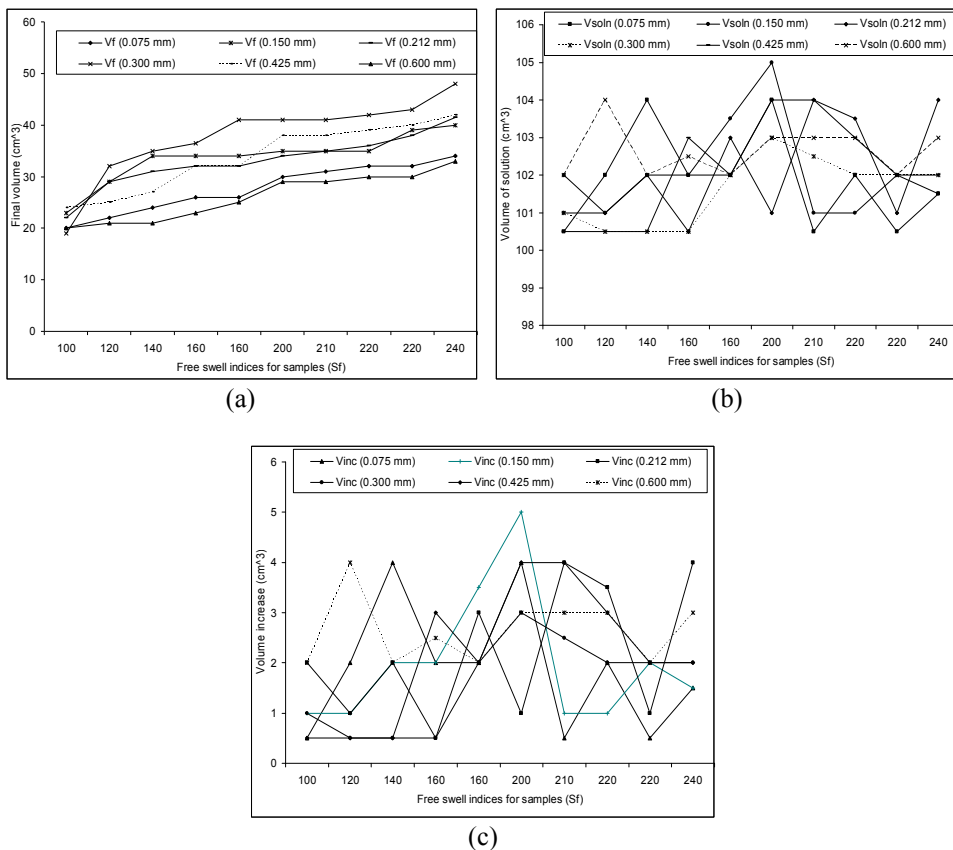


Figure 2. Free swell versus volume (a) Final volume, (b) Volume of solution, (c) Volume increase

As the free swell increases, the volume of solution V_{soln} is seen to drop and rise continuously again till it reaches its peak value of 104 cm³. The undulation of the curve represents the changes that may be experienced in the water level of the environment the free swell of the 0.075mm orange peels composite is taking place. In other words, the free

swell of 0.075mm orange peels particulate will increase when it is used as structural component in a water-based application even when the volume of the water body (volume of solution) reduces. For the interaction of increase in volume V_{inc} and free swell indices a similar curve with smaller magnitude was produced. This is because the V_{inc} curve shows how the original body of water increases in volume when the free swell of the orange peels composites is taking place.

It is necessary to measure the mass of water to see how it may affect the free swell of particle sweet orange peels. To this end, three mass measurements, namely, the mass of water that represents the mass of the original body of water before immersion of the composite, mass of solution, which translates to the mass of water body, which comprises of the composite that has undergone free swell. The mass increase represents that increment in the mass of water body taking place during the free swell process is shown in Figure 3. The mass of water and solution are represented by two tables like curve with similar movements but with different magnitude. The mass of solution is seen to rise steeply as free swell takes place. It reaches a point 96.55 before dropping to rise to a peak of 96.99 g at a free swell of 200 %. The rise and fall in the mass continues till it exits the graph. The behavior of the curve represents the changes expected in the mass of water environment where the 0.075 mm orange peek component may be used. Two density measurements were used to understand the relationship of density changes with the free swell indices of the 0.075 mm sample as described by Figure 4. The first is the density of solution which is given by a straight line curve that is parallel with the free swell indicating that the density of the solution has no effect on the free swell indices of 0.075 mm orange peels. The incremental density is the instantaneous change in density of the 0.075 mm orange peels as the free swell changes. Its interaction with free swell indices produces a curve that is undulating. It is important to understand what happens to the orange peels particulate density with every change in free swell indices.

The curve is seen in Figure 4 to have a peak of 6.92 g/cm³ which translates to a free swell of 220 %. At this point the density increment drops sharply to 2.45g/cm³. This explains the fact that as the free swell rises, there is a change in the density of the material that is undergoing free swell. This instantaneous change in density may however be a positive increment or negative increment leading to a rise or fall in the values as indicated in the curve. Such changes are caused by different mass and volumetric changes that are peculiar only to the material.

The relationship between the volume measurements and free swell indices of the 0.150 mm sample is described graphically by three different curves in Figure 2. As expected, the final volume V_f gives a linear relationship with the free swell indices of the oranges peels particulates. This is an indication that the free swell is dependent on the values of the final volume of the 0.150 mm orange peels particulate. In other words, every increase or decrease in the final volume is followed by a corresponding change in free swell indices. Practically the final volume measurement of a component made with 0.150 mm orange peels particulate in a water-based application can be used to determine the amount of free swell that has taken place. The relationship of volume of solution V_{soln} and increase in volume V_{inc} against free swell produced similar curves with different magnitudes. Their influence on the free swell indices can be said to be the same as shown graphically. The volume of solution curve rises steadily with the free swell indices until it

reaches a peak of 105 before dropping to 101.5 cm³ as it exits the graph. However, the free swell indices increase continuously till a peak value of 300 %. In life applications, the free swell of composites made of the 0.150 mm orange peels will rise continuously till it reaches a peak value before decreasing gradually. This is because when the free swell of composites reaches a peak, no further increase can take place even though the volume of water is increasing.

The V_{inc} is the difference between the volume of water body experiencing free swell of a 0.150mm sample and the original body of water. In other words, the volume increase represents the increment in the volume of a given body of water after the 0.150mm orange peels composite has been immersed and free swell is taking place. Figure 3 shows the relationship between the mass measurements and free swell indices of 0.150mm sample. The mass of water M_w represents the mass of an original body of water before immersion of the 0.150mm orange peels composite. The mass of solution M_{soln} represents the mass of a given body of water after the immersion of a 0.150mm orange peels composite undergoing free swell. The mass increase M_{inc} is the incremental difference between the masses stated earlier during free swell. Two similar curves of different magnitude were produced as seen in Figure 3. The mass of solution reaches a peak at free swell indices of 250 %. This indicates the free swell indices of 0.150mm orange peels composite would increase the mass of the water body to a peak value when the free swell indices is at a value of 250 %.

Figure 4 is the relationship between density measurements and free swell indices of the 0.150 mm sample. The density of the solution d_{soln} is given between 0.95 and 0.97 g/cm³ for all the values of free swell indices. This produces a straight line curve that runs parallel with the free swell indices along the graph. In other words, the free swell is not affected by the density of the solution neither is the density of solution affected by the free swell. The density increase d_{inc} curve however shows an undulation as the free swell indices increase. It rises early to 3.41 g/cm³ and climbs to 3.66 g/cm³ before declining to 0.4 g/cm³ as the free swell indices increases. From this point it climbs rapidly to 3.74 g/cm³ and to a peak of 4.61 g/cm³ before dropping in value and rising again. The movement of the curve makes us to understand the instantaneous change in density that occurs within the material during free swell increase. Therefore, as the 0.150 mm orange peels component experiences free swell, it would experience incremental change in density which may be positive or negative. The movement of the density increase curve shows the mass and volume changes that is occurring within the material during free swell and is only peculiar to the material. This helps to understand the density changes that are occurring within the material simultaneously with free swell in real life applications.

The curves which describe the relationship between the volume measurements and free swell indices of the 0.212 mm sample are shown in Figure 2. The final volume V_f rises linearly with the free swell indices S_f from 22 to 41.5 cm³, indicating a direct dependence on the V_f by the free swell indices. It is expected, that if put in practical usage, the final volume of the 0.212 mm orange peels component could be used to determine the amount of free swell that has taken place. The volume of solution V_{soln} and the increase in volume V_{inc} behaved similarly against free swell with similar curves but varying magnitudes. Both curves reached their peaks at a free swell of 250 and 315 with a value of 104 cm³. From here, it can be seen that the free-swell behavior of the 0.212 mm orange peels

particulate affects the volume of solution in a different way. This is because after reaching a peak of 104 cm^3 at a free swell of 250%. The V_{solt} drops briefly and rises again till it attains the peak value again as the free swell indices reaches a peak of 315 %. When used in a water-based application, the 0.212 mm orange peels component is expected to cause a rise in the volume of the water environment till it reaches a peak. The volume is expected to drop briefly from this peak value as the free swell of the material increase. The volume of the water environment V_{solt} rises to a peak again with the free swell indices.

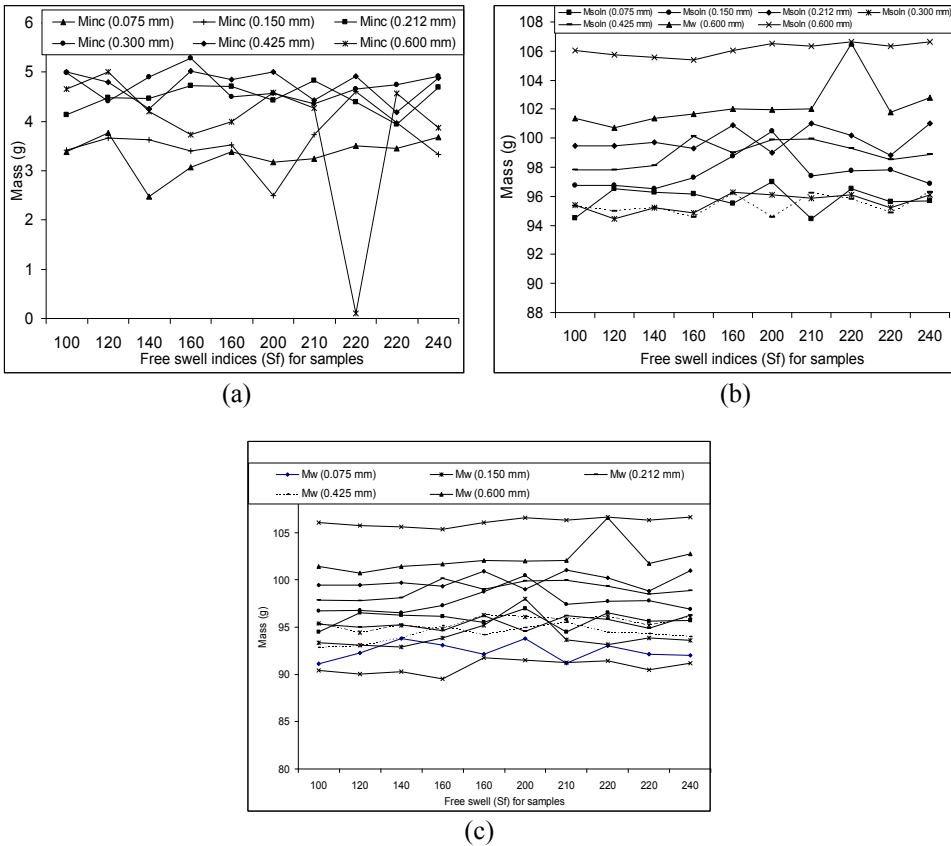


Figure 3. Free swell indices (S_f) for samples versus mass (all sample sizes) versus (a) mass increase, (b) mass of solution, (c) mass of water

The mass measurement relationship with the free swell indices is given in Figure 3. The mass of water M_w represents the mass of a natural body of water which has not had the effects of free swell of a composite. The mass of solution M_{soltm} represents the mass of a natural body of water after the immersion of the 0.212 orange peel reinforced composite which experiences free swell, while the mass increase M_{inc} is the difference of both

masses. Their relationship with free swell indices produces two similar curves of different magnitudes. Of particular interest is the M_{soltn} curve which has rises and drops till it reaches a peak value of 101.03g when the free indices is at 250%. Further increase in free swell indices brings about a drop and rise in the M_{soltn} until it rises to a value of 101g again.

It is clear that the free swell behavior brings about a commensurate influence on the mass of the body of water environment just as it does with the volume. In addition, the free swell behavior of this material makes it possible for the mass of water environment in which it is being used to rise to a peak even as the free swell indices reach a peak. This again is the property of the orange peels particulate that makes it affect the body of water in which it is being used in terms of mass and volume changes. This will help us to know and predict the kind of changes expected in a body of water environment where the material is put into use.

The density measurement is plotted against the free swell indices of sample as given in Figure 4. The d_{inc} rises early from 2.07 to 4.48 g/cm³ and reduces sharply to 2.24 g/cm³ while the free S_f increase from 120 to a value of 210%. At a S_f value of 220% it reaches a maximum value of 9.44 g/cm³ forming an elongated peak on the curve. From this point, the d_{inc} drops and rises in value as the S_f increases continuously. This undulation continues till the S_f reaches a peak value of 315% and the d_{inc} finally drops to 1.18 g/cm³. Once again the movement of the curve shows that the change in S_f brings about an instantaneous change in the density of the material undergoing free swell. Worthy of note is the fact that very increase in free swell did not bring about a corresponding increase in d_{inc} . The increment in the density may be positive or negative due to mass and volume changes caused by water absorption. This would be helpful in understanding the changes that may occur in the density of the 0.212 mm orange peels reinforced composite as its peculiar property when experiencing free swell.

The relationship between the volume measurements and free swell indices of the 0.300 mm orange peels particulate is represented by three curves in Figure 2. The final volume V_f , volume of solution V_{soltn} and V_{inc} were all plotted simultaneously against the free swell indices S_f . The V_f is seen to have a linear relationship with the free swell indices indicating that the free swell is dependent on the values of final volume. Thus, every increase or decrease in V_f is followed by a corresponding change in S_f . If the orange peel particulates were to be used as reinforcement in making composites for immersion based operations, its free swell would be determined from the final volume it attains. The V_{soltn} represents the volume of the water environment in which the free swell of the 0.300mm orange peels component is taking place. The V_{soltn} starts from a point 101 and drops briefly to 100.5 cm³ where it stabilises as the S_f indices moves from 90 to 265. As the S_f stabilises at 310 %, the V_f rises to 103 cm³ and drops back to 102.5 cm³. As the S_f increase further to a peak of 380 %, the V_{soltn} drops to a stable value of 102 cm³. The free swell is observed to attain its highest value of 380% in the sample which also has the widest range of free swell indices from 90-380 %. The movement of the curve shows the expected influence of the free swell of the 0.300mm on the body of water in which it is being used. The V_{soltn} curve represents the expected changes in the water level of the environment where the 0.300mm sample is being put to use. The V_{inc} curve shows the increment in the original volume of water body caused by the free swell. The curve of V_{inc}

goes further to show what changes are caused by the free swell to the original volume of water body during the free swell process. The mass relationship of the sample against the free swell indices is given in Figure 3. The mass of water M_s and solution M_{soln} represents the mass of the original water body and mass of the water body containing the orange peels composite undergoing free swell respectively. The M_s curve reaches a peak at 96.28 which corresponds to a free swell index of 310 %. At this point of the free swell, the M_{soln} continues to undulate till it reaches a maximum value of 96.1 when S_f is at a peak of 380. The free swell behaviours of the sample shows how it would influence the mass of the water body or environment in which it may be used.

The density measurements and free swell indices of the 0.300mm sample resulted into two different curves as seen in Figure 4. The d_{soln} which is the density of solution during free swell represents the density of the water body which contains the orange peels composite. Throughout the course of the free swell, the d_{soln} is between the values of 0.93-0.95 g/cm³. This produces a straight line curve on the graph indicating that the free swell indices do not affect the d_{soln} significantly. The density increase d_{inc} against free swell indices gave a different kind of curve. The d_{inc} begins at a value of 4.98 g/cm³ when S_f is 90% and climbs rapidly to 8.84 and 9.8 g/cm³ as the S_f increases from 220 to 250% respectively. The d_{inc} reaches a peak of 10.56 g/cm³ and drops rapidly to 2.25 g/cm³ at a free swell of 310 %. The value of the d_{inc} undulates as the S_f increases further to a peak of 380. The movement of the curve shows that the sample experiences high incremental density from the early stages of free swell. The density increment may be positive or negative depending on the mass and volume changes experienced by the material. Thus, after reaching a peak of 10.56 g/cm³ at a S_f of 265%, the d_{inc} begins to experience decrement in value. This behaviour and instantaneous changes is caused by the peculiar free swell property of the 0.300mm sample. This would be helpful in understanding the expected changes of the material when employed in water-base applications.

The relationship between volume measurements and free swell indices of the 0.425 mm orange peel particulates is also described graphically in Figure 2. As expected, the S_f rises from 140 to 320 % as V_f increases from 24 cm³ to a peak of 42 cm³. In other words, the V_f has a direct relationship with the S_f i.e. every increase or decrease in V_f brings about the same changes in the S_f . The V_{soln} curve starts as a straight line and rises to 103 before descending to 102 cm³ as the S_f increased from 140 to 220%. The V_{soln} stabilizes at a peak value of 104 cm³ as the S_f remains constant at 280 %. From this stable point, the V_{soln} descends to 102 cm³ as the S_f rises to a peak of 320%. Practically, it is expected that the free swell behaviour of a component made with sample does not increase the volume of overall water body initially. Further increase in S_f would bring about a rise in the water level of the environment and subsequent decrease due to the influences of free swell. The V_{inc} curve goes further to show what happens to the volume of a body of water as the orange peels reinforced composite begins to experience free swell. In Figure 3, the relationship between mass measurements and free swell indices of the sample is presented. The relationship between mass measurements and free swell indices of the sample is described by three curves in Figure 3. The mass of water M_w and mass of solution M_{soln} represents the mass of the original body of water and the mass of the body of water containing the component respectively.

The mass increase M_{inc} , is the increment on the original body of water as a result of free swell behaviour of the orange peels reinforced composite. The M_{soltn} is seen to rise and fall as the S_f indices makes steady increase. This movement is shown graphically in the M_{soltn} curve. However, the influence of the S_f on M_w is seen in the M_{inc} . Therefore, as an original body of water begins to experience the free swell of the orange peels reinforced composite. It experiences an increment represented by M_{inc} which progresses as the free swell increases. Finally, the interaction between density measurements and free swell indices of orange peels reinforced composite is presented in Figure 4 by two curves. The d_{soltn} which ranges from 0.96-0.98 g/cm^3 is plotted as a straight line curve as the S_f increases from 140 to 220 %, this indicates that it has no influence on the S_f either. Thus, the density of the water body or environment does not change due to the influence of the orange peels reinforced composite undergoing free swell within it. The d_{inc} starts at 10 g/cm^3 when the S_f is 140 % dropping gently and rising till it gets to a peak of 14.2 as the S_f increases to 170 %. This produces an elongated peak on the d_{inc} curve, further increase in S_f , brings about a sharp decline in the values of d_{inc} to 1.67 g/cm^3 . As the S_f increases, the d_{inc} continues to rise and drop producing an undulation. This continues till a value of 2.45 g/cm^3 at a peak S_f value of 220 %. The movement of the d_{inc} curve indicates the instantaneous changes in density that should be expected in the orange peels reinforced composite undergoing free swell. These changes could be positive or negative owing to the mass and volume changes peculiar to the material undergoing free swell. The d_{inc} is seen to proceed rapidly at the early stages of free swell between 140 and 170 %, but for latter stages of the free swell, it is seen to be unstable in nature.

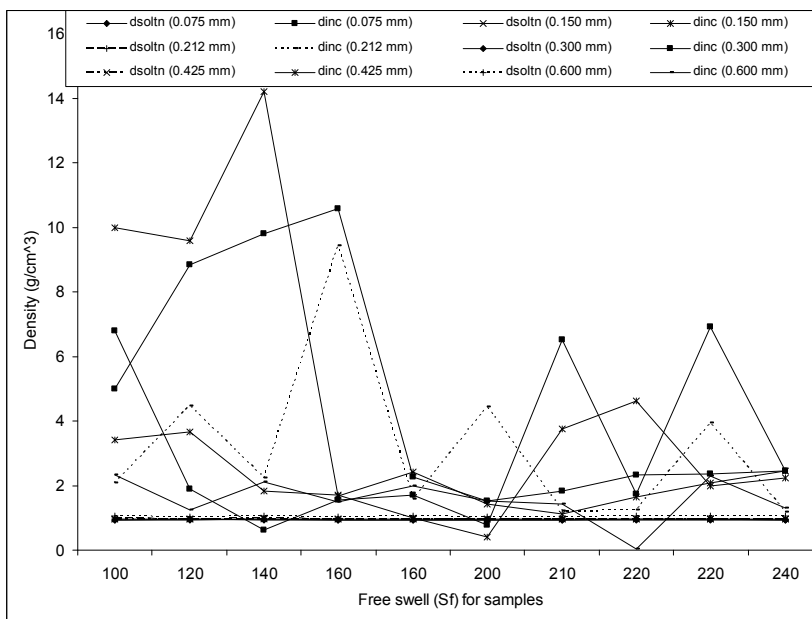


Figure 4. Free swell indices (S_f) for samples versus density for all sample sizes

The last sample to be considered in this investigation is the 0.600mm orange peels particulate sample. For the interaction of volume measurement against the free swell indices, three curves were plotted in Figure 2. Worthy of note is that the 0.600 mm sample has the lowest range of free swell indices ranging from 100 to 230 %. This is due to its large grain size and coarse nature which reduces its water absorption and subsequent swelling capacity. In practical applications, the orange peels reinforced composite is expected to have a much lower free swell than other components made with other sample sizes which may make it preferable to designers and composite manufacturers. The V_f curve rises gradually between 20 and 33 cm³ with the free swell indices indicating a direct dependence on the V_f by the S_f for the sample. The volume of solution V_s represents the volume of water body which contains the orange peels reinforced composite experiences free swell. The volume increase curve represents the increment in the original body of water as the free swell is taking place. The V_{soltn} rises to an early peak of 104 cm³ when the S_f is stable at 110 % but drops in value to 102.5 cm³ at a S_f of 130 %. Further increase in the value of S_f brings about an undulation in the value of V_{soltn} before stabilising at 103 cm³. When the orange peels reinforced composite attains a S_f of 200 %, the V_{soltn} drops in value again till it is stable at 103 cm³ while the S_f reaches a peak of 230 %. What this translates to is that, when using a 0.600 mm orange peel reinforced composite, the overall volume of the water environment rises in the same way the V_{soltn} curve has increased. This means that for every rise in free swell, the body of water is expected to change the same way the V_{soltn} curve has moved. However, every rise in free swell may not bring a corresponding rise in V_{soltn} . Thus, this relationship described graphically in Figure 3 helps to know and understand the expected changes in the volume of water body as a result of the 0.600mm orange peels composite that is undergoing free swell.

The relationship between the mass measurements and free swell indices of the orange peel particulates is presented in Figure 3 by 2 different curves. The mass of water M_w represents the mass of a typical body of water while the mass of solution M_{soltn} on the other hand represents the changes in mass of the water body when it is experiencing the free swell of a 0.600mm orange peel component. As expected there is an overall increase in M_w (water body) where the free swell is taking place. The values of M_{soltn} is seen to undulate as the S_f increases, eventually reaching a peak of 106.66g as the S_f attains a maximum value. The M_{inc} curve shows the trend at which the original water body M_w increases during the free swells of the 0.600mm component to give mass of solution M_{soltn} . The relationship between the density measurements and free swell indices of the 0.600 mm sample produced 2 different curves as shown in Figure 4. The density of solution d_{soltn} represents the density of the water body where the free swell of the material is taking place. The d_{soltn} ranges in value from 1.02 – 1.04 g/cm³ and as such the curve is represented as a straight line over all the values of free swell across the graph. This indicates that the S_f does not change the d_{soltn} in anyway.

The d_{inc} curve represents the instantaneous change in density of the 0.600 mm orange peels component undergoing free swell. As the free swell indices attains a value of 100, the d_{inc} rises rapidly to a peak value of 2.33 g/cm³. In other words, the free swell brings about a rapid instantaneous change in its density. As the S_f continues to increase, the value of d_{inc} is seen to undulate continuously. This is represented in the d_{inc} curve. At a S_f value of 200%, the d_{inc} rises to 2.29 from 0.03 g/cm³. As the S_f reaches a peak of 230%,

the d_{inc} drops to a stable value of 1.29 g/cm^3 . The density increase curve indicates the changes expected in a 0.600 mm orange peels reinforced composite undergoing free swell as it is being used in a water-based application. The increment in density may however be positive or negative as reflected in the d_{inc} curve due to the different mass and volume changes experienced by the material. These changes are as a result of the free swell behaviour which is peculiar only to the material.

CONCLUSION

The Holtz and Gibbs free swell scheme has been used to determine the free swell properties of orange peel particulate green composite reinforcement. The particle size changes and effects have been investigated. The following conclusions can be drawn. (1) The free swell index is controlled by particulate size, final volume of the particulate dissolved in water; (2) For each of the sample sizes, namely, 0.075, 0.150, 0.212, 0.300, 0.425 and 0.600mm, the free swell S_f was found to have a direct dependence on final volume V_f ; (3) The free swell behaviour of the 0.075, 0.150, 0.212, 0.300, 0.425 and 0.600 mm particulate samples describes the expected influences of the free swell of 0.075, 0.150, 0.212, 0.300, 0.425 and 0.600 mm components on the mass, volume and density of the water environment (V_{soltm} , M_{soltm} , d_{soltm} , M_{inc} , V_{inc}) where they are being used as well as the density increments of the different component (d_{inc}) (4) The sample has the highest free swell indices value of 380% and the highest range of free swell indices from 90 to 380%. This means that in practical usage, the free swell indices of a component made with 0.300 mm orange peel particulates is expected to be more than that of the remaining samples, covering a wider range. (5) The 0.600 mm sample has the lowest peak free swell indices value of 230% and the lowest range of free swell indices between 100 to 130%. It is expected that the free swell indices of a component made with 0.600 mm would be less than that of the remaining samples.

Acknowledgement

The authors are grateful to Mr. Salami of the Soil Mechanics Laboratory, University of Lagos, Lagos.

REFERENCES

1. Holtz, W. G; Gibbs, H. J. *Engineering properties of Expansive Clays*, Transactions of the American Society of Civil Engineers, 1956; p. 121.
2. Kamal, G.M; Anwar, F; Hussain, A.I; Sari, N; Ashraf, M.Y. Yield and chemical composition of citrus essential oils as affected by drying pretreatment of peels, *International Food Research Journal*, **2011**,18 (4), 1275-1282.
3. Ezejiolor, T.I.N; Eke, N.V; Okechukwu, R.I; Nwoguikpe, R.N; Duru, C.M; Waste to wealth industrial raw materials potentials of peels of Nigerian sweet orange (*Citrus sinensis*), *African Journal of Biotechnology*, **2011**, 10 (33), 6257-6264.

4. Islam, M.R; Muslim, T; Rahman, MA. Investigation of orange peel: derivation of isolated cellulosic material and analysis of the fatty acids composition, *Dhaka University Journal of Science*, **2011**, 60 (1), 77-78.
5. Chede, P.S. Photochemical analysis of citrus sinensis peel, *International Journal of Pharma and Bio-sciences*, **2013**, 4 (1), 339-343.
6. Verzera, A; Trozzi, A; Dugo, G; Di bella, G; Cotroneo, A. Biological lemon and sweet orange essential oil composition, *Flavour and Fragrance Journal*, **2004**, 19 (6), 544-548.
7. Marthey, J.A. Fractionation of orange peels phenols in ultra-filtered molasses and mass balance studies of their anti-oxidant levels, *Journal of Agriculture Food and Chemistry*, **2004**, 52, 7586-7592.
8. Yeoh, S; Shi, J; Laugrish, T.A.G. Comparisons between techniques for water based extraction of pectin from orange peels, *Desalination*, **2008**, 218, 229-237.
9. Pandharipande, S; Makode, H. Separation of oil and pectin from orange peel and study of effect of pH of extracting medium on the yield of pectin, *Journal of Engineering Research and Studies*, **2012**, 3 (2), 6-9.
10. Vora, J.D; Matthews, R.F; Crandall, P.G; Cook, R. Preparation and chemical composition of orange oil concentrates, *Journal of Food Science*, **1983**, 48 (4), p. 1197.
11. Pino, J; Sarchez, M; Sanchez, R; Rocal, E. Chemical composition of orange oil concentrates, *Nahrung/Food*, **2006**, 36 (6), 539-542.
12. Banidadr, S; Asempour, H. Effect of ferric salt orange peel solid fraction on photo-oxidation and biodegradability of LDPE films, *Iranian Polymer Journal*, **2012**, 21 (7), 463-471.
13. Van den Brom, C.R; Anac, I; Roskamp, R.F; Retsch, M; Jonas, U; Menges, B; Preece, J.A. The swelling behaviour of thermo responsive hydrogel/silical nano-particle composites, *Journal of Material Chemistry*, **2010**, 20, 4827-4839.
14. Abd-El-Salam, M.H; El-Gamal, S; Abd El-Maqsoud, D.M; Mohsen, M. Correlation of electrical and swelling properties with nano free-volume structure of conductive silicone rubber composite, *Polymer Composites*, **2013**, 34 (12), 2105-2115.
15. Masoodi, R; Pillai, K.M. A study on moisture absorption and swelling in bio-based jute-epoxy composites, *Journal of Reinforced Plastics and Composites*, **2012**, 31, 5285-5294.
16. Ojha, S; Regharendra, G; Acharya, S.K; Kumar, P. Fabrication and study of mechanical properties of orange peel reinforced polymer composite, *Caspain Journal of Applied Sciences Research*, **2012**, 1 (13), 190-192.
17. Aigbodion, V.S; Atuanya, C.V; Igogori, E.A; Ihom P. Development of high density polyethylene/orange peels particulate bio-composite, *Gazi University of Journal of Science*, **2013**, 26 (1), 107-117.
18. Tao, N.G; Hu, Z.Y; Liu, Q; Xu, J; Cheng, Y.J; Guo, L.L; Guo, W.W; Deng, X.X. Expression of phytoene synthase gene is enhanced during fruit ripening of navel orange (*Citrus Sinensis*), *Plant Cell Reports*, **2007**, 26, 837-843.

ИСПИТИВАЊЕ СЛОБОДНОГ БУБРЕЊА ПАРТИКУЛА ПОМОРАНЦИНЕ КОРЕ

Олувасеј А. Аџибаде¹, Џонсон О. Агумсој², Сандеј А. Оке³

^{1,2} Департман металуршког и инжењерства материјала, Факултет инжењерства, Универзитет у Лагосу, Лагос, Нигерија

³ Департман машинства, Факултет инжењерства, Универзитет у Лагосу, Лагос, Нигерија

Партикуле коре од поморанце представљају погодан материјал за израду спортске опреме и друге индустријске примене, занимљив како са економског тако и са еколошког аспекта. Изведени су експерименти слободног бубрења како би се испитало понашање материјала од поморанцине коре као пунилаца армираних композиита који се користе у спољним условима у присуству воде. Експериментални подаци су прикупљани у току 10 дана свака 24 сата. Примењен је модел Холца и Гибса за слободно бубрење, који укључује следећих пет параметара: слободно бубрење (S_f ; крајњу запремину (V_f); масу воде (M_w); масу раствора (M_s и запремину раствора (V_s). Испитиване партикуле су биле пречника 0,075, 0,150, 0,212, 0,300, 0,425 и 0,600 mm. Анализа је показала разлике у способностима бубрења у води партикула различитих величина, на основу чега може да се изведе закључак о могућем понашању партикула од поморанцине коре у условима спољне примене.

Кључне речи: параметри бубрења, слободно бубрење, зелени композити

Received: 24 December 2014.

Accepted: 20 October 2015.

A COMPARISON OF DIFFERENT METHODS TO REMOVE DISSOLVED OXYGEN: APPLICATION TO THE ELECTROCHEMICAL DETERMINATION OF IMIDACLOPRID

Ana D. Đurović^{1*}, Zorica S. Stojanović¹, Snežana Ž. Kravić¹, Zvonimir. J. Suturović¹,
Tanja Ž. Brezo¹, Nada L. Grahovac² and Spasenija D. Milanović¹

¹ University of Novi Sad, Faculty of Technology, Bulevar cara Lazara 1, 21000 Novi Sad, Serbia

² Institute of Field and Vegetable Crops, Maksima Gorkog 30, 21000 Novi Sad, Serbia

This study compares different methods for the removal of oxygen from the solution prior to the chronopotentiometric determination of the insecticide imidacloprid on glassy carbon electrode. The research included the application of the chemical method involving addition of sulfite ion, and the physical method of purging the sample with nitrogen stream, as well as their combination. By comparing analytical signals of imidacloprid, chemical method showed almost the same efficiency as conventional physical method, while the best reproducibility was achieved by applying chemical method with addition of the saturated sodium sulfite solution. The method is very simple and can be applied for deoxygenation of the solution prior to the chronopotentiometric analysis. The application of the chemical deoxygenation significantly shortened duration of the chronopotentiometric analysis of imidacloprid from approximately 15 min to 1 min.

KEY WORDS: imidacloprid, sulfite ion, chemical deoxygenation.

INTRODUCTION

Imidacloprid is a systemic insecticide that belongs to a group of neonicotinoids (1). According to the mechanism of action, it acts on the insect's central nervous system, causing irreversible blocking of postsynaptic nicotinic acetylcholine receptors (1). Since its discovery and utilization in practical use, imidacloprid has become the most selling insecticide worldwide used for crop protection and pest control (1-3). Extensive usage of imidacloprid in agriculture requires a systematic control of its content in environmental samples.

Most of the methods used for the determination of imidacloprid are based on the use of chromatographic methods (4-7). Although these techniques exhibit high sensitivity and selectivity, they are complicated, time consuming, expensive, and require highly trained personnel. On the contrary, electroanalytical techniques are of great interest due to their advantages, including high sensitivity, comparative simplicity, rapid response and low

* Corresponding author: Ana D. Đurović, University of Novi Sad, Faculty of Technology, Bulevar cara Lazara 1, 21000 Novi Sad, Serbia, e-mail: djurovic.ana@tf.uns.ac.rs

cost. There are several studies about the application of electroanalytical methods for the determination of imidacloprid, which are based on the irreversible reduction of the analyte on the working electrode (8 - 10). This electroreduction is carried out in two steps. In the first step the nitro group is reduced to a hydroxylamine, and in the second step to an amine (8). Although the applied electrochemical techniques are of short duration and do not require complicated sample preparation, most of time before the analysis is spent on the removal of dissolved oxygen from the solution, as an inevitably required step in the imidacloprid electroanalysis.

The electrochemical reduction of dissolved oxygen results in high residual currents and the production of H_2O_2 and OH^- , which may affect the studied electrochemical process in a certain potential range (11, 12). Since imidacloprid is electroactive in the same potential range where oxygen reduction occurs, in order to avoid drawback procedures by dissolved oxygen, it has to be removed from the solution before the analysis. Therefore, many different methods are developed for deoxygenation. In general, the dissolved oxygen can be removed from solution by chemical or physical means. Among physical methods, purging of samples with an inert gas (usually nitrogen or argon) is commonly used. The time required for effective removal of oxygen varies with the gas flow-rate, solution volume and geometry of the process glass, and lasts 10-15 min, thus representing the most time-consuming step in the entire analysis (13). Although physical methods of deoxygenation are quite effective, they have a number of disadvantages. Namely, the oxygen could diffuse back into the system through tubing and joints, and it is difficult to deoxygenate more than one sample at the same time (14, 15).

Other methods for oxygen removal include the use of electrochemical or chemical (zinc) scrubbers, nitrogen-activated nebulizers, and chemical reduction (12). Chemical reduction can be extremely effective. It is carried out by addition of a substance to the tested solution that rapidly reacts with oxygen. In the choice of a substance for chemical reduction, it is important to avoid reaction between the reductant and the target analyte. The most common reductant reported in the literature is sulfite ion (11, 12, 16). In its application it should be kept in mind that in polarography its application is limited to the solutions of pH greater than 8, due to the appearance of polarographic waves (17). Beside sulfite ion, ascorbic acid is also used for oxygen reduction (18).

This study compares different methods of deoxygenation prior to the chronopotentiometric determination of imidacloprid on glassy carbon electrode. The investigation included physical deoxygenation with nitrogen purging, chemical deoxygenation by addition of sulfite ion to the tested solution, as well as combination of physical and chemical methods. The objective was to simplify and shorten the procedure of oxygen removal as much as possible, in order to perform chronopotentiometric determination of imidacloprid by obtaining a high and reproducible signal of the analyte.

EXPERIMENTAL

Reagents and solutions

All chemicals used were of analytical grade purity. Double distilled water was used throughout. Imidacloprid stock solution (0.4 g/dm^3) was prepared by dissolving an appro-

appropriate amount of the reference standard of imidacloprid (Dr. Ehrenstorfer, Augsburg, Germany) in double distilled water. Britton-Robinson buffer, prepared from equimolar 0.04 mol/dm³ stock solutions of orthophosphoric, boric and acetic acids was used as a supporting electrolyte. All three acids were purchased from Lach-Ner, Brno, Czech Republic. The appropriate pH value (7.5) of the buffer was adjusted by 0.2 mol/dm³ sodium hydroxide solution (Lach-Ner, Brno, Czech Republic). The saturated solution of sodium sulfite (230 g/dm³) was prepared immediately before the analysis by dissolving an appropriate amount of sodium sulfite (Centrohem, Stara Pazova, Serbia) in double distilled water.

Apparatus

All chronopotentiometric investigations were performed on a stripping analyzer with three-electrode cell. The working electrode was a glassy carbon disk of total surface area 7.07 mm². A platinum wire ($\varphi=0.7$ mm, $l=7$ mm) served as a counter electrode, and the reference electrode was Ag/AgCl (KCl, 3.5 mol/dm³). All values of the potential were shown versus Ag/AgCl. Electric stick stirrer was also an integral part of the three-electrode system. The analyses were performed in special glass vessels (volume of 50 cm³) with tapered bottom. The pH values were measured with a digital pH meter model MA 5705 (Iskra, Kranj, Slovenia).

General procedure

The model system, consisting of the supporting electrolyte and imidacloprid was used in all experiments. The Britton-Robinson buffer pH 7.5 was used as supporting electrolyte: 20 cm³ was pipetted into the process glass, followed by addition of a certain volume of the imidacloprid stock solution. For the chemical removal of dissolved oxygen from the solution, appropriate volume (0.6, 0.8 and 1.0 cm³) of the saturated solution of sodium sulfite was added to the model system. For the physical deoxygenation, the solution was purged with nitrogen for appropriate time (5, 10 and 15 min), while the solution was constantly stirred. For removing traces of oxygen from nitrogen, the gas was first purged through a pyrogallol solution, and then through the Britton-Robinson buffer, to saturate gas stream in order to prevent evaporation of the sample. Nitrogen was allowed to escape through a tube that was immersed in the double distilled water. During nitrogen purging the working electrode was kept in a special glass with double distilled water. When a combination of nitrogen purging and reduction with sulfite ion was applied for oxygen removal, 0.4 cm³ of saturated sodium sulfite solution was added to the model system, the apparatus was blanked, and the solution was purged with nitrogen for 5 min.

After removing the oxygen, the solution was stirred for 15 s, followed by a quiet period (10 s), and the analysis was performed. For comparison, the deoxygenated supporting electrolyte was used as a blank. The chronopotentiogram was recorded in a potential range from -0.91 V to -1.42 V. All experiments were performed at room temperature (23±2°C).

RESULTS AND DISCUSSION

In chronopotentiometry, the signal of the imidacloprid was not noticeable due to multitude of peaks that occurred on the chronopotentiogram owing to the oxygen reduction on the working electrode. As a consequence, the final potential of the analysis of -1.42 V was inaccessible, even by applying the maximum current of -50 μA , indicating that the dissolved oxygen had to be removed from the solution.

Preliminary experiments were focused on the background chronopotentiograms recorded for the blank after applying chemical deoxygenation by adding different volumes (0.6, 0.8 and 1 cm^3) of saturated sodium sulfite solution. Further background chronopotentiograms were recorded for the blank deoxygenated by purging nitrogen for 5, 10 and 15 min. The experiments were performed in triplicate for each value. In the case of chemical method, the addition of 0.8 cm^3 of saturated sodium sulfite solution yielded the best appearance of the chronopotentiograms. Namely, the recorded chronopotentiogram was sharp with no-signal baseline.

After the addition of imidacloprid to the blank, the analytical signal appeared at the potential of -1.2 V (9). After prolonged standing of the tested solutions in air, or after multiple addition of solution of imidacloprid to the process glass, only 15 s of stirring prior to the recording was enough to perform the analysis. The applied concentration of sulfite ion was enough to maintain the concentration of dissolved oxygen at a level that did not affect the performance of the chronopotentiometric analysis.

When dissolved oxygen was removed by nitrogen purging, 10 min was sufficient to that purpose, and a longer time did not contribute to a better appearance of the background chronopotentiogram. However, further deoxygenation in duration of 2 min was required because of the oxygen creeping in from the outside. The combination of sulfite ion and nitrogen purging (0.4 cm^3 of saturated sodium sulfite solution and 5 min) did not produce satisfactory result regarding the background chronopotentiograms with nitrogen purging shorter than 10 min.

In order to choose a method for oxygen removal aiming the imidacloprid chronopotentiometric determination, analytical signals of 15 mg/dm^3 imidacloprid obtained after applying different deoxygenation procedures were considered. The results are shown in Table 1.

Table 1. Analytical signals of imidacloprid in dependence of the applied method for dissolved oxygen removal

Deoxygenation method	Analytical signal (s)	RSD (%)
Nitrogen 15 min	0.87 \pm 0.05*	2.87
Nitrogen 10 min	0.88 \pm 0.05	2.84
Nitrogen 5 min	0.58 \pm 0.03	2.59
Nitrogen 5 min and 0.4 cm^3 of saturated Na_2SO_3 solution	0.66 \pm 0.05	3.79
0.6 cm^3 of saturated Na_2SO_3 solution	0.88 \pm 0.06	3.41
0.8 cm^3 of saturated Na_2SO_3 solution	0.90 \pm 0.03	1.67
1 cm^3 of saturated Na_2SO_3 solution	0.84 \pm 0.05	2.98

* \bar{X} mean \pm 2SD, n = 3.

The highest signals were obtained after the addition of sulfite ion and after 10 and 15 min of nitrogen purging, and the lowest after the nitrogen purging for 5 minutes (0.58 s), while a poor reproducibility was observed by applying the combination of nitrogen purging and sulfite ion addition (RSD = 3.79%). By comparing the height and appearance of the signals when different methods for deoxygenation were used, it can be seen that they were practically the same. These results indicate that there was no chemical reaction between sulfite ion and the target analyte. The best reproducibility was achieved by applying chemical deoxygenation with addition of 0.8 cm³ of saturated sodium sulfite solution (RSD = 1.67%). Thanks to the much easier performance, and short duration, chemical deoxygenation with addition of 0.8 cm³ of saturated sodium sulfite solution can be accepted as optimal in terms of the reduction of imidacloprid on glassy carbon electrode.

The chronopotentiometric method using optimal deoxygenation procedure was applied for the determination of imidacloprid content in commercial formulations. Commercial formulations containing imidacloprid as an active ingredient were properly diluted with double distilled water, and finally with Britton-Robinson buffer. Imidacloprid was determined by the calibration curve method, and the obtained results are presented in Table 2. The obtained values for the imidacloprid content were in good agreement with the manufacturer specification, indicating that the optimized chemical deoxygenated procedure can be used for the determination of imidacloprid in commercial formulations.

Table 2. Contents of imidacloprid in the commercial formulations determined by the chronopotentiometric method involving the optimized deoxygenated procedure

Commercial formulation	Imidacloprid content claimed by the manufacturer [g/kg]	Imidacloprid content found by chronopotentiometric method with optimized deoxygenated procedure [g/kg]
Confidor 70 WG	700	699.27 ± 10.56*
Imidor 70 WS	700	708.88 ± 8.04

*X_{mean} ± 2SD, n = 3.

CONCLUSION

Chemical reduction of dissolved oxygen by adding sulfite ion provides the conditions suitable for the chronopotentiometric analysis of imidacloprid. Namely, the reaction between the sulfite ion and dissolved oxygen was almost instant, allowing that in duration of 30 s of stirring the solution, the dissolved oxygen was at a level that enabled the analysis. Thus, conventional time-consuming step of purging of sample with inert gas was avoided. The method was also distinguished by its simplicity, because it required only a saturated solution of sulfite ion, compared to a complicated apparatus when nitrogen was used. By comparing the analytical signals, it was found that sulfite ion did not react with the analyte; the best reproducibility was achieved by adding 0.8 cm³ of the saturated sodium sulfite solution. Given all stated advantages, the deoxygenation procedure with sulfite ion accompanied with chronopotentiometric analysis can be used as a routine tool for the imidacloprid determination in food and water quality control.

Acknowledgement

This investigation was financially supported by the Ministry of Education, Science and Technological Development of the Republic of Serbia (Grant III 46009).

REFERENCES

1. Roberts, T.R.; Hutson, D.H. *Metabolic Pathways of Agrochemicals. Part 2: Insecticides and Fungicides*, The Royal Society of Chemistry: Cambridge, 1999; pp 111-121.
2. Jeschke, P.; Nauen, R. Neonicotinoid Insecticides. In *Insect Control Biological and Synthetic Agents*; Gilbert, L.J., Gill, S.S., Eds.; Elsevier, 2010; pp 61-114.
3. Jeschke, P.; Nauen, R.; Schindler, M.; Elbert, A. Overview of the status and global strategy for neonicotinoids. *J. Agric. Food Chem.* **2011**, *59* (7), 2897-2908.
4. Xiao, Z.; Yang, Y.; Li, Y.; Fan, X.; Ding, S. Determination of neonicotinoid insecticides residues in eels using subcritical water extraction and ultra-performance liquid chromatography-tandem mass spectrometry. *Anal. Chim. Acta* **2013**, *777*, 32-40.
5. Jovanov, P.; Guzvány, V.; Franko, M.; Lazić, S.; Sakač, M.; Milovanović, I.; Nedeljković, N. Development of multiresidue DLLME and QuEChERS based LC-MS/MS method for determination of selected neonicotinoid insecticides in honey liqueur. *Food Res. Int.* **2014**, *55*, 11-19.
6. Ko, A-Y.; Rahman, M.M.; Abd El-Aty, A.M.; Jang, J.; Park, J-H.; Cho, S-K.; Shim, J-H. Development of a simple extraction and oxidation procedure for the residue analysis of imidacloprid and its metabolites in lettuce using gas chromatography. *Food Chem.* **2014**, *148*, 402-409.
7. Masiá, A.; Campo, J.; Blasco, C.; Picó, Y. Ultra-high performance liquid chromatography-quadrupole time-of-flight mass spectrometry to identify contaminants in water: an insight on environmental forensics. *J. Chrom. A* **2014**, *1345*, 86-97.
8. Navalón A.; El-Khattabi, R.; Gonzáles-Casado, A.; Vilches, J.L. Differential-pulse polarographic determination of the insecticide imidacloprid in commercial formulations. *Microchim. Acta* **1999**, *130* (4), 261-265.
9. Guzvány, V.J.; Gaál, F.F.; Bjelica L.J.; Ökrész, S.N. Voltammetric determination of imidacloprid and thiametoxam. *J. Serb. Chem. Soc.* **2005**, *70* (5), 735-743.
10. Chen, M.; Meng, Y.; Zhang, W.; Zhou, J.; Xie, J.; Diao, G. β -Cyclodextrin polymer functionalized reduced-graphene oxide: application for electrochemical determination imidacloprid. *Electrochim. Acta* **2013**, *108*, 1-9.
11. Wallace, G.G. Dissolved oxygen: the electroanalytical chemists dilemma. *TrAC.* **1985**, *4* (6), 145-148.
12. Wang, J. *Analytical electrochemistry*; Third edition, Wiley-VCH: New Jersey, 2006; pp.118-119.
13. Fraga, J.M.G.; Abizanda, A.I.J.; Moreno, F.J.; León, J.J.A. Application of principal component regression to the determination of Captopril by differential pulse polarography with no prior removal of dissolved oxygen. *Talanta* **1998**, *46* (1), 75-82.

14. Florence, T.M.; Farrar, Y.J. Removal of oxygen from polarographic solutions with ascorbic acid. *J. Electroanal. Chem. Interfacial Electrochem.* **1973**, *41* (1), 127-133.
15. Reinke, R.; Simon, J. The online removal of dissolved oxygen from aqueous solutions used in voltammetric techniques by the chromatomembrane method. *Anal. Bioanal. Chem.* **2002**, *374* (7-8), 1256-1260.
16. Wong, G.T.F.; Zhang, L-S. Chemical removal of oxygen with sulfite for the polarographic or voltammetric determination of iodate or iodide in seawater. *Mar. Chem.* **1992**, *38* (1-2), 109-116.
17. Heyrovský, J.; Zuman, P. *Practical polarography: An Introduction for Chemistry Students*; Academic press: London and New York, 1968, pp.27-28.
18. Butler, I.B.; Schoonen, M.A.A.; Rickard, D.T. Removal of dissolved oxygen from water: a comparison of four common techniques. *Talanta* **1994**, *41* (2), 211-215.

ПОРЕЂЕЊЕ РАЗЛИЧИТИХ МЕТОДА ЗА УКЛАЊАЊЕ РАСТВОРЕНОГ КИСЕОНИКА: ПРИМЕНА ПРИ ЕЛЕКТРОХЕМИЈСКОМ ОДРЕЂИВАЊУ ИМИДАКЛОПРИДА

Ана Д. Ђуровић¹, Зорица С. Стојановић¹, Снежана Ж. Кравић¹, Звонимир Ј. Сутуровић¹, Тања Ж. Брезо¹, Нада Ј. Граховић², Спасенија Д. Милановић¹

¹ Универзитет у Новом Саду, Технолошки факултет, Булевар цара Лазара 1, 21000 Нови Сад, Србија

² Институт за ратарство и повртарство, Максима Горког 30, 21000 Нови Сад, Србија

У овој студији поређене су различите методе за уклањање раствореног кисеоника из раствора пре хронопотенциометријског одређивања инсектицида имидаклоприда на електроди од стакластог угљеника. Истраживање је обухватало примену хемијске методе додатком сулфитног јона и физичке методе провођење струје азота кроз узорак у трајању од 5, 10 и 15 мин, као и њихову комбинацију. Поређењем аналитичких сигнала имидаклоприда, хемијска метода показала је скоро исту ефикасност као и конвенционална физичка метода, док је најбоља репродуктивност остварена применом хемијске методе уз додатак 0,8 cm³ zasiћеног раствора натријум сулфита. Метода је веома једноставна и може се применити за уклањање кисеоника из раствора пре извођења хронопотенциометријске анализе. Применом хемијске деоксигенације значајно се скраћује трајање хронопотенциометријске анализе имидаклоприда са 15 мин на 1 мин.

Кључне речи: имидаклоприд, сулфитни јон, хемијска деоксигенација.

Received: 15 June 2015.

Accepted: 23 September 2015.

LATTICE BOLTZMANN SIMULATION OF TWO-SIDED LID-DRIVEN FLOW IN DEEP CAVITIES

Nataša Lj. Lukić^{1*}, Predrag M. Tekić², Jelena B. Rađenović² and Ivana M. Šijački¹

¹ University of Novi Sad, Faculty of Technology, Bulevar cara Lazara 1, 21000 Novi Sad, Serbia

² University of Novi Sad, Faculty of Science, Trg Dositeja Obradovića 3, 21000 Novi Sad, Serbia

The present study is concerned with two-sided lid-driven incompressible flow in rectangular, deep cavities applying lattice Boltzmann method. After validating the code for the square cavity, solutions for cavities with an aspect ratio 1.5 and 4 were obtained for the Reynolds numbers of 100, 400, 1000 and 3200. The influence of the Reynolds number and aspect ratio on the flow pattern and on the characteristics of vortices inside the cavity was studied. Symmetric flow pattern was obtained for all investigated cases. The middle of the cavity is mostly influenced by the increase in the aspect ratio. Critical aspect ratio, at which the birth of a primary vortex in the middle of the cavity takes place, was determined to be between 2.7 and 2.725.

KEY WORDS: lattice Boltzmann method, two-sided lid-driven cavity, deep cavity, aspect ratio, antiparallel.

INTRODUCTION

Recently, the lattice Boltzmann method (LBM) has become an alternative way for computational fluid dynamics (CFD) (1-4). Unlike conventional methods, which are based on macroscopic continuity equations, it utilizes the particle distribution function to describe collective behavior of fluid molecules. The kinetic features of the LBM enable it to be a very effective numerical tool for simulating complex geometries of flows (5-7), multiphase flows (8, 9), magnetohydrodynamic systems (10, 11), and so on.

Lid-driven cavity flow has been studied extensively, and it is one of the most popular fluid problems in the CFD field. This is mainly because of the simplicity of the cavity geometry, which allows easy and straightforward coding while maintaining complex flow features. In the literature, it is possible to find a great number of papers on the lid-driven cavity flow (12-18). References in these papers do not include works on the lattice Boltzmann simulation of lid-driven cavity flow. Since the driven cavity flow is a benchmark problem for numerical methods. It was also the subject of numerous lattice Boltzmann studies (11, 19-27).

* Corresponding Author: Nataša Lj. Lukić, University of Novi Sad, Faculty of Technology, Bulevar cara Lazara 1, 21000 Novi Sad, Serbia, e-mail: nlukic@tf.uns.ac.rs

Most of previous studies were carried out on one-sided lid-driven cavity flow. A detailed analysis demonstrating the capabilities of the lattice Boltzmann method to simulate cavity flow was presented by Hou et al. (20). The results obtained in their study compared perfectly for Reynolds (Re) number up to 7500 with Navier-Stokes solution results of Ghia et al. (14). Patil et al. (23) investigated the lid-driven flow in rectangular, deep cavities with aspect ratios of 1.5-4 and Re number of 50-3200, with a particular focus on the dynamics of the primary and corner-vortices. Cheng and Hung (28) studied the effects of the aspect ratio (ranging from 0.1 to 7) and Re number (0.01 to 5000) on the vortex structure using lattice Boltzmann method.

Kuhlmann et al. (29, 30) introduced the case of two-sided lid-driven cavity flow, in which the flow driven by two facing walls moving in opposite directions was investigated. They observed that two-dimensional flows are not unique and depend upon the cavity aspect ratio and Re number. Albensoeder et al. (31) investigated numerical solutions of two-sided lid driven cavity flow and found existence of numerous flow states. Luo et al. (15) used a continuation method to predict flow solutions for a two-sided lid-driven flow with an aspect ratio of 1.96 and calculated five distinct flows for $Re < 2000$. Cavity flow driven by the motion of two horizontal bounding walls was investigated by Gaskell et al. (17). Streamlines for flow with different aspect and speed ratios were presented in their work. Only a few works have performed a simulation of the two-sided lid-driven flow using LBM (27, 32). Perumal and Dass (32) investigated the flow driven by parallel and antiparallel motion of two facing walls in a square cavity at different Re numbers. In their study, Tekić et al. (27) presented results for parallel and antiparallel motion in a staggered cavity and determined an asymmetric steady-state flow pattern for parallel motion of lids.

The main objective of the present work is to study the incompressible flow in a two-sided lid-driven cavity utilising LBM method and examine the influence of the aspect ratio and Re number on the flow pattern with an emphasis on the vortex structure. Figure 1 shows a schematic diagram of two-sided lid-driven cavity with the aspect ratio $K=H/L$, where H is the cavity depth and L the cavity width.

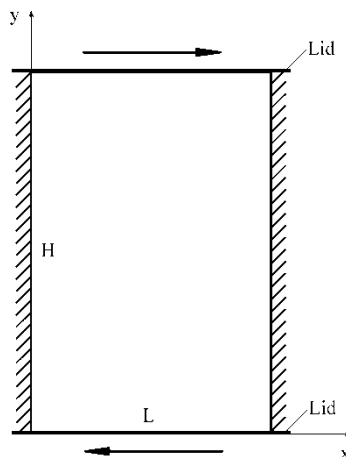


Figure 1. Schematic diagram of the two-sided lid-driven cavity – antiparallel motion

MATHEMATICAL FORMULATION

Lattice Boltzmann equation

This section gives a brief introduction to the lattice Boltzmann method. More detailed description can be found elsewhere (1, 33).

The lattice Boltzmann equation (LBE) reads:

$$\frac{\partial f}{\partial t} + \xi \cdot \Delta f = \Omega. \quad [1]$$

After applying simple Bhatnagar-Gross-Krook (BGK) approximation on the collision term (Ω), a space discretized LBE is as follows:

$$f_i(x + e_i \Delta t, t + \Delta t) - f_i(x, t) = -\frac{1}{\tau} [f_i(x, t) - f_i^{eq}(x, t)] \quad [2]$$

where $f_i(x, t)$ and $f_i^{eq}(x, t)$ are the distribution function and the equilibrium distribution function, respectively, e_i is a discrete velocity vector and τ is the single relaxation time related to the kinematic viscosity of the fluid:

$$\tau = \frac{6\nu + 1}{2}. \quad [3]$$

The nine-velocity square lattice model (D2Q9) is commonly used for simulating two-dimensional (2-D) flows. The equilibrium distribution function for isothermal incompressible flow and D2Q9 model reads:

$$f_i^{eq} = \rho w_i \left[1 + \frac{3}{c^2} e_i \cdot u + \frac{9}{2c^4} (e_i \cdot u)^2 - \frac{3}{2c^2} u \cdot u \right] \quad [4]$$

where w_i and u are the weight parameters and velocity of the fluid, respectively. Discrete velocity vectors are defined as:

$$\begin{aligned} e_0 &= (0, 0) \\ e_i &= (\pm c, 0), (0, \pm c) \quad i = 1, 2, 3, 4 \\ e_i &= (\pm c, \pm c) \quad i = 5, 6, 7, 8 \end{aligned} \quad [5]$$

where $c = \Delta x / \Delta t$, Δx and Δt are the lattice grid spacing and the time step, respectively. Weight parameters for each velocity vector are $w_0 = 4/9$, $w_{1,3,5,7} = 1/9$, and $w_{2,4,6,8} = 1/36$. The macroscopic density and velocity of the fluid are obtained from the distribution function as follows:

$$\rho = \sum_{i=1}^8 f_i \quad [6]$$

$$\rho u = \sum_{i=1}^8 e_i f_i.$$

Boundary conditions

Dirichlet boundary conditions in nondimensional form are:

$$\left. \begin{array}{l} \text{Left and right walls :} \quad u, v = 0, \text{ at } x = (0, N) \\ \text{Bottom wall :} \quad u = \pm u_{ref}, v = 0, \text{ at } y = 0 \\ \text{Top wall :} \quad u = u_{ref}, v = 0, \text{ at } y = KN \end{array} \right\} \quad [7]$$

where N and KN are the number of lattice nodes in the x and y direction, respectively.

‘Finite-difference velocity gradient’ (34) model has been implemented on the stationary walls. This is the default non-local boundary condition based on an algorithm proposed by Skordos (35). Velocity gradients are estimated employing a finite difference scheme over adjacent neighbors. Latt et al. (34) suggested that these boundary conditions exhibit considerably higher numerical stability and thus are dedicated for use in high Reynolds number flows.

“Finite-difference velocity gradient” model, incorporating the equilibrium scheme (20), has been implemented on the moving walls. The values of flow variables (u, v, ρ) are reset to their prescribed constant values. The distribution function is taken as the equilibrium distribution function f_i^{eq} corresponding to these flow variables (23). The corner points are treated as part of the stationary walls (20).

The initial density $\rho(x, 0)$ is set to a value of 2.7 (20). The velocities at all nodes are taken as zero at the start of simulations. The initial equilibrium distribution function $f_i^{eq}(x, 0)$ is evaluated based on these conditions, while the initial distribution function is taken as $f_i(x, 0) = f_i^{eq}(x, 0)$.

Each numerical step of the LBM consists of streaming and collision. Computations were carried out with a code developed by the authors and written in C++ programming language.

RESULTS AND DISCUSSION

Validation of results for one-sided lid-driven cavity

Before presenting the results on two-sided, the validation of the results for one-sided lid-driven cavity flow was performed through comparison with the results reported in the literature. The grid resolution for square cavity was taken as 256 x 256. Figure 2 shows the steady-state u and v velocity profiles through the geometric center of the cavity for different Re numbers. It is clear that the present results are in good agreement with the results obtained by Chen et al. (36).

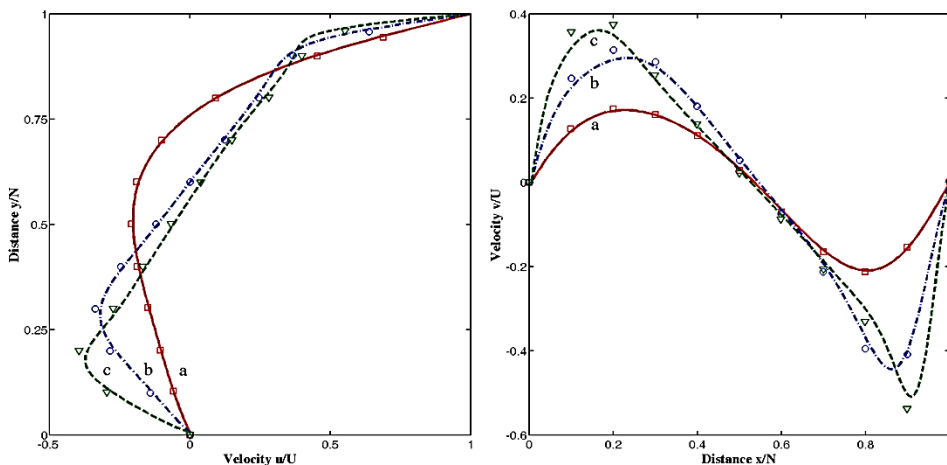


Figure 2. The velocity profiles u and v along the vertical and horizontal centrelines for $K=1$. (a) $Re=50$; (b) $Re=400$; (c) $Re=1000$. Symbols: solutions of Ref. (33); Lines: present study.

Two-sided lid-driven cavity

A two-dimensional incompressible flow driven by two facing lids moving in the opposite directions with an equal velocity for cavities with aspect ratios of 1.5 and 4 is presented here. All simulations employed 256×384 and 256×1024 nodes for cavities with the aspect ratios $K=1.5$ and 4, respectively. Grid size was chosen since the results, listed in Table 1, did not change significantly with further mesh refinement (using 384×576 nodes). Figures 3 and 4 show stream function and vorticity contours for different Re numbers and cavities with the aspect ratios of 1.5 and 4, respectively. It can be seen that an odd number of vortices is present considering that two-vortex flow is counted as a single vortex. For $K=1.5$ and $Re=50$, shown in Figure 3a, two co-rotating (clockwise direction) vortices are identified with a saddle point at the center of the cavity. This flow is known as the two-vortex flow (15, 30). As the Re number increases, two-vortex flow disappears with two vortices merging into a single vortex which occupies the entire cavity (Figure 3b). When $Re=1000$, two secondary vortices appear at the top-left and bottom-right corners of the cavity. As expected, secondary vortices gain in size for $Re=3200$ (see Figures 3c-d).

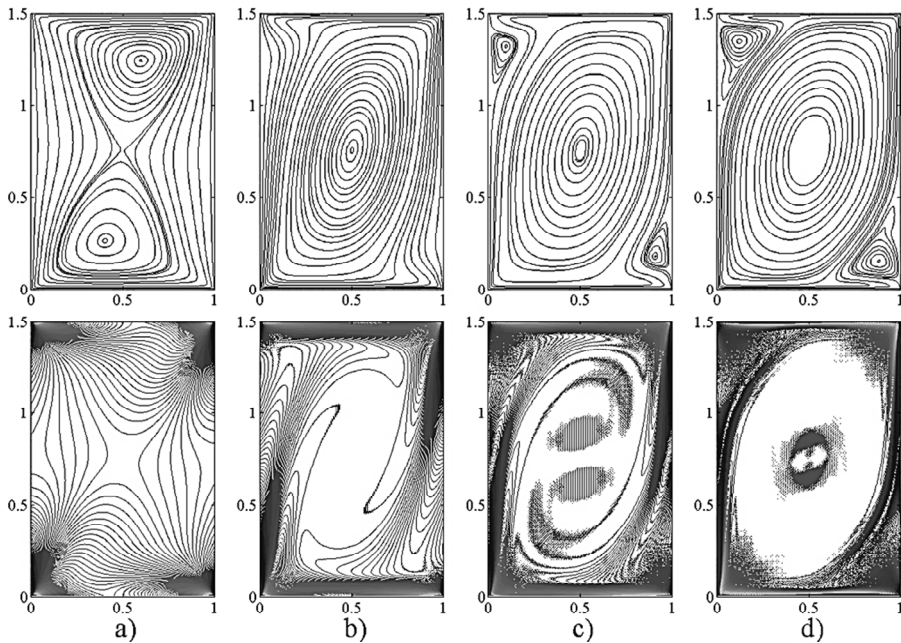


Figure 3. Streamfunction (top row) and vorticity (bottom row) contours for two-sided lid-driven cavity flow at various Re numbers-antiparallel motion. Aspect ratio $K=1.5$.
a) $Re=50$; b) $Re=400$; c) $Re=1000$; d) $Re=3200$

Streamfunction and vorticity contours, computed for cavity with the aspect ratio $K=4$ and $Re=50$, are shown in Figure 4a. It can be noticed that two primary vortices adjacent to the moving lids and rotating in a clockwise direction are present. Also, in the middle of the cavity, two-vortex flow appears. The two-vortex flow gains in strength and occupies more space at the expense of the vortices adjacent to the moving lids when $Re=400$ (see Figure 4b). For $Re=1000$, two secondary vortices adjacent to the solid walls are observed. These vortices are bounded with two heteroclinic connections between two points on the same wall, as shown in Figure 4c. Two vortex flow disappears for $Re=3200$ (see Figure 4d), with two secondary vortices now fully merged into one vortex located in the center of the cavity. More detailed discussion on the merger of secondary vortices is given in the next section.

As the Re number is increased from 50 to 1000, the centers of the inside top and bottom vortices move away from the center of the cavity towards the left and right solid walls, respectively. However, when $Re=3200$, the centers of the vortices are located closer to the center of the cavity.

The vorticity contours plotted in Figures 3 and 4 confirm findings of Patil et al. (23): as the Re number is increased, primary vortices adjacent to the moving lids become more prominent and larger in size and therefore the viscous effects are confined to the boundary layers close to the walls.

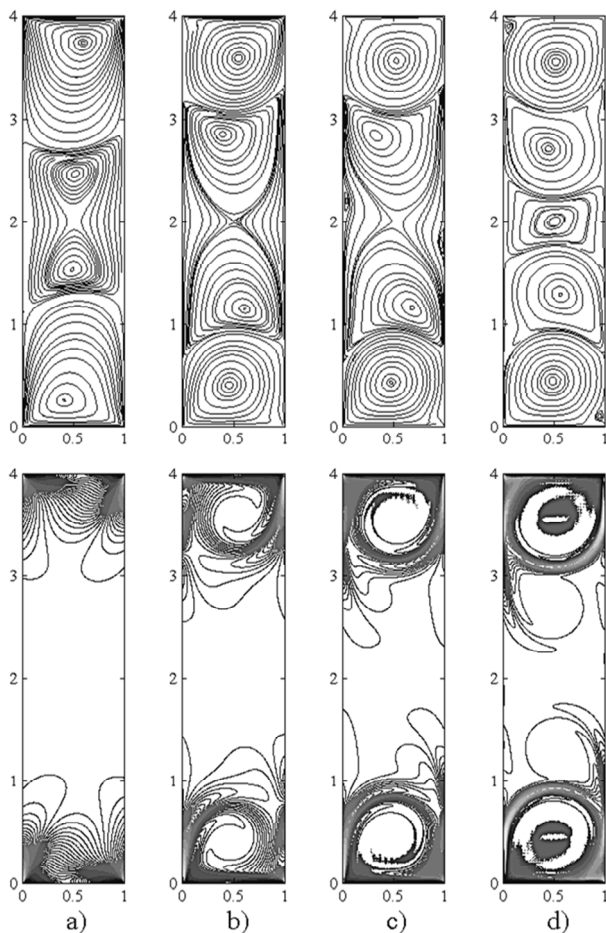


Figure 4. Streamfunction (top row) and vorticity (bottom row) contours for two-sided lid-driven cavity flow at various Re numbers – antiparallel motion. Aspect ratio $K=4$. a) $Re=50$; b) $Re=400$; c) $Re=1000$; d) $Re=3200$

Table 1 lists the locations and values of streamfunction and vorticity in the centers of the primary vortices appearing in the cavity with the aspect ratios of 1.5 and 4 for different Re numbers. It can be seen that for $K=4$, the computed vorticity in the centers of primary vortices adjacent to the moving lids (indexed as 1 and 4) decreases as the Re number increases. On the other hand, the vorticity value of the interior primary vortices (indexed as 2 and 3) increases with the Re number until $R=1000$. However, for $Re=3200$, the vorticity value is found to decrease. Similar behavior of the primary vortices (vortex adjacent to the moving lid and the vortex below that) was also observed for one-sided lid-driven cavity (23, 28).

Table 1. Values of streamfunction and vorticity in the centers of primary vortices for different Re and aspect ratios

<i>Re</i>	(<i>x</i> _{c1} , <i>y</i> _{c1})	Ψ_1, Ω_1	(<i>x</i> _{c2} , <i>y</i> _{c2})	Ψ_2, Ω_2
50 ^a	0.5998, 1.2429	-0.1026, -3.0513	0.4050, 0.2590	-0.1026, -3.0560
50 ^b	0.5958, 3.7552	-0.1017, -3.2429	0.5165, 2.4731	1.39E-04, 0.0162
400 ^a	0.5025, 0.7530	-0.1280, -1.6593		
400 ^b	0.5486, 3.6018	-0.1140, -2.2293	0.3950, 2.8622	9.87E-03, 0.3910
1000 ^a	0.5025, 0.7530	-0.1303, -1.5647		
1000 ^b	0.5296, 3.5689	-0.1166, -2.0089	0.3267, 2.8514	0.0124, 0.4899
3200 ^a	0.5095, 0.7589	-0.2498, -1.0939		
3200 ^b	0.5185, 3.5644	-0.2218, -1.6730	0.4442, 2.7181	0.0356, 0.4704
<i>Re</i>	(<i>x</i> _{c3} , <i>y</i> _{c3})	Ψ_3, Ω_3	(<i>x</i> _{c4} , <i>y</i> _{c4})	Ψ_4, Ω_4
50 ^a				
50 ^b	0.4904, 1.5214	1.41E-04, 1.62E-02	0.4111, 0.2493	-0.1017, -3.2191
400 ^a				
400 ^b	0.6119, 1.1436	9.87E-03, 0.3883	0.4593, 0.4040	-0.1140, -2.2304
1000 ^a				
1000 ^b	0.6792, 1.1579	1.26E-02, 0.4988	0.4754, 0.4287	-0.1161, -1.9945
3200 ^a				
3200 ^b	0.5617, 1.2915	0.0363, 0.4640	0.4874, 0.4451	-0.2199, -1.6695

^a Aspect ratio K=1.5 (256 x 384);

^b Aspect ratio K=4.

Effect of the aspect ratio

Previously, the effect of the Re number for the aspect ratios of 1.5 and 4 was considered. Now our interest is to determine the effect of the aspect ratio on the flow pattern, particularly, the evolution of primary vortices for Re=50.

According to Gürcan et al. (37, 38), there are four key stages during Stokes flow transformation in the cavity as the aspect ratio is increased: the appearance of a saddle point; the appearance of secondary vortices on the cavity walls; connection of secondary vortices with the saddle point, and the disappearance of the two-vortex substructure. Figure 5 shows the streamfunction contours for Re=50 and different aspect ratios. As can be seen, the increase in the aspect ratio results in the same changes in the flow pattern as discussed by Gürcan et al. (38). With the increase in the aspect ratio, two secondary vortices increase in size and move towards the center of the cavity. Figure 5a shows the streamfunction contours for the cavity of the aspect ratio of 2.575, at which secondary vortices reach the saddle point in the center of the cavity. Hence, four heteroclinic connections between the saddle point and solid walls are present (37, 38). As K increases to 2.675 (Figure 5b), two heteroclinic connections remain in the cavity, connecting the points on the two facing walls. When K=2.7, flow pattern at the center of the cavity highly resembles cat's eye flow. At a critical aspect ratio, between $2.7 \leq K_c \leq 2.725$, the centers of two small co-rotating vortices

reach the saddle point and fully merge to form a single vortex at the centre of the cavity (the disappearance of the two-vortex flow).

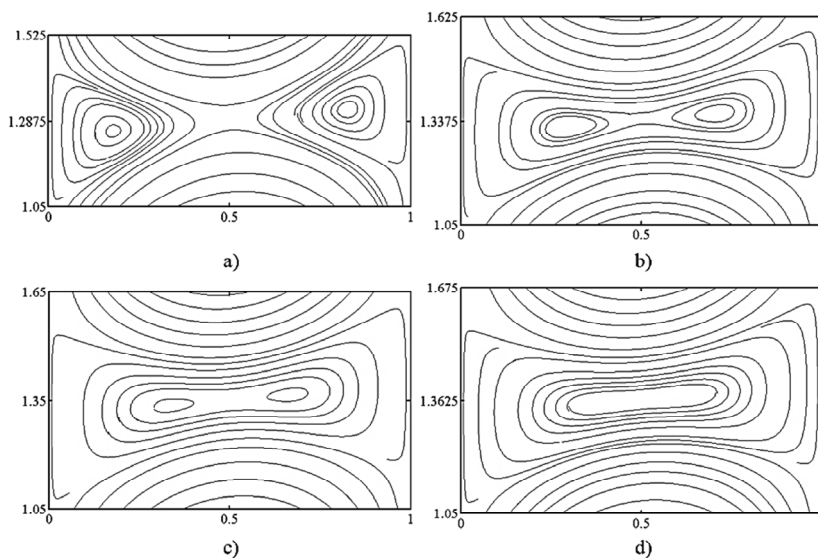


Figure 5. Streamfunction contours for $Re=50$: a) $K=2.575$; b) $K=2.675$; c) $K=2.7$; d) $K=2.72$.

CONCLUSION

In this paper, two-sided lid-driven flow inside deep cavities was simulated using lattice Boltzmann method. Flow was induced by the antiparallel movement of two facing lids. The code was successfully validated on a square lid-driven cavity benchmark problem. After the code validation, steady-state symmetric patterns were obtained for two-sided deep cavity flow with antiparallel motion for all investigated Reynolds numbers and aspect ratios. Odd number of vortices is present also, with the appearance of two-vortex flow in some cases. The middle region of the deep cavity is mostly affected by the increase in the aspect ratio. Critical aspect ratios, at which primary vortices arise from two secondary ones, were determined to be between $2.7 \leq K_c \leq 2.725$ for Reynolds number 50.

Acknowledgement

This research was financially supported by the Ministry of Education, Science and Technological Development of the Republic of Serbia (Project No. 172025).

REFERENCES

1. Succi, S.: *The Lattice Boltzman Equation for Fluid Dynamics and Beyond*, Oxford University Press: Oxford, 2001; p 368.
2. Yu, D.; Mei, R.; Luo, L.-S.; Shyy, W. Viscous flow computations with the method of lattice Boltzmann equation. *Prog. Aerosp. Sci.* **2003**, *39*, 329-367.
3. Luo, L.-S. In *The lattice-gas and lattice Boltzmann methods: Past, present, and future*, Proc Int Conf Appl Comput Fluid Dyn, Beijing, 2000; Wu, J.; Zhu, Z., Eds. Beijing, 2000; pp 52-83.
4. Sukop, M.C.; Thorne, D.T.J.: *Lattice Boltzmann Modeling: An Introduction for Geoscientists and Engineers*, Springer: Berlin, 2007; p 172.
5. He, X.; Chen, S.; Doolen, G.D. A Novel Thermal Model for the Lattice Boltzmann Method in Incompressible Limit. *J. Comput. Phys.* **1998**, *146* (1), 282-300.
6. Shi, Y.; Zhao, T.S.; Guo, Z.L. Thermal lattice Bhatnagar-Gross-Krook model for flows with viscous heat dissipation in the incompressible limit. *Phys. Rev. E* **2004**, *70*,
7. Marković, J.Đ.; Lukić, N.L.; Jokić, A.I.; Ikonić, B.B.; Ilić, J.D.; Nikolovski, B.G. 2D simulation and analysis of fluid flow between two sinusoidal parallel plates using lattice Boltzmann method. *Chem. Ind. Chem. Eng. Q.* **2013**, *19* (3), 369-375.
8. Shan, X.; Chen, H. Lattice Boltzmann model for simulating flows with multiple phases and components. *Phys. Rev. E* **1993**, *47*, 1815-1819.
9. Guo, Z.; Zhao, T.S. Discrete velocity and lattice Boltzmann models for binary mixtures of nonideal fluids. *Phys. Rev. E* **2003**, *68*, 035302, 1-4.
10. You-Sheng, X.; Yang, L.; Guo-Xiang, H. Using Digital Imaging to Characterize Threshold Dynamic Parameters in Porous Media Based on Lattice Boltzmann Method. *Chin. Phys. Lett.* **2004**, *21* (12), 2454-2457.
11. Guo, Z.; Zhao, T.S. Lattice Boltzmann model for incompressible flows through porous media. *Phys. Rev. E.* **2002**, *66*, 036034, 1-9.
12. Erturk, E. Discussions on driven cavity flow. *Int. J. Numer. Meth. Fluids* **2009**, *60*, 275-294.
13. Shankar, P.N.; Deshpande, M.D. Fluid Mechanics in the Driven Cavity. *Annu. Rev. Fluid Mech.* **2000**, *32* (1), 93-136.
14. Ghia, U.; Ghia, K.N.; Shin, C.T. High-Re solutions for incompressible flow using the Navier-Stokes equations and a multigrid method. *J. Comput. Phys.* **1982**, *48* (3), 387-411.
15. Luo, W.-J.; Yang, R.-J. Multiple fluid flow and heat transfer solutions in a two-sided lid-driven cavity. *Int. J. Heat Mass Tran.* **2007**, *50*, 2394-2405.
16. Erturk, E.; Corke, T.C.; Gökçöl, C. Numerical solutions of 2-D steady incompressible driven cavity flow at high Reynolds numbers. *Int. J. Numer. Meth. Fluids* **2005**, *48* (7), 747-774.
17. Gaskell, P.H.; Savage, M.D.; Summers, J.L.; Thompson, H.M. Stokes flow in closed, rectangular domains. *Appl. Math. Model.* **1998**, *22* (9), 727-743.
18. Wahba, E.M. Multiplicity of states for two-sided and four-sided lid driven cavity flows. *Comput. Fluids.* **2009**, *38*, 247-253.

19. Ding, L.; Shi, W.; Luo, H.; Zheng, H. Investigation of incompressible flow within 1/2 circular cavity using lattice Boltzmann method. *Int. J. Numer. Meth. Fluids* **2009**, *60*, 919-936.
20. Hou, S.; Zou, Q.; Chen, S.; Doolen, G.D.; Cogley, A.C. Simulation of Cavity Flow by the Lattice Boltzmann Method. *J. Comput. Phys.* **1995**, *118*, 329.
21. Lü, X.-Y.; Zhang, C.-Y.; Liu, M.-R.; Kong, L.-J.; Li, H.-B. Thermal lattice Boltzmann simulation of viscous flow in a square cavity. *Int. J. Mod. Phys. C* **2005**, *16* (6), 867-877.
22. Miller, W. Flow in the driven cavity calculated by the lattice Boltzmann method. *Phys. Rev. E* **1995**, *51*, 3659-3669.
23. Patil, D.V.; Lakshmisha, K.N.; Rogg, B. Lattice Boltzmann simulation of lid-driven flow in deep cavities. *Comput. Fluids* **2006**, *35*, 1116-1125.
24. Zhen-Hua, C.; Bao-Chang, S.; Lin, Z. Simulating high Reynolds number flow in two-dimensional lid-driven cavity by multi-relaxation-time lattice Boltzmann method. *Chin. Phys.* **2006**, *15* (8), 1855-1863.
25. Che Sidik, N.A.; Osman, K.; Khudzairi, A.Z.; Ngali, Z. Numerical investigation of lid-driven cavity flow based on two different methods: lattice Boltzmann and splitting method. *Jurnal Mekanikal* **2008**, *25*, 1-8.
26. Chen, S. A large-eddy-based lattice Boltzmann model for turbulent flow simulation. *Appl. Math. Comput.* **2009**, *215*, 591-598.
27. Tekić, P.M.; Rađenović, J.B.; Lukić, N.L.; Popović, S.S. Lattice Boltzmann simulation of two-sided lid-driven flow in a staggered cavity. *Int. J. Comp. Fluid Dyn.* **2010**, *24* (9), 383-390.
28. Cheng, M.; Hung, K.C. Vortex structure of steady flow in a rectangular cavity. *Comput. Fluids* **2006**, *35*, 1046-1062.
29. Kuhlmann, H.C.; Wanschura, M.; Rath, H.J. Elliptic instability in two-sided lid-driven cavity flow. *Eur. J. Mech. B-Fluid.* **1998**, *17* (4), 561-569.
30. Kuhlmann, H.C.; Wanschura, M.; Rath, H.J. Flow in two-sided lid-driven cavities: non-uniqueness, instabilities, and cellular structures. *J. Fluid Mech.* **1997**, *336* (267-299), 267-299.
31. Albensoeder, S.; Kuhlmann, H.C.; Rath, H.J. Multiplicity of Steady Two-Dimensional Flows in Two-Sided Lid-Driven Cavities. *Theoret. Comput. Fluid Dynamics* **2001**, *14*, 223-241.
32. Perumal, D.A.; Dass, A.K., Simulation of flow in two-sided lid-driven square cavities by the lattice Boltzmann method. In *Advances in Fluid Mechanics VII*, Rahman, M.; Brebbia, C. A., Eds. WIT Press: 2008; Vol. 59, pp 45-54.
33. Mohamad, A.A.: *Applied Lattice Boltzmann Method for Transport Phenomena, Momentum, Heat and Mass Transfer*, Sure Print: Dalbrent, Canada, 2007.
34. Latt, J.; Chopard, B.; Malaspinas, O.; Deville, M.; Michler, A. Straight velocity boundaries in the lattice Boltzmann method. *Phys. Rev. E* **2008**, *77* (5), 056703.
35. Skordos, P.A. Initial and boundary conditions for the lattice Boltzmann method. *Phys. Rev. E* **1993**, *48*, 4823-4842.

36. Chen, S.; Tölke, J.; Krafczyk, M. A new method for the numerical solution of vorticity–streamfunction formulations. *Comput. Method. Appl. M.* **2008**, *198* (3-4), 367-376.
37. Gürçan, F.; Wilson, M.C.T.; Savage, M.D. Eddy genesis and transformation of Stokes flow in a double-lid-driven cavity. Part 2: deep cavities. *Proceedings of the Institution of Mechanical Engineers, Part C: Journal of Mechanical Engineering Science* **2006**, *220* (12), 1765-1774.
38. Gürçan, F.; Gaskell, P.H.; Savage, M.D.; Wilson, M.C.T. Eddy genesis and transformation of Stokes flow in a double-lid driven cavity. *Proceedings of the Institution of Mechanical Engineers, Part C: Journal of Mechanical Engineering Science* **2003**, *217* (3), 353-364.

СИМУЛАЦИЈА ТОКА ФЛУИДА У ДУБОКИМ ШУПЉИНАМА СА ДВА ПОКРЕТНА ЗИДА ПРИМЕНОМ LATTICE BOLTZMANN МЕТОДЕ

Наташа Љ. Лукић¹, Предраг М. Текић², Јелена Б. Рађеновић², Ивана М. Шијачки¹

¹ Универзитет у Новом Саду, Технолошки факултет, Булевар цара Лазара 1, 21000 Нови Сад, Србија

² Универзитет у Новом Саду, Природно-математички факултет, Трг Доситеја Обрадовића 3, 21000 Нови Сад, Србија

У овом раду је симулирано кретање нестишљивог флуида у дубоким правоугаоним шупљинама коришћењем lattice Boltzmann-ове методе. Кретање флуида омогућују два наспрамна покретна зида. Ради тестирања саме методе, прво је извршена симулација познатог тест проблема, квадратне шупљине са једним покретним зидом. Након провере имплементације и тачности алгоритма на струјање флуида у квадратној шупљини, симулиран је модел тока флуида у дубоким шупљинама са два покретна зида, за супротнострујно кретање истих. Испитан је утицај сразмере шупљине (однос висине и ширине) и Рејнолдсовог броја на ток флуида и карактеристике вртлога формираних унутар правоугаоне шупљине. Сразмера шупљине је варирана између 1,5 и 4 док су вредности Рејнолдсовог броја: 100; 400; 1000 и 3200. Симетричност флуидног тока је утврђена у свим испитиваним условима као и непаран број вртлога (уколико се дво-вртложни ток посматра као један вртлог). Са порастом Рејнолдсовог броја секундарни вртлози добијају на снази. С друге стране, повећање сразмере шупљине највише утиче на ток флуида у централном делу. Утврђено је да критична вредност односа висине и ширине шупљине, при којој се јавља примарни вртлог у средишту шупљине, износи између 2,7 и 2,725 за Рејнолдс 50.

Кључне речи: lattice Boltzmann метода, два покретна зида, дубока шупљина, сразмера, супротнострујни

Received: 3 July 2015.

Accepted: 19 September 2015.

CORRELATION AND PRINCIPAL COMPONENT ANALYSIS IN CERAMIC TILES CHARACTERIZATION

Sanja O. Podunavac-Kuzmanović, Jonjaua G. Ranogajec and Strahinja Z. Kovačević*

University of Novi Sad, Faculty of Technology, Bulevar cara Lazara 1, 21000 Novi Sad, Serbia

The present study deals with the analysis of the characteristics of ceramic wall and floor tiles on the basis of their quality parameters: breaking force, flexural strength, absorption and shrinking. Principal component analysis was applied in order to detect potential similarities and dissimilarities among the analyzed tile samples, as well as the firing regimes. Correlation analysis was applied in order to find correlations among the studied quality parameters of the tiles. The obtained results indicate particular differences between the samples on the basis of the firing regimes. However, the correlation analysis points out that there is no statistically significant correlation among the quality parameters of the studied samples of the wall and floor ceramic tiles.

KEY WORDS: Principal component analysis, correlation analysis, floor tiles, wall tiles, chemometrics.

INTRODUCTION

Ceramic tiles are widely used decorative building material in modern buildings, and the same holds also for the ancient ones. They have technical and esthetical functions (1,2). Whether indoor or outdoor, they are used as wall and floor tiles with different microstructure, porosity, thermal and mechanical properties (3-5). The raw material composition of ceramic tiles is a mixture of clay minerals (kaoline, illite and montmorillonite), feldspar, quartz, and carbonates. The mineral nature of the mixture determines the quality and the function of the tiles. The production of tiles is a complex process since it contains many different technological segments. In the beginning of the tile production, the raw material preparation, which includes excavation, classification and grinding of raw material components, presents the dominant segment of the tile production. The wet grinding process gives the best distribution of raw material components and moisture in the prepared green body, as well as the best particle size distribution. After the raw material preparation, further processes as shaping, drying, firing and glazing have to be done in order to obtain the final products of desirable characteristics.

* Corresponding author: Dr Strahinja Kovačević, University of Novi Sad, Faculty of Technology, Bulevar cara Lazara 1, 21000 Novi Sad, Serbia; email: strahko@tf.uns.ac.rs

There are very complicate relationships among the characteristics of material sampled from different production stages and the characteristics of the final products. Evidently, many parameters have to be taken into consideration for understanding the existing functions. One of useful approaches in this field could be chemometric studies.

Despite the prefix *chemo-*, which refers to chemistry, chemometric studies have found their application, not only in analytical chemistry (6), but also in food engineering (7), pharmaceutical engineering (8), biotechnology (9), microbiology (10) and forensics (11). Chemometrics enables simultaneous evaluation of an almost unlimited number of data, facilitating the clarification of theoretical and practical problems, including mathematical or statistical methods such as regression analysis (linear and multiple linear regression, principal component regression, partial least squares regression, artificial neural networks regression, etc.) and pattern recognition methods (cluster analysis, principal component analysis, partial least squares discriminant analysis, etc.). Chemometrics has become an important tool in engineering data analysis since it can reveal some features of the analyzed system which are not obvious.

The aim of this study was to examine the correlations between the tile characteristics: percentage of shrinking, water absorption, breaking force, and flexural strength, obtained at the different firing temperatures, and to find possible similarities and dissimilarities among the tiles by applying principal component analysis.

EXPERIMENTAL

Materials

There were 14 floor tiles (dimensions 450 x 450 x 8 mm) and 14 wall tiles (dimensions 250 x 400 x 8.5 mm) sampled from the technological lines of the ceramic tile company „Zorka-Keramika“, Šabac; seven samples of each group (wall/floor tiles) were fired at a defined temperature, Table 1. The analyzed characteristics of the 28 samples were: percentage of shrinking, water absorption, breaking force, and flexural strength.

Table 1. Parameters of the used firing regimes

Floor tiles	
Firing regime	Temperature/cycle (°C / min)
Regime 1	1180/37
Regime 2	1185/37
Wall tiles	
Firing regime	Temperature/cycle (°C / min)
Regime 1	1105/40
Regime 2	1110/40

The shrinking and water absorption values were determined according to the SRPS ISO 10545-3 standard (12), while the breaking force and flexural strength values were established following the standard SRPS ISO 10545- 4 (13) with ZMGi, VEB Thüringer, Rauenstein device.

Mathematical approach

The statistical analysis was carried out by the NCSS and the Statistica 10.0 software. The principal component analysis (PCA) is one of chemometric methods which transforms the initial data set into a set of values of linearly uncorrelated variables. The result is given in a set of vector samples called principal components (PCs) presented in a score form and in loadings plots. The regression analysis, in general, is a statistical process commonly used for establishing relationships among the existing variables. In the present study, the linear regression analysis was used in order to find the existing correlations among the studied parameters, the characteristics of the tiles, and to derive possible mathematical models. Prior to the PCA analysis, the data were standardized by min-max normalization method.

A major part of every formed mathematical model is its validation. Cross-validation principle is mainly used when the accuracy of the predicting mathematical models is investigated. One of these methods, called leave-one-out (LOO) cross-validation, was applied in this investigation.

RESULTS AND DISCUSSION

The PCA was used in order to determine a connection between the used firing regimes and the characteristics of the produced tile samples. The data used in the PCA analysis are given in Table 2 and Table 3.

Table 2. Values of characteristic parameters for the analyzed floor tiles

Firing regime	Tile sample number	Shrinking (%)	Absorption (%)	Breaking force (N)	Flexural strength (N/mm ²)
Regime 1	1	8.00	0.21	2378	60.932
	2	8.08	0.23	2602	63.253
	3	8.03	0.34	2777	71.22
	4	8.30	0.36	2363	56.003
	5	8.50	0.36	2436	56.269
	6	8.40	0.50	2511	61.108
	7	8.30	0.33	2550	60.504
Regime 2	8	8.10	0.20	2877	69.812
	9	8.15	0.18	2767	65.492
	10	8.00	0.21	3439	81.396
	11	8.00	0.26	2655	62.841
	12	8.26	0.26	2887	71.859
	13	8.22	0.27	2690	63.768
	14	8.25	0.21	2629	60.754

Table 3. Values of characteristic parameters for the analyzed wall tiles

Firing regime	Tile sample number	Shrinking (%)	Absorption (%)	Breaking force (N)	Flexural strength (N/mm ²)
Regime 1	1	0.59	17.37	653	24.48
	2	0.59	16.57	656	24.59
	3	0.65	16.19	674	25.27
	4	0.65	15.95	657	25.27
	5	0.65	16.07	686	26.39
	6	0.65	16.52	647	27.25
	7	0.72	16.79	667	29.64
Regime2	1	0.55	15.20	765	27.97
	2	0.54	15.44	742	27.13
	3	0.55	15.88	769	28.11
	4	0.63	16.25	733	27.43
	5	0.64	16.34	678	25.41
	6	0.63	16.44	688	25.80
	7	0.63	15.84	699	26.91

The results of the PCA analysis are given in Figure 1. Figure 1b shows that the samples can not be classified only based on the studied parameters. The obtained loading plot (Figure 1a), shows that all the studied parameters strongly influence the distribution of the samples along the PC1 axis.

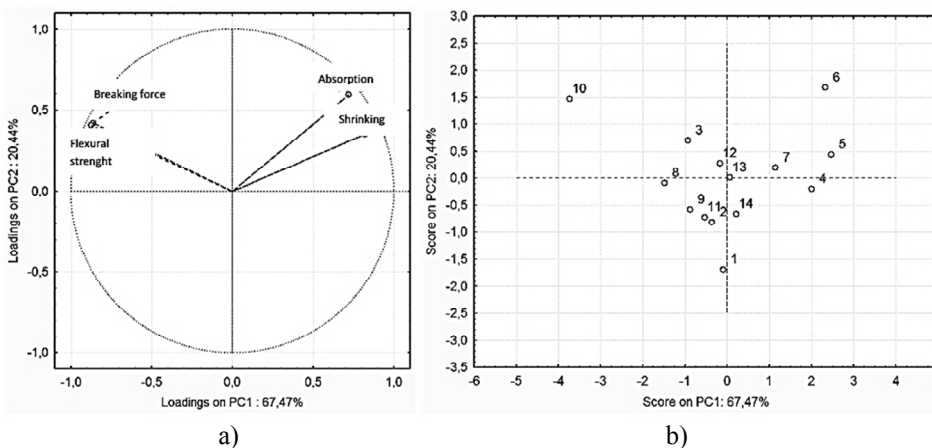


Figure 1. Loadings (a) and score (b) plot for the floor tiles

Loadings plot in Figure 2a indicates that some particular separation of the samples could be observed along the PC1 axis. In this case, the samples can be classified mostly based on the studied parameters (breaking force and absorption value) and that can be

seen on the score plot in Figure 2b. The tile samples from the number 1 to 7, which were treated by the firing regime 1, have mostly positive values for the PC1, but the tile samples from the number 8 to 14, which were treated by the firing regime 2, have negative values for the PC2. This score plot also shows that there is a significant difference in the absorption and breaking force among the wall tile samples treated by two different firing regimes.

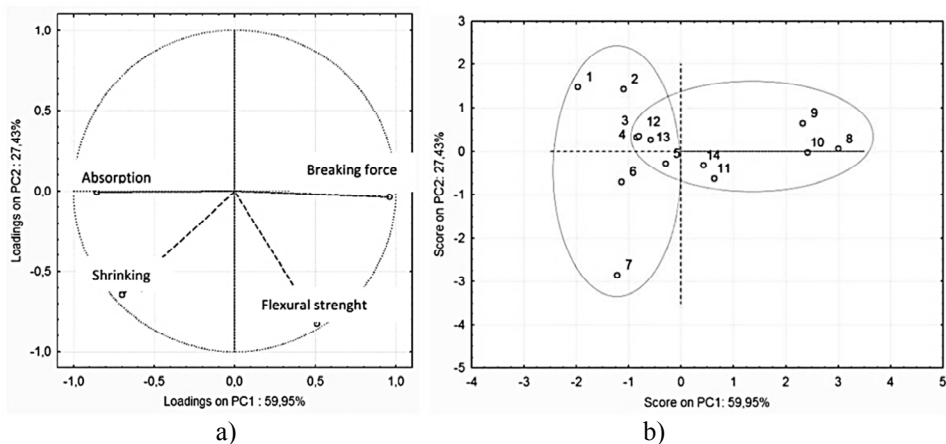


Figure 2. Loadings (a) and score (b) plot for the wall tiles

Correlations between all the studied parameters were considered. The statistical characteristics of the correlations among the studied parameters of the tiles quality are given in Table 4. The obtained results indicate weak linear relationships among the studied parameters of the wall and floor tiles, the fact being also confirmed by cross-validation (Table 5).

The correlation coefficient values closer to 1 represent better fit of the regression, while high values of the *F*-test indicate the significance of the model. Root mean square error (*RMSE*) is the variation of the residuals or the variation about the regression line. It should have a low value for the regression to be significant. The lower predicted residuals sum of the squares (*PRESS*) value, the better the predictability of the model. If the *PRESS* value is less than the total sum of squares (*TSS*) value, the model predicts better and can be considered significant. High values of r^2_{cv} and r^2_{adj} (r^2_{cv} , $r^2_{adj} > 0.6$) indicate high predictivity of the equations. If r^2 , r^2_{cv} are negative, this fact indicates a very poor mathematical model.

In this study, the correlations among the studied parameters have very poor statistical characteristics, certainly they cannot be applied for a precise prediction of the dependent variable. The polynomial regression did not result in any acceptable model as well.

Table 4. Basic statistical parameters of the linear relationships among the studied parameters

Model	Tiles type	Firing regime	Y	X	a	b	RMSE	F	r ²
1	Floor tiles	1	absorption	shrinking	0.3510	-2.556	0.0753	4.725	0.4859
2		1	flexural strength	shrinking	-17.66	206.7	4.137	4.138	0.4528
3		1	flexural strength	absorption	-7.162	63.71	5.544	0.0889	0.0175
4		2	absorption	shrinking	0.0520	-0.203	0.0388	0.0000	0.0000
5		2	flexural strength	shrinking	-26.06	280.1	7.086	0.9960	0.1661
6		2	flexural strength	absorption	-34.53	75.83	7.644	0.1540	0.0299
7	Wall tiles	1	absorption	shrinking	-3.098	18.48	0.5152	0.3850	0.0715
8		1	flexural strength	shrinking	37.19	2.218	0.8917	20.454	0.8036
9		1	flexural strength	absorption	0.0860	24.7	2.012	0.0001	0.0000
10		2	absorption	shrinking	8.337	10.94	0.2910	10.497	0.6774
11		2	flexural strength	shrinking	-15.79	36.37	0.7922	5.110	0.5054
12		2	flexural strength	absorption	-1.48	50.52	0.8334	4.135	0.4526

Table 5. Cross-validation parameters of the obtained linear models

Model	r ² _{cv}	r ² _{adj}	PRESS	TSS	S _{PRESS}
1	-0.1216	0.3830	0.0618	0.0551	0.090
2	-0.1394	0.3434	178.2	156.4	5.05
3	-0.4176	0.0000	221.7	156.4	5.63
4	-0.8534	0.0000	0.0140	0.0075	0.040
5	-1.195	0.0000	661.1	301.1	9.72
6	-0.6378	0.0000	493.2	301.1	8.39
7	-2.170	0.0000	4.531	1.430	0.800
8	0.5751	0.7643	8.599	20.24	1.11
9	-1.459	0.0000	49.77	20.24	2.67
10	0.3860	0.6128	0.8056	1.312	0.340
11	0.0300	0.4065	6.153	6.344	0.940
12	0.0677	0.3432	5.914	6.344	0.920

CONCLUSIONS

The obtained results describe the similarities and dissimilarities between the analyzed samples of the wall and floor tiles on the basis of their quality characteristics: absorption, flexural strength, shrinking and breaking force. Principal component analysis revealed the separation of the tiles depending on the applied firing regimes. There is no high-quality mathematical model, confirmed by basic and cross-validation statistical parameters, which successfully correlates quality characteristics of the analyzed tile samples.

Acknowledgement

These results are the part of the projects No. 172012 and III 45008 supported by the Ministry of Education, Science and Technological Development of the Republic of Serbia.

REFERENCES

1. Fanger, P.O. *Thermal Comfort*. New York: McGraw-Hill Book Company, 1970.
2. Rhee, S.K. Porosity. Thermal Conductivity Correlations for Ceramic Materials. *Materials Science and Engineering*. **1975**, *20*, 89-83.
3. Effting, C.; Folgueras, M.V.; Guths, S.; Alarcon, O.E. Microstructural characterization of ceramic floor tiles with the incorporation of wastes from ceramic tile industries. *Mater. Res.* **2010**, *13*, 319-323.
4. Suvaci, E.; Tamsu, N. The role of viscosity on microstructure development and stain resistance in porcelain stoneware tiles. *Journal of the European Ceramic Society* **2010**, *30*, 3071–3077
5. Catarino, L.; Sousa, J.; Martins, I.M.; Vieira, M.T.; Oliveria, M.M. Ceramic products obtained from rock wastes. *Journal of materials processing technology* **2003**, *143-144*, 843-845.
6. Jokić, S.; Podunavac Kuzmanović, S.; Jevrić, L.; Sudar, R.; Vidović, S.; Aladić, K.; Kovačević, S. HPLC Retention behaviour of Triacylglycerols Extracted from Soybean Oil by Supercritical CO₂. *Croat. Chem. Acta* **2014**, *87* (3), 261-269.
7. Malbaša, R.; Jevrić, L.; Lončar, E.; Vitas, J.; Podunavac-Kuzmanović, S.; Milanović, S.; Kovačević, S. Chemometric Approach to Texture profile Analysis of Kombucha Fermented Milk products. *J. Food Sci. Technol.* **2014**, in press DOI: 10.1007/s13197-014-1648-4
8. Kovačević, S. Z.; Podunavac-Kuzmanović, S. O.; Jevrić, L. R.; Djurendić, E. A.; Ajduković, J. J. Non-linear assessment of anticancer activity of 17-picolyl and 17-picolinylidene androstane derivatives – Chemometric guidelines for further syntheses. *Eur. J. Pharm. Sci.* **2014**, *62*, 258-266.
9. Dodić, J.; Grahovac, J.; Kalajdžija, N.; Kovačević, S.; Jevrić, L.; Podunavac Kuzmanović, S. Chemometric Approach to Prediction of Antibacterial Agent Production by *Streptomyces hygroscopicus*. *Appl. Biochem. Biotechnol.* **2014**, *174*, 534-541.
10. Kovačević, S. Z.; Podunavac Kuzmanović, S. O.; Jevrić, L. R. Multivariate Regression Modelling of Antifungal Activity of Some Benzoxazole and Oxazolo[4,5-*b*]pyridine Derivatives. *Acta Chim. Slov.* **2013**, *60*, 756-762.
11. Gadzuric, S. B.; Podunavac Kuzmanovic, S. O.; Jokic, A. I.; Vranes, M. B.; Ajdukovic, N.; Kovacevic, S. Z. Chemometric estimation of post-mortem interval based on Na⁺ and K⁺ concentrations from human vitreous humour by linear least squares and artificial neural networks modelling. *Aust. J. Forensic Sci.* **2014**, *46* (2), 166-179.
12. SRPS ISO 10545-3, Ceramic tiles - Part 3: Determination of water absorption, apparent porosity, apparent relative density and bulk density.
13. SRPS ISO 10545- 4, Ceramic tiles - Part 4: Determination of modulus of rupture and breaking strength.

КОРЕЛАЦИОНА АНАЛИЗА И АНАЛИЗА ГЛАВНИХ КОМПОНЕНАТА У КАРАКТЕРИЗАЦИЈИ КЕРАМИЧКИХ ПЛОЧИЦА

*Сања О. Подунавац-Кузмановић, Јоњауа Г. Раногајец, Страхинца З. Ковачевић**

Универзитет у Новом Саду, Технолошки факултет, Булевар цара Лазара 1, 21000 Нови Сад

У раду је описана анализа карактеристика подних и зидних плочица на основу параметера њиховог квалитета: силе лома, савојне чврстоће, упијања и скупљања. Анализа главних компонената је примењена са циљем утврђивања потенцијалних сличности и разлика између анализираних узорака на основу поменутих карактеристика, као и режима печења. Такође, примењена је и корелациона анализа како би се утврдиле корелације између испитиваних параметара квалитета плочица. Резултати указују на одређене разлике између плочица на основу режима печења. Међутим, корелациона анализа указује на непостојање значајних корелација између испитиваних карактеристика квалитета керамичких зидних као и подних плочица.

Кључне речи: анализа главних компонената, корелациона анализа, подне керамичке плочице, зидне керамичке плочице, хемометрија.

Received: 14 September 2015.

Accepted: 20 October 2015.

SEQUENTIAL MICRO AND ULTRAFILTRATION OF DISTILLERY WASTEWATER

*Vesna M. Vasić**, Marina B. Šćiban, Dragana V. Kukić, Jelena M. Prodanović
and Nikola R. Maravić

University of Novi Sad, Faculty of Technology, Bulevar cara Lazara 1, 21000 Novi Sad, Serbia

Water reuse and recycling, wastewater treatment, drinking water production and environmental protection are the key challenges for the future of our planet. Membrane separation technologies for the removal of all suspended solids and a fraction of dissolved solids from wastewaters, are becoming more and more promising. Also, these processes are playing a major role in wastewater purification systems because of their high potential for recovery of water from many industrial wastewaters. The aim of this work was to evaluate the application of micro and ultrafiltration for distillery wastewater purification in order to produce water suitable for reuse in the bioethanol industry. The results of the analyses of the permeate obtained after micro and ultrafiltration showed that the content of pollutants in distillery wastewater was significantly reduced. The removal efficiency for chemical oxygen demand, dry matter and total nitrogen was 90%, 99.2% and 99.9%, respectively. Suspended solids were completely removed from the stillage.

KEY WORDS: distillery wastewater, microfiltration, ultrafiltration, water reuse

INTRODUCTION

Water is one of the most important resources, but also one of the most sensitive. Compared to other industrial sectors, the food industry uses a much greater amount of water for product unit [1]. The largest quantity of these waters appears as a wastewater. Water and wastewater costs are becoming an increasingly important economic factor for small and medium-sized enterprises. This applies particularly to the food and beverage industries [2].

Based on the data of Water management basis of the Republic of Serbia (RS) [3], total production of wastewaters in the Autonomous Province (AP) of Vojvodina is 766,041.00 m³/day of which about 60% are industry wastewaters. Even 72.7% of organic pollution originates from industry wastewaters. Emission from the food industry is 84.04% of total industrial pollution in AP Vojvodina. Of total organic load from all point sources, municipal and industrial, food industry participates with 60%. Such production of wastewaters is a major problem both from the economic and environmental protection point of view.

* Corresponding author: Vesna M. Vasić, University of Novi Sad, Faculty of Technology, Bulevar Cara Lazara 1, 21000 Novi Sad, Serbia, e-mail: vesnavasic@tf.uns.ac.rs

Of the total amount of wastewaters (municipal and industrial wastewaters) in AP Vojvodina, only 10% is purified, while more than 65% of industrial plants do not treat their wastewaters [4]. The highest percentage of industrial polluters (54.76%) discharge their wastewaters into the river (with or without previous treatment), then into the city sewer (19.04%), the channel (18.45%), the creek 3.57%, etc. [3]. Therefore, reducing the wastewater quantity and the possibility of its reuse are one of the greatest challenges facing industry today.

The aim of this work was to evaluate the application of micro and ultrafiltration for distillery wastewater purification in order to produce water suitable for the reuse in the bioethanol industry.

EXPERIMENTAL

Material

The experiments were performed using distillery wastewater from the ethanol factory Reachem, Srbobran Serbia, where it was obtained from starch feedstock.

Microfiltration experiment

The experiment was carried out in a cross-flow microfiltration unit shown in Figure 1. The feed (1) was circulated by a centrifugal pump (WPEm 3400r) (2) under the condition of complete recirculation of the fluid. The experiment was performed under the transmembrane pressure (TMP) of 2 bar. The permeate (6) was constantly drained away from the system, collected and analyzed. The TMP and feed flow rate were adjusted by the regulation valves and measured by the pressure gauges (3a, 3b) and the flow-meter (5). The experiment was performed under the TMP of 2 bar and feed flow rate of 300 L/h. The multichannel ceramic membrane used (NOVASEP, France) had the nominal pore size of 200 nm with the length of 400 mm. The useful membrane surface was 0.0501 m². All experiments were carried out at room temperature (25°C). The system and membrane were cleaned according to the following procedure:

- short rinsing with water, without recirculation, in order to remove residual stillage from the system
- 15 minutes rinsing with water (with recirculation)
- 30 minutes washing with 5% solution of Ultrasil (with recirculation)
- 15 minutes rinsing with distilled water (with recirculation)
- short rinsing with distilled water (without recirculation)
- the membrane was further cleaned by immersing in 10% solution of HCl, during 24 h

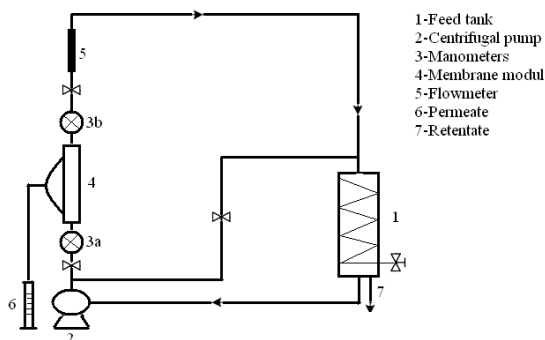


Figure 1. Schematic of the apparatus for microfiltration

Ultrafiltration experiment

Ultrafiltration experiment was carried out using a Milipore Stirred Ultrafiltration Cell Model 8200 with maximum vessel volume of 0.2 L (Figure 2). The ultrafiltration conditions were as follows: pressure of the inert gas 4 bar, stirring agility 100 rpm, and the volume of wastewater that was filtered 150 ml. The wastewater was filtered through a polyethersulfone membrane with the molecular weight cut-off (MWCO) of 10,000 Da; the permeate was drained away from the system, collected and analyzed. The filtration was stopped when the flow rate decreased significantly. The experiments were carried out at room temperature (25°C).



Figure 2. Laboratory apparatus for „dead-end“ ultrafiltration

Analytical methods

Feed and permeate samples were analyzed for dry matter, ash, organic dry matter, suspended solids and chemical oxygen demand (COD) according to the Standard Methods [5]. Total nitrogen was determined by the Kjeldahl method [6].

RESULTS AND DISCUSSION

The wastewater was analyzed just after bringing it from the factory, and the results are presented in Table 1.

Table 1. Results of the analysis of the distillery wastewater, MF and UF permeates

Parameter	Wastewater	MF permeate	UF permeate
pH	5.07	5.07	5.07
Dry Matter (DM) [mg/L]	73477	16250	5800
Ash [mg/L]	7950	2660	1790
Organic DM [mg/L]	65527	13590	4010
% of Organic DM [%DM]	89	83	69
Suspended Solids (SS) [mg/L]	51480	-	-
Ash of SS [mg/L]	4710	-	-
Organic Dry Matter of Suspended Solids [mg/L]	46770	-	-
% of Organic DM of SS[%]	90	-	-
% of Suspended Solids in Dry Matter[%]	70	-	-
Total Nitrogen [mg/L]	4193	826	280
COD [mgO ₂ /L]	90000	17654	9073
Turbidity [NTU]		39	0.75

As can be seen from Table 1, the analyzed wastewater has high values of COD, dry matter and total nitrogen. About 70% of dry matter is in the form of suspended solids, of which 90% is organic matter. Considering the presented results, it can be seen that distillery wastewater is highly polluted and it should not be disposed in the environment without previous treatment. Further, distillery wastewater was passed through the microfiltration membrane, permeate was collected analyzed, and subsequently nanofiltered using dead-end ultrafiltration membrane with MWCO 10000 Da.

Based on the presented results it can be said that the values of COD, dry matter and total nitrogen decreased after the microfiltration compared to the initial values of wastewater. The removal efficiency was 80.4%, 78% and 80.4%, respectively. The suspended solids were completely removed from the wastewater. The permeate with reduced content of organic matter and free from suspended solids could be recirculated in the mashing processes. This would reduce the amount of water needed for the bioethanol production process.

The permeate obtained after microfiltration still contains a large amount of organic matter, so ultrafiltration was conducted in order to improve the quality of the permeate.

Based on the results presented for UF permeate (Table 1) it can be seen that after the sequential micro and ultrafiltration the content of pollutants in distillery wastewater was significantly reduced. The removal efficiency for COD, dry matter and total nitrogen was 90%, 99.2% and 99.9%, respectively. Also, the turbidity was significantly lower in the UF permeate compared with that obtained after microfiltration. The permeate obtained in this way could be used as a dilution water in the fermentation step. However, additional

analyses are needed in order to determine the presence of inhibitory compounds which can affect the ethanol yield. Usually, these are organic acids, glycerol and acetaldehyde, arising as by-products in the bioethanol production process [7].

Modern tendencies are increasingly focused on the reuse of wastewater [1, 2, 8, 9]. Bialas et al. [10] investigated the effect of recirculation of starch stillage on ethanol yield. Their results showed that there is no change in the ethanol yield even when the 75% of water was replaced with stillage. Mohaghehi and Schell [11] also investigated the possibility of reuse of stillage in the ethanol production process. Three fermentations in series were conducted with different initial concentrations of sugar and replacing 10% or 20% of water with stillage. It was determined that, at low concentration of sugar and with 10% of recirculated stillage, the ethanol yield was insignificantly changed. However, with the increase of sugar concentration and quantity of recirculated stillage, the yield was gradually reduced.

Even though all discussions in the previous subsections motivate water reuse, the decision to reuse depends on economic feasibility. Treatment and discharge are often cheaper than reuse, but not always. The goals of water reuse, especially the goal such as zero discharge, are often too costly to achieve in one phase [12]. Therefore, it is very important to evaluate all stages of the wastewater treatment process, especially in the context of additional treatment costs required to achieve higher quality of the water.

Membrane separation technologies play a major role in the advanced wastewater treatment systems because of its potential for recovery of water from many industrial wastewaters [13]. Murthy and Chaudhari [14] evaluated the distillery wastewater purification with the combined use of UF and reverse osmosis (RO) processes. The percentage rejections of TDS, BOD, color, chlorides, sulfates and potassium were 97.9, 97.9, 93.2, 99.8, 99.7 and 94.65%, respectively. Similar results were obtained by Nataraj et al. [15], with the use of hybrid NF and RO processes for the removal of contaminants to obtain a good water recovery rate. The water reclaimed by NF and RO processes could be reused for either municipal or industrial purposes.

The results obtained in this work are a basis for further investigations of the reuse of distillery wastewater in terms of the effect of recirculated water on the fermentation process and ethanol yield, as well as economic of the process.

CONCLUSION

Reducing of wastewater quantity and the possibility of its reuse are one of the greatest challenges facing industry today. The experiments conducted in this study showed that combined micro and ultrafiltration are promising techniques for recovery of water from stillage. Based on the presented results it can be concluded that the described processes were effective in purification of distillery wastewater with removal efficiency for COD, dry matter and total nitrogen of 90%, 99.2% and 99.9%, respectively. The composition of the permeate obtained after micro and ultrafiltration points out to the possibility of its reuse in the bioethanol production process.

Acknowledgement

This research was supported by the grant „Improved treatment procedures for food industry wastewaters purification“ number 114-451-2105/2014-02 from the Provincial Secretariat for Science and Technological Development of the Autonomous Province of Vojvodina.

REFERENCES

1. Mavrov, V. and Bélières, E.: Reduction of water consumption and wastewater quantities in the food industry by water recycling using membrane processes. *Desalination* **2000**, *131*, 75-86.
2. Blöcher, C., Noronha, M., Fünfroeken, L., Dorda, J., Mavrov, V., Janke, H.D. and Chmiel, H.: Recycling of spent process water in the food industry by an integrated process of biological treatment and membrane separation. *Desalination* **2002**, *144*, 143-150.
3. Jovičić M.: Water management basis of the Republic of Serbia (in Serbian), Ministry of Agriculture Forestry and Water Management of the Republic of Serbia and Institute for Water Management “Jaroslav Černi”, Belgrade, 2001 pp. 130-132.
4. CEDEF (Central European Development Forum), Korišćenje i tretman komunalnih i industrijskih otpadnih voda u Republici Srbiji, Republika Srbija Autonomna Pokrajina Vojvodina, Pokrajinski sekretarijat za urbanizam, graditeljstvo i zaštitu životne sredine (2015) p. 10.
5. APHA (American Public Health Association), Standard Methods for the Examination of water and wastewater, 20th ed., APHA, AWWA, WEF, Washington DC, 1998.
6. MEBAK, Brautechnische Analysenmethoden, Bd. I, III Auflage (in German), 1997; pp 171-174.
7. Maiorella, B., Blanch, H.W. and Wilke C.R.: By-product inhibition effects on ethanolic fermentation by *Saccharomyces cerevisiae*. *Biotechnol. and Bioeng.* **1983**, *25*,103-121.
8. Zhang, W., Xiong, R. And Wei G.: Biological flocculation treatment on distillery wastewater and recirculation of wastewater. *J. Hazard. Mater.* **2009**, *172*, 1252-1257.
9. Hafez, A., Khedr, M. and Gadallah H.: Wastewater treatment and water reuse of food processing industries. Part II: Techno-economic study of a membrane separation technique. *Desalination* **2007**, *214*, 261-272.
10. Białas W., Szymanowska D. and Grajek W.: Fuel ethanol production from granular corn starch using *Saccharomyces cerevisiae* in a long term repeated SSF process with full stillage recycling. *Bioresource Technol.* **2010**, *101*, 3126-3131.
11. Mohagheghi A. and Schell D.J.: Impact of Recycling Stillage on Conversion of Dilute Sulfuric Acid Pretreated Corn Stover to Ethanol. *Biotechnol. and Bioeng.* **2010**,*105*, 992-996.
12. Byers, W., Lindgren, G., Noling, C. and Peters, D.: Industrial Water Management, A Systems Approach. 2nd ed., Center for Waste Reduction Technologies, American Institute of Chemical Engineers, New York, 2003.

13. Rai U.K., Muthukrishnan M. and Guha B.K.: Tertiary treatment of distillery wastewater by nanofiltration. *Desalination* **2008**, *23*, 070-78.
14. Murthy Z.V.P. and Chaudhari L.B.: Treatment of distillery spent wash by combined UF and RO processes. *Global Nest J.* **2009**, *11*, 235-240.
15. Nataraj S.K., Hosamani K.M. and Aminabhavi T.M.: Distillery wastewater treatment by the membrane based nanofiltration and reverse osmosis processes. *Water Res.* **2006**, *40*, 2349-2356.

СЕКВЕНЦИЈАЛНА МИКРО И УЛТРАФИЛТРАЦИЈА ОТПАДНЕ ВОДЕ ИЗ ДЕСТИЛЕРИЈЕ

*Весна М. Васић, Марина Б. Шћибан, Драгана В. Кукић, Јелена М. Продановић,
Никола Р. Маравић*

Универзитет у Новом Саду, Технолошки факултет, Булевар цара Лазара 1, 21000 Нови Сад, Србија

Поновна употреба воде, пречишћавање отпадних вода, производња воде за пиће и заштита животне средине најважнији су изазови са којима се наша планета сусреће. Мембранске технологије се последњих година интензивно користе за третман отпадних вода у циљу смањења њиховог загађења као и могућности поновне употребе. Посебно се ово односи на прехранбену индустрију која троши велике количине воде за своје производне процесе, при чему се највећа количина ове воде јавља као отпадна вода. Током истраживања изведених у оквиру овог рада испитана је могућност употребе микро и ултрафилтрације за пречишћавање отпадне воде из дестилерије, у циљу сагледавања састава добијеног пермеата који би се могао поново употребити у индустрији биоетанола. За експерименте је коришћена керамичка мембрана за микрофилтрацију са пречником пора од 200 nm и мембрана за ултрафилтрацију од полиетерсулфона са MWCO (Molecular Weight Cut Off) од 10000 Da. Резултати су показали да је након процеса секвенцијалне микро и ултрафилтрације загађење отпадне воде у значајној мери смањено. Ефикасност уклањања ХПК, суве материје и азота била је 90%, 99,2% and 99,9%, редом. Такође, суспендоване честице су у потпуности уклоњене из отпадне воде. Састав добијеног пермеата указује на могућност његове рецикулације у производни процес, чиме би се значајно смањила запремина ефлуента и потрошња воде потребне за припрему сировина и ферментацију.

Кључне речи: Отпадна вода, микрофилтрација, ултрафилтрација, рецикулација

Received: 7 July 2015.
Accepted: 16 October 2015.

POLICE ASPECTS OF THE FORENSIC METHODS OF THE STUDY OF PERCENTAGE OF WATER CONTENT OF THE DETERMINE THE AGE OF THE FRESCOES

Vojkan M. Zorić^{1,2}, Željko Nikač³ and Radovan Radovanović³

¹ University of Novi Sad, Faculty of Sciences, Trg Dositeja Obradovića 4, 21000 Novi Sad, Serbia,

² Ministry of Interior, CPD-National Criminalistical-Technical Center, Kneza Miloša 103, 11000 Belgrade, Serbia

³ The Academy of Criminalistic and Police Studies, Belgrade-Zemun, Serbia

The novels of the Criminal Procedure Code (CPC) Republic of Serbia have introduced the concept of prosecutorial investigation in relation to that of evidence, special evidentiary actions and other software for the operation of the criminal prosecution. The meaning of novels is to conduct harmonization of standards with solutions of modern criminal law practice, particularly with regard to EU standards Serbia applying for membership in the Union. Preventing the most serious forms of crime is the focus of authorized bodies Serbia and in this context combating and preventing all forms of forgery, as is the case with forgeries frescoes and selling them on the world market. In exposed paper the method determining age of the frescoes is proposed. It is based on the use of closed Markov's graphs with three cells. The measurements of contents of water molecules in surrounding area can be done only for the space in which the frescoes is located. This means that followed exposed method is non destructive.

KEY WORDS: Police, Forensics, Humidity concentration, Markov's graph, frescoes.

INTRODUCTION

After the social changes in Serbia in late 2000 launched a process of social reform, transformation of the police and state authorities, new and harmonization of legislation with the EU. Started the transition of Security sector reform and police, secret service and other subjects in the national security.

In the field of criminal law is modelled on the developed world adopted several new regulations, such as the Penal Code, Criminal Procedure Code, the Law on Confiscation of the Proceeds from Crime, Law on organization and jurisdiction of the authorities in combating organized crime, corruption and other most serious forms of crime.

In the field of criminal procedural law adopted a new Code of Criminal Procedure (1), which has been repeatedly amended and supplemented, and was modelled on the German model finally adopted the amended text that introduces into practice the concept of prose-

* Corresponding autor: Vojkan M.Zorić, University of Novi Sad, Faculty of Sciences, Trg Dositeja Obradovića 4, 21000 Novi Sad, Serbia, e-mail: vzoric@df.uns.ac.rs; Ministry of Interior, CPD-National Criminalistical-Technical Center, Kneza Miloša 103, 11000 Belgrade, Serbia; vojkan.zoric@mup.gov.rs

cutorial investigation. According to this model, the state (public) prosecutor shall conduct the investigation and preliminary investigation procedure (1, Art.43-49) and it's subordinate to the police and all authorities at that stage. The state prosecutor ordered the police implement specific actions in the function of collecting evidence (1, Art.285), and in this respect the police acts and has specific powers (1, Art.286-294) that are characteristic police standard, criminal and other. At present the CPC of evidence (1, Art.85-160) as well as hearing the defendant, the hearing of witnesses, expert analysis, investigation, verification of documents, checking accounts and suspicious transactions, seizure and search of objects (people, things, a). In accordance with the Convention against Transnational Organized Crime (Palermo Convention) (2) in CPC are built special evidentiary actions (2, Art.161-187), such as secret surveillance of communication, secretly monitoring and recording, computer search data, controlled delivery and covert coroner.

For the purpose of this paper is of particular importance is the expertise, evidentiary action (2, Art.113-132). In order to determine forgeries frescoes, other works of art and rare objects of special importance sampling as a method of expertise in a broad sense.

Determining of age of the frescoes is very important problem. This problem becomes very serious since the number of forgeries and forgers increases permanently. Control whether the paint is original or forgery is complicated by the fact that during analysis the paint should not be damaged.

It is the reason why we propose a method which is not destructive (in the sense of damaging of the frescoes). The method consists in determining of humidity contents i.e. in measuring of ppm of molecules water expressed in per cents. This method is applicable in all cases, because the paint and its environment always contain some per cent of molecules water. The paint and environment exchange molecules of water and therefore humidity per cent changes in time.

Since the room is not hermetically isolated of wider environment this fact must be taken into account from the moment of creation. It is obvious that the exchange of water molecules between room and wider environment influences the humidity of the frescoes.

The Marcov's graphs will be used in calculations. The graphs will have three cells and will be closed. The cells correspond to the paint, to the room and to wider environment. The fact that the system is closed means that the sum of concentrations will be constant in time. The choice of closed system in the same time means that the effects of absorption of water molecules by walls, furniture etc. are neglected, although they really exist.

GENERAL REMARKS ABOUT FORGERIES AND FORENSIC EXPERTISE OF FRESCOES

We considered two approaches:

(a) *Falsification* of art, rare items and weapons (old and trophy) is a phenomenon that is now very much in the world and brings enormous profits for all participants in the criminal chain. On the other hand, the customers, the state and the international community are equally damaged by this kind of crime because it distorts economic interests, originality and value of artworks and objects Raritan. An additional problem is the foreign elements of these offenses, which leads to the necessity of cooperation among all countries and international organizations.

Art Mafia is now synonymous with organized criminal groups engaged in both the theft and resale of original paintings and rare objects, as well as forgery and selling these items on the market (3). The organization brings together a wide circle of people – thieves, forgers, perpetrators, transporters and other participants in the criminal chain that connects a common goal - the achievement of extra profits.

The fight against counterfeiters includes measures at national and international level, both normative and operational. Certainly the most important role is played by Interpol as the International Criminal Police Organization, which consisted of specialized line of work that follows forgeries, smuggling and all forms of crime in this and related fields (4). Interpol coordinate joint actions and take other measures and actions as well as invitations to national police (Romania - forger stolen art objects, Lithuania-list of damaged and owners, Poland and Norway - Project Joint investigation teams for legal and smuggled heritage), international meetings (IX International meeting on theft and smuggling of art objects, cultural treasures and antiques-Lion, 11-13-03.2015), cooperation with specialized agencies (UNESCO Venice Office, SEE, EU, private sector), the publication of Protection of the National Convention of the goods (Mali and Bhutan, 18.02.2013), posters (The Most Wanted Works of Art, Dec. 2014), meetings of the expert group (IEG - Interpol Expert Group, 27-28.02.2014. (5)), the publication of stolen goods from war zones (Afghanistan, Iraq), a special international standard (Object ID) containing a description and characteristics of object recognition, the International Red List of ICOM (International Council of Museums, Red Lists) archaeological objects, vulnerable regions and localities from which they steal, smuggle and resale cultural objects and others. A list is compiled with the help of Getty International Institute continues to deliver International Council of Museums.

b) *Counterfeits* frescoes in the above sense are rare, but as forms of crimes and present the subject of attention of professional and general public. Because of the special values, historical, cultural and other reasons, it is extremely important work state Officials involved in the discovery of these works and their further processing. The detection of counterfeit is particularly important forensic work and the use of appropriate forensic methods, which help obtain material evidence and provides the basis for the prosecution of perpetrators.

BASIC FORMULAS DETERMINING HUMIDITY

In the previous section it was said that the analysis will be based on closed Marcov's graphs with three cells.

The mentioned graph is given on Figure 1.

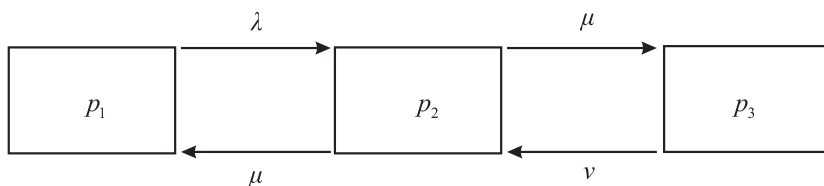


Figure 1. The closed Marcov's graph with three c

On this graph p_1 represents concentration of water molecules in the frescoes, p_2 is concentration of water molecules in the room while p_3 is concentration water molecules in wider environment.

Scheme on Figure 1 represents graphical algorithm for forming the system of differential equations determining time dependence of concentrations p_1 , p_2 and p_3 . This system is as follows:

$$\begin{aligned} \dot{p}_1 &= -\lambda p_1 + \mu p_2 \\ \dot{p}_2 &= -2\mu p_2 + \lambda p_1 + \nu p_3 \\ \dot{p}_3 &= -\nu p_3 + \mu p_2 \end{aligned} \tag{2.1}$$

where λ, μ, ν are distribution frequencies. Summing these equations we obtain that

$$\dot{p}_1 + \dot{p}_2 + \dot{p}_3 = \frac{d}{dt}(p_1 + p_2 + p_3) = 0$$

wherefrom it follows that:

$$p_1(t) + p_2(t) + p_3(t) = const. \tag{2.2}$$

The last formula is the proof that Marcov's graph is closed.

The system of differential equations [2.2] can be translated into system of linear algebraic equations by means of Laplace's transformation (6, 7). It means that all equations of the system [2.1] will be multiplied with $e^{-\omega t}$ and integrated with respect to t from zero to infinity. The described procedure gives the system of algebraic equations:

$$(\omega + \lambda)q_1(\omega) - \mu q_2(\omega) = p_1(0) \tag{2.3}$$

$$-\lambda q_1(\omega) + (\omega + 2\mu)q_2(\omega) + \nu q_3(\omega) = p_2(0) - \mu q_2(\omega) + (\omega + \nu)q_3(\omega) = p_3(0)$$

The notation used in [2.3] is:

$$q_s(\omega) = \int_0^{\infty} dt e^{-\omega t} p_s(t), \quad s = 1, 2, 3 \tag{2.4}$$

The formula:

$$q_s(\omega) = \int_0^{\infty} dt e^{-\omega t} \dot{p}_s(t) = \omega q_s(\omega) - p_s(0), \tag{2.5}$$

$s = 1, 2, 3$

was used, also. The solutions of the system [2.3] are given by:

$$\begin{aligned} q_1(\omega) &= \frac{p_1(0)\omega^2 + [(2\mu + \nu)p_1(0) + \mu p_2(0)]\omega + \mu\nu H}{\omega(\omega - \Omega_1)(\omega - \Omega_2)} \\ q_2(\omega) &= \frac{p_2(0)\omega^2 + [(\nu + \lambda)p_2(0) + \lambda p_1(0) + \nu p_3(0)]\omega + \lambda\nu H}{\omega(\omega - \Omega_1)(\omega - \Omega_2)} \end{aligned} \tag{2.6}$$

where $H = p_1(0) + p_2(0) + p_3(0)$ and

$$\Omega_1 = -\frac{2\mu + \nu + \lambda}{2} + \frac{1}{2}\sqrt{4\mu^2 + \nu^2 + \lambda^2 - 2\nu\lambda} \tag{2.7}$$

$$\Omega_2 = -\frac{2\mu + \nu + \lambda}{2} - \frac{1}{2}\sqrt{4\mu^2 + \nu^2 + \lambda^2 - 2\nu\lambda} \tag{2.8}$$

Time dependance of concentrations $p_s(t)$; $s = 1, 2, 3$ can be found by application of inverse Laplace transformation (8):

$$p_s(t) = \frac{1}{2\pi i} \int_{c-i\infty}^{c+i\infty} d\omega e^{\omega t} q_s(\omega), \quad s = 1, 2, 3 \quad [2.9]$$

The contour in complex ω plane for calculation of Bromvich integral (9,10) is given on Figure 2.

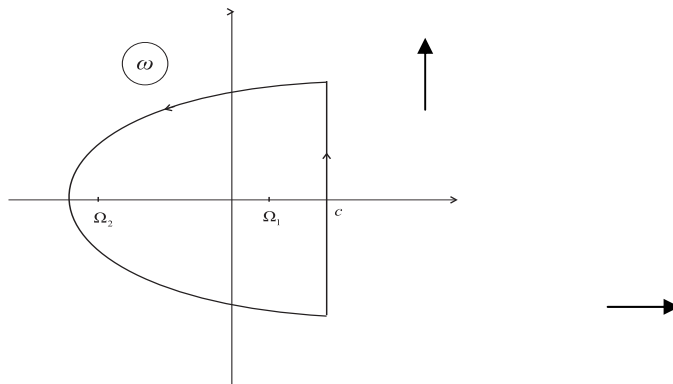


Figure 2. Contour in complex plane for finding of inverse Laplace transformation

Since all functions $q_s(\omega)$ have three simple poles $\omega=0$, $\omega=W_1$ and $\omega=W_2$, the integral [2.9] is sum of residues in poles 0, W_1 and W_2 . The formula for finding of residuum at simple pole is:

$$\text{Res} f(z) = \lim_{z \rightarrow z_0} (z - z_0) f(z) \quad [2.10]$$

Applying the formulas [2.9] and [2.10] to [2.6] we obtain the solutions of the system of differential equations [2.]:

$$p_1(t) = \frac{\mu\nu H}{\Omega_1\Omega_2} + \frac{p_1(0)\Omega_1^2 + [(2\mu + \nu)p_1(0) + \mu p_2(0)]\Omega_1 + \mu\nu H}{\Omega_1(\Omega_1 - \Omega_2)} e^{\Omega_1 t} - \frac{p_1(0)\Omega_2^2 + [(2\mu + \nu)p_1(0) + \mu p_2(0)]\Omega_2 + \mu\nu H}{\Omega_2(\Omega_1 - \Omega_2)} e^{\Omega_2 t} \quad [2.11]$$

$$p_2(t) = \frac{\lambda\nu H}{\Omega_1\Omega_2} + \frac{p_2(0)\Omega_1^2 + [(\lambda + \nu)p_2(0) + \lambda p_1(0) + \nu p_3(0)]\Omega_1 + \lambda\nu H}{\Omega_1(\Omega_1 - \Omega_2)} e^{\Omega_1 t} - \frac{p_2(0)\Omega_2^2 + [(\lambda + \nu)p_2(0) + \lambda p_1(0) + \nu p_3(0)]\Omega_2 + \lambda\nu H}{\Omega_2(\Omega_1 - \Omega_2)} e^{\Omega_2 t} \quad [2.12]$$

$$p_3(t) = \frac{\lambda\mu H}{\Omega_1\Omega_2} + \frac{p_3(0)\Omega_1^2 + [(2\mu + \lambda)p_3(0) + \mu p_2(0)]\Omega_1 + \lambda\mu H}{\Omega_1(\Omega_1 - \Omega_2)} e^{\Omega_1 t} - \frac{p_3(0)\Omega_2^2 + [(2\mu + \lambda)p_3(0) + \mu p_2(0)]\Omega_2 + \lambda\mu H}{\Omega_2(\Omega_1 - \Omega_2)} e^{\Omega_2 t} \quad [2.13]$$

These formulas will be used for determining of the age of the frescoes.

DETERMINING AGE OF THE FRESCO

Determining of age of the fresco requires series of measurements of water contents. It should be pointed out that we do not know when was the initial momentum $t = 0$, since we do not know when the fresco was finished. Consequently, initial concentrations $p_1(0)$, $p_2(0)$ and $p_3(0)$ are unknown. There is a possibility to determine initial concentration of H_2O molecules in the fresco using computer scheme of paint distribution of fresco. With help of this scheme we can reproduce paints of investigated fresco and measure its humidity. It could be equal to initial concentration $p_i(0)$.

Concerning measurements we must remember that the fresco must not be damaged, which means that no measurements should be done on the fresco. It also means that the formula [2.11] will not be used. Measurements of humidity percentage of wider environment are not recommended due to the possible fluctuations of humidity in wider area (rain, snow, wind etc.). On the bases of above reasoning it remains to measure H_2O contents in different moments in time in the room where the fresco is located. The humidity fluctuations in the room are very rare. Besides, the paint is in direct contact with air of the room (see Markov's graph). This direct contact gives more perceptible changes of humidity. Since the wider environment and the paint are not in direct contact, the changes of humidity of wider environment $p_3(t)$ would be weak, and this requires longer time intervals between two consecutive measurements. The final conclusion from preceding discussion is that all measurements are related to determining the concentrations $p_2(t)$. The first measurement concentration p_2 gives $p_2(T)$, where T is the age of the fresco in the moment of measurement. This concentration will be denoted with B_1 .

On the basis of the formula [2.12], written for $t = T$ we get the following expression formula:

$$R = \frac{B_1 - \Phi(x, y, T, B_0) - F(x, y, T, z, H)}{2 \sinh yT} e^{xT} \quad \& \quad f(x, y, z, T, H, B_0) \quad [3.14]$$

Where

$$x = \frac{2\mu + \nu + \lambda}{2}, y = \frac{1}{2} \sqrt{4\mu^2 + \nu^2 + \lambda^2 - 2\nu\lambda}, z = \nu\lambda, B_0 = p_2(0), B_1 = p_2(T) \quad [3.15]$$

The functions Φ and F , figuring in [3.14] are given by:

$$\Phi(x, y, T, B_0) = B_0 \frac{y \cosh yT - x \sinh yT}{y} e^{-xT} \quad [3.16]$$

$$F(x, y, T, z, H) = \left[\frac{1}{x^2 - y^2} - \frac{x \sinh yT + y \cosh yT}{y(x^2 - y^2)} e^{-xT} \right] zH \quad [3.17]$$

The time unit in the formula [3.14] is one year. There appear six unknown values in [3.14]: x, y, z, T, H and B_0 . To determine these unknown parameters, we must carry out six measurements of concentration $p_2(t)$. The interval τ between two consecutive measurements can be taken to be one month, or half a month. In the first case $\tau = 1/12$ and in the second case $\tau = 1/24$. The first of these measurement must be done a month or half amount after the first measurement which has got value $B_1 = p_2(t)$.

The values of concentration obtained in moments $T + \tau, T + 2\tau, \dots, T + 6\tau$, will be denoted by B_2, B_3, \dots, B_7 , respectively. So we obtain the following system of the equations:

$$\begin{aligned}
 B_2 &= F(x, y, T + \tau, z, H) + \Phi(x, y, T + \tau, B_0) + [2e^{-x(T+\tau)} \sinh(T+\tau)] f(x, y, z, T + \tau, H, B_0) \\
 B_3 &= F(x, y, T + 2\tau, z, H) + \Phi(x, y, T + 2\tau, B_0) + [2e^{-x(T+2\tau)} \sinh(T+2\tau)] f(x, y, z, T + 2\tau, H, B_0) \\
 B_4 &= F(x, y, T + 3\tau, z, H) + \Phi(x, y, T + 3\tau, B_0) + [2e^{-x(T+3\tau)} \sinh(T+3\tau)] f(x, y, z, T + 3\tau, H, B_0) \\
 B_5 &= F(x, y, T + 4\tau, z, H) + \Phi(x, y, T + 4\tau, B_0) + [2e^{-x(T+4\tau)} \sinh(T+4\tau)] f(x, y, z, T + 4\tau, H, B_0) \\
 B_6 &= F(x, y, T + 5\tau, z, H) + \Phi(x, y, T + 5\tau, B_0) + [2e^{-x(T+5\tau)} \sinh(T+5\tau)] f(x, y, z, T + 5\tau, H, B_0) \\
 B_7 &= F(x, y, T + 6\tau, z, H) + \Phi(x, y, T + 6\tau, B_0) + [2e^{-x(T+6\tau)} \sinh(T+6\tau)] f(x, y, z, T + 6\tau, H, B_0)
 \end{aligned}
 \tag{3.18}$$

Besides, in order to find the age of the paint T , which is the main goal of our analysis, we must find the distribution frequencies μ, ν and λ . These frequencies cannot be calculated directly from the formulas [3.18]. They can be determined with the help of the values of x, y and z which are included into [3.18]. Knowing x, y and z , we can find μ, ν and λ from the relations [3.15]. The solving of the system of equations [3.18], requires the use of numerical methods. The same requires the solving of the system [3.15]. Finishing this section we quote the following illustrative example:

For: $\tau = 1/24$;

$$\begin{aligned}
 B_1 &= 2.7; B_2 = 2.7002; B_3 = 2.7005; B_4 = 2.7007; \\
 B_5 &= 2.70085; B_6 = 2.70095; B_7 = 2.701;
 \end{aligned}
 \tag{3.19}$$

we obtained:

$$T = 65.25 \text{ years}; H = 10; B_0 = 1.93; x = 0.12547; y = 0.005966; z = 0.000047 \tag{3.20}$$

Substituting [3.20] into [3.15], we found the values for distribution frequencies:

$$\lambda = 0.011179; \mu = 0.004847; \nu = 0.04221.$$

It is seen the results obtained in this example are realistic (11,12).

CONCLUSION

Because of the special values, historical, cultural and other reasons, it is extremely important work state Officials involved in the discovery of these works and their further processing. The detection of counterfeits is particularly important forensic work and the use of appropriate forensic methods, which help obtain material evidence and provides the basis for the prosecution of perpetrators.

The proposed method of determining the age of the frescoes has given satisfactory result: the age T can be determined without touch on the paint. The theory is based on really existing situation. Some idealizations are introduced by the fact that closed Markov's graph is used. This eliminated actually existing effect consisting of influence of walls, furniture etc. to the humidity of room. The main shortage of this approach is the moment of selling the fresco, since it occurs out of the room included in our theory. In quoted illustrative example only one set of six values B was used. In practice the more realistic result could be obtained with n sets of six values B . These n sets would be obtained by changing of intervals τ between two successive measurements. In this way we should obtain n sets of results of the type [3.20]. The values given in [3.20] would be calculated as arithmetic means of n values or as expectable values of them.

Acknowledgement

This work was supported by the Serbian Ministry of Education, Science and Technological Development, Grant No. TR34019.

The authors owe special gratitude to his teacher, academician prof. dr Bratislav Tošić.

REFERENCES

1. "RS Official Gazette" No.72/11, 101/11, 121/11, 32/13 and 45/13.
2. Law on Ratification of the UN Convention against Transnational Organized Crime, the Additional Protocols, "FRY Official Gazette- International Treaties", No. 06/01. (Palermo Convention).
3. Todorovic, M: *Forgeries of art goods*, MOI RS, *Security*, 1, Belgrade, **1993**, p.589-598.
4. Nikač, Ž: Transnational cooperation between countries in the fight against crime – Interpol and Europol, The Institute for textbooks and teaching aids RS, Belgrade, 2003; p.134-135.
5. Source: www.interpol.int, Crime areas, Works of Art (accessed: 8 March 2015).
6. Meyn S.P., Tweedie R.L: *Markov Chains and Stochastic Stability*, Springer, 2005.
7. Donaldson, T.: *A Laplace Transform Calculus for Partial Differential Operators*, Providence: AMS, 1974.
8. Lipson, H.: The Introduction of Fourier Methods into Crystal-Structure Determination, *Notes and Records of the Royal Society of London*, **1990**, 44 (2), 257-264.
9. Dodson, C.T.J. Introduction to Laplace Transforms for Engineers, School of Mathematics, Manchester University, www.maths.manchester.ac.uk/kd/ma2m1/laplace.pdf
10. Howye, J.M. *Complex Analysis*, London, Springer, 2001.
11. Zorić, V.M. Analysis of mechanical oscillations the colored coating and method of application results of forensic investigations, PhD Thesis, University of Novi Sad, Serbia, 2009.
12. Zorić, V.M. *Forensic Investigation of colored layers*, Zadužbina Andrejević, Beograd, 2014.

ПОЛИЦИЈСКИ АСПЕКТИ ФОРЕНЗИЧКИХ МЕТОДА СТУДИЈЕ ПРОЦЕНТА САДРЖАЈА ВОДЕ КОД ОДРЕЂИВАЊА СТАРОСТИ ФРЕСАКА

Војкан М. Зорић^{1,2}, Жељко Никач³, Радован Радовановић³

¹ Универзитет у Новом Саду, Природно-математички факултет, Трг Доситеја Обрадовића 4,
21000 Нови Сад, Србија

² Министарство унутрашњих послова, УКП-Национални криминалистичко-технички Центар, Булевар
Михајла Пупина 2, 11000 Београд, Србија

³ Криминалистичко-полицијска академија, Прегревица, 11080 Београд – Земун, Србија

Новеле о кривичном поступку (ЗКП) Републике Србије имају уводни концепт тужилачке истраге у вези са овим доказима, посебне доказне радње и други софтвер за функционисање кривичног гоњења. Значење новела је да спроведе усклађивање стандарда са решењима савременог кривичног закона у пракси, посебно у вези са стандардима ЕУ Србије, која се пријављује за чланство у Унији. Спречавање најозбиљнијих облика криминала је фокус надлежних органа Србије и у том контексту је спречавање и борба против свих облика фалсификата, као што је случај са фалсификатима фресака и уметничких слика и њихова продаја на светском тржишту. У изложеном раду је предложен метод одређивања старости фресака. Он се заснива на коришћењу затворених Марковљевих графова са три хелије. Мерења садржаја молекула воде у околини може се урадити само за простор у коме се налазе фреске. То значи да је следећи изложени метод који се користи – неструктиван.

Кључне речи: Полиција, фореника, концентрација влажности, Марковљеви графови, фреске.

Received: 9 February 2015.

Accepted: 15 July 2015.

BIOCHEMICAL AND PHARMACEUTICAL ENGINEERING

GLYCEROL AS A CARBON SOURCE FOR XANTHAN PRODUCTION BY *Xanthomonas campestris* ISOLATES

Bojana Ž. Bajić*, Zorana Z. Rončević, Siniša N. Dodić, Jovana A. Grahovac
and Jelena M. Dodić

University of Novi Sad, Faculty of Technology, Bulevar cara Lazara 1, 21000 Novi Sad, Serbia

The success of xanthan biosynthesis depends on several factors, most importantly the genetic potential of the production microorganism and cultivation media composition. Cultivation media composition affects the yield and quality of the desired product as well as production costs. This is why many studies focus on finding cheap alternative raw materials, especially carbon sources, to replace commercially used glucose and sucrose. In addition to the Xanthomonas campestris ATCC 13951 which is the primary industrial production microorganism, other Xanthomonas strains can produce xanthan as well. Under the same conditions, different strains produce different amounts of the biopolymer of varying quality. The aim of this paper is to compare producibility of phytopathogenic X. campestris strains, isolated from the environment with the reference X. campestris ATCC 13951 strain and to estimate the possibility of xanthan production using alternative glycerol-based media than the synthetic glucose-based media. Submerged cultivation on the medium based on glucose or glycerol (2.0 %w/v) was performed using the reference strain and eight isolated X. campestris strains. In order to assess the success of biosynthesis, xanthan yield and rheological properties were determined. Strains isolated from the environment produced yields between 2.98 g/L and 12.17 g/L on the glucose-based medium and 1.68 g/L and 6.31 g/L on the glycerol-based medium. Additionally, X. campestris ATCC 13951 provided the highest yield when using glucose (13.24 g/L), as well as glycerol-based medium (7.44 g/L). The obtained results indicate that in the applied experimental conditions and using all tested strains, glycerol is viable as a carbon source for the production of xanthan.

KEY WORDS: xanthan, *Xanthomonas campestris*, glycose, glycerol

INTRODUCTION

In many industrial areas, the use of microbial polysaccharides, among which xanthan has a prominent place, has increased significantly. Xanthan is the biopolymer with the highest economic importance and is the subject of numerous research studies due to its

* Corresponding author: Bojana Ž. Bajić, University of Novi Sad, Faculty of Technology, Bulevar cara Lazara 1, 21000 Novi Sad, Serbia, e-mail: baj@uns.ac.rs

unique rheological properties such as a high degree of pseudoplasticity and high viscosity, even at low concentrations (1, 2).

Biotechnological, or more precisely microbiological, production has been an integral part of everyday life since the earliest civilizations, but since the early 20th century microorganisms have been exploited in controlled conditions in order to produce a desired product. Industrial production mainly uses reference strains of production microorganisms, which are preserved in culture collections. However, there is a growing interest in isolating new strains with improved properties. Since these production microorganisms are isolated from the environment, they are more resistant to environmental changes than the strains from a culture collection, which gives the option of manipulating the process parameters in order to improve production. There is a possibility that newly isolated strains could synthesize metabolites that have yet to be exploited in typical conditions for biotechnological production. Additionally, it is possible that strains from the environment will synthesize desired products from unusual substrates, which opens up the option of using intermediary and by-products of various industries as substrates for the biotechnological production.

Bacterial strains belonging to the genus *Xanthomonas* may produce xanthan, however, some species are more efficient, such as *Xanthomonas campestris*. The strains from the culture collections, mainly *X. campestris* pv *campestris* NRRL-B 1459 or ATCC 13951, have been extensively used for industrial xanthan production (3, 4). Although xanthan produced by these bacteria has commercially significant rheological properties, it lacks marketability compared to the polymers from algae or plants due to high production costs, which is the reason why its process efficiency should be increased. In order to achieve this goal there have been suggested various approaches and techniques, one of which is the isolation and selection from the natural environments and screening of *X. campestris* strains for enhanced xanthan production (5). The ability to biosynthesize xanthan and infectivity towards plants (phytopathogenicity) such as cabbage, cauliflower and others are directly correlated (6), which is why it is significant to test the productivity of strains isolated from the environment.

Xanthan produced using different *X. campestris* strains shows variations in yield and viscosity, which can be seen in a large number of studies. Additionally, selected production strains display different behavior in altered cultivation conditions. Therefore, the composition of the cultivation medium for xanthan biosynthesis greatly influences the quantity and quality of the produced biopolymer, which is why it is essential to determine the optimal production medium for each strain in order to establish its industrial potential (1, 7).

The commercial media used for the production of xanthan contain glucose or sucrose as the carbon source, whose cost represents a critical factor in its production process from an economic perspective. If xanthan would be produced on a medium with a low-cost carbon source, production costs would decrease (8), which is why numerous waste effluents have been suggested as alternative carbon sources (2, 9). Glycerol, the main by-product of the biodiesel production process, is one such cheap and available substrate used for the biotechnological production of various products, one of which is xanthan (10, 11).

The aim of this paper is to compare the producibility of phytopathogenic *Xanthomonas campestris* strains, isolated from the environment with the reference strain *X. campestris*

ATCC 13951 and to estimate the possibility of xanthan production using a glycerol-based medium, and compare the process efficiency to that involving synthetic media with glucose.

EXPERIMENTAL

Production microorganism

Nine *Xanthomonas campestris* strains were used as the producing microorganism for xanthan biosynthesis. The reference strain ATCC 13951 and eight strains isolated from the agricultural land of Vojvodina were stored on yeast maltose (YM[®], Difco) agar slants. The strains were isolated from the infected leaves of several different cruciferous plants, such as cabbage (I2, I4, I6, I8), kale (I1, I7) and cauliflower (I3, I5). The isolate was identified as *Xanthomonas campestris* on the basis of its morphological and physiological characteristics according to Bergey's Manual of Determinative Bacteriology (12). Cultures were subcultured at four-week intervals to maintain good viability and stability.

Cultivation media

The medium used for the inoculum preparation was YM[®] broth, while xanthan production was performed on the media containing glucose or glycerol (Table 1). Literature data (11) were used for the formulation of the cultivation medium based on glycerol. The pH value of the medium was adjusted to 7.0±0.2 and then sterilized by autoclaving under standard conditions.

Table 1. Media composition for xanthan production

Medium compound	Glucose medium [g/L]	Glycerol medium [g/L]
Glucose	20	-
Glycerol	-	20
Yeast extract	3.0	-
Urea	-	0.9
KH ₂ PO ₄	3.0	3.0
(NH ₄) ₂ SO ₄	1.5	-
MgSO ₄ ·7H ₂ O	0.3	-

Xanthan production

Xanthan production was carried out simultaneously in 300 mL Erlenmeyer flasks with 100 mL of the cultivation medium. Inoculation was performed by adding 10% (v/v) of the inoculum prepared in aerobic conditions at 26°C in a laboratory shaker (KS 4000i control, IKA[®], Germany) at 150 rpm for 48 h. Biosynthesis was carried out in batch mode under aerobic conditions for 5 days at a temperature of 30°C and agitation rate of 150 rpm.

Analysis of the cultivation broth

At the end of the process, samples of the cultivation broths were analyzed. Rheological properties of the cultivation broth samples were determined using a controlled-stress rheometer HAAKE RS600 (Thermo-Electron Corporation, Germany) with cone-plate C60/ITi sensor, at $25 \pm 0.1^\circ\text{C}$, and shear rates from 0 to 1000 1/s. Rheological parameters were calculated according to the Ostwald de Vaele equation.

The samples of the cultivation broth were centrifuged at 10,000 rpm for 10 min (Hettich Rotina 380 R, Germany). The obtained supernatants were filtered through a $0.45\ \mu\text{m}$ nylon membrane (Agilent Technologies, Germany) and then analyzed by HPLC (Thermo Scientific Dionex UltiMate 3000 series), to determine the residual glucose and glycerol content. The HPLC instrument was equipped with a HPG-3200SD/RS pump, WPS-3000(T)SL autosampler (10 μL injection loop), ZORBAX NH_2 column (250 mm x 4.6 mm, 5 μm) and a RefractoMax520 detector. In order to determine glucose content, 75% (v/v) acetonitrile was used as the eluent at a flow rate of 1.2 mL/min and an elution time of 20 min at a column temperature of 25°C , while 70 % (v/v) acetonitrile was used as an eluent in order to determine glycerol content with a flow rate of 1.0 mL/min, elution time of 10 min and column temperature of 30°C .

Product separation

After the biosynthesis, the product separation from the cultivation medium was carried out in order to evaluate xanthan production. In this study, xanthan was recovered from the supernatant, which was obtained after ultracentrifugation (Hettich Rotina 380 R, Germany) of the cultivation broth at 10,000 rpm for 10 min, by precipitation with 96% (v/v) ethanol in the presence of KCl as the electrolyte. Ethanol was gradually added to the supernatant at 15°C until the alcohol content in the mixture was 60% (v/v), at constant stirring. A saturated solution of KCl was added when half of the necessary ethanol amount was poured into the supernatant in a quantity to obtain a final content of 1% (v/v). The obtained mixture was kept at 4°C for 24 h in order to dehydrate the precipitated xanthan, and then centrifuged at 3500 rpm for 15 min (Tehtnica LC-321, Slovenia). The precipitated polymer was then dried to constant weight at 60°C in order to determine raw xanthan yield. Ethanol used for precipitation of xanthan was recycled by distillation.

RESULTS AND DISCUSSION

In accordance with the defined aim of the paper, xanthan biosynthesis was performed using nine different production microorganism strains on a cultivation medium containing glucose or glycerol as the sole carbon source. In order to assess the success of biosynthesis, the rheological properties of the cultivation broths were determined at the end of the process.

The rheological properties were defined by flow curves of the cultivation broths which were a result of xanthan production by different production microorganism strains in the cultivation medium containing glucose (Figure 1) or glycerol (Figure 2) as the car-

bon source. Flow curves represent the relationship between the shear rate D (1/s) and the shear stress τ (Pa). As the figures show, the solutions are pseudoplastic in nature which is characteristic of xanthan solutions (7).

The rheological parameters, consistency factor and flow behavior index, as well as the coefficient of correlation are presented in Table 2. High values of the correlation coefficient match the experimental results and the aforementioned functional dependence, meaning the cultivation broths are pseudoplastic systems. The viscosity depends on the amount of xanthan in the cultivation broth, molecular weight and inter-molecular structures which are formed due to functional groups in the molecule. A change in the viscosity of the cultivation broth is a clear indicator of xanthan being produced (7). Given that the viscosity, which is a direct measurement of the quality of a fluid (8), and the consistency factor (K) are proportional, the values of the consistency factor K (Table 2) indicate a different quality and quantity of the synthesized biopolymer.

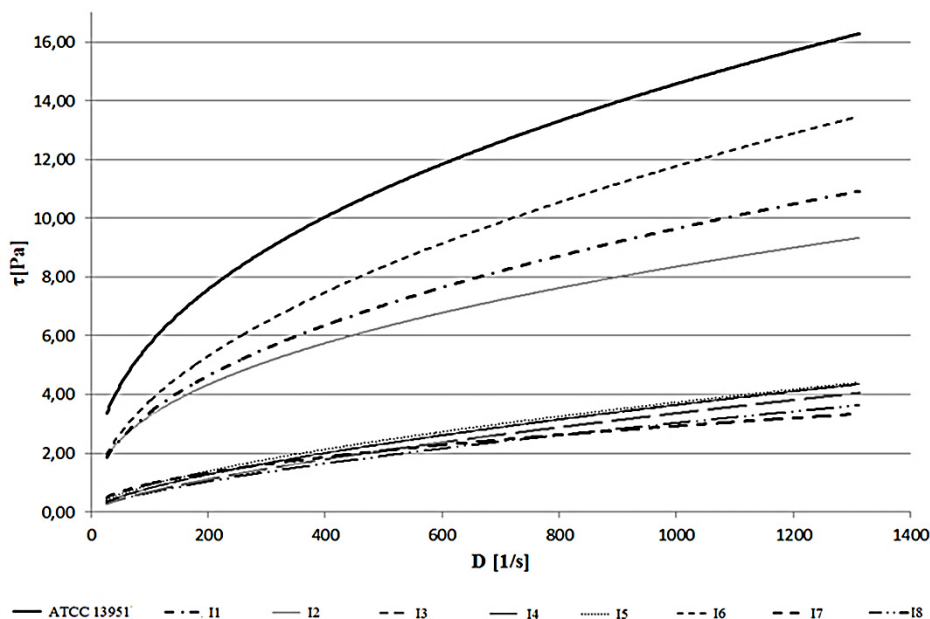


Figure 1. Flow curves of the glucose-based cultivation medium obtained after the xanthan biosynthesis

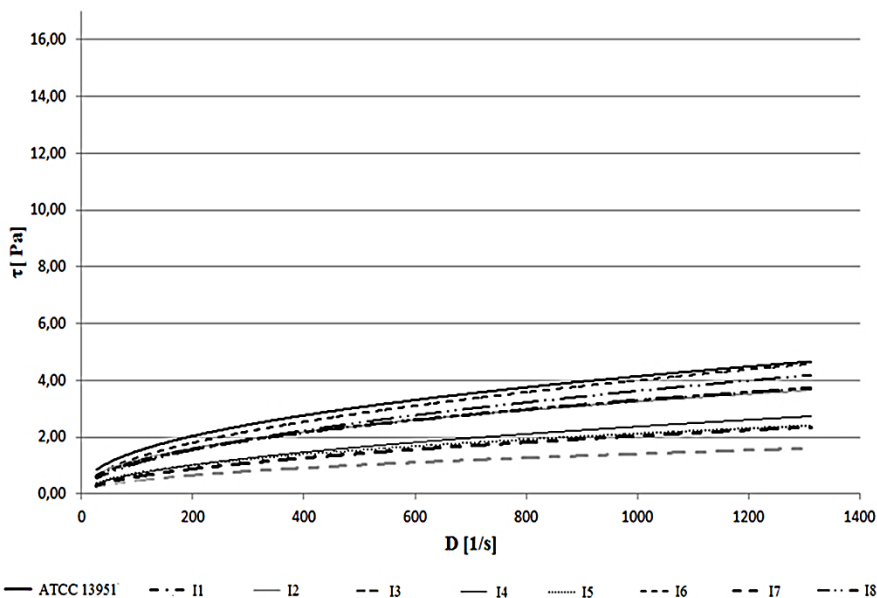


Figure 2. Flow curves of the glycerol-based cultivation medium obtained after the xanthan biosynthesis

Table 2. Rheological parameters and coefficient of correlation for cultivation broths obtained after the biosynthesis using nine *X. campestris* strains on the glucose- and glycerol-based media

<i>X. campestris</i> strain	Glucose-based medium			Glycerol-based medium		
	K [Pa·s ⁿ]	N [1]	R ²	K [Pa·s ⁿ]	n [1]	R ²
ATCC 13951	0.8760	0.4070	0.9986	0.1977	0.4403	0.9876
11	0.4142	0.4955	0.9933	0.1370	0.4605	0.9950
12	0.4981	0.4081	0.9925	0.1622	0.4338	0.9716
13	0.0289	0.6884	0.9788	0.0539	0.4727	0.9376
14	0.0401	0.6527	0.9860	0.0633	0.5246	0.9144
15	0.0540	0.6132	0.9793	0.0880	0.4615	0.9646
16	0.3841	0.4955	0.9974	0.1301	0.4961	0.9292
17	0.0998	0.4891	0.9738	0.0552	0.5230	0.9477
18	0.0307	0.6649	0.9814	0.1370	0.4605	0.9950

The consistency factor is the highest when the *Xanthomonas campestris* ATCC 13951 strain is used in the glucose-based medium (0.8760 Pa·sⁿ) and the glycerol-based medium (0.1977 Pa·sⁿ). The values of this rheological parameter using other strains range between 0.0289-0.4981 Pa·sⁿ for the glucose-based medium and 0.0539-0.1622 Pa·sⁿ for the gly-

cerol-based medium. Based on the obtained results for the strains isolated from the environment on tested media, both glucose- and glycerol-based media, the lowest consistency factor was obtained for the isolate I3 (0.0289 Pa·sⁿ and 0.0539 Pa·sⁿ, respectively), while the highest consistency factor was observed for the isolate I2 (0.4981 Pa·sⁿ and 0.1622 Pa·sⁿ, respectively). The values of the flow behavior index (n) that range from 0.4070 and 0.6884 for the glucose-based medium and from 0.4338 to 0.5246 for the glycerol-based medium, are lower than 1, also confirm the pseudoplastic characteristics of the cultivation media. The rheological parameters, consistency factor and flow behavior index, obtained in this research have values similar to, but slightly lower than, the values reported in the literature (13).

According to the experimental plan, the cultivation broths were precipitated in order to determine the product yield. The obtained results show that the xanthan production by *X campestris* was influenced by the strain as well as by the composition of the cultivation medium (Table 3), which is in accordance with the literature data (14, 15). When using the glucose-based medium, in applied experimental conditions, the values of xanthan yield varied between 2.98 g/L and 13.24 g/L. The highest values were obtained using ATCC 13951 strain, while the strain I5 produced the lowest yield. In addition to the high values obtained with the ATCC 13951 strain, two strains isolated from the environment, I1 and I2, also produced high values of xanthan, which are 10.71 g/L and 12.17 g/L, respectively. The obtained values are slightly lower than the values (14.74 g/L) listed in the literature (3). Additionally, there are yield differences when glycerol-based medium was used. The yields range between 7.24 g/L for ATCC 13951 and 1.68 g/L for the isolate I5. The highest yield values are slightly higher than the values listed in the literature (11). From an economical point of view, when glycerol is used as a sole carbon source the obtained yield values are low, but the mere possibility of using this alternative carbon source in the biotechnological production of xanthan is very significant.

Table 3. Xanthan yield, sugar conversion and conversion into product obtained using *X. campestris* strains on the glucose- and glycerol-based media

<i>X. campestris</i> strain	Glucose-based medium			Glycerol-based medium		
	Xanthan Yield, P [g/L]	Sugar conversion* [%]	Conversion** [%]	Xanthan Yield [g/L]	Sugar conversion* [%]	Conversion** [%]
ATCC 13951	13.24	89.15	66.22	7.44	68.70	37.20
I1	11.71	72.34	58.55	3.86	62.70	19.29
I2	12.17	85.18	60.86	3.56	40.55	17.82
I3	5.29	57.23	26.44	1.94	62.55	9.72
I4	6.60	54.03	32.99	2.41	44.30	12.03
I5	2.98	16.71	14.90	1.68	54.80	8.40
I6	9.94	73.70	49.69	6.31	61.00	31.57
I7	3.65	54.32	18.26	2.90	52.55	14.48
I8	4.96	35.89	24.82	4.60	53.40	22.99

*sugar conversion [%] = (S₀-S)/S₀·100

**conversion [%] = P/S₀·100

S₀ - sugar content in the inoculated medium

S - sugar content after 120 h of cultivation

In addition to xanthan yield, values of the sugar conversion and conversion to product are highest when *X. campestris* ATCC 13951 is used as the production microorganism on both the glucose- and glycerol-containing medium. These results are in accordance with the literature, which lists this strain as the most widely used in xanthan production research (4, 16). These results can be explained by the fact that the composition of the cultivation medium and the environmental conditions used were most beneficial for the production microorganism. In order to increase product yield and quality by using strains isolated from the environment and select the best production microorganism, future research is necessary.

Further research will especially focus on the optimization of the xanthan production process on glycerol-based cultivation media, as well as media based on other industrial effluents, in order to simulate a model plant for xanthan production which is a necessary step to transfer the technology from the laboratory to the industrial level. If a plant were designed to produce xanthan using one of the screened production microorganisms and the same process parameters as in this paper, glycerol-based cultivation medium would not be adequate. However, if this media would be one of the substrates, it would have to be previously optimized and enriched regarding basic media components and raw glycerol could be used instead of technical glycerol. Another approach is to focus on the production microorganism through the process of screening and/or genetic modification.

CONCLUSIONS

The results obtained in this research indicate that all used *X.campestris* strains isolated from the environment can be used for xanthan production, and the obtained yields point out to clear differences between the tested strains. The use of *X. campestris* ATCC 13951 provided the highest yield when using a medium based on glucose (13.24 g/L) and glycerol (7.44 g/L). The strains isolated from the environment produced xanthan yields between 2.98 g/L and 12.17 g/L g/L on the glucose-based medium and 1.68 g/L and 6.31 g/L on the glycerol-based medium. Although the yield values on the glycerol- based medium are lower than on the standard glucose-based medium, the obtained results indicate that glycerol is viable as a carbon source in the applied experimental conditions using all tested strains for the production of xanthan. Further research should encompass the optimization of the glycerol-based media, as well as the process parameters, in order to increase yield and quality of the desired product. It should also focus on the use of raw glycerol from biodiesel production as an alternative cheap substrate.

Acknowledgement

The study is a result of the research conducted within the Project 114-451-799/2015 funded by the Provincial Secretariat for Science and Technological Development of the Autonomous Province of Vojvodina.

REFERENCES

1. Rosalam, S.; England, R. Review of xanthan gum production from unmodified starches by *Xanthomonas campestris* sp. *Enzyme Microb. Tech.* **2006**, *39* (2), 197-207.
2. Faria, S.; de Oliveira Petkowicz, C.L.; de Morais, S.A.L.; Terrones, M.G.H.; de Resende, M.M.; de França, F.P.; Cardoso, V.L. Characterization of xanthan gum produced from sugar cane broth. *Carbohydr. Polym.* **2011**, *86* (2), 469-476.
3. Leela, J.K.; Sharma, G. Studies on xanthan production from *Xanthomonas campestris*. *Bioproc. Biosyst. Eng.* **2000**, *23* (6), 687-689.
4. Kassim, M.B.I. Production and characterization of the polysaccharide “xanthan gum” by a local isolate of the bacterium *Xanthomonas campestris*. *Afr. J. Biotechnol.* **2011**, *10* (74), 16924-16928.
5. Kamal, F.; Mehrgan, H.; Assadi, M.M.; Mortazavi, S.A. Mutagenesis of *Xanthomonas campestris* and selection of strains with enhanced xanthan production. *Iranian Biomedical Journal.* **2003**, *7* (3), 91-98.
6. Ramírez, M.E.; Fucikovský, L.; García-Jiménez, F.; Quintero, R.; Galindo, E. Xanthan gum production by altered pathogenicity variants of *Xanthomonas campestris*. *Appl. Microbiol. Biotechnol.* **1988**, *29* (1), 5-10.
7. García-Ochoa, F.; Santos, V.E.; Casas, J.A.; Gómez, E. Xanthan gum: production, recovery, and properties. *Biotechnol. Adv.* **2000**, *18* (7), 549-579.
8. Nery, T.B.R.; da Cruz, A.J.G.; Druzian, J.I. Use of green coconut shells as an alternative substrate for the production of xanthan gum on different scales of fermentation. *Polímeros.* **2013**, *23* (5), 602-607.
9. Kurbanoglu, E.B.; Kurbanoglu, N.I. Ram horn hydrolysate as enhancer of xanthan production in batch culture of *Xanthomonas campestris* EBK-4 isolate. *Process. Biochem.* **2007**, *42* (7), 1146-1149.
10. Rončević, Z.Z.; Bajić, B.Ž.; Grahovac, J.A.; Dodić, S.N.; Dodić, J.M. Effect of the initial glycerol concentration in the medium on the xanthan biosynthesis. *Acta Periodica Technologica.* **2014**, *45* (1), 239-246.
11. Brandão, L.V.; Assis, D.J.; López, J.A.; Espiridião, M.C.A.; Echevarria, E.M.; Druzian, J.I. Bioconversion from crude glycerin by *Xanthomonas campestris* 2103: xanthan production and characterization. *Braz. J. Chem. Eng.* **30**, 4 (2013) 737-746.
12. Breed, R.S.; Murray, E.G.D.; Smith, N.R. *Bergey's manual of determinative bacteriology*. Williams & Wilkins Co.: Baltimore, 1957; pp 152-183.
13. Dodić, J.M.; Rončević, Z.Z.; Bajić, B.Ž.; Grahovac, J.A.; Dodić, S.N. Possibility of xanthan production on glycerol containing media, Food Science Conference 2013, Budapest, 7-8th November 2013, Book of proceedings, pp 161-164.
14. Moreira, A.S.; Vendruscolo, J.L.S.; Gil-Turnes, C.; Vendruscolo, C.T. Screening among 18 novel strains of *Xanthomonas campestris* pv *pruni*. *Food Hydrocolloid.* **2001**, *15* (4-6), 469-474.
15. Antunes, A.E.C.; Moreira, A.S.; Vendruscolo, J.L.S.; Vendruscolo, C.T. Screening of *Xanthomonas campestris* pv *pruni* strains according to their production of xanthan and its viscosity and chemical composition. *Braz. J. Food Technol.* **2003**, *6* (2), 317-322.

16. Kumara, S.M.; Khan, B.A.; Rohit, K.C.; Purushotham, B. Effect of carbon and nitrogen sources on the production of xanthan gum from *Xanthomonas campestris* isolated from soil. *Arch. Appl. Sci. Res.* **2012**, 4 (6), 2507-2512.

ГЛИЦЕРОЛ КАО ИЗВОР УГЉЕНИКА У ПРОИЗВОДЊИ КСАНТАНА ПРИМЕНОМ ИЗОЛАТА *Xanthomonas campestris*

Бојана Ж. Бајић, Зорана З. Рончевић, Синиша Н. Додић, Јована А. Граховац,
Јелена М. Додић

Универзитет у Новом Саду, Технолошки факултет, Булевар цара Лазара 1, 21000 Нови Сад, Србија

Успешност биосинтезе ксантана зависи од неколико фактора међу којима су веома значајни генетски потенцијал производног микроорганизама и састав хранљиве подлоге. Састав подлоге утиче на квалитет и принос жељеног производа, али и на трошкове производње. Због тога се многа истраживања баве испитивањем могућности примене јефтиних и доступних сировина као алтернатива за глукозу и сахарозу, комерцијално најчешће примењиваних извора угљеника. Поред соја *Xanthomonas campestris* ATCC 13951 који је највише примењиван производни микроорганизам за индустријску производњу, ксантан могу продуковати и други сојеви рода *Xanthomonas*, при чему различити сојеви под истим условима продукују различиту количину биополимера различитог квалитета. Циљ овог рада јесте упоређивање производних способности фитопатогених сојева *X. campestris*, изолованих из природног окружења са референтним сојем и упоређивање могућности производње ксантана на подлози са глицеролом као извором угљеника у односу на уобичајено примењивану синтетичку подлогу са глукозом. У оквиру експерименталног дела рада изведена је субмерзна култивација референтног соја *Xanthomonas campestris* ATCC 13951 и осам изолата на подлогама чије су основа глукоза односно глицерол (2,0 % w/v). Како би се проценила успешност биосинтезе у примењеним експерименталним условима, одређене су реолошке карактеристике добијених култивационих течности, као и приноси ксантана. Изолати из природног окружења продуковали су ксантан у количини од 2.98-12.17 g/L на хранљивој подлози са глукозом, односно од 1.68-6.31 g/L на хранљивој подлози са глицеролом. Међутим, применом референтног соја *X. campestris* ATCC 13951 остварени су највећи приноси ксантана на обе хранљиве подлоге (13.24 g/L за глукозу и 7.44 g/L за глицерол). Како су сви проучавани сојеви синтетисали ксантан на глицеролу као једином извору угљеника, сирови глицерол може бити предмет истраживања као јефтинији извор угљеника у подлогама за производњу ксантана.

Кључне речи: ксантан, *Xanthomonas campestris*, глукоза, глицерол

Received: 1 September 2015.

Accepted: 20 October 2015.

OPTIMIZATION OF ALCOHOLIC FERMENTATION USING IMMOBILIZED YEAST CELLS IN CALCIUM ALGINATE GEL

Jovana J. Đuran*, Zorana Z. Rončević, Bojana Ž. Bajić, Siniša N. Dodić, Jovana A. Grahovac, Aleksandar I. Jokić and Jelena M. Dodić

University of Novi Sad, Faculty of Technology, Bulevar cara Lazara 1, 21000 Novi Sad, Serbia

*Ethanol is an important industrial chemical with emerging potential as a biofuel to replace fossil fuels. In order to enhance the efficiency and yield of alcoholic fermentation, combined techniques such as cells immobilization and media optimization have been used. The aim of this study was the optimization of sodium alginate concentration and glucose and yeast extract content in the media for ethanol production with immobilized cells of *Saccharomyces cerevisiae*. Optimization of these parameters was attempted by using a Box–Behnken design using the response surface methodology. The obtained model predicts that the maximum ethanol content of 7.21% (v/v) is produced when the optimal values of sodium alginate concentration and initial content of glucose and yeast extract in the medium are 22.84 g/L, 196.42 g/L and 3.77 g/L, respectively. To minimize the number of yeast cells "eluted" from the alginate beads and residual glucose content in fermented media, additional two sets of optimization were made. The obtained results can be used for further techno-economic analyses of the process to select the optimum conditions of the fermentation process for industrial application.*

KEY WORDS: Ethanol, *Saccharomyces cerevisiae*, immobilization, optimization, RSM.

INTRODUCTION

Due to the diminishing fossil fuel reserves, there is a strong need for alternative energy sources. In the past decades, biofuels have been considered as an alternative fuel for the future. Ethanol, environmentally friendly and renewable energy source produced through fermentation of sugars, has become one of the most promising biofuels. Efficient ethanol production requires a rapid fermentation leading to high ethanol concentrations. Fermentation of media with high initial sugar concentration has been suggested as an effective way for increasing the ethanol yield (1). However, in the media with high sugar and ethanol content, yeast growth and metabolic activities are significantly inhibited. The inhibition can be caused by osmotic stress, and by the product and substrate concentrations (2). In order to decrease these problems, cells immobilization has been used. Entrapment in calcium alginate gel is one of the most commonly used techniques for the

* Corresponding author: Jovana J. Đuran, University of Novi Sad, Faculty of Technology, Bulevar cara Lazara 1, 21000 Novi Sad, Serbia, e-mail: dju@tf.uns.ac.rs

cells immobilization because of the simple immobilization procedure, the high cell density in the gel and the non-toxic carrier (3, 4). Comparing with the suspended yeast, the advantages of using calcium alginate entrapped yeast cells in alcoholic fermentation are the greater specific rate of ethanol production by 40–50%, and twice as fast glucose consumption (5).

The optimization of fermentation conditions, particularly nutritional and environmental parameters, which greatly influence the product yield and economics of the process, are very important to improve ethanol production (6). Also, for alcoholic fermentation with immobilized yeast cells it is very important to define the optimal concentration of cells carrier to avoid the carrier degradation due to the separation of carbon dioxide and mass transfer limitation caused by low porosity of the carrier.

Response surface methodology (RSM) is a statistical technique for the modelling and optimization of multiple variables, to determine the optimum process conditions by combining experimental designs with interpolation by first- or second-order polynomial equations in a sequential testing procedure (7). This statistical technique provides useful information for scale-up of any bioprocess and also to develop and improve the usage of semi-continuous or continuous production process. RSM has already been successfully applied for the optimization of ethanol production with immobilized cells of *Saccharomyces cerevisiae* (8, 9).

The aim of this study was the optimization of sodium alginate concentration and glucose and yeast extract content in media for ethanol production with immobilized cells of *Saccharomyces cerevisiae*.

EXPERIMENTAL

Producing microorganism and cells immobilization

Fresh baker's yeast (Alltech, Senta, Serbia) was used as producing microorganism throughout this research. Yeast was suspended in sterilized 0.9% (w/v) NaCl to form basic cells suspension which was used for the cells immobilization.

The cells-alginate mixture was formed by mixing of sodium alginate solutions (20, 40 and 60 g/L concentration) with basic cells suspension in a 1:4 volume ratio. Previously, sodium alginate solutions were sterilized in autoclave at 121°C and pressure of 2.1 bar for 20 min and stored overnight at 20°C. The cells-alginate mixture was then cast into beads by dropping from peristaltic pump with a tube of 3 mm in diameter into the sterile 20 g/L CaCl₂ solution which was stirred continuously (magnetic stirrer, 150 rpm) at room temperature. The beads were hardened by keeping in a CaCl₂ solution for 20 min with gentle agitation. Finally, these beads were washed with sterile distilled water to remove excess Ca²⁺ ions and untrapped cells before being used for the fermentation process. The average diameter of the beads was approximately 3.0 mm.

Fermentation media

According to the defined aim of the study and the applied experimental design, in media for ethanol production, content of glucose (50-200 g/L) and yeast extract (0-4 g/L)

were varied. The media were adjusted to the pH 5.0 with 10% (v/v) sulfuric acid and sterilized by autoclaving at 121°C and a pressure of 2.1 bars for 20 min.

Fermentation conditions

The experiments were carried out in 300 mL Erlenmeyer flasks containing 100 mL of fermentation medium of the appropriate composition. The inoculation was performed in sterile conditions by adding immobilized biocatalysts so that the medium contains a yeast cells number that guarantees a stable fermentation (10^8 cfu/mL). The fermentations were carried out in batch mode under anaerobic conditions for 48 h at the temperature of 30°C and agitation rate of 150 rpm.

Analytical methods

At the end of the process, the samples of fermented media were analyzed. Number of yeast cells "eluted" from the alginate beads was determined with Neubauer Haemocytometer under 400x magnification using an optical microscope (Wild M20, Heerbrugg, Switzerland).

Residual glucose content was determined by high-performance liquid chromatography. The samples of fermented media were centrifuged at 4000 rpm for 15 min, filtered through a 0.45 μ m nylon membrane (Agilent Technologies Inc, Germany), and then analyzed. The HPLC instrument (Thermo Scientific Dionex UltiMate 3000 series) was equipped with a pump HPG-3200SD/RS, autosampler WPS-3000(T)SL (10 μ L injection loop), column ZORBAX NH₂ (250 mm x 4.6 mm, 5 μ m) and detector RefractoMax520. Acetonitrile 75% (v/v) was used as eluent at a flow rate of 1.2 mL/min and elution time of 20 min at column temperature of 25°C.

Ethanol was determined directly from the samples of fermented media by gas chromatography. The GC instrument (HP 5890 Series II GC, Agilent Technologies Inc, USA) was equipped with a stainless steel Carbowax 20 M column and flame ionization detector. The column temperature was 85°C and the carrier gas was helium. The injector and detector temperatures were maintained at 150°C.

Experimental design and optimization by RSM

The Box-Behnken design with three factors at three levels and three repetitions in the central point and response surface methodology (RSM) were used to optimize ethanol production by immobilized cells of *Saccharomyces cerevisiae*. According to this experimental design, 15 experiments were conducted. Glucose content, X_1 (g/L), yeast extract content, X_2 (g/L) and concentration of sodium alginate, X_3 (g/L) were used as the independent variables (factors), and ethanol concentration, Y_1 (% v/v), number of yeast cells "eluted" from alginate beads, Y_2 (10^6 cfu/mL) and residual content of glucose, Y_3 (g/L) were chosen for the dependent variable (responses). The three levels of each independent variable were coded as -1, 0, and +1, which corresponded to the lower, middle, and higher values, respectively. The experimental design is given in Table 1.

Table 1. Box-Behnken experimental design and varied values of factors

Experiment	Coded factor level			Varied factor value [g/L]		
	X ₁	X ₂	X ₃	Glucose	Yeast extract	Sodium alginate
1	-1	-1	0	50	0	40
2	1	-1	0	200	0	40
3	-1	1	0	50	4	40
4	1	1	0	200	4	40
5	-1	0	-1	50	2	20
6	1	0	-1	200	2	20
7	-1	0	1	50	2	60
8	1	0	1	200	2	60
9	0	-1	-1	125	0	20
10	0	1	-1	125	4	20
11	0	-1	1	125	0	60
12	0	1	1	125	4	60
13	0	0	0	125	2	40
14	0	0	0	125	2	40
15	0	0	0	125	2	40

The relations between the independent variables and the responses were calculated by the second-order polynomial equation:

$$Y_i = b_0 + \sum b_i X_i + \sum b_{ii} X_i^2 + \sum b_{ij} X_i X_j \quad [1]$$

where Y_i is the selected response; b_0 is the intercept, and b_i , b_{ii} and b_{ij} are the linear, quadratic and interaction regression coefficient, respectively, while X_i and X_j are the varied factors.

Statistical analyses of the experimental results were performed using Statistica software v. 12.0. The method of desirability function was applied for the determination of optimal values of examined factors (Design-Expert 8.1).

RESULTS AND DISCUSSION

Among biofuels, ethanol has experienced unseen levels of attention. Therefore, improvement in its production technology is of huge economic importance. Techniques for rapid fermentation that leads to higher ethanol concentrations in fermented media are desirable (10). The combination of yeast cells immobilization and optimization of media for alcoholic fermentation has been suggested as good solution to increase ethanol yield (8). In this study, optimization of sodium alginate concentration and glucose and yeast extract content in the fermentation medium was carried out using response surface methodology and Box-Behnken experimental design.

Data analysis

Based on the results of experiments formulated by the Box-Behnken design and regression analysis, quadratic polynomial equations were established to identify the relation between the selected responses (Y_1 – ethanol concentration, Y_2 – number of yeast cells "eluted" from alginate beads and Y_3 – residual content of glucose) and examined factors (X_1 – glucose content, X_2 – yeast extract content and X_3 – concentration of sodium alginate). The results of the statistical analyses, i.e. coefficients of regression equations, their significance and coefficient of determination (R^2) for selected responses are given in Table 2.

A positive sign for the values of the regression equations coefficients of interaction indicates a synergistic effect, while a negative sign represents an antagonistic effect of the factors on the selected response. The significance of each coefficient was determined by the p -value. The coefficients of regression equations, at a confidence level of 95%, are significant if their p -values are less than 0.05. These coefficients are bolded in Table 2.

The fitting of the experimental data to the regression model was checked and suitably explained by the coefficient of determination (R^2). The R^2 values closer to 1 suggest the better correlation between the observed and predicted values. The high values of the determination coefficient obtained for all responses (Table 2) indicate good fit of the experimental data to Equation [1]. These values suggest that only 1.8% of the total variations for the ethanol concentration and residual glucose content and 3.8% of the total variations for "eluted" yeast cells number could not be explained by the obtained model.

Table 2. Coefficients of regression equations, their significance and coefficient of determination (R^2) for selected responses

Response	Y_1		Y_2		Y_3	
Effect	Coefficient	p -value	Coefficient	p -value	Coefficient	p -value
Intercept						
b_0	-0.270660	0.621060	77.83889	0.075316	17.58565	0.021650
Linear						
b_1	0.029273	0.001161	-1.28539	0.007595	-0.04037	0.417905
b_2	0.093609	0.517033	-6.92708	0.480234	3.20208	0.070296
b_3	0.020710	0.309814	-1.27625	0.350419	-0.71979	0.012892
Quadratic						
b_{11}	-0.000046	0.024669	0.00550	0.002557	0.00018	0.284909
b_{22}	0.046963	0.070765	1.76250	0.259947	-0.30104	0.217013
b_{33}	-0.000213	0.347094	0.00544	0.711323	0.00786	0.014158
Interaction						
b_{12}	0.004815	0.000260	-0.01633	0.665228	-0.00033	0.953701
b_{13}	0.000209	0.010580	0.01045	0.032285	-0.00010	0.861922
b_{23}	-0.001908	0.377678	-0.02437	0.862119	-0.03812	0.121751
R^2	0.982		0.962		0.982	

The most significant response in the alcoholic fermentation is the ethanol concentration in the fermented medium. In order to understand the interactions of the examined

factors and determine their optimum values to achieve the maximum ethanol concentration, three-dimensional response surface plots, which are the graphical representations of the regression equation, were generated. These plots are presented in Figures 1-3. Each figure represents the effects of two factors on the selected response, whereas the third variable was maintained at the central value from the experimental design.

The effects of the initial content of glucose and yeast extract on ethanol concentration in fermented media at a constant sodium alginate concentration (40 g/L) are presented in Figure 1. From this response surface plot it is evident that, in the applied experimental conditions, ethanol production increased with increasing initial glucose and yeast extract content in the fermentation media. A maximum ethanol content of about 7.0% (v/v) is predicted by the model for the maximum values of glucose and yeast extract content, i.e. 175-200 g/L and 3-4 g/L, respectively.

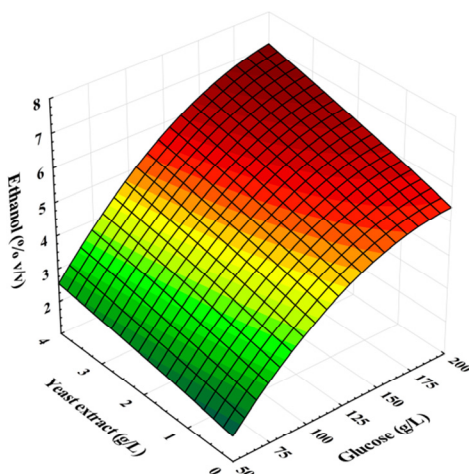


Figure 1. The effects of the initial glucose and yeast extract content on the ethanol production at a constant sodium alginate concentration (40 g/L)

The effects of the initial yeast extract content and sodium alginate concentration on the ethanol concentration in fermented media at constant initial glucose content (125 g/L) are presented in Figure 2. As in the previous case, the results shown in this figure indicate that the ethanol yield does not depend on the sodium alginate concentration. However, the initial yeast extract content in the fermentation media influenced the ethanol production. The value of selected response increases from about 4.0% (v/v) to about 5.5% (v/v), with an increase of the initial yeast extract content regardless of the sodium alginate concentration.

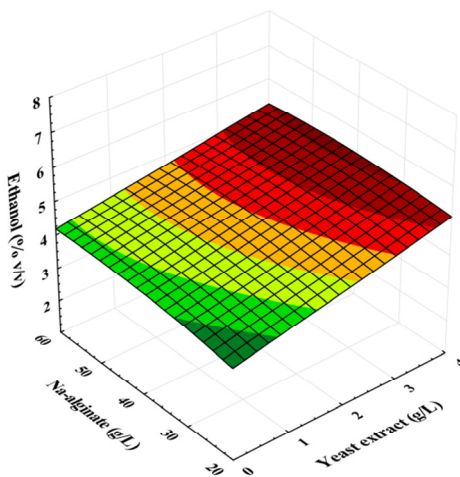


Figure 2. The effects of the initial yeast extract content and sodium alginate concentration on the ethanol production at a constant glucose content (125 g/L)

Although assimilable nitrogen is necessary for cells growth, its influence on the ethanol production by suspended yeast cells is also very significant (2, 11). As it can be seen from the response surface plots presented in Figures 1 and 2, a higher initial yeast extract content leads to a higher final ethanol concentration in the fermented medium, regardless of the immobilized cells system used.

The response surface plot presented in Figure 3 illustrates the effects of the initial glucose content and sodium alginate concentration on ethanol production at a constant initial yeast extract content (2 g/L).

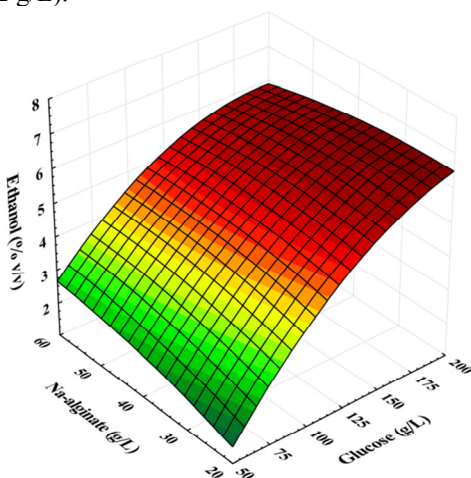


Figure 3. The effects of the initial glucose content and sodium alginate concentration on the ethanol production at a constant yeast extract content (2 g/L)

As it can be seen from the results presented on this figure, the increase of the glucose content in the medium results in the maximum ethanol concentration. On the other hand, it is evident that the ethanol production does not depend on the sodium alginate concentration used for yeast cell immobilization for all initial glucose contents. According to the predictions of the model, the ethanol yield is at a maximum (6.5% v/v) at the maximum values of the initial glucose content (175-200 g/L), regardless of the sodium alginate concentration. These results are in agreement with the fact that a combination of a high sugar in the medium and immobilized yeast cells lead to high ethanol production (12, 13).

Optimization of bioethanol production

The final use of response surface methodology is the process optimization. A form for optimization of the process with two or more outputs is the use of a desirability function (D) which was proposed by Derringer and Suich in 1980. Individual response surfaces are determined for each response. The predicted values obtained from each response surface are transformed to a dimensionless scale d_i . The scale of the desirability function ranges between $d=0$ (for an unacceptable response value) and $d=1$ (for a completely desirable one). Desirability function is calculated by combining the individual desirability values using the geometric mean: $D = (d_1 \times d_2 \times \dots \times d_m)^{1/m}$. This function has been frequently used during the optimization of multiple response processes in science and engineering (14).

In this study, the concept of desirability function was used to optimize glucose and yeast extract content in the fermentation medium as well as sodium alginate concentration used for the immobilization of yeast cells. Depending on the selected responses, three sets of optimization were made, and the obtained results are presented in Table 3.

Table 3. The optimal values of parameters and selected response

Factors and responses	Goal	Predicted value	Goal	Predicted value	Goal	Predicted value
	First set		Second set		Third set	
Glucose (g/L)	in range	196.42	in range	197.28	in range	135.48
Yeast extract (g/L)	in range	3.77	in range	3.87	in range	4.00
Na-alginate (g/L)	in range	22.84	in range	46.83	in range	41.02
Ethanol (% v/v)	maximize	7.21	maximize	6.98	maximize	6.10
"Eluted" cell number (cfu/mL·10 ⁶)	in range	8.10	minimize	0.03	minimize	0.15
Residual glucose (g/L)	in range	42.95	in range	69.82	minimize	7.21
Desirability	1.00		1.00		0.92	

If the only goal of the optimization is to achieve maximum ethanol concentration in fermented media (first set), which is a direct indicator of the success of the alcoholic fermentation, the desirability function has maximum value (1.00) at the initial contents of

glucose and yeast extract of 196.42 g/L and 3.77 g/L, respectively, and sodium alginate concentration of 22.84 g/L. By applying media with such nutrients contents and using that concentration of sodium alginate for yeast cells immobilization the model predicts ethanol concentration of 7.21% (v/v), number of "eluted" yeast cells of $8.10 \cdot 10^6$ cfu/mL and residual glucose content of 42.92 g/L.

In the alcoholic fermentation with immobilized *Saccharomyces cerevisiae* it is very important to minimize "elution" of yeast cells from the alginate beads. Therefore, the second set of optimization was performed to maximize the ethanol concentration and minimize the number of "eluted" yeast cells in the applied experimental conditions. The developed model with the desirability function of 1.00 predicts that the maximum ethanol concentration of 6.98% (v/v) and minimum number of "eluted" yeast cells of $0.03 \cdot 10^6$ cfu/mL are achieved when the optimal values of sodium alginate concentration and initial content of glucose and yeast extract in the fermentation medium are 46.83 g/L, 197.28 g/L and 3.87 g/L, respectively.

The composition of the fermentation medium is of critical importance for the success of the bioprocess. When defining the media composition it must be taken into account that the higher process efficiency can be achieved when the residual nutrients content is minimal. In addition, the unused nutrients represent losses from an economic viewpoint. Also, the processing wastewater with the high level of organic pollution before discharge into the environment increases the cost of the production process (15). Hence, in the third set of optimization, in addition to achieving the maximum ethanol concentration in the fermented medium and minimum number of "eluted" yeast cells, the minimum residual content of glucose was selected as response. The established model predicts that the maximum ethanol concentration of 6.10% (v/v), minimum number of "eluted" yeast cell of $0.15 \cdot 10^6$ cfu/mL and minimum amount of residual glucose of 7.21 g/L are produced when the optimal values of sodium alginate concentration and initial content of glucose and yeast extract in the medium for bioethanol production with immobilized cells of *Sacharomyces cerevisiae* are 41.02 g/L, 135.48 g/L and 4 g/L, respectively.

The results obtained in all three sets of optimization represent the basis for further techno-economic analyses of the process to select the optimum fermentation conditions for the ethanol production at an industrial scale. In addition, the results of the first optimization set represent the basis for further research which would include the prolongation of fermentation time over the applied 48 h, aimed at minimization of the unmetabolized glucose content in the fermented medium. On the other hand, in order to justify the use of immobilized yeast cells for ethanol production on media with lower initial sugar content (third set), future research should include application of semi-continuous or continuous fermentation process.

CONCLUSIONS

The response surface methodology based on a Box-Behnken design was successfully employed to optimize the ethanol production by immobilized cells of *Saccharomyces cerevisiae* in the applied experimental conditions. The obtained second-order polynomial models gave a satisfactory description of the experimental data. The optimized variable

factors were determined as follows: glucose content of 135.48 g/L, yeast extract content of 4 g/L and sodium alginate concentration of 41.02 g/L. Under the optimum conditions, the model predicts a maximum ethanol yield of 6.10% (v/v), minimum number of "eluted" yeast cells of $0.15 \cdot 10^6$ cfu/mL and minimum amount of residual glucose of 7.21 g/L. The results obtained in this study can be used for further techno-economic analyses of the process, to select the optimum conditions of ethanol production process for industrial application.

Acknowledgement

The authors gratefully acknowledge the support of the Ministry of Education, Science and technological Development of the Republic of Serbia, Project Number: TR-31002.

REFERENCES

1. Najafpour, G.; Younesi, H.; Ismail, K.S.K. Ethanol fermentation in an immobilized cell reactor using *Saccharomyces cerevisiae*. *Biores. Tech.* **2004**, *96* (3), 251-260.
2. Bafrcnová, P.; Šmogrovičová, D.; Sláviková, I.; Pátkova, J.; Dömény, Z. Improvement of very high gravity ethanol fermentation by media supplementation using *Saccharomyces cerevisiae*. *Biotechnol. Lett.* **1999**, *21* (4), 337-341.
3. Ghorbani, F.; Younesi, H.; Sari, A.E.; Najafpour, G. Cane molasses fermentation for continuous ethanol production in an immobilized cells reactor by *Saccharomyces cerevisiae*. *Renew. Eng.* **2011**, *36* (2), 503-509.
4. Behera, S.; Kar, S.; Mohanty, R.C.; Ray, R.C. Comparative study of bio-ethanol production from mahula (*Madhuca latifolia L.*) flowers by *Saccharomyces cerevisiae* cells immobilized in agar agar and Ca-alginate matrices. *Appl. Eng.* **2010**, *87* (1), 96-100.
5. Pátková, J.; Šmogrovičová, D.; Dömény, Z.; Bafrcnová, P. Very high gravity worth fermentation by immobilised yeast. *Biotechnol. Lett.* **2000**, *22* (14), 1173-1177.
6. Grahovac, J.; Dodić, J.; Dodić, S.; Popov, S.; Jokić, A. Optimization of ethanol production from thick juice: A response surface methodology approach. *J. Flue.* **2012**, *93*, 221-228.
7. Ferreira, S. L. C.; Bruns, R. E.; Ferreira, H. S.; Matos, G. D.; David, J. M.; Brandão, G. C.; da Silva, E. G. P.; Portugal, L. A.; dos Reis, P. S.; Souza, A. S.; dos Santos, W. N. L. Box-Behnken design: An alternative for the optimization of analytical methods. *Anal. Chim. Acta.* **2007**, *597* (2), 179-186.
8. Rončević, Z.; Dodić, J.; Grahovac, J.; Dodić, S.; Bajić, B.; Vučurović, D.; Tadijan, I. Optimization of C:N:P ratio in media for bioethanol production with immobilized cells of *Saccharomyces cerevisiae*, Proceedings, 9th Conference on Sustainable Development of Energy, Water and Environment Systems, 20-27th September 2014, Venice – Istanbul, SDEWES2014.0330, p.1-10.
9. Sasikumar, E.; Viruthagiri T. Optimization of Process Conditions Using Response Surface Methodology (RSM) For Ethanol Production from Pre-treated Sugarcane Bagasse: Kinetics and Modeling. *Bioenerg. Res.* **2008**, *1*, 239-247.

10. Pradeep, P.; Reddy, O. V. S.; Mohan, P. R.; Ko, S. Process optimization for ethanol production from very high gravity (VHG) finger millet medium using response surface methodology. *I. J. of Biotech.* **2012**, *10* (3), 168-174.
11. Pradeep P.; Krishna Goud G.K.; Reddy O.V.S. Optimization of very high gravity (VHG) finger millet (Ragi) medium for ethanolic fermentation by yeast. *Chiang Mai J Sci.* **2010**, *37*, 116-123.
12. Mei, X.; Liu, R.; Shen, F; Wu, H. Optimization of Fermentation Conditions for the Production of Ethanol from Stalk Juice of Sweet Sorghum by Immobilized Yeast Using Response Surface Methodology. *Eng. And Fuels.* **2009**, *23*, 487-491.
13. Behera, S.; Kar, S.; Mohanty, R.C.; Ray, R.C. Comparative study of bio-ethanol production from mahula (*Madhuca latifolia* L.) flowers by *Saccharomces cerevisiae* cells immobilized in agar agar and Ca-alginate matrices. *Appl Energy* **2010**, *87*, 96-100.
14. Jeong, I. J.; Kim, K. J. An interactive desirability function method to multiresponse optimization. *Eur. J. Oper. Res.* **2009**, *195* (2), 412-426.
15. Rončević, Z.; Bajić, B.; Grahovac, J.; Dodić, J.; Dodić S. Effect of the initial glycerol concentration in the medium on the xanthan biosynthesis. *APTEFF* **2014**, *45* (1), 239-246.

ОПТИМИЗАЦИЈА АЛКОХОЛНЕ ФЕРМЕНТАЦИЈЕ ЋЕЛИЈАМА КВАСЦА ИМОБИЛИСАНИМ У КУГЛИЦАМА КАЛЦИЈУМ-АЛГИНАТА

Јована Ј. Ђуран, Зорана З. Рончевић, Бојана Ж. Бајић, Синиша Н. Додић, Јована А. Граховац, Александар И. Јокић, Јелена М. Додић

Универзитет у Новом Саду, Технолошки факултет, Булевар цара Лазара 1, 21000 Нови Сад, Србија

Чињеница да је биоетанол обновљив и еколошки прихватљив извор енергије довела је до драстичног повећања његових производних капацитета, а самим тим и до потражње за ефикасном техником ферментације. Алкохолна ферментација подлога са високим садржајем шећера је један од начина да се повећа ефикасност производње етанола. У циљу бољег искоришћења супстрата и очувања метаболичке активности ћелија квасца у условима повећање концентрације инхибитора значајну улогу има примена имобилисаних ћелијских система. У алкохолној ферментацији се у највећој мери примењује метод имобилизације ћелија квасца умрежавањем у куглицама калцијум-алгината због једноставног поступка имобилизације у благим условима као и могућности умрежавања велике количине ћелија. Осим примене имобилисаних система унапређење алкохолне ферментације могуће је остварити оптимизацијом састава хранљиве подлоге. Циљ овог истраживања је оптимизација концентрације натријум-алгината, као и садржаја глукозе и екстракта квасца у хранљивој подлози за алкохолну ферментацију имобилисаним ћелијама *Saccharomyces cerevisiae*. Експерименти базирани на Вох-Веһкен-овом дизајну изведени су шаржним поступком у ерленмајерима запремине 300 ml у трајању од 48 h на температури од 28°C, при брзини мешања од 200 o/min под анаеробним условима. Оптимизација алкохолне ферментације је извршена применом методе жељене функције

у комбинацији са полиномским зависностима посматраних одзива. Највећи садржај етанола од 7,21% (v/v) постиже се када су оптималне вредности концентрације натријум-алигината и почетних садржаја глукозе и екстракта квасца у подлози 22,84 g/l, 196,42 g/l и 3,77 g/l, редоследом. Овај принос добијен је оптимизацијом за коју жељена функција има вредност 1,00. Како би се минимизовао број ћелија квасца "испраних" из куглица носача, као и садржај неискоришћене глукозе у проферментисаној подлози урађена су још два сета оптимизације. Добијени резултати представљају основу за даљу техно-економску анализу процеса која би разрешила оправданост мањег садржаја етанола у проферментисаној подлози са циљем уштеде састојака хранљиве подлоге и смањења органског оптерећења отпадних токова.

Кључне речи: Етанол, *Saccharomyces cerevisiae*, имобилизација, оптимизација, RSM.

Received: 27 August 2015.
Accepted: 30 September 2015.

CHEMOMETRIC ESTIMATION OF THE RETENTION BEHAVIOR OF SELECTED ESTRADIOL DERIVATIVES

Milica Ž. Karadžić¹*, Davor M. Lončar², Lidija R. Jevrić¹, Sanja O. Podunavac-Kuzmanović¹, Strahinja Z. Kovačević¹ and Stela D. Jokić³

¹ University of Novi Sad, Faculty of Technology, Bulevar cara Lazara 1, 21000 Novi Sad, Serbia

² SUPERLAB, Milutina Milankovića 25, 11070 Novi Beograd, Serbia

³ J.J. Strossmayer University of Osijek, Faculty of Food Technology, F. Kuhača 18, 31000 Osijek, Croatia

Quantitative structure-retention relationship (QSRR) analysis has been performed in order to correlate the retention of selected estradiol derivatives with their calculated molecular lipophilicity. The lipophilicity descriptors were derived computationally and most important were selected. Linear regression (LR) was used for model establishing. Statistical quality of the generated models was determined by standard statistical and cross-validation statistical parameters. Statistically significant and physically meaningful models were obtained. The prediction results are very well correlated with the experimentally observed data. Given predictive ability of the established models indicates that they could be used for predicting the chromatographic behavior of the similar molecules in normal-phase high-performance thin-layer chromatography.

KEY WORDS: estradiol derivatives, chromatography, QSRR, lipophilicity, linear regression

INTRODUCTION

One of the steroid hormones that naturally occurs in the human body is estradiol. It is also an estrogen sex hormone, the primary female sex hormone. Estradiol can be found in most vertebrates as well as many insects, fish and other animal species (1). In many studies, the identification and quantitation of estradiol is a subject of interest. The most sensitive method and widely used technique for estradiol determination is liquid chromatography (LC) (2-5). In environmental analyses, reversed-phase high pressure liquid chromatography (RP HPLC) with different detectors is used (6). Although being less sensitive, the method of thin layer chromatography (TLC) can be used for estradiol determination (7,8).

For understanding the chromatographic processes, it is very useful to establish the mathematical models. Quantitative structure-retention relationship (QSRR) is a technique for determining relationships between chromatographic properties of investigated mole-

* Corresponding author: Milica Ž. Karadžić, University of Novi Sad, Faculty of Technology, Bulevar cara Lazara 1, 21000 Novi Sad, Serbia, e-mail: mkaradzic@hotmail.com

cules and molecular descriptors. In QSRR studies, two groups of input data are needed, dependent and independent variables (9). The use of computational methods increases, particularly for prediction of the influence of various factors on biological activity and for establishing correlations between them. A very important step in establishing the QSRR models is to select the most suitable descriptors for predicting retention. In this paper, molecular lipophilicity descriptors were calculated using suitable software for molecular design.

One of the most important physicochemical properties of a molecule that determines its bioactivity is its lipophilicity. Estimation of the lipophilic character of new, potentially biologically active compounds is considered as one of the first parameters to be determined. Lipophilicity is a molecular property that expresses the relative affinity of a solute for aqueous and organic phases (10). Rapidly increasing use of lipophilicity in modeling of the biological processes indicates the great need for valid procedures for quantification of this physicochemical property.

The aim of this study was to characterize the physicochemical properties of estradiol derivatives and to find the possible relationship between retention characteristics and lipophilicity parameters of investigate compounds in order to understand the separation mechanism in the given chromatographic system. Additionally, the task was to evaluate if established models can be used for the prediction of the retention behavior in given chromatographic systems and to mark the best predictive model for ten estradiol derivatives. Ten estradiol derivatives were examined using normal-phase high-performance thin-layer chromatography (NP HPTLC).

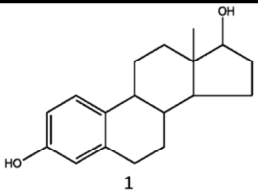
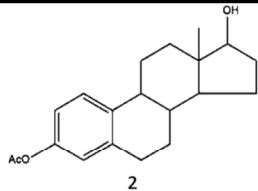
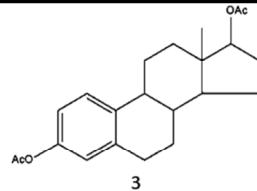
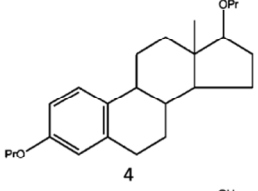
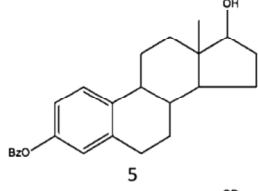
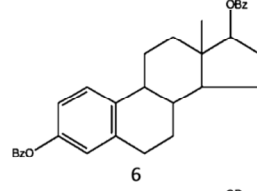
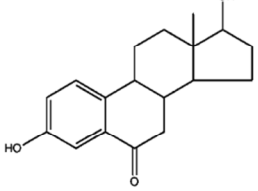
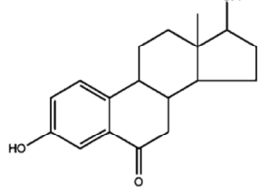
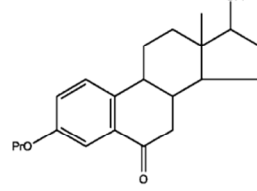
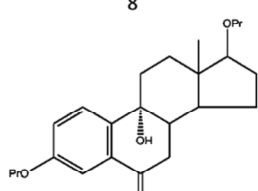
EXPERIMENTAL

Thin-layer chromatography

High performance TLC was performed on 10 x 10 cm plates that were pre-coated with silica gel 60 with fluorescence indicator (Merck, Darmstadt, Germany). The investigated compounds were dissolved in methanol (2 mg/ml). Glass capillaries were used to apply samples on the plates 1 cm from the edge. The mobile phases were benzene-acetone (9:1 v/v) and benzene-ethyl acetate (9:1; 8:2 v/v). After chromatograms development, the plates were dried at the room temperature (20-22°C) and spots were detected under UV light ($\lambda = 254$ nm). The R_F values are averages from at least three chromatograms developed for each solute-mobile phase combination. All solvents used in the analysis were of analytical grade purity.

The names and 2D chemical structures of 10 investigated estradiol derivatives are presented in Table 1.

Table 1. 2D chemical structures and names of studied compounds

		
		
		
		
1	3,17- β -dihydroxy-estra-1,3,5(10)-trien	
2	2-acetoxy-17- β -hydroxy-estra-1,3,5(10)-trien	
3	3,17- β -diacetoxy-estra-1,3,5(10)-trien-1,3,5(10)-trien	
4	3,17- β -dipropionyloxy-estra-1,3,5(10)-trien	
5	3-benzoyloxy-17- β -hydroxy-estra-1,3,5(10)-trien	
6	3,17- β -dibenzoyloxy-estra-1,3,5(10)-trien	
7	3,17- β -dihydroxy-estra-1,3,5(10)-trien-6-on	
8	3-hydroxy-17- β -propionyloxy-estra-1,3,5(10)-trien-6-on	
9	3,17- β -dipropionyloxy-estra-1,3,5(10)-trien-6-on	
10	3,17- β -dipropionyloxy-9- α -hydroxy-estra-1,3,5(10)-trien-6-on	
AcO - acetoxy group; BzO - benzoyl group; Pr - propionyl group		

Molecular modeling and molecular descriptors

For 2D molecular structures, ChemBioDraw Ultra v12.0 software was used and 3D structures were obtained by ChemBio3D Ultra v12.0 program (11). The 3D models were subjected to energy minimization using molecular mechanism force field method (MM2). The minimization was performed until the root mean square (RMS) value reached a value smaller than 0.1 kcal/Åmol. The values of the lipophilicity descriptors for each molecule in the data set are computed using the software MarvinSketch v6.1, ChemBio3D Ultra v12.0, ALOGPS 2.1, Molinspiration and PaDEL Descriptor (12-15). ChemBio3D Ultra v12.0 calculates lipophilicity descriptors from 3D structure and all other programs calculate lipophilicity descriptors from 2D structure. Software ALOGPS 2.1. is considered as an accurate tool for predicting the lipophilicity and aqueous solubility of molecules (16).

QSRR analysis

LR was used for QSRR analysis. The LR analysis is used for modeling the relationship between the dependent variable and just one independent variable. It attempts to model the relationship between two variables by fitting a linear equation to observed data. Standard statistical parameters: Fisher's criteria (F), correlation coefficient (r) and standard deviation (s) and *cross-validation* parameters: *cross-validated* coefficient of determination (r_{cv}^2), adjusted coefficient of determination (r_{adj}^2), predictive residual sum of squares (PRESS), total sum of squares (TSS), PRESS/TSS ration and standard deviation based on predicted residual sum of squares (S_{PRESS}) were used for model validation. High values of *cross-validation* parameters ($r_{cv}^2, r_{adj}^2 > 0.5$) indicate that the derived QSRR models have a high predictive ability (17). The QSRR modeling was conducted using NCSS&GESS software (18).

RESULTS AND DISCUSSION

Chromatographic data

Chromatographic retention data (R_M) of the investigated compounds are shown in Table 2. In the mobile phases, benzene (Bz) was used as a diluent and acetone (Ac) and ethyl acetate (EtAc) as the modifiers. As it can be concluded, at the same concentration of the modifier the retention of compounds is higher in the eluent with ethyl acetate. This suggests a higher solubility of the compounds in acetone. The higher concentration of the modifier in the mobile phase Bz-EtAc causes a decrease of retention. Also, the replacement of the hydroxy group with an acetyl group (molecules 1 and 2, 2 and 3, 1 and 3) leads to the decrease of the retention values. The same pattern can be noticed when the hydroxy group is replaced with a propionyl group (molecules 1 and 4, 3 and 4, 7 and 8, 7 and 9, 8 and 9). If the hydroxy group is replaced with a benzoyl group (molecules 1 and 5) a decrease of the retention values is also observed. The compounds in which the hydroxyl group is replaced with an acetyl, propionyl or benzoyl group are less retained, and they are less polar than the compounds that have hydroxyl group. This chromatographic behavior is described by the

phenomenon in the normal-phase chromatography: non-polar components pass more quickly through the layer/column than polar components.

Table 2. Chromatographic retention data of studied compounds

	R_M		
	Bz-An 9:1	Bz-EtAc 9:1	Bz-EtAc 8:2
1	0.259	0.589	0.087
2	-0.158	0.043	-0.358
3	-0.525	-0.399	-1.005
4	-0.589	-0.410	-1.817
5	-0.337	-0.176	-0.513
6	-0.395	-1.065	-1.399
7	0.753	1.235	0.550
8	0.347	0.689	0.158
9	-0.167	0.035	-0.327
10	0.288	0.653	0.122

QSRR analysis

The calculated lipophilicity descriptors are presented in Table 3. It can be concluded that the values of the lipophilicity descriptors are similar, with exception of AlogP and AlogP₂, which are very small for the majority of the compounds.

Table 3. Calculated lipophilicity descriptors for ten investigated compounds

Comp	logP ¹	LogP ²	AlogP _s ³	AClogP ³	milLogP ³	AlogP ³	MlogP ³	XlogP ₂ ³	XlogP ₃ ³	milLogP ⁴	ALogP ⁵	ALogP ₂ ⁵	CrippenLogP ⁵	MLogP ⁵	XLogP ⁵
1	3.75	3.91	3.57	3.84	3.43	3.81	3.63	4.23	4.01	3.43	0.44	0.19	3.61	3.22	3.47
2	3.66	3.88	3.91	4.07	3.46	3.85	3.98	4.42	2.81	3.46	-0.25	0.06	3.58	3.45	1.95
3	4.10	4.11	4.88	4.55	4.16	4.23	4.34	5.16	3.38	4.17	0.47	0.23	3.83	3.33	3.66
4	5.50	5.42	5.49	5.48	5.19	5.56	4.77	5.67	4.32	5.19	0.85	0.73	4.40	3.44	4.40
5	5.71	5.78	5.25	5.54	5.78	5.51	5.08	6.14	4.47	5.78	1.01	1.01	5.18	3.66	4.91
6	8.21	7.91	7.07	7.51	8.19	7.56	6.42	8.60	6.70	8.19	1.67	2.80	5.12	3.88	4.73
7	2.60	2.55	2.52	3.33	2.53	2.82	2.98	2.86	2.81	2.53	3.25	10.56	6.99	4.54	6.53
8	3.74	3.44	3.39	4.29	3.59	3.87	3.58	3.85	3.86	3.59	-0.11	0.01	3.19	3.11	1.88
9	4.35	4.07	4.03	4.98	4.29	4.57	4.16	4.30	4.43	4.29	0.35	0.12	4.16	3.34	2.88
10	3.27	3.00	3.41	4.23	3.72	3.56	3.39	2.92	3.17	3.72	0.46	0.21	4.77	3.55	3.32

¹MarvinSketch v6.1; ²ChemBio3D Ultra v12.0; ³ALOGPS 2.1; ⁴Molinspiration; ⁵PaDEL Descriptor

The LR analysis was carried out in order to correlate chromatographic retention (R_M) and calculated lipophilicity values and to determine the best QSRR models that can predict retention behavior. The best LR models that cover all three mobile phases (Table 2) are described by the following equations:

$$\text{Bz-An 9:1} \quad R_M = 1.7631 - 0.4389 \cdot \text{AlogPs} \quad (1)$$

$$\text{Bz-EtAc 9:1} \quad R_M = 2.4695 - 0.5478 \cdot \text{AlogPs} \quad (2)$$

$$\text{Bz-EtAc 8:2} \quad R_M = 2.3460 - 0.6644 \cdot \text{AlogPs} \quad (3)$$

It can be seen that the retention behavior is best described by the AlogPs lipophilicity descriptor. The statistical quality of established equations was determined by the standard statistical and cross-validation parameters (Table 4).

Table 4. Statistical and *cross-validation* parameters for established LR models described by equations 1-3

Eq.	r	F	s	r^2_{cv}	r^2_{adj}	PRESS	TSS	PRESS/TSS	S_{PRESS}
1	0.9057	67.24	0.1479	0.8436	0.8922	0.2541	1.6246	0.1564	0.1594
2	0.8927	58.24	0.1984	0.8201	0.8774	0.4618	2.5676	0.1799	0.2149
3	0.8244	32.87	0.3203	0.6073	0.7994	1.6061	4.0898	0.3927	0.4008

In this study, the high values of r^2_{cv} , r^2_{adj} and F and the low values of PRESS and S_{PRESS} indicate a high predictive ability of the QSRR models described by equations 1-3.

For the confirmation of the absence of a systematic error, the residuals of the predicted R_M values were plotted against the experimentally observed R_M values (Figure 1).

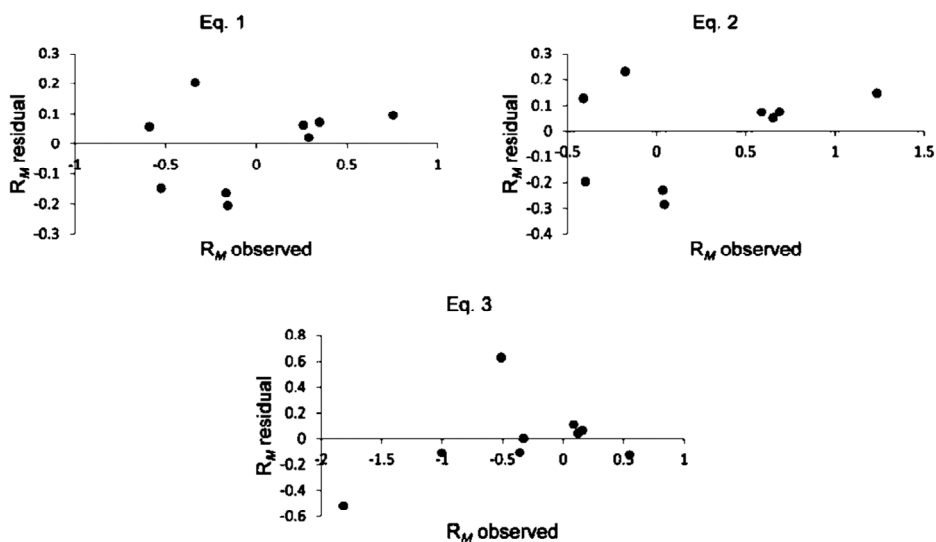


Figure 1. Experimentally observed *versus* residual R_M values

All presented results indicate that the LR models can be successfully used to predict the R_M values of the investigated estradiol derivatives. Based on the result of the given *cross-validation* parameters (Table 4) and graphs (Fig.1) it can be concluded that the best models are described by equations 1 and 2, i.e. for the eluent that contains 10 % acetone and ethyl acetate as modifiers. By the same criteria, the model described by equation 3 is also satisfactory.

In some future NP HPTLC experiments, for suitable solvent systems, the established LR models with the AlogPs lipophilicity descriptor can be used for the prediction of the retention behavior of estradiol derivatives and similar compounds. In addition, it can be concluded that by the lipophilicity parameter, the retention in NP HPTLC can be predicted as good as in reversed-phase thin-layer chromatography.

CONCLUSION

In this paper, the QSRR analysis using LR models was performed in order to identify the most important factors and quantify their influence, to select descriptors that best describe the retention behavior, and to derive mathematical models that could be able to predict the NP HPTLC chromatographic behavior of the investigated estradiol derivatives. The most appropriate molecular descriptor is AlogPs and the best statistical results were obtained with 10% acetone and 10% ethyl acetate as modifiers. Predictive power of the established models allows us to estimate the retention behavior for estrogen derivatives and similar compounds, and understand their behavior in an NP HPTLC system. Considering the small set of molecules encompassed by this study, the predictive ability of the generated models is limited.

Acknowledgment

This paper was performed within the framework of the research projects CMST COST Action No. 1105, and projects No. 172012 and 172014 and 31055 supported by the Ministry of Education, Science and Technological Development of the Republic of Serbia.

REFERENCES

1. Mechoulam, R.; Brueggemeier, R.W.; Denlinger, D.L. Estrogens in insects. *Cell. Mol. Life Sci.* **1984**, *40* (9), 942-944.
2. López de la Alda, M. J.; Barceló, D. New developments in liquid chromatography mass spectrometry for the determination of micropollutants. *J. Chromatogr. A* **2000**, *892* (1-2), 391-406.
3. Lagana, A.; Fago, G.; Marino, A.; Santarelli, D. Liquid chromatography tandem mass spectrometry applied to the analysis of natural and synthetic steroids in environmental waters. *Anal. Lett.* **2001**, *34* (6), 913-926.
4. Ingrand, V.; Herry, G.; Beausse, J.; de Roubin, M. R. Analysis of steroid hormones in effluents of wastewater treatment plants by liquid chromatography–tandem mass spectrometry. *J. Chromatogr. A* **2003**, *1020* (1), 99-104.

- Kimura, A.; Taguchi, M.; Arai, H.; Hiratsuka, H.; Namba, H.; Kojima, T. Radiation-induced decomposition of trace amounts of β -estradiol in water. *Radiat. Phys. Chem.* **2004**, *69* (4), 295-301.
- Lopez de Alda, M. J.; Barcelo, D. Use of solid-phase extraction in various of its modalities for sample preparation in the determination of estrogens and progestogens in sediment and water. *J. Chromatogr. A* **2001**, *938* (1-2), 145-153.
- Medina, M. B.; Schwartz, D. P.; Thin-layer chromatographic detection of zeranol and estradiol in fortified plasma and tissue extracts with Fast Corinth V. *J. Chromatogr.* **1992**, *581* (1), 119-128.
- Novaković, J.; Pacáková, V.; Ševčík, J.; Cserháti, T. Quantitative structure-chromatographic retention relationship study of six underivatized equine estrogens. *J. Chromatogr. B* **1996**, *681* (1), 115-123.
- Karadžić, M.Ž.; Jevrić, L.R.; Podunavac-Kuzmanović, S.O.; Lončar, E.S.; Kovačević, S.Z. Structure-retention relationship study of 2,4-dioxotetrahydro-1,3-thiazole derivatives. *J. Liq. Chromatogr. R. T.* **2015**, *38* (12), 1247-1253.
- Jevrić, L. R.; Velimirović, S. D.; Koprivica, G. B.; Mišljenović, N. M.; Kuljanin T. A.; Tepić, A. N. 2012. Prediction of s-triazine components lipophilicity of total herbicides. *Romanian Biotechnological Letters* 17:6882-6892.
- ChemBioOffice 2012. Perkin Elmer Informatics. <http://www.cambridgesoft.com/>.
- Chem Axon, Ltd. <http://www.chemaxon.com/>.
- VCCLAB, 2005. Virtual Computational Chemistry Laboratory. <http://www.vcclab.org>.
- Molinspiration Cheminformatics, <http://www.molinspiration.com/>.
- Yap, C.W. PaDEL-Descriptor. An open source software to calculate molecular descriptors and fingerprints. *J. Comput. Chem.* **2011**, *32* (7), 1466-1474.
- Tetko, I.; Tanchuk, V. Application of associative neural networks for prediction of lipophilicity in ALOGPS 2.1 program. *J. Chem. Inf. Comp. Sci.* **2002**, *42* (5), 1136-1145.
- Karadžić, M.Ž.; Jevrić, L.R.; Kovačević, S.Z.; Podunavac-Kuzmanović, S.O. Retention data from normal-phase thin-layer chromatography in characterization of some 1,6-anhydrohexose and D-aldopentose derivatives by QSRR method. *J. Liq. Chromatogr. R. T.* **2015**, *38* (10), 1044-1051.
- Hintze, J. NCSS and GESS, NCSS, LLC, Kaysville, Utah. <http://www.ncss.com/>.

ХЕМОМЕТРИЈСКА ПРОЦЕНА РЕТЕНЦИОНОГ ПОНАШАЊА ОДАБРАНИХ ДЕРИВАТА ЕСТРАДИОЛА

Милица Ж. Караџић¹, Давор М. Лончар², Лидија Р. Јеврић¹, Сања О. Подунавац-Кузмановић¹, Страхиња З. Ковачевић¹, Стела Д. Јокић³

¹ Универзитет у Новом Саду, Технолошки факултет, Булевар цара Лазара 1, 21000 Нови Сад, Србија

² СУПЕРЛАБ, Милутина Миланковића 25, 11070 Нови Београд, Србија

³ Ј.Ј. Штросмајер Универзитет у Осиеку, Прехрамбено-технолошки факултет, Ф. Кухача 18, 31000 Осиек, Хрватска

Анализа корелација између хемијске структуре и ретенције (QSRR) је примењена у циљу дефинисања корелације између ретенције одабраних деривата естрадиола и њихове рачунате молекулске липофилности. Дескриптори липофилности су

добијени компјутерски и изабрани су најбитнији. Линеарна регресија (LR) је коришћена за успостављање модела. Статистички квалитет генерисаних модела је одређен стандарним статистичким и крос валидационим статистичким параметрима. Статистички значајни и физички смислени модели су задржани. Предикт резултати су веома добро корелирани са експерименталним подацима. Предиктивна способност утврђених модела указује да они могу бити коришћени за предикцију хроматографског понашања сличних молекула у нормално фазној танкослојној хроматографији високог учинка (NP HPTLC).

Кључне речи: деривати естрадиола, хроматографија, анализа корелација између хемијске структуре и ретенције, липофилност, линеарна регресија

Received: 1 September 2015.

Accepted: 2 October 2015.

INFLUENCE OF IONIC STRENGTH ON THE RHEOLOGICAL PROPERTIES OF HYDROXYPROPYLMETHYL CELLULOSE–SODIUM DODECYLSULFATE MIXTURES

Jaroslav M. Katona*, Alena Tomšik, Sandra Dj. Bučko and Lidija B. Petrović

University of Novi Sad, Faculty of Technology, Bulevar cara Lazara 1, 21000 Novi Sad, Serbia

Mixtures of polymers and surfactants are commonly found in a range of products of pharmaceutical, cosmetic, and food industry. Interaction between polymers and surfactants influences different properties of these products, e.g. stability, flow properties, phase behavior, etc. It is known from previous work that an interaction in binary mixtures of hydroxypropylmethyl cellulose (HPMC) and sodium dodecylsulfate (SDS) takes place when SDS concentration (C_{SDS}) is higher than the critical association concentration (CAC) and lower than the polymer saturation point (PSP). The interaction results in the formation of an HPMC–SDS complex. The objective of this work was to study the effect of the ionic strength on the HPMC–SDS complex formation by rheological investigation. The HPMC/SDS mixtures composed of 0.70 % wt. HPMC, and 0.00 % to 2.50 % wt. SDS were prepared in deionized water, 0.01M and 0.05M NaCl solution. It was found that an increase in the ionic strength influences the HPMC–SDS complex formation by increasing the zero shear viscosity of the mixtures in the interaction region ($CAC < C_{SDS} < PSP$), while a decrease in the viscosity is observed for $C_{SDS} > PSP$. The HPMC/SDS mixtures showed a shear thinning or a shear thickening flow properties depending on C_{SDS} . The flow properties were influenced by the ionic strength of the mixtures.

KEY WORDS: polymer–surfactant interaction, nonionic cellulose ethers, hydroxypropylmethyl cellulose, ionic strength

INTRODUCTION

Polymers and surfactants are commonly found in many food, pharmaceutical and chemical industry products. An interaction between a polymer and a surfactant often takes place when they are jointly found in a solution. The polymer–surfactant interaction influences physico–chemical properties of the solutions and is often employed to achieve different effects such as emulsification, colloidal stability, viscosity enhancement, gel formation, solubilization, phase separation, etc. Details of polymer–surfactant interaction depend on molecular characteristics and concentration of both polymer and surfactant (1, 2, 3).

* Corresponding author: Jaroslav M. Katona, University of Novi Sad, Faculty of Technology, Bulevar cara Lazara 1, 21000 Novi Sad, Serbia, jkatona@uns.ac.rs

Hydroxypropylmethyl cellulose (HPMC) is a nonionic water-soluble cellulose ether. It is obtained by partial substitution of hydroxyl groups of cellulose with hydrophobic hydroxypropyl and methyl groups. The substituents make HPMC a typical amphiphilic polymer with properties such as ability to adsorb at air-water and oil-water interface, emulsification, self-assembly, and association with other amphiphilic molecules (4, 5). In this regard, the addition of low molar mass surfactants, especially anionics such as sodium dodecylsulfate (SDS), to HPMC solution may result in a polymer-surfactant interaction. The HPMC-SDS interaction takes place when the SDS concentration (C_{SDS}) exceeds the critical association concentration (CAC), which is a minimal surfactant concentration required for the onset of association of the surfactant and the polymer (6). The HPMC-SDS interaction takes place via hydrophobic moieties of the components, where SDS binds to HPMC chains and thereby brings about formation of the HPMC-SDS complex. The binding and complex formation support physical cross-links between entangled HPMC chains, which result in an increase in the viscosity of the HPMC/SDS mixtures. At the same time, formation of negatively charged SDS micelles along HPMC chains progressively converts the nonionic polymer into a polyanion. As C_{SDS} is further increased, the electrostatic repulsive forces between the neighboring HPMC chains start to dominate, the network structure is gradually lost, and consequently, the viscosity of the HPMC/SDS mixture drops. Individual HPMC chains become fully solubilized with SDS when C_{SDS} reaches the polymer saturation point (PSP). The increase in C_{SDS} above PSP causes only a slight decrease in the viscosity of the HPMC/SDS mixtures as a result of formation of free SDS micelles in the solution, which brings about slight conformational changes of the SDS-solubilized HPMC chains (7, 8, 9).

In this work, the influence of the ionic strength on the formation of the HPMC-SDS complex was studied by a rheological investigation of HPMC/SDS mixtures of different SDS concentration and different ionic strength.

EXPERIMENTAL

Materials

Hydroxypropylmethyl cellulose (trade name Methocel K100M CR, methoxyl content 22.6 %, hydroxypropyl content 10.5 %) was obtained from Colorcon Ltd., England. The viscosity average molar mass was $M_v=717,490$ g/mol, and the overlap concentration was $c^*=0.072$ % w/v, as determined by capillary viscometry (10). Sodium dodecylsulfate purity >99 %, was obtained from Merck, Germany. The critical micelle concentration determined at 20°C by conductometric titration was CMC=0.244 % w/v. All samples were used without any further purification. Demineralized water was used as a solvent.

Preparation of solutions

The HPMC stock solutions of different ionic strength (0.00M, 0.01M and 0.05M NaCl) were prepared by dispersing HPMC powder in the corresponding NaCl solutions at 80–90°C by gentle stirring. The stock solutions were left for 24 h at room temperature before further use. Stock solutions of SDS of different ionic strength (0.00M, 0.01M and

0.05M NaCl) were prepared by dissolving SDS in the corresponding NaCl solutions at 20°C.

The HPMC/SDS mixtures of desired ionic strength (0.00M, 0.01M and 0.05M NaCl) were containing 0.7 % w/w HPMC and 0.00–2.50 % w/w SDS, and were prepared by mixing HPMC stock solutions with the SDS stock solutions and appropriate dilution with NaCl solutions. The mixtures were vigorously hand-mixed, and were left for 48 h prior to further use.

Rheological measurements

Rheological measurements were performed on a RheoStress 600HP rheometer (ThermoHAAKE, Germany), at 20°C. The cone and plate geometry was used ($d=60$ mm, $\theta=1^\circ$), and the steady-state controlled rate method was employed to measure apparent viscosity η at different shear rates (11). The apparent viscosity was normalized against the zero shear viscosity η_0 (i.e. η/η_0) when plotting the viscosity curves. The zero shear viscosity was determined at sufficiently low shear rates, where the apparent viscosity is shear rate independent and a Newtonian plateau is observed.

RESULTS AND DISCUSSION

The zero shear viscosity of HPMC/SDS mixtures of different ionic strength

The influence of C_{SDS} on the zero shear viscosity of HPMC/SDS mixtures of different ionic strength is shown in Figure 1.

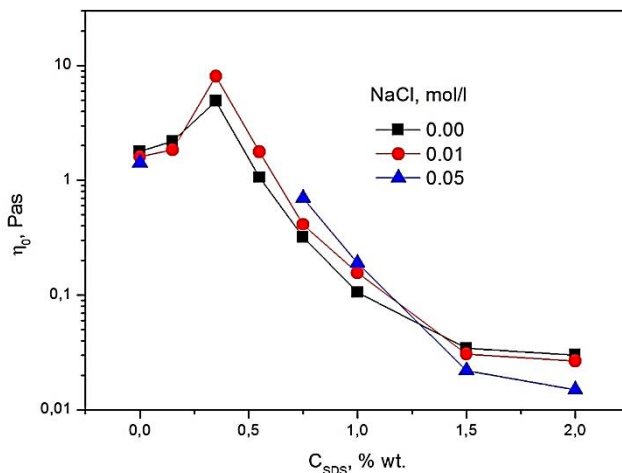


Figure 1. Influence of SDS concentration on the zero shear viscosity of the HPMC/SDS mixtures of different ionic strength

It can be seen that the increase in C_{SDS} increased the viscosity of the 0.00M NaCl HPMC/SDS mixture, to reach a maximum at $C_{SDS}=0.35$ % wt. The increase in the viscosity is due to the formation of the HPMC–SDS complex, which takes place when C_{SDS} is higher than the critical association concentration $CAC=0.15$ % wt. The complex formation takes place via hydrophobic interactions, where SDS molecules bind to the HPMC chains. SDS forms micelles around the hydrophobic moieties of the neighboring HPMC chains, which strengthens the network of entangled HPMC chains and results in an increase in viscosity (12, 13). Further increase in C_{SDS} brings about a decrease in the viscosity of the HPMC/SDS mixture. The binding of SDS causes an increase in the negative net charge of HPMC chains and thus electrostatic repulsion between neighboring HPMC chains takes place, which results in gradual disentanglement of chains, network looseness, and consequently, in a drop in the viscosity of the mixtures (14). The changes in the viscosity of the HPMC/SDS mixtures take place no more, and a constant value is reached at the C_{SDS} of 1.50 % wt. This indicates that the HPMC–SDS interaction is finished, and that C_{SDS} reached the polymer saturation point (*PSP*). At the *PSP*, all hydrophobic moieties of the HPMC chains are fully solubilized with SDS micelles, the intermolecular links between the neighboring HPMC chains are broken, and the 3D network structure is completely lost (8, 9).

The same trends in the change of the zero shear viscosity as a function of C_{SDS} are observed when the ionic strength of the HPMC/SDS mixtures is increased, indicating the same HPMC–SDS interaction mechanism. However, at increased ionic strength, the viscosity in the interaction region is higher when compared to the zero ionic strength mixture, Figure 1. This is especially true for the 0.05 % wt. NaCl mixtures (data not shown), where for the C_{SDS} ranging from 0.15 to 0.55 % wt., the viscosity was so high that it was not possible to prepare homogeneous samples for rheological measurements. The increased viscosity comes from the pronounced charge screening effect of Na^+ ions, which enables formation of SDS micelles with higher aggregation number around the hydrophobic moieties of HPMC chains (1, 15). This strengthens the network and results in an increase in the viscosity. At $C_{SDS}>PSP$, an increase in the ionic strength of the HPMC/SDS mixtures leads to a decrease in the viscosity. Namely, the charge screening makes HPMC chains solubilized by SDS effectively less charged, which makes them smaller, and this consequently brings about a decrease in the viscosity of the mixtures.

Influence of shear rate on the viscosity of HPMC/SDS mixtures of different ionic strength

The viscosity curves of the HPMC/SDS mixtures having different concentration of SDS and 0.00M NaCl ionic strength are shown in Figure 2. The mixtures with $C_{SDS} < 0.35$ % wt. and >1.50 % wt. show a typical shear thinning flow behavior, where viscosity decreases on the increase in the shear rate. However, when $C_{SDS}=0.55–1.00$ % wt. shear thinning is observed only at lower shear rates. When a critical shear rate is reached, the viscosity of the mixtures sharply increases, flow profile changes from shear thinning to shear thickening, indicating a shear–induced structure formation (16).

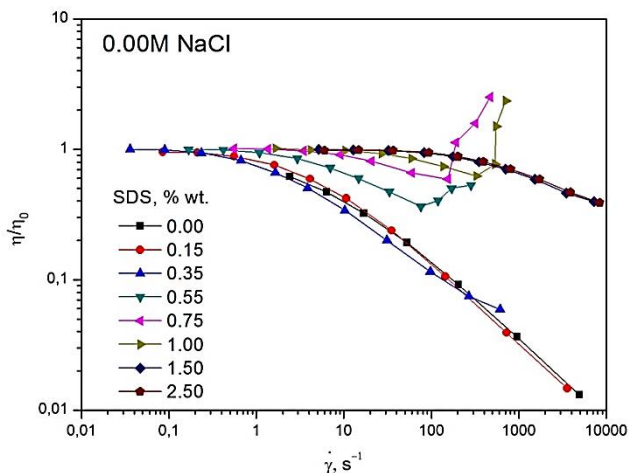


Figure 2. Viscosity curves of the HPMC/SDS mixtures containing 0.7 % wt. HPMC, 0–2.50 % wt. SDS, and 0.00M NaCl

The shear thickening flow is also observed when ionic strength of HPMC/SDS mixtures is increased, Figure 3 and Figure 4, where the shear thickening region extends to higher SDS concentrations. In the 0.01M NaCl mixtures the shear thickening flow is observed up to $C_{SDS}=1.50$ % wt., while in the 0.05% wt. NaCl mixtures the shear thickening flow is observed up to $C_{SDS}=2.00$ % wt., indicating that an increase in ionic strength of HPMC/SDS mixtures supports the shear-induced structure formation.

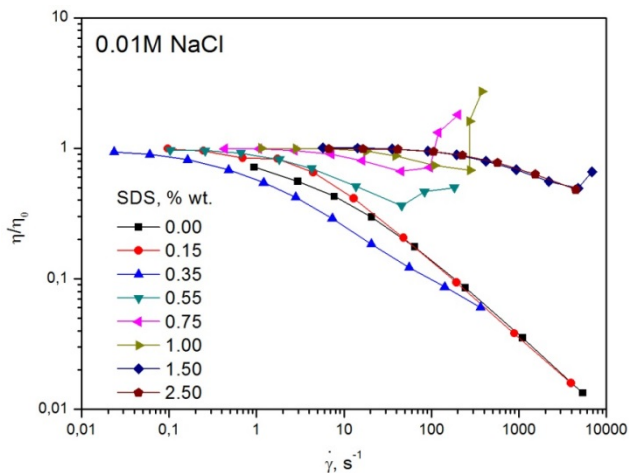


Figure 3. Viscosity curves of HPMC/SDS mixtures containing 0.7 % wt. HPMC, 0–2.50 % wt. SDS, and 0.01M NaCl

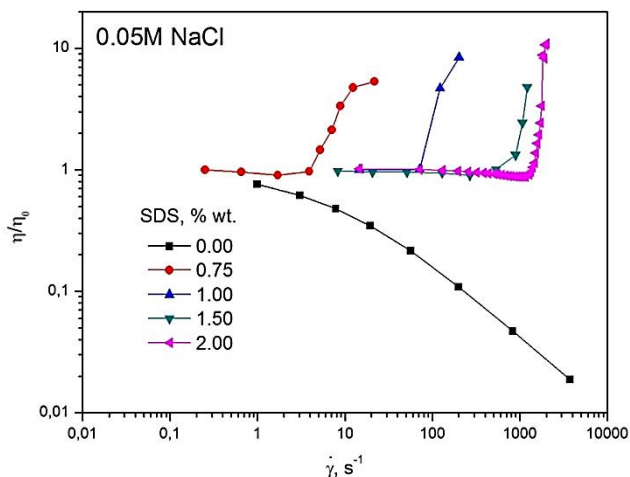


Figure 4. Viscosity curves of HPMC/SDS mixtures containing 0.7 % wt. HPMC, 0–2.50 % wt. SDS, and 0.05M NaCl.

The influence of the SDS concentration on the critical shear rate, i.e. the shear rate where the onset of shear thickening takes place, for the HPMC/SDS mixtures of different ionic strength is shown in Figure 5.

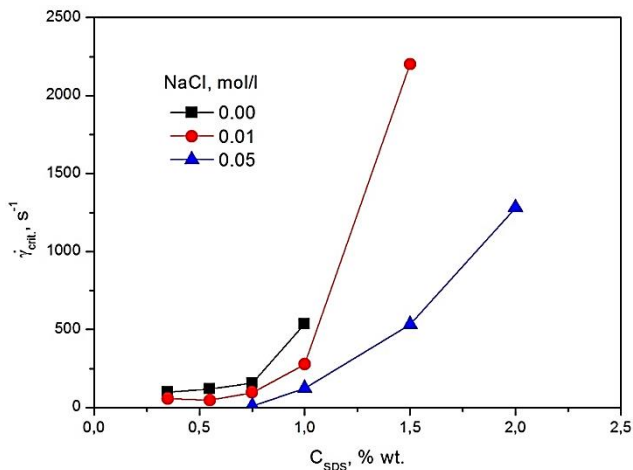


Figure 5. Influence of the SDS concentration on the critical shear rate for the HPMC/SDS mixtures of different ionic strength

It can be seen that the critical shear rate increases when the C_{SDS} of the HPMC/SDS mixture is increased, regardless of the ionic strength of the mixtures. This indicates that for a more solubilized HPMC–SDS complex a larger shear is needed to bring about conformational changes of the HPMC chains. The conformational changes make the new

hydrophobic moieties available for the establishment of the intermolecular link supported by SDS binding, and eventually lead to an increase in viscosity. On increasing the ionic strength of the HPMC/SDS mixtures the critical shear rate decreases. This is attributed to the charge of the screening effect of Na^+ ions, which makes the HPMC–SDS complex effectively less charged and thus more flexible and prone to conformational changes under the effect of shear, as opposed to highly charged polyanions having a rigid, rod-like conformation.

CONCLUSION

Interaction in the HPMC/SDS mixtures takes place when C_{SDS} is higher than the critical association concentration $\text{CAC}=0.15$ % wt. and ends at the polymer saturation point $\text{PSP}=1.50$ % wt. The increase in the ionic strength of the HPMC/SDS mixtures influence the interaction, as evidenced by an increase in the viscosity of the mixtures in the interaction region ($\text{CAC}<C_{\text{SDS}}<\text{PSP}$), and a decrease in viscosity for $C_{\text{SDS}}>\text{PSP}$. The HPMC/SDS mixtures show a shear thinning or shear thickening flow behavior, depending on C_{SDS} and ionic strength of the mixtures, indicating that a product design having desirable rheological properties can be achieved by careful tuning of polymer–surfactant interactions.

Acknowledgement

This work was supported by the Ministry of Education, Science and Technological Development of the Republic of Serbia, Grant No. III46010. It was done within COST MP1106 and CM1101 action framework.

REFERENCES

1. Lindman, B. Surfactant–Polymer Systems. In *Handbook of Applied Surface and Colloid Chemistry*; Holmberg, K., Ed.; John Wiley & Sons Ltd.: West Sussex, 2002; pp 445-463.
2. Antunes, F.E.; Marques, E.F.; Miguel, M.G.; Lindman, B. Polymer–vesicle association. *Adv. Colloid Interface Sci.* **2009**, *147-148*, 18-35.
3. Taylor, D.J.F.; Thomas, R.K.; Penfold, J. Polymer/surfactant interactions at the air/water interface. *Adv. Colloid Interface Sci.* **2007**, *132*, 69-110.
4. Camino, N. A.; Perez, O. E.; Sanchez, C. C.; Patino, J. M. R.; Pilosof, A. M. R. Hydroxypropylmethylcellulose surface activity at equilibrium and adsorption dynamics at the air–water and oil–water interfaces. *Food Hydrocolloids* **2009**, *23*, 2359-2368.
5. Futamura, T.; Kawaguchi, M. Characterization of paraffin oil emulsions stabilized by hydroxypropyl methylcellulose. *J. Colloid Interface Sci.* **2012**, *367*, 55-60.
6. Winnik, F. M.; Regismont, S. T. A. Fluorescence methods in the study of the interactions of surfactants with polymers. *Colloids Surf., A* **1996**, *118*, 1-39.
7. Nilsson, S. Interactions between Water-Soluble Cellulose Derivatives and Surfactants. 1. The HPMC/SDS/Water System. *Macromolecules* **1995**, *28*, 7837-7844.

8. Katona, J.; Sovilj, V.; Petrović, L. Rheological investigation on dynamic and structure of separated phases in polymer mixture–ionic surfactant ternary system. *Carbohydr. Polym.* **2008**, *74*, 193-200.
9. Picullel, L.; Egermayer, M.; Sjostrom, J. Rheology of Mixed Solutions of an Associating Polymer with a Surfactant. Why Are Different Surfactants Different? *Langmuir* **2003**, *19*, 3643-3649.
10. Tirrel, M. Fundamentals in Polymer Solutions. In *Interactions of Surfactants with Polymers and Proteins*; Goddard, D. E.; Ananthapadmanabhan, K.P., Eds.; CRC Press: Florida, 1993; pp 203-269.
11. Schramm, G. A. *Practical Approach to Rheology and Rheometry*; Gebrueder HAAKE GmbH: Karlsruhe, 2000; pp 36-64.
12. Su, J.C.; Liu, S.Q.; Joshi, S.C.; Lam, Y.C. Effect of SDS on the gelation of hydroxypropylmethylcellulose hydrogels. *J. Therm. Anal. Calorim.* **2008**, *93*, 495-501.
13. Nilsson, S.; Thuresson, K.; Hansson, P.; Lindman, B. Mixed Solutions of Surfactant and Hydrophobically Modified Polymer. Controlling Viscosity with Micellar Size. *J. Phys. Chem. B* **1998**, *102*, 7099-7105.
14. Silva, S.M.C.; Antunes, F.E.; Sousab, J.J.S.; Valentea, A.J.M.; Pais, A.A.C.C. New insights on the interaction between hydroxypropylmethyl cellulose and sodium dodecyl sulfate. *Carbohydr. Polym.* **2011**, *86*, 35-44.
15. Nystrom, B.; Kjoniksen, A.-L.; Lindman, B. Effect of temperature, surfactant, and salt on the rheological behavior in semidilute aqueous systems of a nonionic cellulose ether. *Langmuir* **1996**, *12*, 3233-3240.
16. Clasen, C.; Kulicke, W. M. Determination of viscoelastic and rheo-optical material functions of water-soluble cellulose derivatives. *Prog. Polym. Sci.* **2001**, *26*, 1839-1919.

УТИЦАЈ ЈОНСКЕ ЈАЧИНЕ НА РЕОЛОШКЕ ОСОБИНЕ СМЕША ХИДРОКСИПРОПИЛМЕТИЛ ЦЕЛУЛОЗЕ И НАТРИЈУМ ДОДЕЦИЛСУЛФАТА

*Јарослав М. Катона, Алена Томишиќ, Сандра Ђ. Бучко, Лидија Б. Петровић,
Јадранка Л. Фрај*

Универзитет у Новом Саду, Технолошки факултет, Булевар цара Лазара 1, 21000 Нови Сад, Србија

Производи фармацеутске, козметичке, прехранбене и хемијске индустрије врло често у свом саставу садрже смеше полимера и сурфактаната. Интеракција између полимера и сурфактаната утиче на низ особина тих производа као што су нпр. стабилност, реолошке особине, сепарација фаза и сл. Познато је да до интеракције између хидроксипропилметил целулозе (ХПМЦ) и натријум додецилсулфата (СДС) долази када је концентрација СДС $C_{СДС}$ већа од критичне концентрације асоцијације (ЦАЦ) а мања од концентрације засићења полимера (ПСП). Као последица дате интеракције долази до формирања ХПМЦ–СДС комплекса. Циљ овог рада је испитивање утицаја јонске јачине на формирање ХПМЦ–СДС комплекса путем рео-

лошких мерења. У том циљу, припремљене су ХПМЦ/СДС смеше које су садржале 0,70 % м/м ХПМЦ, 0,00 % м/м до 2,50 % м/м СДС у дејонизованој води, и 0,01М и 0,05М растворима NaCl. Добијени резултати указују да вискозитет при нултој брзини смицања смеша ХПМЦ/СДС расте са повећањем јонске јачине у опсегу ХПМЦ–СДС интеракције ($\zeta_{\text{АПЦ}} < \zeta_{\text{СДС}} < \text{ПСП}$), док опада за $\zeta_{\text{СДС}} > \text{ПСП}$. ХПМЦ/СДС смеше показују псеудопластично или дилатантно протицање у зависности од $\zeta_{\text{СДС}}$. Јонска јачина такође утиче на реолошке особине смеша.

Кључне речи: полимер–сурфактант интеракција, нејонски етри целулозе, хидроксипропилметил целулоза, јонска јачина

Received: 22 May 2015.

Accepted: 15 July 2015.

CHROMATOGRAPHIC LIPOPHILICITY AS A PREDICTOR OF ANTIPROLIFERATIVE ACTIVITY OF 17-PICOLYL AND 17-PICOLINYLIDENE ANDROSTANE DERIVATIVES TOWARD PROSTATE CANCER

Strahinja Z. Kovačević^{1*}, Sanja O. Podunavac-Kuzmanović¹, Lidija R. Jevrić¹,
Evgenija A. Djurendić², Jovana J. Ajduković² and Pavle T. Jovanov³

¹ University of Novi Sad, Faculty of Technology, Bulevar cara Lazara 1, 21000 Novi Sad, Serbia

² University of Novi Sad, Faculty of Sciences, Department of Chemistry, Biochemistry and Environmental Protection, Trg Dositeja Obradovića 8, 21000 Novi Sad, Serbia

³ University of Novi Sad, Institute of Food Technology, Bulevar cara Lazara 1, 21000 Novi Sad, Serbia

The present study describes the quantitative retention – (anticancer) activity relationship analysis of a series of 17-picoyl and 17-picolinylidene androstane derivatives based on the chromatographic data obtained by reversed-phase high performance liquid chromatography (C18-RP-HPLC) in a mobile phase consisting of 90% of methanol and 10% of water. The obtained retention factor or chromatographic lipophilicity factor ($\log k_{0,90}$) was correlated with the antiproliferative activity of studied compounds (IC_{50}) toward androgen-receptor negative prostate cancer cell line (AR-neg. PC-3). Correlation analysis was carried out by applying non-linear artificial neural networks (ANNs) method. Statistical validation showed that the obtained ANNs can successfully predict the IC_{50} values of structurally similar androstane derivatives.

KEY WORDS: Prostate cancer, chemometrics, chromatography, lipophilicity, molecular modeling.

INTRODUCTION

Lipophilicity is a molecular parameter widely used in estimation of biological and environmental behavior of many substances (1-3). There are several experimental methods for its approximation, such as shake-flask method with water-octanol partition system, potentiometric titration, etc. or computational approaches. One of the experimental approaches for lipophilicity determination is chromatography, usually on reversed phases (RP) (4). There are many studies which deal with the chromatographic determination of lipophilicity, mostly by high performance liquid chromatography (HPLC) and thin layer

* Corresponding author: Strahinja Z. Kovačević, University of Novi Sad, Faculty of Technology, Bulevar cara Lazara 1, 21000 Novi Sad, Serbia, e-mail: strahko@uns.ac.rs

chromatography (TLC) (5-7). The chromatographic lipophilicity is usually expressed as the R_M^0 parameter (TLC) or $\log k_0$ (HPLC). These parameters refer to the retention of a compound in pure water (0% of the modifier in the mobile phase). However, the chromatographic lipophilicity (R_M or $\log k$) can be determined in different stable chromatographic conditions with mobile phases which are a combination of certain volume fractions of water and a modifier (usually methanol or acetonitrile).

A series of eighteen 17 α -picolyl and 17(*E*)-picolinyliden androstane derivatives showed significant antiproliferative activity toward androgen-receptor negative prostate cancer cell line (AR-neg. PC-3) and was analyzed applying the quantitative structure-activity relationship (QSAR) approach (8). In a recent study (9), the chromatographic lipophilicity of these compounds was determined by the RP-HPLC method applying C18 stationary phase and the mobile phase composed of 90% of methanol and 10% of water. The obtained lipophilicity parameter was defined as $\log k_{0,90}$.

The main aim of the present study was to find possible correlations between the experimentally obtained chromatographic lipophilicity ($\log k_{0,90}$) of the analyzed androstane derivatives and their antiproliferative activity toward AR-neg. PC-3 cells defined by IC_{50} values. This is so-called quantitative retention-activity relationship (QRAR) approach. This approach emphasizes the significance of the chromatographic lipophilicity parameter in the prediction of different biological properties (anticancer activity, antifungal activity, antibacterial activity, etc).

In this study, the correlation analysis was carried out using artificial neural networks (ANNs) as a non-linear approach. ANNs were applied in many QSAR and QSRR (quantitative structure-retention relationship) studies with great success (10,11). They can find the complex relationships between the variables and enable the prediction of certain characteristics (biological behavior, physico-chemical parameters, etc.) on the basis of certain easily available parameters (molecular descriptors).

EXPERIMENTAL

The IUPAC names of the investigated androstane derivatives 1-18 and their antiproliferative activity (IC_{50}) toward AR-neg. PC-3 cell line are given in Table 1. The basic structures of the analyzed derivatives are given in Figure 1. The compounds were synthesized and tested according to the previously described procedures (12-14). The complete RP-HPLC determination, with diode array detector (DAD) and evaporative light scattering detector (ELSD), of chromatographic lipophilicity of studied derivatives is given in the reference (9). The molecular descriptors were calculated on the basis of 2D chemical structures by using SimulationPuls ADMET Predictor program. Regression analysis and ANN modeling were carried out by using Statistica 10, NCSS 2007 and Microsoft Excel software.

Table 1. The IUPAC names and IC₅₀ values of studied compounds

No.	IUPAC name	IC ₅₀ (μM)	Reference
1	17α-picolylyl-androst-5-en-3β,17β-diol	6.30	(12)
2	4β,5β-epoxy-17β-hydroxy-17α-picolylyl-androstane-3-one	65.50	(12)
3	5α,6α-epoxy-17α-picolylyl-androstane-N-oxide-3β,17β-diol	33.60	(14)
4	17α-picolylyl-androst-4-en-3β,17β-diol	22.30	(14)
5	17β-hydroxy-17α-picolylyl-androst-4-en-3β-yl acetate	31.30	(14)
6	17β-hydroxy-17α-picolylyl-androst-4-ene-3,6-dione	4.30	(14)
7	4,17β-dihydroxy-17α-picolylyl-androsta-4,6-dien-3-one	25.60	(14)
8	17α-picolylyl-androsta-3,5-dien-17β-ol	24.70	(14)
9	17α-picolylyl-androst-5-en-3β,4β,17β-triol	52.10	(14)
10	17(E)-picolinyliden-androst-4-en-3-one	12.90	(12)
11	4β,5β-epoxy-17(E)-picolinyliden-androstane-3-one	14.30	(12)
12	17(E)-picolinyliden-androst-4-en-3-one-N-oxide	10.10	(12)
13	3β-acetoxy-17(E)-picolinyliden-androst-5-ene-N-oxide	0.55	(12)
14	4-methoxy-17(E)-picolinyliden-androst-4-en-3-one	34.10	(14)
15	17(E)-picolinyliden-androst-4-en-3β-ol	10.10	(13)
16	17(E)-picolinyliden-androst-4-en-3β-yl acetate	66.20	(13)
17	17(E)-picolinyliden-androst-4-ene-3,6-dione	88.90	(13)
18	17(E)-picolinyliden-androsta-3,5-diene	19.90	(14)

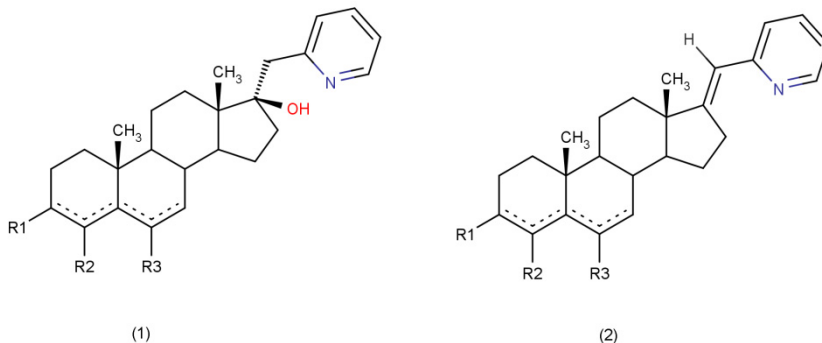


Figure 1. The basic structures of (1) 17-picolylyl and (2) 17-picolinylidene androstane derivatives

The rings A and B of the steroid core in the studied compounds are modified by different substituents, such as acetoxy, epoxy, N-oxide and methoxy functional groups.

Before the ANN modeling, the output data were normalized in the range from 0 to 1, applying the *min-max* normalization formula:

$$y_{norm} = (1 - \Delta U - \Delta L) \cdot ((y - y_{min}) / (y_{max} - y_{min})) + \Delta L \quad [1]$$

where y_{norm} , y_{max} and y_{min} are the normalized, maximum and minimum value of the dependent variable y , and ΔU , ΔL are the values of margins which limit extrapolation ability of the network ($\Delta U = \Delta L = 0.01$) (15).

RESULTS AND DISCUSSION

The ANN models were obtained by self-training (ST) ANN module in Statistica 10 program. Radial basis function (RBF) network was applied as a type of network. It is an ANN that uses radial basis functions as activation functions. The RBF values depend only on the distance from the origin of a Euclidean space, so that:

$$\phi(x) = \phi(\|x\|) \quad [2]$$

The RBF artificial neural network can be presented as the sum of N radial basis functions:

$$y(x) = \sum_{i=1}^N \omega_i \phi(\|x - x_i\|) \quad [3]$$

x_i – center, ω_i – weights

The output value of an RBF network is a linear combination of radial basis functions of the input data and neuron parameters. The input data (independent variables) were $\log k_{0.90}$ and S+SF parameters. The S+SF factor represents the ratio of the equilibrium solubility of an ionizable chemical compound's salt to its intrinsic solubility. It was obtained by *in silico* calculations by SimulationPlus software. The output data were normalized IC_{50} values. During the ST-ANN regression modeling 200 networks have been trained and the number of hidden neurons varied in the range of 2-12. The data used for the ST-ANN modeling are shown in Table 2.

Table 2. The data used for the ST-ANN modeling of antiproliferative activity of studied androstanes

Compound	Set	Input data		Output data
		$\log k_{0.90}$	S+SF	$IC_{50}(\text{norm}) \text{ exp.}$
1	Training	0.048	1070.0	0.0738
2	Training	0.093	1250.0	0.7304
3	Validation	-0.431	94.8	0.3766
4	Training	-0.128	1070.0	0.2513
5	Validation	0.439	1910.0	0.3511
6	Training	-0.389	1110.0	0.0516
7	Test	-0.413	1030.0	0.2879
8	Test	0.750	2010.0	0.2779
9	Training	-0.423	506.0	0.5818
10	Training	0.276	2590.0	0.1470
11	Training	0.266	2550.0	0.1625
12	Training	-0.053	303.0	0.1159
13	Test	0.371	356.0	0.0100
14	Training	0.350	3300.0	0.3821
15	Validation	0.414	1960.0	0.1159
16	Training	0.770	3700.0	0.7382
17	Training	-0.074	2080.0	0.9900
18	Training	1.194	3440.0	0.2246

The whole set of data was divided into three subsets: training set (12 compounds), test set (3 compounds) and validation set (3 compounds). The test set must be used to determine generalization error, while validation set is used to find the best ANN configuration and training parameters (by comparing the validation set error and the training set error during training).

The ANN modeling resulted in two acceptable networks with satisfactory characteristics (Table 3). The architecture of the obtained networks is the following: **2–10–1**, referring to the number of input data – the number of hidden neurons – the number of output data. The correlation coefficients and root mean square errors of the training set (R_{train} , $RMSE_{train}$), test set (R_{test} , $RMSE_{test}$) and validation set (R_{valid} , $RMSE_{valid}$) describe the statistical performance of the networks as very good. The R and $RMSE$ values indicate a good fitting of the data, which is confirmed by the graphical comparison of the experimental and predicted IC_{50} data (Figure 1), as well as the experimental IC_{50} and residuals (Figure 2).

Table 3. The characteristics of the obtained ANN models

Net name	Hidden activation	Output activation	R_{train}	R_{test}	R_{valid}	$RMSE_{train}$	$RMSE_{test}$	$RMSE_{valid}$
ANN1	Gaussian	Identity	0.9745	0.8096	0.5940	0.0023	0.0039	0.0149
ANN2			0.9826	0.9896	0.5763	0.0015	0.0032	0.0169

As it can be seen from Figure 2, the determination coefficients are higher than 0.80, the slope of the linear relationship is very close to 1, while the intercept is close to zero for both models. These facts are another confirmation of the assumption of the good quality of the ANN models. The relatively small dissipation of the points around linear relationship can be observed as well.

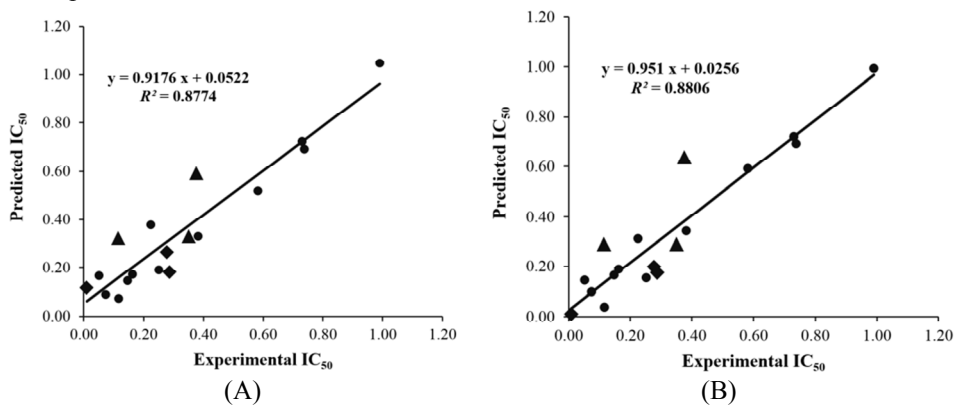


Figure 2. Comparison of the experimental and predicted IC_{50} data for the network ANN1 (A) and the network ANN2 (B) (● - training set, ♦ - test set, ▲ – validation set)

The graphical comparison of the experimental and predicted data can give an insight into the real prediction ability of the formed regression models and the ideal dependence

between these data is linear, with the intercept equal to 0 and slope equal to 1. The comparison of the experimental data and residuals (Figure 3) shows the random distribution of the residuals around the $y = 0$ axis and their relatively low amplitude, which is another confirmation of the reliability of the established ANN models.

Global sensitivity analysis (GSA) was applied to estimate the influence of every input variable on variations in the values of the parameters of the ANN model, which also have an influence on the output values. The GSA coefficients of input variables describe the change in the network's outputs due to the variations in the parameters that affect the network. A large sensitivity index of an input parameter suggests that the network's performance can be significantly changed with small variation in the input parameter (16).

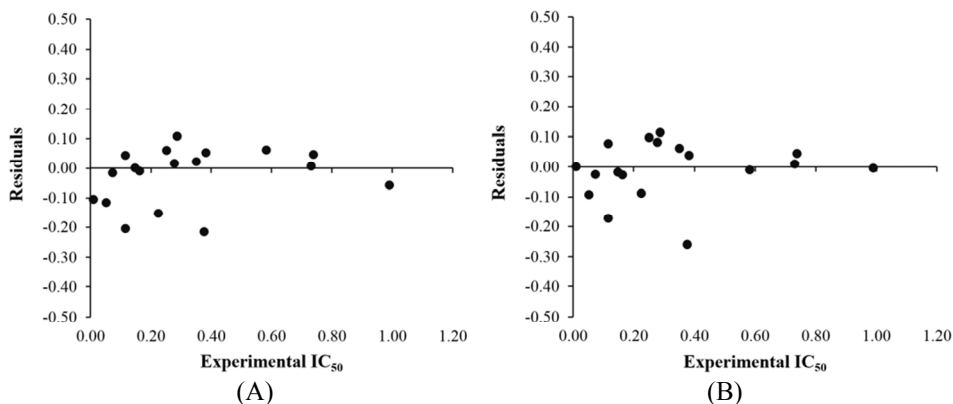


Figure 3. Comparison of the experimental IC_{50} data and the residuals for the network ANN1 (A) and the network ANN2 (B)

The GSA coefficient equal to 1 or less is a sure sign that the variable should be omitted from the ANN model (16). The results of GSA for the ANN models are shown in Table 4. Each variable has a significantly higher GSA coefficient than 1, which indicates the significance of the variables in the models.

Table 4. GSA coefficients of the input data for the obtained ANN models

Network	$\log k_{0.90}$	S+SF
ANN1	10.23	23.86
ANN2	11.51	21.04
Average	10.87	22.45

It must be emphasized that the presented ANN models predict the antiproliferative activity of the analyzed androstane derivatives in normalized form, so it is necessary to transform the predicted value in natural form by using the equation for *min-max* normalization.

CONCLUSIONS

The presented results indicate the possibility of the application of the experimentally obtained lipophilicity parameter ($\log k_{0,90}$) in the prediction of the antiproliferative activity (IC_{50}) of 17 α -picolyl and 17(*E*)-picolinylidene androstane derivatives toward prostate cancer cells. Also, another important parameter in the prediction of IC_{50} values is the *in silico* S+SF descriptor. The non-linear artificial neural networks were the most suitable regression method in defining these QRAR mathematical models. As a result of the ANN modeling, two ANN models with satisfactory statistical characteristics were obtained. The obtained models indicate that the chromatographic lipophilicity, determined under controlled chromatographic conditions, could be used as a reliable predictor of anticancer activity of structurally similar androstane derivatives.

Acknowledgement

This paper was performed within the framework of the research project No. 114-451-347/2015-02, financially supported by the Provincial Secretariat for Science and Technological Development of Vojvodina.

REFERENCES

1. Nasal, A.; Siluk, D.; Kaliszan, R. Chromatographic retention parameters in medicinal chemistry and molecular pharmacology. *Curr. Med. Chem.* **2003**, *10*, 381-426.
2. Kaliszan, R. QSRR: Quantitative structure-(chromatographic) retention relationships. *Chem. Rev.* **2007**, *107*, 3212-3246.
3. Heberger, K. Quantitative structure-(chromatographic) retention relationships. *J. Chromatogr. A* **2007**, *1158*, 273-305.
4. Jevrić, L. R.; Koprivica, G. B.; Mišljenović, N. M.; Jovanović, B. Ž. Chromatographic behavior and lipophilicity of s-triazine derivatives on silica gel impregnated with paraffin oil. *APTEFF* **2010**, *41*, 159-168.
5. Kovačević, S. Z.; Podunavac-Kuzmanović, S. O.; Jevrić, L. R.; Lončar, E. S. Assessment of chromatographic lipophilicity of some anhydro-D-aldose derivatives on different stationary phases by QSRR approach. *J. Liq. Chromatogr. Relat. Technol.* **2015**, *38*, 492-500.
6. Kovačević, S. Z.; Jevrić, L. R.; Podunavac-Kuzmanović, S. O.; Lončar, E. S. Chemometric estimation of the RP TLC retention behaviour of some estrane derivatives by using multivariate regression methods. *Cent. Eur. J. Chem.* **2013**, *11*, 2031-2039.
7. Jokić, S.; Podunavac-Kuzmanović, S. O.; Jevrić, L. R.; Sudar R.; Vidović, S.; Aladić, S.; Kovačević, S. HPLC Retention Behavior of Triacylglycerols Extracted from Soybean Oil by Supercritical CO₂. *Croat. Chem. Acta* **2014**, *87*, 261-269.
8. Kovačević, S. Z.; Podunavac-Kuzmanović, S. O.; Jevrić, L. R.; Djurendić, E. A.; Ajduković, J. J. Non-linear assessment of anticancer activity of 17-picolyl and 17-picolinylidene androstane derivatives – Chemometric guidelines for further syntheses. *Eur. J. Pharm. Sci.* **2014**, *62*, 258-266.

9. Kovačević, S. Z.: Kovačević, S. Z. Chemometric modeling of chromatographic behavior and biological activity of a series of androstane derivatives (Hemometrijsko modelovanje hromatografskog ponašanja i biološke aktivnosti serije androstanskih derivata). Ph.D. Thesis, University of Novi Sad, July 2015.
10. Garkani-Nejad, Z.; Jalili-Jahani, N. Modeling the activity of 2-phenylnaphtalene inhibitors using self-training artificial neural networks. *Cent. Eur. J. Chem.* **2010**, *8*, 877-885.
11. Garkani-Nejad, Z. Use of self-training artificial neural networks in a QSRR study of a diverse set of organic compounds. *Chromatographia* **2009**, *70*, 869-874.
12. Djurendić, E. A.; Daljev, J.; Sakač, M.; Čanadi, J.; Jovanović Šanta, S.; Andrić, S.; Klisurić, O.; Kojić, V.; Bogdanović, G.; Djurendić-Brenesel, M.; Novaković, S.; Penov Gaši, K. Synthesis of some epoxy and/or N-oxy 17-picolyl and 17-picolinylidene-androst-5-ene derivatives and evaluation of their biological activity. *Steroids* **2008**, *73*, 129-138.
13. Djurendić, E. A.; Ajduković, J. J.; Sakač, M. N.; Čanadi, J. J.; Kojić, V. V.; Bogdanović, G. M.; Penov Gaši, K. M. 17-Picolinylidene-substituted steroid derivatives and their antiaromatase and cytotoxic activity. *ARKIVOC* **2009**, *13*, 311-323.
14. Djurendić, E. A.; Ajduković, J. J.; Sakač, M. N.; Čanadi, J. J.; Kojić, V. V.; Bogdanović, G. M.; Penov Gaši, K. M. Synthesis and cytotoxic activity of some 17-picolyl and 17-picolinylidene androstane derivatives. *Eur. J. Med. Chem.* **2012**, *54*, 784-792.
15. Jayalakshmi, T.; Santhakumaran, A. Statistical normalization and back propagation for classification. *IJCTE* **2011**, *3*, 89-93.
16. Shojaeefard, M. H.; Akbari, M.; Tahani, M.; Farhani, F. Sensitivity analysis of the artificial neural network outputs in friction stir lap joining of aluminium to brass. *Adv. Mater. Sci. Eng.* **2013**, *2013*, 1-7.

ПРЕДВИЂАЊЕ АНТИКАНЦЕРОГЕНЕ АКТИВНОСТИ 17-ПИКОЛИЛ И 17-ПИКОЛИНИЛИДЕН АНДРОСТАНСКИХ ДЕРИВАТА НА ОСНОВУ ХРОМАТОГРАФСКЕ ЛИПОФИЛНОСТИ

Страхиња З. Ковачевић¹*, Сања О. Подунавац-Кузмановић¹, Лидија Р. Јеврић¹,
Евгенија А. Ђурендић², Јована Ј. Ајдуковић², Павле Т. Јованов³

¹ Универзитет у Новом Саду, Технолошки факултет, Булевар цара Лазара 1, 21000 Нови Сад, Србија

² Универзитет у Новом Саду, Природно-математички факултет, Департман за хемију, биохемију и заштиту животне средине, Трг Доситеја Обрадовића 8, 21000 Нови Сад, Србија

³ Универзитет у Новом Саду, Институт за прехранбене технологије, Булевар цара Лазара 1, 21000 Нови Сад, Србија

Изведена анализа описује квантитативне зависности између ретенционог понашања серије 17-пиколил и 17-пиколинилиден андростанских деривата, дефинисаног помоћу течне хроматографије високих перформанси на обрнутим фазама (C18-RP-HPLC) са мобилном фазом састављеном од 90% метанола и 10% воде, и њихове антипролиферативне активности (IC₅₀) према ћелијама андроген-рецептор негативног канцера простате (AR-neg. PC-3). Ретенциони фактор (log*k*_{0,90}), односно хрома-

тографска липофилност, корелиран је са IC_{50} вредностима испитиваних деривата применом нелинеарне методе вештачких неуронских мрежа. Статистичка валидација показала је да добијене неуронске мреже могу успешно бити примењене за предвиђање антипролиферативне активности структурно сличних андростанских деривата.

Кључне речи: Канцер простате, хеометрија, хроматографија, липофилност, моделовање молекула.

Received: 5 August 2015.
Accepted: 11 October 2015.

ESTIMATION OF CHROMATOGRAPHIC LIPOPHILICITY OF SOME D-HOMO ANDROSTENE DERIVATIVES

Nada U. Perišić Janjić¹, Katarina M. Penov Gaši¹, Evgenija A. Djurendić¹, Marina P. Savić¹, Strahinja Z. Kovačević², Stela D. Jokić³ and Sanja O. Podunavac-Kuzmanović^{2*}

¹ University of Novi Sad, Faculty of Sciences, Department of Chemistry, Biochemistry and Environmental Protection, Trg Dositeja Obradovića 8, 21000 Novi Sad, Serbia

² University of Novi Sad, Faculty of Technology, Bulevar cara Lazara 1, 21000 Novi Sad, Serbia

³ J.J. Strossmayer University of Osijek, Faculty of Food Technology, F. Kuhača 18, 31000 Osijek, Croatia

Quantitative structure-retention relationship (QSRR) method was applied to study the chromatographic behaviour of D-homo-androstene derivatives 1-7. Retention constants (R_M^0) of the analysed derivatives were determined by reversed-phase high-performance thin-layer chromatography (RP HPTLC) on C18 plates by using four mobile phase mixtures: methanol-water, acetone-water, acetonitrile-water, and dioxane-water. Correlation analysis based on multiple regression method was applied in order to model chromatographic retention by means of nine different lipophilicity descriptors ($\log P$). The developed QSRR models were cross-validated and high-quality validation parameters were obtained by leave-one-out method. It was found that the derived QSRR models have a good predictive ability.

KEY WORDS: QSRR, chemometrics, RP HPTLC, lipophilicity

INTRODUCTION

Androgens are a group of chemically related sex steroid hormones. These steroid hormones orchestrate growth and development of the male reproductive system. Later in life, these hormones trigger male puberty, influencing vocals, body ornamentation, muscle mass, and behaviour such as sex drive and aggressiveness. Like all steroid hormones, androgens produce effects by docking with receptors on the cell's membrane surface or inside the cell in the liquid cytoplasm. Receptor binding triggers different chemical signaling systems depending on receptor location (1). Androgens are converted to other steroid hormones through enzymatically catalyzed reactions (2-4).

The physicochemical properties predicted from structure are helpful in the search of new molecules of similar or increased biological activity. The development of steroidal drugs is often followed by research on structure-activity relationship (SAR) studies (5-7). Quantitative structure-activity relationship (QSAR) approach, including multivariate data

* Corresponding author: Sanja Podunavac-Kuzmanović, University of Novi Sad, Faculty of Technology, Bulevar cara Lazara 1, 21000 Novi Sad, Serbia, e-mail: sanya@uns.ac.rs

analysis in combination with statistical design, has become extensively used. This method represents an attempt to correlate biological activities of compounds with structural or molecular descriptors including physicochemical, electronic, geometrical, topological or thermodynamic parameters. Progress in the use of QSAR methods has shown the importance of the hydrophobic or lipophilic nature of biologically active molecules. Octanol-water partition coefficient, referred to as $\log P$, is a frequently used parameter in organic synthetic chemistry. It is a quantitative descriptor of lipophilicity, one of the key determinants of pharmacokinetic properties (8). $\log P$ is commonly used in QSAR studies and drug design, since this property is related to drug absorption, metabolism, bioavailability and toxicity. There are many methods for estimating $\log P$, experimental as well as computational. The traditional shake flask method is often replaced by alternative methods, such as reversed-phase liquid chromatography (RPLC). Chromatographic methods are experimentally simple, low cost, accurate, and have high-throughput. Quantitative structure-retention relationship (QSRR) analysis is among the most extensively studied manifestations of linear free-energy relationships (LFER). These are the statistically derived relationships between the structures of solutes and their chromatographic retention (9). The application of RP HPTLC, as well as normal-phase (NP) HPTLC chromatographic data of androstene derivatives to a QSRR and QSAR studies has been described in our previous papers (10,11). In this context, the aim of the present study was to investigate chromatographic behaviour of *D-homo*-androstene derivatives **1-7** and determine the quantitative relationships between the retention constants and their chemical structures. A central object of this study was to establish multivariate quantitative lipophilicity-retention relationships and to derive the high quality models which correlate the lipophilicity of these compounds with their retention data.

EXPERIMENTAL

The structures of the investigated androstene derivatives 1-7 are presented in Fig. 1. The compounds were synthesized according to earlier described procedures (12,13). The chemical structures of the molecules were drawn by HyperChem software (HyperCube Inc, Version 7.5). Semiempirical AM1 calculations were used for compounds geometry optimization by the program implemented in HyperChem. Chromatographic analysis was performed on 10 cm x 10 cm HPTLC plates coated with C_{18} silica F₂₅₄ (Merck). The solvent mixtures used as mobile phases are listed in Table 1.

Table 1. The solvent mixtures used as mobile phases

Mobile phase	Volume fraction of organic modifier, φ
Methanol-water	0.5-0.9
Acetone-water	0.5-0.8
Acetonitrile-water	0.5-0.7
Dioxane-water	0.5-0.7

The compounds investigated were separately dissolved in methanol (1 mg/ml), and 0.2 μ l of the solutions were spotted on the plates. Chromatograms were developed by the ascending technique at room temperature, without previous saturation of the chamber with the solvent. The plates were dried at room temperature and the spots were visualized under UV light at $\lambda = 254$ nm. The R_f values were the averages of at least three measurements. For the subsequent calculations, the mean R_M values were used, which were calculated by use of the following equation: $R_M = \log(1/R_f - 1)$. The calculated R_M values for different concentrations of organic solvent were used to check the linearity of their relationship with the volume fraction of the organic modifier according to the equation: $R_M = R_M^0 + m\varphi$, where φ is the volume fraction of organic solvent in the mobile phase, R_M^0 (intercept) is the R_M value extrapolated to zero concentration of organic modifier (best estimation of the lipophilicity), and m (slope) is related to the specific hydrophobic surface area of the androstene derivatives.

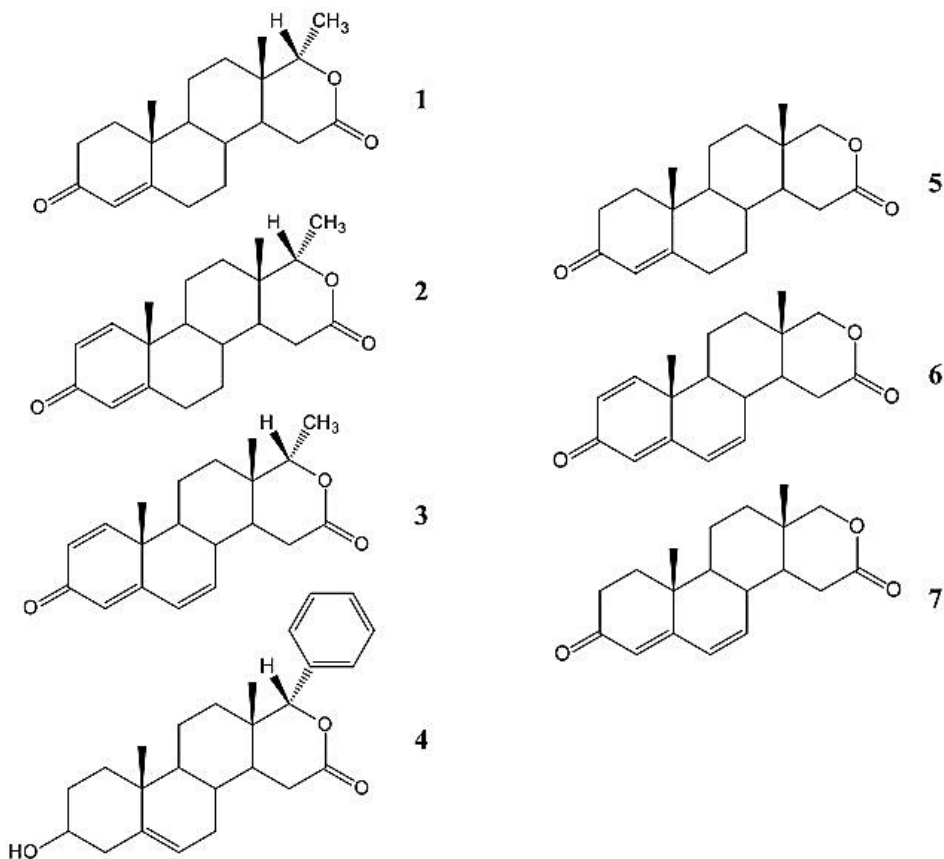


Figure 1. Chemical structures of the investigated compounds

The partition coefficients ($ACDlogP$, $AlogP$, $IlogP$, $AB/logP$, $milogP$, $\log P_{Kow}$, $XlogP$, $CSlogP$, $ClogP$) were calculated for the compounds by using different theoretical

procedures from the internet data (Table 2). The complete regression analysis including linear and multilinear regression (MLR) was carried out by NCSS 2007 Statistical Software.

Table 2. Calculated partition coefficients obtained by different software

Cmpd	ACDlogP	AlogP	IlogP	ABlogP	mlogP	logP _{K_{ow}}	XlogP	CSlogP	ClogP
1	2.99	2.76	3.25	2.69	3.54	2.73	3.88	3.92	2.79
2	3.01	2.56	3.21	2.65	3.51	2.51	4.38	3.87	3.15
3	2.62	2.56	1.32	2.61	3.01	2.30	4.22	3.75	2.73
4	4.23	4.24	4.75	4.33	4.75	3.65	5.05	5.14	3.87
5	2.61	2.55	2.97	2.45	3.17	2.02	3.26	3.73	2.32
6	2.12	2.09	1.03	2.22	2.64	1.88	3.77	3.53	2.21
7	2.11	1.95	3.02	2.26	2.67	2.09	3.26	3.57	1.84

RESULTS AND DISCUSSION

The obtained R_M values were plotted against the organic modifier concentration in the mobile phase (ϕ). In all the cases, the linear relationships were obtained between R_M values and ϕ . This linearity is indicative of reversed-phase chromatography. The theoretical R_M^0 values for 0% organic modifier in the mobile phase were determined from the linear equations. The results from regression analysis of these relationships are compiled in Table 3. The obtained statistical parameters illustrate good quality of the correlations.

Table 3. Correlation data for the partition RP HPTLC equation $R_M = R_M^0 + m\phi$

Compound	R_M^0	m	r	s
Methanol-water				
1	2.018	-2.447	0.989	0.065
2	1.494	-1.956	0.995	0.039
3	1.540	-1.938	0.997	0.029
4	2.714	-2.868	0.983	0.101
5	1.871	-2.203	0.986	0.078
6	1.790	-2.193	0.992	0.051
7	3.271	-3.470	0.997	0.055
Acetone-water				
1	0.911	-1.418	0.975	0.041
2	0.726	-1.278	0.985	0.035
3	0.919	-1.590	0.966	0.045
4	1.448	-2.003	0.973	0.054
5	1.137	-1.686	0.987	0.028
6	1.102	-1.655	0.994	0.029
7	1.611	-2.070	0.997	0.020

Table 3. Continuation

Compound	R_M^0	m	r	s
Acetonitrile-water				
1	1.929	-2.670	0.994	0.026
2	1.893	-2.693	0.993	0.028
3	2.009	-3.015	0.996	0.024
4	2.721	-4.011	0.998	0.022
5	2.203	-3.200	0.992	0.038
6	2.097	-3.183	0.993	0.029
7	3.055	-4.580	0.994	0.040
Dioxane-water				
1	2.252	-3.821	0.991	0.047
2	1.385	-2.554	0.988	0.031
3	1.401	-2.633	0.990	0.034
4	3.031	-4.633	0.997	0.032
5	1.942	-3.237	0.997	0.023
6	1.833	-3.306	0.996	0.024
7	3.579	-5.239	0.995	0.048

Correlations Between Retention Constants and Specific Hydrophobic Surface Area

In order to elucidate the relationship between the lipophilicity (R_M^0) and the specific hydrophobic surface area (m) of androstene derivatives 1-7, the relationships between these two hydrophobicity parameters were studied. In all of the solvents, the linear correlations were observed between the intercept R_M^0 and the slope (m), as shown in the equations given in Table 4.

Table 4. Equations of the relationship between R_M^0 and m

Modifier	Equation	r	S
Methanol-water	$R_M^0 = -0.770 - 1.176 m$	0.995	0.074
Acetone-water	$R_M^0 = -0.648 - 1.059 m$	0.981	0.067
Acetonitrile-water	$R_M^0 = 0.197 - 0.622 m$	0.993	0.058
Dioxane-water	$R_M^0 = -0.775 - 0.820 m$	0.996	0.082

From the data presented in Table 4, as well as from the plots presented in Fig. 2, it is evident that highly significant relationships were found between the lipophilicity and specific hydrophobic surface area with all the mobile phases.

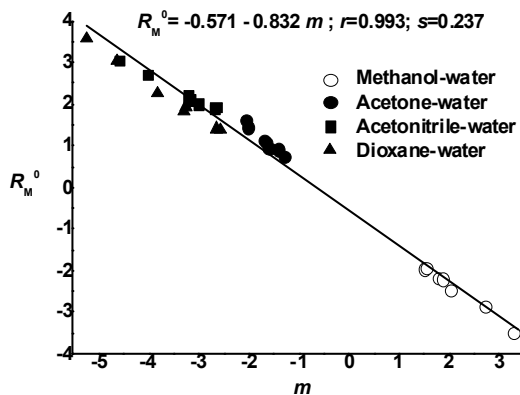


Figure 2. Correlation between R_M^0 and m

This finding indicates that the investigated androstene derivatives behave as a homologous series of solutes. The good correlation between R_M^0 and m reflect the suitability of the systems examined for estimating the lipophilicity of the compounds. These chromatographic data (R_M^0 and m), which describe the partitioning between a non-polar stationary and a polar mobile phase, may therefore be appropriate for the assessment of the lipophilicity. Also, it can be concluded from the obtained data, that RP-HPTLC on C18 can successfully be used for the determination of the lipophilicity parameters of androstene derivatives. Therefore, these parameters can be applied in QSRR studies.

Correlations Between Retention Constants in Different Organic Modifiers

The obtained R_M^0 values depend on the modifier used. Lower R_M^0 values were obtained with acetone-water as mobile phase (average value 1.151), than for methanol-water (average value 2.100), dioxane-water (average value 2.203), and acetonitrile-water (average value 2.272). Different mutual relationships were observed between the R_M^0 values calculated for the different modifiers (Table 5).

Table 5. Correlations between R_M^0 values determined using different mobile phases

Equation	R	s
$R_{M}^0_{MeOH} = 0.161 + 1.685 R_{M}^0_{Acet}$	0.930	0.265
$R_{M}^0_{MeOH} = -1.110 + 1.413 R_{M}^0_{ACN}$	0.955	0.214
$R_{M}^0_{MeOH} = 0.361 + 0.789 R_{M}^0_{Diox}$	0.994	0.079
$R_{M}^0_{Acet} = -0.577 + 0.760 R_{M}^0_{ACN}$	0.969	0.085
$R_{M}^0_{Acet} = 0.361 + 0.789 R_{M}^0_{Diox}$	0.916	0.137
$R_{M}^0_{ACN} = 1.178 + 0.497 R_{M}^0_{Diox}$	0.926	0.184

MeOH = methanol, Acet = acetone, ACN = acetonitrile, Diox = dioxane

The slope and intercept values in Table 5 depend on the mobile phase used. High values of the correlation coefficient for these relationships indicate that chromatographic behaviour of the investigated androstene derivatives is similar in all the mobile phases.

Correlations Between Retention Constants and logP values

To obtain the quantitative effects of the lipophilicity parameters of androstene derivatives on their retention constants, QSRR analysis with nine different partition coefficients ($\log P$) was applied. Usually, lipophilicity parameters are linearly related to retention constants, but in the more general case this relationship is not linear (14). Therefore, a complete regression analysis was made, resorting to (multi)linear, quadratic and cubic relationships. It is obtained that the fitting equations improve when resorting to higher order (second or third order) polynomials. Among the presented lipophilicity parameters, $C\log P$ has the highest correlation with R_M^0 for all the eluents. Therefore, this lipophilicity parameter was retained and used to find two-variable polynomials between the R_M^0 and $\log P$ values. The introduction of a second parameter improves the statistical indices of the QSRR model. The second parameter brings about some variations in these relationships, showing that similar QSRR models can be obtained with different combination of partition coefficients (Table 6). The best QSRR models with two variables were obtained with second order polynomials. The resulted models are as following:

Methanol-water

$$R_M^0 = 1.142 C\log P^2 - 0.463 \log P_{K_{oww}}^2 - 7.529 C\log P + 3.611 \log P_{K_{oww}} + 7.736$$
$$r = 0.999; \quad s = 0.045; \quad n = 7; \quad F = 316.42 \quad [1]$$

Acetone-water

$$R_M^0 = 0.442 C\log P^2 - 0.069 \log P_{K_{oww}}^2 - 3.083 C\log P + 1.023 \log P_{K_{oww}} + 3.826$$
$$r = 0.999; \quad s = 0.013; \quad n = 7; \quad F = 1108.36 \quad [2]$$

Acetonitrile-water

$$R_M^0 = 1.207 C\log P^2 - 0.618 \log P_{K_{oww}}^2 - 7.270 C\log P + 4.285 \log P_{K_{oww}} + 5.809$$
$$r = 0.996; \quad s = 0.045; \quad n = 7; \quad F = 316.42 \quad [3]$$

Dioxane-water

$$R_M^0 = 1.106 C\log P^2 - 0.315 \log P_{K_{oww}}^2 - 7.895 C\log P + 3.505 \log P_{K_{oww}} + 8.423$$
$$r = 0.997; \quad s = 0.105; \quad n = 7; \quad F = 92.11 \quad [4]$$

These results clearly show that by selecting the appropriate lipophilicity descriptors it is possible to obtain several mathematical models with excellent statistical characteristics. Moreover, owing to the errors in the experimental data, small statistical differences between QSRR polynomials are not significant. From Eqs. 1-4, it is evident that for modelling of retention for the set of androstene derivatives $C\log P$ and $\log P_{K_{oww}}$ is prominent. The statistical quality of the regression equations was justified by the parameters like r , s and probability factor related to the F -ratio. Cross-validation statistical technique has been applied for the observation of the quality with regard to predictive ability of these

models. It calculates the following parameters: *PRESS* (predicted residual sum of squares), *SSY* (total sum of squares), r^2_{CV} (cross-validation determination coefficient), and r^2_{adj} (adjusted determination coefficient). Statistical data presented in Table 6 indicate that very good mathematical models were obtained for all of the mobile phases. The high r^2_{CV} values, observed in cases of Eqs. 1-4, are indicative of their reliability in the prediction of the retention constant. For the verification of the predictive power of the developed models, the predicted R_M^0 values of the analysed compounds were calculated by using different $\log P$ values and compared with the experimental ones. The predicted retention constants for all of the mobile phases are presented in Table 7. Based on the magnitude of residue, there is a close agreement between the observed and calculated retention.

Table 6. Cross-validation parameters

Equation	<i>PRESS</i>	<i>SSY</i>	<i>PRESS/SSY</i>	r^2_{CV}	r^2_{adj}
1	0.2462	2.5843	0.0953	0.9047	0.9953
2	0.0182	0.7532	0.0242	0.9758	0.9986
3	0.0406	1.1805	0.0344	0.9656	0.9771
4	0.1237	4.0987	0.0302	0.9698	0.9838

The propagation of the residuals on both sides of zero indicates that no systemic error exists in the development of regression models.

Table 7. Predicted R_M^0 values of androstene derivatives calculated by using Equations 1-4

Solvent Comp.	Methanol-water		Acetone-water		Acetonitrile-water		Dioxane-water	
	R_M^0	Residue	R_M^0	Residue	R_M^0	Residue	R_M^0	Residue
1	2.025	0.007	0.918	0.007	1.976	0.047	2.229	-0.023
2	1.496	0.002	0.728	0.002	1.901	0.008	1.345	-0.040
3	1.547	0.007	0.904	-0.015	1.932	-0.077	1.511	0.110
4	2.712	-0.002	1.468	0.020	2.721	0.000	3.035	0.004
5	1.819	-0.052	1.144	0.007	2.228	0.025	1.856	-0.086
6	1.825	0.035	1.102	0.000	2.104	0.007	1.855	0.022
7	3.272	0.001	1.609	-0.002	3.046	-0.009	3.591	0.012

On the basis of the correlations between R_M^0 and $\log P$, all of the mobile phases are suitable for the RP HPTLC systems for the determination of octanol/water partition coefficients, and thus of the lipophilicity of the molecules. Our findings suggest the usefulness of the chromatographic method in fast characterization of the lipophilicity of structurally closely related molecules.

CONCLUSIONS

The retention constants (R_M^0) of seven *D-homo*-androstene derivatives were compared for four mobile phase mixtures: methanol-water, acetone-water, acetonitrile-water, and dioxane-water. Linear relationships were found between R_M^0 and specific hydrophobic

surface area (m) for all of the mobile phases; this is characteristic of closely related compounds. Also, there are the linear correlations among the R_M^0 values calculated for the different mobile phases. High quality QSRR models that relate R_M^0 and two variables were obtained with second order polynomials. It can be concluded that for modelling of the retention for the analysed set of androstene derivatives $ClogP$ and $\log P_{Koww}$ are prominent. It indicates that these models can be successfully applied to predict the chromatographic behaviour of this class of compounds.

Acknowledgement

This paper was performed within the framework of the research projects CMST COST Action No. 1306, and projects No. 172012 and 172014 supported by the Ministry of Education, Science and Technological Development of the Republic of Serbia and the project No. 114-451-958/2015-02, financially supported by the Provincial Secretariat for Science and Technological Development of Vojvodina.

REFERENCES

1. Shahidi, N. T. A review of the chemistry, biological action, and clinical applications of anabolic-androgenic steroids. *Clin. Ther.* 2001, 23, 1355-1390.
2. Palomino, E. Chemical modulation of activity in steroidal estrogens. In *Biochemistry and Function of Sterols*; Parish, E. J., Ed.; CRC Press: New York, 1997; pp 245-256.
3. Dufort, I.; Soucy, P.; Lacoste, L.; Luu-The, V. Comparative biosynthetic pathway of androstenol and androgens. *J. Steroid Biochem. Mol. Biol.* 2001, 77, 223-227.
4. Numazawa, M.; Yamguchi, S. 6-Phenylaliphatic-substituted androst-4-ene-3,17-diones as aromatase inhibitors: structure activity relationships. *J. Steroid Biochem. Mol. Biol.* 1998, 67, 41-48.
5. Kovačević, S. Z.; Podunavac-Kuzmanović, S. O.; Jevrić, L. R.; Djurendić, E. A.; Ajduković, J. J. Non-linear assessment of anticancer activity of 17-picoyl and 17-picolinylidene androstane derivatives – Chemometric guidelines for further syntheses. *Eur. J. Pharm. Sci.* 2014, 62, 258-266.
6. Kovačević, S. Z.; Podunavac Kuzmanović, S. O.; Jevrić, L. R. Multivariate regression modelling of antifungal activity of some benzoxazole and oxazolo[4,5-b]pyridine derivatives. *Acta Chim. Slov.* 2013, 60 (4), 756-762.
7. Kovačević, S. Z.; Podunavac Kuzmanović, S. O.; Jevrić, L. R.; Kalajđžija, N. D. Neural network modelling of antifungal activity of a series of oxazole derivatives based on in silico pharmacokinetic parameters. *APTEFF*, 2013, 44, 249-258.
8. Di, L.; Kerns, E. H. Profiling drug-like properties in discovery research. *Curr. Opin. Chem. Biol.* 2003, 7, 402-408.
9. Kovačević, S. Z.; Podunavac Kuzmanović, S. O.; Jevrić, L. R.; Lončar, E. S. Assessment of chromatographic lipophilicity of some anhydro-D-aldose derivatives on different stationary phases by QSRR approach. *J. Liq. Chromatogr. Relat. Technol.* 2015, 38 (4), 492-500.

10. Perišić-Janjić, N.; Djaković-Sekulić, T.; Stojanović, S.; Penov-Gaši, K. Evaluation of the lipophilicity of some dehydroepiandrosterone derivatives using RP-18 HPTLC chromatography. *Chromatographia* 2004, 60, 201-205.
11. Perišić-Janjić, N.; Djaković-Sekulić, T.; Stojanović, S.; Penov-Gaši, K. HPTLC chromatography of androstene derivatives. Application of normal phase thin-layer chromatographic retention data in QSAR studies. *Steroids* 2005, 70, 137-144.
12. Penov Gaši, K.; Stojanović, S.; Sakač, M.; Popsavin, M.; Jovanović Šanta, S.; Stanковић, S.; Klisurić, O.; Andrić, N.; Kovačević, R. Synthesis and anti-aromatase activity of some new steroidal D-lactones. *Steroids* 2005, 70, 47-53.
13. Penov Gaši, K.; Stojanović, S.; Sakač, M.; Djurendić, E.; Csanadi, J.; Molnar-Gabor, D.; Lazar, D.; Kovačević, R. Synthesis and biological activity of some 17 α -substituted homolactones of androst-5-ene derivatives. *Collect. Czech. Chem. Commun.* 2005, 70, 1387-1396.
14. Lien, E. J. *Side Effects and Drug Design*. Marcel Dekker: New York, 1987; pp 41-162.

ПРОЦЕНА ХРОМАТОГРАФСКЕ ЛИПОФИЛНОСТИ D-ХОМО АНДРОСТЕНСКИХ ДЕРИВАТА

Нада У. Перушић Јањић¹, Катарина М. Пенов Гаши¹, Евгенија А. Ђурендић¹,
Марина П. Савић¹, Страхиња З. Ковачевић², Стела Д. Јокић³,
Сања О. Подунавац-Кузмановић^{2*}

¹ Универзитет у Новом Саду, Природно-математички факултет, Департман за хемију, биохемију и заштиту животне средине, Трг Доситеја Обрадовића 3, 21000 Нови Сад, Србија

² Универзитет у Новом Саду, Технолошки факултет, Булевар цара Лазара 1, 21000 Нови Сад, Србија

³ Ј. Ј. Штросмајер Универзитет у Осијеку, Прехрамбено-технолошки факултет, Ф. Кухача 18, 31000 Осијек, Хрватска

У раду је представљено дефинисање хроматографског понашања D-хomo андростенских деривата 1-7. Ретенционе константе (R_M^0) испитиваних деривата дефинисане су помоћу танкослојне хроматографије високих перформанси на обрнутим фазама (RP HPTLC) на C18 плочама коришћењем четири мобилне фазе: метанол-вода, ацетон-вода, ацетонитрил-вода и диоксан-вода. Примењена је корелациона анализа заснована на мултиплој линеарној (полиномској) регресији са циљем моделовања хроматографског понашања на основу девет дескриптора липофилности ($\log P$). Добијени QSRR модели су валидовани унакрсном валидацијом. Оптималне вредности параметара унакрсне валидације указују на значајну предиктивну моћ добијених модела.

Кључне речи: QSRR, хеометрија, RP HPTLC, липофилност.

Received: 14 July 2015.

Accepted: 11 October 2015.

BASIL (*Ocimum basilicum* L.) ESSENTIAL OIL AND EXTRACTS OBTAINED BY SUPERCRITICAL FLUID EXTRACTION

Zoran P. Zeković¹*, Snežana Dj. Filip², Senka S. Vidović¹, Dušan S. Adamović³ and Ahmed M. Elgndi¹

¹ University of Novi Sad, Faculty of Technology, Bulevar cara Lazara 1, 21000 Novi Sad, Serbia

² University of Novi Sad, Technical Faculty Mihajlo Pupin, Djure Djakovica b.b., 23000 Zrenjanin, Serbia

³ Institute of Field and Vegetable Crops, Maksima Gorkog 30, 21000 Novi Sad, Serbia

*The extracts obtained from sweet basil (*Ocimum basilicum* L.) by hydrodistillation and supercritical fluid extraction (SFE) were qualitative and quantitative analyzed by GC-MS and GC-FID. Essential oil (EO) content of basil sample, determined by an official method, was 0.565% (V/w). The yields of basil obtained by SFE were from 0.719 to 1.483% (w/w), depending on the supercritical fluid (carbon dioxide) density (from 0.378 to 0.929 g mL⁻¹). The dominant compounds detected in all investigated samples (EO obtained by hydrodistillation and different SFE extracts) were: linalool, as the major compound of basil EO (content from 10.14 to 49.79%, w/w), eugenol (from 3.74 to 9.78%) and δ -cardinene (from 3.94 to 8.07%). The quantitative results of GC-MS from peak areas and by GC-FID using external standard method involving main standards, were compared and discussed.*

KEY WORDS: *Ocimum basilicum* L., essential oil, extracts, gas chromatography, composition

INTRODUCTION

Ocimum basilicum L. (sweet basil) is a plant belonging to the *Lamiaceae* family, and the most cultivated variety in the world (especially in Mediterranean countries). The basil leaves can be used fresh or dried, as a spice, to enhance the flavor of foods. Essential oil (EO) extracted from fresh leaves and flowers can be used as aroma additives in food, pharmaceuticals, and cosmetics (1). There are several types of basil oil traded commercially. Extracted from different varieties of sweet basil, these are known as European (French or sweet basil), Egyptian, Reunion (Comoro), Bulgarian and Java basil oils (2). The plants of this species generally present a fresh, minty and sweet flavor, with linalool, methylchavicol and various sesquiterpenes being responsible for this (3). Many investigators have studied the chemical composition of the basil EO, and it has been found to be very variable, with linalool, methylchavicol, eugenol and/or methyl cinnamate as the main constituents (3-6). There are various classifications that include the extensive range

* Corresponding author: Zoran P. Zeković, University of Novi Sad, Faculty of Technology, Bulevar cara Lazara 1, 21000 Novi Sad, Serbia, e-mail: zzekovic@tf.uns.ac.rs

of subspecies of this herb. One of them is based on the content of linalool and methylchavicol (estragole), which are the two major components of *O. basilicum* L. EO (7), yielding four chemotypes: chemotype A and chemotype B, with linalool and methylchavicol as the main component of the EO, respectively; chemotype AB, the principal constituent of which is linalool, but with a relatively high content of methylchavicol; and chemotype BA, which contains methylchavicol as the main constituent, followed by linalool. The basil EO content, as well as EO composition varies depending on the environment and the *O. basilicum* chemotype. For example, samples from Fiji have EO content only 0.2% (dominant compounds: linalool 22.3%, methyl eugenol 24.7% and (E)-methyl cinnamate 23.6%), samples from Cuba have a much higher EO content of 1.9-2.5% (dominant compounds: methyl chavicol 66.8%, 1,8-cineol 5.4% and linalool 5.0%), and samples from Burkina Faso have content of EO of 0.7-1.8% (dominant compounds: 1,8-cineol 60.2%, α -terpineol 6.5% and β -pinene 5.7%) (8).

Supercritical fluid extraction (SFE) is regarded as a promising alternative technique to steam distillation (or hydrodistillation) and solvent extraction for the extraction of flavor and fragrance compounds from natural materials. Carbon dioxide is the most commonly used supercritical fluid in food and pharmaceutical industry. It is non-toxic, non-explosive and easy removable from the product, and possesses relatively low critical temperature and pressure ($T_c = 31.1^\circ\text{C}$, $p_c = 73.8$ bar). The solvent properties of carbon dioxide can be described as a function of fluid density (9). Selection of the extraction pressure and temperature range is an important factor affecting the final composition of the extract and process yield, since the solubility of every component in the supercritical fluid will primarily depend on these parameters (10).

In this study two chromatographic methods (GC-MS and GC-FID) were used and compared for the qualitative and quantitative determination of basil extract compounds, i.e. chemical composition of basil EO (obtained by hydrodistillation) and different basil extracts (obtained by SFE using carbon dioxide).

EXPERIMENTAL

Plant material and chemicals

Sweet basil (*Ocimum basilicum* L.) was cultivated by the Department for Organic Production and Biodiversity, Bački Petrovac, Institute of Field and Vegetable Crops, Serbia (year 2011). The collected plant material (basil leaves and flowers) were dried and stored at room temperature. The moisture of material (after drying at 105°C , 2 h) was 11.44% (w/w). The sample was ground and sieved using sieve sets produced by Erweka, Germany (mean particle size 0.657 mm).

Commercial carbon dioxide (Messer, Novi Sad, Serbia) was used for SFE. All other chemicals were of analytical reagent grade.

Hydrodistillation

The EO content was determined using the Ph. Jug. IV procedure (11).

Supercritical carbon dioxide extraction

The extraction process was carried out on a laboratory-scale high pressure extraction plant (HPEP, NOVA, Swiss, Effretikon, Switzerland), described previously (12). The main plant parts and properties, by manufacturer specification, were: the diaphragm type compressor (with pressure range up to 1000 bar), extractor (internal volume 200 mL, maximum operating pressure of 700 bar), separator (internal volume 200 mL, maximum operating pressure of 250 bar), pressure control valve, temperature regulation system, and regulation valves. Maximum carbon dioxide mass flow rate is 5.7 kg h⁻¹.

The sample of basil (50.0 g) was placed in the extractor vessel. The flow rate of carbon dioxide was 3.225 g min⁻¹, the pressure 100 and 300 bar, and of the temperature 40 and 50°C (values higher than carbon dioxide T_c, but relatively low, to avoid thermal decomposition). The separator conditions were 15 bar and 23°C. The extraction was carried out and the extraction yield was measured after 4 hours of the process. After each extraction, the obtained extract was placed in a glass bottle, sealed and stored at 4°C to prevent any possible degradation.

GC-MS and GC-FID

The GC-MS experiments were carried out on a GC/MS Agilent Technologies Series 6890N/5975B (Santa Clara, California, USA), and an HP-5 MS capillary column (30.0 m x 0.25 mm I.D., film thickness 0.25 µm) was used. The working conditions were: the helium flow rate: 2 ml min⁻¹, temperature: injector 250°C; detector 300°C; initial 60°C with a linear increase of 4°C min⁻¹ to 150°C, detector: 35-550 D, total analysis time: 58.06 min. The injected volume of investigated sample solution in methylene chloride (about 1 mg mL⁻¹) was 5 µL, using split-ratio 1:30. The compounds were identified using the NIST 05 and Wiley 7n mass data base. The results of compound content were expressed as relative (area) percent (%).

For the quantitative determination (to measure contents of basil EO compounds) use was made of a flame ionization detector (FID). The standard compounds ((+)-limonene, eucalyptol, linalool, α-terpineol, methylchavicol and geraniol) were purchased from Carl Roth GmbH (Germany). The GC conditions were the same as for GC-MS. Each standard was dissolved in methylene chloride, and then, different concentrations (from 1 to 500 µg mL⁻¹) were obtained as standard solutions. After the GC-FID analyzes, six equations (for six standard compounds), which describe the dependence of the compound concentration on the peak area, were obtained (min. value of correlation coefficient was 0.99). The final result was expressed as compound content (C) in % (w/w).

In this work, triplicate tests were done for each sample, and the results are presented as mean value.

RESULTS AND DISCUSSION

The content of EO, determined by the official procedure (11) was 0.565% (V/w). The samples of EO were characterized qualitative and quantitative by two chromatographic methods, GC-MS and GC-FID (Figure 1 and Table 1). The predominant compounds in

EO were linalool (50.09%), indicating that the investigated sample of basil is of chemotype A, δ -cadinene (8.11%), and germacrene (5.76%). Other EO compounds, with the content higher than 3%, were: γ -cadinene (3.13%), methylchavicol (3.30%), β -selinene (3.58%), eugenol (3.76%) and α -bergamotene (4.13%). The results (Table 1), expressed as relative (area) percent of compound (GC-MS), are very similar to those obtained by “real” quantitation by external standard method (GC-FID), expressed as compound content in % (w/w). This conclusion could be explained by the nature of the EO compounds which are all evaporable, and, at the other hand, by the EO isolation procedure, i.e. hydrodistillation (or steam distillation). The composition of EOs of different drugs can be very similar. For example, EOs of sweet basil (*O. basilicum* L.) and coriander (*Coriandrum sativum* L.) have the same main compound – linalool (50.09% and 52.4%, respectively) and a lot of other constituents (camphor, geraniol, α -terpineol) (13). Therefore, for a quantitative analysis of similar samples (other aromatic plants EOs), GC-MS method could be successfully used. In this way, the result of the EOs composition and compounds content can be obtained much easier and faster, using only GC-MS (with no need for standards and calibration as in the GC-FID method).

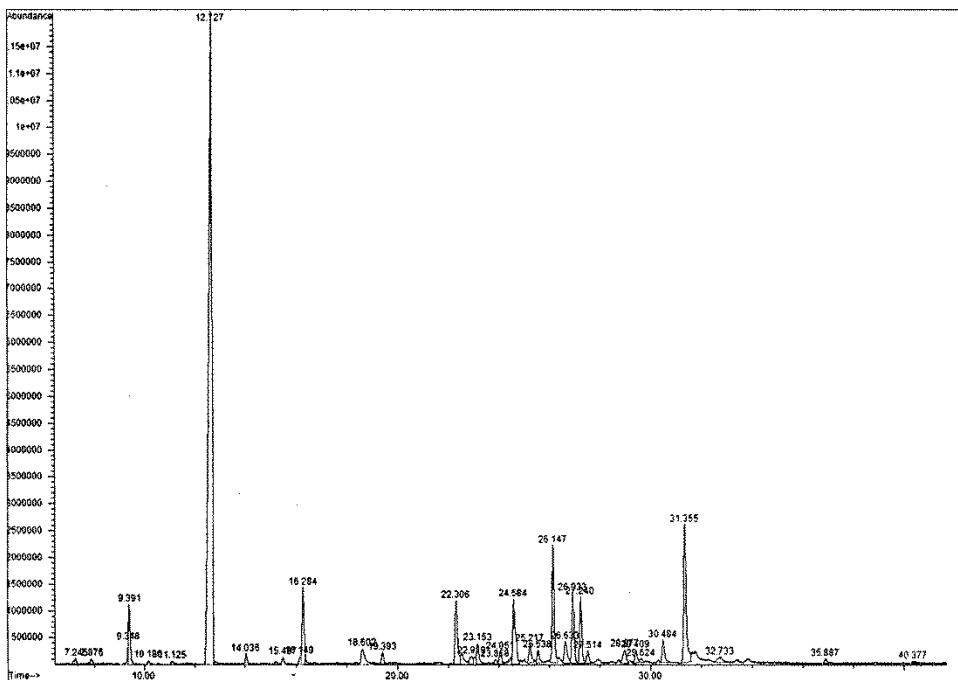


Figure 1. GC chromatogram of basil EO obtained by hydrodistillation

Table 1. Results of GC-MS and GC-FID analyses of basil EO obtained by hydrodistillation

EO				
Compound	Area percent (%)	C* (% w/w)	EY**	t_R*** (min)
β-Pinene	0.39	0.39	2.20	7.245
Myrcene	0.29	0.29	1.64	7.876
(+)-Limonene	0.39	0.41	2.32	9.348
1,8-Cineole (Eucalyptol)	2.50	2.69	15.20	9.391
<i>Trans</i> -β-Ocimene	0.19	0.19	1.07	10.180
Linalool	50.09	49.79	281.31	12.727
Camphor	0.49	0.48	2.71	14.036
Terpinene-4-ol	0.33	0.33	1.86	15.483
α-Terpineol	0.35	0.46	2.60	16.149
Methylchavicol	3.30	3.38	19.10	16.284
Geraniol	1.53	1.66	9.38	18.600
Bornyl acetate	0.55	0.54	3.05	19.393
Eugenol	3.76	3.74	21.13	22.306
β-Elemene	1.15	1.14	6.44	23.153
<i>Trans</i> -Caryophyllene	0.67	0.66	3.73	24.051
α-Bergamotene	4.13	4.11	23.22	24.584
α-Humulene	1.03	1.02	5.76	25.217
β-Cubebene	0.69	0.69	3.90	25.538
Germacrene	5.76	5.73	32.37	26.147
Germacrene D	1.52	1.51	8.53	26.633
β-Selinene	3.58	3.56	20.11	26.933
γ-Cadinene	3.13	3.12	17.63	27.240
α-Selinene	0.97	0.96	5.42	28.972
Spathulenol	0.72	0.72	4.07	29.409
δ-Cadinene	8.11	8.07	45.60	31.355
Σ n.i.****	4.38	4.36	24.62	
Σ	100.00	100.00	564.97	

* C - compound content

** EY - extraction yield (mg per 100 g of basil)

*** t_R - retention time (min)

**** n.i.- not identified

After the SFE investigations of basil using carbon dioxide (CO₂), the samples of extracts were obtained (see Experimental) using different combinations of pressure and temperature, i.e. solvent density, of supercritical CO₂ for basil extraction (Table 2). The obtained extraction yields presented in Table 2, can not be explained by the increase of the solvent density because the final yield of extract depends also on extraction tempera-

ture, i.e. a higher temperature means a better solubility of basil compounds, which results in a higher extraction yield. It is difficult to explain what is more important for compound extraction in the SFE process – solvent density or temperature. The effect of temperature on compound solubility at a constant pressure is due to two mechanisms: the increase in vapor pressure with temperature resulting in an increased solubility, and the decrease in solvent density causing a decrease in solubility. The solubility of the solute may increase, become constant or decrease with the temperature rise at a constant pressure, depending on whether the solute vapor pressure or the solvent density is predominant (14).

Table 2. SFE conditions and extraction yield

Pressure (bar)	100	100	300	300
Temperature (°C)	50	40	50	40
Density (g mL ⁻¹)	0.378	0.568	0.881	0.929
Extraction yield (% w/w)	0.894	0.719	1.483	1.287

GC-MS and GC-FID results of obtained CO₂ extracts are shown in Table 3.

Table 3. Results of GC-MS and GC-FID analysis of basil extracts obtained by SFE at different extraction conditions

Sample (p, T)	100, 50		100, 40		300, 50		300, 40	
	AP* (%)	C** (% w/w)	AP (%)	C (% w/w)	AP (%)	C (% w/w)	AP (%)	C (% w/w)
1,8-Cineole (Eucalyptol)	0.48	0.25	0.61	0.23	0.89	0.45	2.00	1.10
Linalool	21.33	11.79	27.80	16.60	23.55	10.14	26.09	10.72
Camphor	-	-	0.39	0.23	0.29	0.12	0.38	0.16
α-Terpineol	2.00	0.79	1.03	0.60	1.42	0.54	1.50	0.8
Methylchavicol	1.93	0.62	1.58	0.87	1.19	0.60	1.14	0.66
Geraniol	1.22	0.65	1.25	0.81	1.10	0.56	0.96	0.44
Bornyl acetate	-	-	0.44	0.26	0.40	0.17	0.64	0.26
Eugenol	17.69	9.78	15.56	9.29	13.72	5.91	16.09	6.61
β-Elemen	1.38	0.76	0.99	0.59	0.66	0.28	1.16	0.48
Trans-Caryophyllene	0.81	0.45	0.73	0.44	0.52	0.22	0.61	0.25
α-Bergamotene	5.24	2.90	4.26	2.54	4.14	1.78	5.57	2.29
α-Humulene	1.25	0.69	1.11	0.66	1.07	0.46	1.20	0.49
β-Cubebene	0.98	0.54	0.58	0.35	0.96	0.41	0.86	0.35
Germacrene	5.29	2.92	5.30	3.16	4.30	1.85	5.63	2.31
γ-Elemene	0.75	0.41	-	-	0.67	0.29	-	-
β-Selinene	3.35	1.85	2.94	1.75	2.14	0.92	3.51	1.44
γ-Cadinene	4.83	2.67	4.55	2.72	3.36	1.45	4.31	1.77
α-Selinene	1.88	1.04	0.99	0.59	0.70	0.30	1.29	0.53
Spathulenol	2.26	1.25	2.12	1.27	1.66	0.72	2.01	0.83
δ-Cadinene	13.05	7.21	11.64	6.95	9.16	3.94	10.67	4.38
Σ n.i.	14.27	7.89	16.13	9.64	28.11	12.10	14.38	5.92
Σ	99.99	54.46	100.00	59.56	100.00	43.21	100.00	41.79
Other extracted compounds (%) ^a		45.54		40.44		56.79		58.21

*AP - area percent

** C - compound content

*** n.i. - not identified

^a - Coextracted, non-polar and non-evaporable basil compounds (of course, not present in the basil EO obtained by the hydrodistillation process)

The results from Table 3 show the great difference between the contents of basil EO compounds obtained by the GC-MS method and by the GC-FID method. The percents of the compounds detected by GC-FID in the CO₂ extracts are from 41.79% (sample obtained at 300 bar and 40°C, i.e. solvent density of 0.929 g mL⁻¹) to 59.56% (sample obtained at 100 bar and 40°C, i.e. solvent density of 0.568 g mL⁻¹). On the basis of our previous SFE investigations of different aromatic plants (and other raw materials) carried out during last 20 years (12, 14-28), the best combination of pressure and temperature for EO separation (isolation) is 100 bar and 40°C – the resulting extracts are most similar to “classical” EOs. The other extracted compounds – OEC (Table 3, the last row) from the extracts (mass percent from 40.44 to 58.21%) are not (and could not be, without some kind of derivation, such is esterification) detected by the GC-FID (or GC-MS) method. The highest yield, i.e. content of OEC (58.21%) was obtained using supercritical CO₂ with highest the investigated density (0.929 g mL⁻¹), i.e. the highest solvent "solubility power". On the other hand, the values obtained by GC-MS, result in a "wrong" picture of basil compounds contained in the CO₂ extracts (and, probably, all other extracts obtained using different solvents and extraction procedures). It can be concluded that the GC-MS method can be used only for qualitative and quantitative analyze of "real" EOs obtained by distillation (containing only evaporable compounds).

The predominant compounds in the CO₂ extracts are linalool (from 10.14 to 16.60%), eugenol (from 5.91 to 9.78%) and δ-cadinene (from 3.94 to 7.21%), depending on the SFE conditions, whereas the dominant EO compounds of the same basil sample obtained by hydrodistillation were linalool (49.79%), δ-cadinene (8.07%) and germacrene (5.73%), see Table 1.

The obtained results (Table 3) can be discussed the following way: The compound which is dominant in all the basil products is linalool, whose content in EO was 50.09% (i.e. 49.79%, w/w). The highest content of this compound in CO₂ extracts was obtained at 100 bar and 40°C (16.60%), but the highest extraction yield of linalool was not achieved under these extraction conditions. The extraction yield of the basil SFE at 300 bar and 50°C was 1.483% (Table 2), and linalool content in the extract is 10.14% (Table 3), i.e. 150.38 mg of linalool has been extracted from 100 g of plant material. On the other hand, at 100 bar and 40°C, the extraction yield was 0.719%, linalool content 16.60% and 119.35 mg per 100 g of basil sample was obtained. This sort of calculation is necessary for all compounds of interest (Table 4).

Table 4. Extraction yields of the predominant compounds of the basil CO₂ extracts

Sample (p, T)	EO		100, 50		100, 40		300, 50		300, 40	
	C*	EY**	C	EY*	C	EY	C	EY	C	EY
Linalool	49.79	281.31	10.79	96.46	16.60	119.35	10.14	150.38^a	10.72	137.97
Methylchavicol	3.38	19.10	0.62	5.54	0.87	6.25	0.60	8.90	0.66	8.49
Eugenol	3.74	21.13	9.78	87.43	9.29	66.79	5.91	87.64	6.61	85.07
α-Bergamotene	4.11	23.22	2.90	25.93	2.54	18.26	1.78	26.40	2.29	29.47
β-Selinene	3.56	20.11	1.85	16.63	1.75	12.58	0.92	13.64	1.44	18.53
δ-Cadinene	8.07	45.60	7.21	64.46	6.95	49.97	3.94	58.43	4.38	56.37

* - compound content (% w/w)

** - extraction yield (mg per 100 g of basil)

a - the highest compound SFE yield (bold)

The compound solubility depends on the solvent density, i.e. on the process pressure and temperature. The solvent density of 0.378 g mL^{-1} (100 bar and 50°C) was the most suitable for the extraction of δ -cadinene (the highest compound solubility). The extraction yield was 64.46 mg/100 g (Table 4). The combination of pressure of 300 bar and temperature of 50°C (solvent density 0.881 g mL^{-1}) of CO_2 resulted in the highest yields of linalool (150.38 mg/100 g), methylchavicol (8.90 mg/100 g) and eugenol (87.64 mg/100 g). The best solubility of α -bergamotene and β -selinene was observed at the highest investigated density of CO_2 (0.929 g mL^{-1}), i.e. at the pressure of 300 bar and temperature of 40°C . On the other hand, the obtained extraction yields using SFE were higher for some compounds (eugenol, α -bergamotene and δ -cadinene) than that obtained by hydrodistillation (Table 4). In the same table, the results of compound content (C; %, w/w) show a similarity (more than all other extracts) of the CO_2 extract obtained at 100 bar and 40°C (solvent density 0.568 g mL^{-1}) to basil essential oil obtained by hydrodistillation.

CONCLUSION

In the sweet basil, the determined EO content was 0.565% V/w, with linalool as the predominant compound (50.09%), which indicates that the investigated sample of basil is of chemotype A. The extraction yields obtained by SFE, using CO_2 , were from 0.719 to 1.483% (w/w), depending on the carbon dioxide density (from 0.378 to 0.929 g mL^{-1}). The predominant compounds of the CO_2 extracts were linalool (from 10.14 to 16.60%), eugenol (from 5.91 to 9.78%) and δ -cadinene (from 3.94 to 7.21%), depending on SFE conditions. The GC-MS method can be successfully used only for qualitative and quantitative analyses of "real" EOs, obtained by hydrodistillation (containing only evaporable compounds). On the other hand, for all other extracts (including CO_2 extracts), obtained by different extraction methods and solvents, GC-FID method, using appropriate external standards, is right way for a precise quantitative determination.

Acknowledgement

The authors gratefully acknowledge the financial support of this work by the Ministry of Education, Science and Technological Development of the Republic of Serbia, Project No. TR 31013.

REFERENCES

1. Lee, S.J.; Umamo, K.; Shibamoto, T.; Lee, K.G. Identification of volatile components in basil (*Ocimum basilicum* L.) and thyme leaves (*Thymus vulgaris* L.) and their antioxidant properties. *Food Chem.* **2002**, *91* (1), 131-137.
2. Simon, J.E.; Quinn, J.; Murray, R.G. Basil: A source of essential oils. In *Advances in New Crops*; Janick, J.; and Simon, J.E., Eds.; Timber Press, Portland, OR, **1990**; pp. 484-489.
3. Sheen, L.Y. Flavor characteristic compounds found in the essential oil of *Ocimum basilicum* L. with sensory evaluation and statistical analysis. *J. Agric. Food Chem.* **1991**, *39* (5), 939-943.

4. Grayer, R.J.; Kite, G.C.; Goldstone, F.J.; Bryan, S.E.; Panton, A.; Putievsky, E. Intra-specific taxonomy and essential oil chemo-types in sweet basil, *Ocimum basilicum*. *Phytochem.* **1996**, *43* (5), 1033-1039.
5. Marotti, M.; Piccaglia, R.; Giovanelli, E. Differences in essential oil composition of basil (*Ocimum basilicum* L.) Italian cultivars related to morphological characteristics. *J. Agric. Food Chem.* **1996**, *44* (12) 3926-3929.
6. Schulz, H.; Schrader, B.; Quilitzsch, R.; Pfeffer, S.; Kruger, H. Rapid classification of basil chemotypes by vibrational spectroscopy methods. *J. Agric. Food Chem.* **2003**, *51* (9) 2475-2481.
7. Baritoux, O.; Richard, H.; Touche, J.; Derbesy, M. Effects of drying and storage of herbs and spices on the essential oil. Part I. Basil. *Ocimum basilicum* L.. *Flav. Fragr. J.* **1992**, *7*, 267-271.
8. Keita, S.M.; Vincent, C.; Schmit, J.P.; Ramaswamy, S.; Belanger, A. Effect of various essential oils on *Callosobruchus maculatus* (F.) (Coleoptera: Bruchidae). *J. Stored Prod. Res.* **2000**, *36*, 355-364.
9. Levelet Sengers, J.M.H. Supercritical fluids: Their properties and application. In: *Supercritical Fluids - Fundamentals and Applications*; Kiran E., Debenedetti P.G., Peters C.J., Eds.; Kluwer Academic Publisher, Netherlands, **2000**; pp. 1-29.
10. Diaz-Maroto, M.C.; Perez-Coello, M.S.; Cabezudo, M.D. Supercritical carbon dioxide extraction of volatiles from spices: Comparison with simultaneous distillation-extraction. *J. Chrom. A.* **2002**, *947* (1), 23-29.
11. *Pharmacopoea Jugoslavica, Editio Quarta (Ph. Jug. IV)*, Vol. 1, Federal Institute of Public-Health, Belgrade, Yugoslavia, **1984** (in Serbian).
12. Pekić, B.; Zeković, Z.; Petrović, L.; Tolić, A. Behavior of (-)- α -Bisabolol and (-)- α -Bisabololoxides A and B in Camomile Flower Extraction with Supercritical Carbon Dioxide. *Separ. Sci. Technol.* **1995**, *30* (18), 3575-3584.
13. Zeković, Z.; Adamović, D.; Četković, G.; Radojković, M.; Vidović, S. Essential oil and extract of coriander (*Coriandrum sativum* L.). *Acta Periodica Technologica.* **2011**, *42*, 281-288.
14. Jokić, S.; Svilović, S.; Zeković, Z.; Vidović, S. Mathematical modelling of soybean oil solubility in supercritical carbon dioxide. *Int. J. Food Sci. Tech.* **2011**, *46* (5) 1031-1037.
15. Pekić, B.; Zeković, Z.; Tolić, A. Investigation of the Extraction Kinetics of Camomile Flowers by Supercritical Carbon Dioxide. *J. Serb. Chem. Soc.* **1994**, *59* (4), 249-254.
16. Tolić, A.; Zeković, Z.; Pekić, B. Dependence of Camomile Flower Solubility on Carbon Dioxide Density at Supercritical Extraction. *Separ. Sci. Technol.* **1996**, *31* (13), 1889-1892.
17. Zeković, Z.; Lepojević, Ž.; Vujić, Dj. Supercritical Extraction of Thyme (*Thymus vulgaris* L.). *Chromatographia.* **2000**, *51* (3/4), 175-179.
18. Zeković, Z. Chamomile Ligulate Flowers in Supercritical CO₂-Extraction. *J. Essent. Oil Res.* **2000**, *12*, 85-93.
19. Stojanović, G.; Palić, R.; Alagić, S.; Zeković, Z. Chemical composition and antimicrobial activity of the essential oil and CO₂-extracts of semi-oriental tobacco *Otlja*. *Flavour Frag. J.* **2000**, *15*, 335-338.

20. Zeković, Z.; Lepojević, Ž.; Tolić, A. Modelling of the Thyme - Supercritical Carbon Dioxide Extraction System; I. The Influence of Carbon Dioxide Flow Rate and Grinding Degree of Thyme. *Separ. Sci. Technol.* **2001**, *36* (15), 3459-3472.
21. Zeković, Z.; Lepojević, Ž.; Tolić, A. Modelling of the Thyme - Supercritical Carbon Dioxide Extraction System; II. The Influence of Extraction Time and Carbon Dioxide Pressure. *Separ. Sci. Technol.* **2003**, *38* (3), 541-552.
22. Zeković, Z.; Lepojević, Ž.; Mujić, I. SFE of PMT mixture by supercritical CO₂, CHISA 2006, 17th International Congress of Chemical and Process Engineering, Prague, 27-31 August 2006, Summaries 2, Separation Processes, B3.04, CD-ROM of Full Texts, 1-5.
23. Zeković, Z.; Pfaš-Šovljanski, I.; Grujić, O. Supercritical fluid extraction of hops. *J. Serb. Chem. Soc.* **2007**, *72* (1), 81-87.
24. Tepić, A.; Zeković, Z.; Kravić, S.; Mandić, A. Pigment content and fatty acid composition of paprika oleoresins obtained by conventional and supercritical carbon dioxide extraction. *CYTA J. Food.* **2009**, *7* (2), 95-102.
25. Zeković, Z.; Lepojević, Ž.; Milić, S.; Adamović, D.; Mujić, I. Supercritical CO₂ extraction of mentha (*Mentha piperita* L.) at different solvent densities. *J. Serb. Chem. Soc.* **2009**, *74* (4), 417-425.
26. Vidović, S.; Mujić, I.; Zeković, Z.; Lepojević, Ž.; Milošević, S.; Jokić S. Extraction of Fatty Acids from *Boletus edulis* by Subcritical and Supercritical Carbon Dioxide. *J. Am. Oil Chem. Soc.* **2011**, *88*, 1189-1196.
27. Milošević, S.; Lepojević, Ž.; Zeković, Z.; Vidović, S. Determination of extraction conditions of *Ginkgo biloba* L. leaves by supercritical CO₂ using response surface methodology. *Hem. Ind.* **2011**, *65* (2), 147-157.
28. Jokić, S.; Vidović, S.; Zeković, Z.; Podunavac Kuzmanović, S.; Jevrić, L.; Marić, B. Chemometric analysis of tocopherols content in soybean oil obtained by supercritical CO₂. *J. Supercrit. Fluids.* **2012**, *72*, 305-311.

ЕТАРСКО УЉЕ И ЕКСТРАКТИ БОСИЉКА (*Ocimum basilicum* L.) ДОБИЈЕНИ СУПЕРКРИТИЧНОМ ЕКСТРАКЦИЈОМ

Зоран П. Зековић, Снежана Ђ. Филип², Сенка С. Видовић¹, Душан С. Адамовић³,
Мохамед А. Елгнди¹

¹ Универзитет у Новом Саду, Технолошки факултет, Булевар цара Лазара 1, 21000 Нови Сад, Србија

² Универзитет у Новом Саду, Технички факултет Михајло Пупин, Ђуре Ђаковића б.б, 23000 Зрењанин, Србија

³ Институт за ратарство и повртарство, Максима Горког 30, 21000 Нови Сад, Србија

Екстракти босиљка (*Ocimum basilicum* L.) добијени различитим екстракционим поступцима (хидродестилација и суперкритична екстракција угљен диоксидом) су квалитативно и квантитативно анализирани GC-MS и GC-FID методама. Садржај етарског уља (ЕУ) босиљка, одређен официјалном методом, је износио 0,565% (V/m). Принос суперкритичне екстракције босиљка је био од 0,719 до 1,483% (m/m), у зависности од густине суперкритичног флуида - угљен диоксида (испити-

вани опсег густине растварача је био од 0,378 до 0,929 g/mL). Доминантна једињења која су детектована у свим испитиваним узорцима (ЕУ добијено хидродестилацијом и различити суперкритични екстракти) су: линалоол, као главна компонента ЕУ босилјка (садржај од 10,14 до 49,79%, m/m), еугенол (од 3,74 до 9,78%) и δ -кадинен (од 3,94 до 8,07%). Квантитативни садржај компонената одређен помоћу GC-MS (релативни проценат, %, одређен преко површине пика) и GC-FID (% m/m, одређен применом методе спољашњег стандарда) је упоређен и продискутован.

Кључне речи: *Ocimum basilicum* L., етарско уље, екстракти, гасна хроматографија, састав

Received: 10 December 2014.

Accepted: 22 April 2015.

INSTRUCTION FOR MANUSCRIPT PREPARATION

Acta Periodica Technologica publishes reviews and scientific papers covering all branches of technology: food, chemical, biochemical, pharmaceutical, as well as process engineering and related scientific fields.

Acta Periodica Technologica is published in English. The journal may include supplements from congresses, meetings or symposiums.

Submission of Papers. All correspondence, including submission of the manuscript, notification of the Editor's decision and requests for revision, takes place by e-mail: sdjilas@tf.uns.ac.rs or bastajab@uns.ac.rs.

Submission of paper implies that

- it is prepared according this Instructions,
- it has not been published previously (except in the form of an abstract or as a whole in the proceedings of papers of a scientific meeting, or as part of a published lecture or academic thesis),
- it is not under consideration for publication elsewhere, and
- it will not be published elsewhere in the same form, in English or in any other language, without the written consent of the publisher.

Preparation of manuscripts

Language: Manuscript should be written in English.

Typing: Manuscript must be written in Word with a font size 10 pt, double spaced with wide margins (3 cm) on A4 pages (max. 10 pages for scientific papers). All pages of the manuscript should be numbered. Import tables and figures into the text. Abbreviations and symbols-notation should be explained at first appearing, or on a separate list at the end of manuscript.

General format. The manuscript should contain the following in this order: Title page, ABSTRACT and KEY WORDS, INTRODUCTION, EXPERIMENTAL, RESULTS and DISCUSSION, CONCLUSION, ACKNOWLEDGEMENT and REFERENCES as well as ABSTRACT and KEY WORDS IN SERBIAN LANGUAGE.

Title page: On the first page should be the title without symbols, formulae or abbreviations (capital bold letters). Title should be concise and explanatory of the content of the paper. Full name (name, initial and surname) of authors (without degrees, professional or official titles) should be given under the title, written in italic. Clearly indicate (with asterix) who is responsible for correspondence at all stages of refereeing and publication. Ensure that e-mail address and the full postal address are provided. Affiliation of authors should be given after the author's name. Indicate all affiliations with superscript number immediately after authors name and in front of appropriate address. If the paper was given, wholly or in part, at a scientific meeting, this should be stated in a footnote on the title page.

Abstract of the paper (100-250 words, written in italic) should be given under the title and authors. Abstracts should contain the aim of investigated work, methods, results and conclusion.

Keywords (normal letters, max. 5 keywords) should be listed afterwards.

Introduction should state previous relevant work with appropriate references, the problem investigated and the aim of work.

Experimental. The materials and methods used should be stated clearly in sufficient detail to permit the work to be repeated by others. Only new techniques should be described in detail; known methods must have adequately references.

Results and Discussion. Results should be presented concisely, with tables or illustrations for clarity. The significance of the findings should be discussed without repetition of the material in the Introduction. Adequate number of illustrations, graphs and chemical formulae used must be kept on minimum.

Conclusion. This section should present the main conclusions of the study. Also, conclusions should indicate the significance of contribution and application possibilities of the obtained results.

Acknowledgements: These should be kept to a minimum.

References cited should be indicated in the text using Arabic numerals in brackets (), in the order of appearing. All publications cited in the text should be presented in a list of references given on a separate page. Abbreviations of journal titles should be given according to the Chemical Abstracts Service (CASSI Search Tool; <http://cassi.cas.org>). The list of references should be arranged according to their appearance in the text. Give names of all authors (do not use „et.al.“), with their initials after respective surnames. Include article titles in journals. The abbreviated titles should be followed by the year (**bold**), volume (*italic*), number (in brackets if exists), and first and last page numbers.

Examples:

Journals: Pascual, E.C.; Goodman, B.A; Yerezian, C. Characterisation of Free Radicals in Soluble Coffee by Electron Paramagnetic Resonance Spectroscopy. *J. Agric. Food Chem.* **2002**, 50 (21), 6114–6122.

Books: Morris, R. *The Last Sorcerers: The Path from Alchemy to the Periodic Table*; Joseph Henry Press: Washington, DC, 2003; pp 145–158.

Book with more chapters: Puls, J.; Saake, B. Industrially Isolated Hemicelluloses. In *Hemicelluloses: Science and Technology*; Gatenholm, P., Tenkanen, M., Eds.; ACS Symposium Series 864; American Chemical Society: Washington, DC, 2004; pp 24–37.

Book of Abstracts: Noe, W.; Howaldt, M.; Ulber, R.; Scheper, T. Immunobase elution assay for process control, 8th European Congress on Biotechnology, Budapest, 17–21 August 1997, Book of Abstracts WE 163, p. 246.

Thesis: Linstead, J.B.: Linstead, J.B. Effects of adding natural antioxidants on colour stability of paprika. Ph.D. (or M.S.) Thesis, University of Glasgow, november 2006.

Patent: Lenssen, K. C.; Jantscheff, P.; Kiedrowski, G.; Massing, U. Cationic Lipids with Serine Backbone for Transfecting Biological Molecules. Eur. Pat. Appl. 1457483, 2004.

Unpublished data: Should be cited with one of the following comments „in press“, „unpublished work“ or „personal communication“.

Online citations: Should include the author, title, website and date of access.

Example: Wright, N.A. The Standing of UK Histopathology Research 1997-2002. <http://pathsoc.org.uk> (accessed 7 October 2004).

Abstract and keywords in Serbian language should be given at the end of manuscript (after references), in extended form (max. length 1 page), printed in Cyrillic (normal letters) with the title (capital letters), full name(s) of each author(s) and affiliation(s) (italic letters).

Chemical nomenclature and units. Authors are requested to use SI units and chemical nomenclature following the rules of Chemical Abstracts whenever possible.

Tables. Each Table is numbered with Arabic numeral, followed by the title (**Table 1.** Result...). The table width must be 12,5 cm max.

Figures. Each drawing or figure should also be numbered with Arabic numerals followed by the title (**Figure 1.** Chromatogram of...). Graphs and charts must be prepared by Microsoft Excel or Origin. Schemes must be prepared by Microsoft Visio or Corel Draw. *It is necessary to submit them as separate files in original extension* (xls, xlsx, vdr, cdr). Scanned black&white schemes should be submitted in tif, wmf, or bmp form. Photographs should be submitted in jpg form.

Formulae and Equations. Type formulas and mathematical equations clearly, accurately placing superscripts and subscripts. Equations should be indicated in the text using Arabic numerals in square brackets [].

Additional information

Manuscript should be sent in two hard copies to the address: Faculty of Technology Novi Sad, Bulevar Cara Lazara 1, 21000 Novi Sad, Serbia, to the editor: Professor Dr. Sonja Djilas (for Acta Periodica Technologica) and electronic form to the e-mail: sdjilas@tf.uns.ac.rs or bastajab@uns.ac.rs. Authors are expected to propose the category of manuscript (review, original scientific paper).

Review process. All papers submitted to the journal will be reviewed by at least two independent referees who will be asked to complete the refereeing job within 4-6 weeks. Final decision on publication will be made by the Editorial Board. Manuscripts may be sent back to authors for revision if necessary. Revised manuscript submissions should be made as soon as possible (within 2 weeks) after the receipt of the referees comments.

Proofs. One set of page proofs will be sent by e-mail to the corresponding Author. Please use this proof only for checking the typesetting, editing, completeness and correctness of the manuscript. The author may list the corrections and return to the journal in an e-mail within 48 hours of receipt.

Author service. For inquiries relating to the submission of manuscript, please send an e-mail to the Editor (sdjilas@tf.uns.ac.rs).

УПУТСТВО ЗА ПИСАЊЕ РАДА

Acta Periodica Technologica објављује прегледне и научне радове који покривају све области прехранбене, хемијске и фармацеутске технологије, као и процесног инжењерства и сличних научних области.

Acta Periodica Technologica се штампа на енглеском језику. Часопис може садржавати и додатке везане за конгресе, научне скупове и симпозијуме.

Достављање рукописа. Сва кореспонденција везана за предају рукописа рада, обавештења о одлукама уредника и захтевима за ревизију рукописа врши се електронском поштом са следећих адреса: sdjilas@tf.uns.ac.rs или bastajab@uns.ac.rs.

Да би рукопис био узет у разматрање за објављивање мора да задовољи следеће критеријуме:

- да је припремљен у складу са овим упутством,
- да резултати који су обрађени у рукопису нису претходно публиковани (изузев ако су у форми извода рада или у целини штампани у изводима радова научних скупова, или ако су део објављеног предавања и академске тезе),
- да није предат за штампу у неки други часопис и
- да није или неће бити објављен негде другде у истом облику, на енглеском или неком другом језику, без писане сагласности издавача часописа *Acta Periodica Technologica*.

Ако је рад објављен у целини или само његов део на неком научном скупу, то се мора јасно назначити у фусноти на насловној страни рукописа.

Припрема рукописа:

Језик: Рукопис мора бити написан на енглеском језику.

Припрема: Рукопис мора бити припремљен на максимално 10 страница А4 формата (односи се само на научне радове), у MS Word-у, Times New Roman фонтом са величином слова 10 pt, двоструким проредом и са свим маргинама од по 3 cm. Све странице рукописа морају бити нумерисане. Табеле и слике морају бити постављене на месту појављивања у тексту.

Општи изглед. Рукопис треба да је изложен јасно и да садржи: Насловну страну, Извод рада, Кључне речи, Увод, Експериментални део, Резултате и дискусију, Закључак, Захвалницу и Литературу (све на енглеском језику), као и Извод рада и кључне речи на српском језику.

Насловна страна: На првој страни рукописа треба да стоји наслов рада (без симбола, формула или скраћеница) написан великим болдираним словима. Наслов рада треба да је концизан и јасан и да се односи на садржај рукописа. Испод наслова рада *италик* словима написати пуна имена свих аутора (име, средње слово и презиме), без научних и професионалних звања. Име аутора који је задужен за сву кореспонденцију, током свих фаза рецензије и објављивања рада, јасно означити звездичом. Такође, неопходно је навести и његову e-mail адресу, као и пуну поштанску адресу. Институцију(е) у којој су аутори запослени (или ангажовани) навести испод имена свих аутора. Уколико аутори нису из исте институције иза имена сваког аутора означити бројем у индексу припадност институцији и исти број у индексу написати испред назива одговарајуће институције.

Извод рада (100-250 речи, *италик* слова) написати испод наслова рада и имена аутора. Извод треба да садржи циљ истраживачког рада, методе, резултате и дискусију.

Кључне речи (нормална слова, максимално 5 кључних речи) навести испод Извода рада.

Увод треба да садржи податке везане за претходни истраживачки рад са одговарајућим референцама, као и проблем и циљ истраживања описаних у раду.

Експериментални део. Материјал и методе, који су коришћени у раду, треба да буду јасно и детаљно изложени како би остали научници могли да их понове. Детаљно описати само нове технике и методе, док је за већ познате методе довољно навести одговарајуће референце.

Резултати и дискусија. Резултати морају бити приказани концизно и јасно, у табелама или илустрацијама. Значајност резултата истраживања приказати без понављања материјала изложеног у Уводу. Број и величину табела, илустрација, графика и хемијских формула свести на неопходан минимум.

Закључак треба да покаже значајан допринос проблематике рукописа и могућност њене даље примене.

Захвалница. Текст захвалнице треба да буде што краћи.

Референце у тексту означити по редоследу појављивања арапским бројевима у заградама (). Све публикације наведене у рукопису рада навести и у листи референци на посебној страници текста. Скраћени називи часописа треба да буду написани у складу са Chemical Abstracts Service (CASSI Search Tool; <http://cassi.cas.org>). Списак референци треба написати по редоследу њиховог појављивања у тексту. Навести имена свих аутора (не користити „... и сарадници“), са њиховим иницијалима иза одговарајућег презимена. Иза скраћених назива часописа означити годину издања (**болд**), свеску (*италик*), број (ако постоји), и први и последњи број странице рада.

Примери:

Часописи: Pascual, E.C.; Goodman, B.A.; Yeretizian, C. Characterisation of Free Radicals in Soluble Coffee by Electron Paramagnetic Resonance Spectroscopy. *J. Agric. Food Chem.* **2002**, 50 (21), 6114–6122.

Књиге: Morris, R. *The Last Sorcerers: The Path from Alchemy to the Periodic Table*; Joseph Henry Press: Washington, DC, 2003; pp 145–158.

Књиге са више поглавља: Puls, J.; Saake, B. Industrially Isolated Hemicelluloses. In *Hemicelluloses: Science and Technology*; Gatenholm, P., Tenkanen, M., Eds.; ACS Symposium Series 864; American Chemical Society: Washington, DC, 2004; pp 24–37.

Књиге извода радова: Noe, W.; Howaldt, M.; Ulber, R.; Scheper, T. Immunobase elution assay for process control, 8th European Congress on Biotechnology, Budapest, 17–21 August 1997, Book of Abstracts WE 163, p. 246.

Тезе: Linstead, J.B. Effects of adding natural antioxidants on colour stability of paprika. Ph.D. (or M.S.) Thesis, University of Glasgow, november 2006.

Патенти: Lenssen, K. C.; Jantscheff, P.; Kiedrowski, G.; Massing, U. Cationic Lipids with Serine Backbone for Transfecting Biological Molecules. Eur. Pat. Appl. 1457483, 2004.

Необјављени (непубликовани) подаци: Треба да буду цитирани уз коментар „у штампи“, „необјављени резултати“ „личне белешке“.

Подаци преузети са интернета: Треба да садрже аутора, наслов, интернет адресу и датум приступа подацима: Пример: Wright, N.A. The Standing of UK Histopathology Research 1997-2002. <http://pathsoc.org.uk> (accessed 7 October 2004).

Извод и кључне речи на срском језику треба написати ћириличним писмом на крају рукописа рада (после списка литературних података) и у проширеном облику (највише 1 страница). Наслов рада написати нормалним, великим словима, а испод њега *италик* словима написати имена аутора (име, средње слово и презиме) као и назив институције у којој раде.

Хемијска номенклатура и јединице. Аутори су обавезни да користе SI систем јединица и хемијску номенклатуру која је у складу са правилима Chemical Abstract-а где год је то могуће.

Табеле. Свака табела треба да је нумерисана арапским бројем иза којег следи назив табеле (**Table 1. Result...**). Ширина табеле не сме бити већа од 12,5 цм.

Графици и слике. Сваки график или слику такође треба нумерисати арапским бројем иза којег следи назив (**Figure 1. Chromatogram of...**). Графици морају бити припремљени помоћу програма Microsoft Excel, Origin или Statistica. Шеме морају бити припремљене помоћу програма Microsoft Visio или Corel Draw. Све графике и шеме неопходно је доставити као посебне фајлове у оригиналној екстензији (нпр. xls, xlsx, vdr, cdr). Скениране црно-беле шеме доставити као фајлове са tif, wmf или bmp екстензијом. Фотографије у црно-белој техници доставити као посебне фајлове са jpg екстензијом.

Хемијске формуле и математичке једначине. Написати хемијске формуле и математичке једначине јасно и прецизно и тачно поставити индексе на своја места. Једначине у тексту означити арапским бројевима у угластим заградама []. Значења коришћених скраћеница и симбола треба детаљно објаснити приликом њиховог првог појављивања у тексту или дати посебан списак на посебној страници на крају рукописа.

Додатне информације

Рукопис треба послати уреднику часописа у два одштампана примерка на следећу адресу: Проф. др Соња Ђилас, Технолошки факултет Нови Сад, Булевар цара Лазара 1, 21000 Нови Сад, са назнаком „Рад за часопис Acta Periodica Technologica“. Електронску верзију рукописа послати на следеће e-mail адресе: sdjilas@tf.uns.ac.rs или bastajab@uns.ac.rs. Од аутора се очекује да предложи категорију рукописа рада (прегледни рад или оригинални научни рад).

Рецензија. Сви радови достављени уредништву часописа биће послати на рецензију код најмање два независна рецензента који ће бити замољени да рецензију дос-

тављеног им рукописа изврше у року од 4-6 недеља. Коначну одлуку о публикавању рукописа доноси Уређивачки одбор часописа. Рукопис може бити враћен ауторима на исправку и допуњу, уколико је то неопходно. Исправљен и допуњен рукопис треба вратити уредништву часописа што је пре могуће (најдаље за 2 недеље) након достављања примедби и коментара рецензената ауторима.

Рад припремљен за штампу: У последњој фази припреме рукописа аутору задуженом за кореспонденцију електронском поштом биће достављен рад припремљен за штампу на корекцију искључиво техничке природе и сагласност за штампање. Све корекције аутори достављају електронском поштом у року од 48 сати од пријема рада припремљеног за штампу.

Сва питања везана за објављивање радова у часопису слати на e-mail уредника часописа (sdjilas@tf.uns.ac.rs).

FORMER EDITORS-IN-CHIEF

Prof. Dr. Adalbert Šenborn (1967-1970)
Prof. Dr. Radivoj Žakula (1972-1975)
Prof. Dr. Miroslava Todorović (1976-1994)
Prof. Dr. Biljana Škrbić (1995-1998)

THIS ISSUE OF ACTA PERIODICA TECHNOLOGICA
IS FINANCIALLY SUPPORTED BY:

*Ministry of Education, Science and Technological Development
of Republic of Serbia*

Editorial:

University of Novi Sad, Faculty of Technology,
Bulevar cara Lazara 1, 21000 Novi Sad, Serbia

Phone: +381 21 485 3652

Fax: +381 21 450 413

e-mail: sdjilas@tf.uns.ac.rs

Text-Proof-Reader: Prof. Dr. Luka Bjelica

Typsetting: Branislav Bastaja

Cover design: Živojin Katić

Printed by Futura d.o.o., Petrovaradin

Copies: 200